

Investigation of Sustainable Hydrogen Production from Steam Biomass Gasification

by

Abdussalam Goma Abuadala

A Thesis Submitted in Partial Fulfillment
of the Requirements for The Degree of

Doctor of Philosophy

in

The Faculty of Engineering and Applied Science
Mechanical Engineering

University of Ontario and Institute of Technology

December 2010

© Abdussalam Goma Abuadala, 2010

Abstract

Hydrogen is a by-product of the gasification process and it is environmentally friendly with respect to pollution and emission issues when it is derived from a CO₂-neutral resource such as biomass. It is an energy carrier fuel and has flexibility to convert efficiently to other energy forms to be used in different energy applications like fuel cells.

The proposed research presents literature on previous gasification studies regarding hydrogen production from biomass and updates the obtained results. The main objectives of the thesis are: a) to study hydrogen production via steam biomass (sawdust) gasification; b) to evaluate the produced hydrogen by performing comprehensive analysis by using thermodynamic, exergoeconomic and optimization analyses. Despite details specific to the gasifier, in general, there is a special need to theoretically address the gasifier that gasifies biomass to produce hydrogen. This further study of gasification aspects presents a comprehensive performance assessment through energy and exergy analyses, provides results of the optimization studies on minimizing hydrogen production costs, and provides a thermo-economic analysis for the proposed systems (Systems I, II and III). This thesis also includes the results from the performed study that aims to investigate theoretical hydrogen production from biomass (sawdust) via gasification technology.

Results from the performed parametric study show that the gasification ratio increases from 70 to 107 gH₂ per kg of sawdust. In the gasification temperature studied, system II has the highest energy efficiency that considers electricity production where it increases from 72 % to 82 % and has the lowest energy efficiency that considers hydrogen yield where it increases from 45 % to 55 %. Also, it has the lowest hydrogen cost of 0.103 \$/kW-h. The optimization results show that the optimum gasification temperatures for System I, System II and System III are 1139 K, 1245 K and 1205 K, respectively.

Keywords: Gasifier, Gasification, Biomass, Hydrogen, Thermodynamics, Energy, Exergy, Exergoeconomics, Efficiency, Water Gas Shift, Steam Methane Reformer, Hydrogen Cost.

Acknowledgements

I would like to express my sincere gratitude and appreciation to my supervisor, Professor Ibrahim Dincer. Thank you for giving me the unique opportunity to do research with you. I appreciate your expert guidance and mentorship, your encouragement and support at all levels. Special thanks for your time, patience, and extremely valuable scientific advice.

I would like to thank the examining committee members for their recommendations and detailed review.

This work would not have been possible without the constant support of my family. Special thanks to my dear mom and dad. I shall never forget you - your soul is always with me. I would like also to express my honest and eternal gratitude towards my wife and children Alaa, Awab and Nibrass for having supported me through this journey.

Last but not least, I am indebted to my friends Dr. Ahmed Elgadi, Dr. Fateh Alej, Dr. Gaith Bsheesh and Dr. Omar Ramadan, who have helped me in terms of guidance and moral support.

Table of Contents

ABSTRACT.....	II
ACKNOWLEDGEMENTS.....	III
TABLE OF CONTENTS.....	IV
LIST OF TABLE CAPTIONS.....	IIX
LIST OF FIGURE CAPTIONS.....	X
LIST OF SYMBOLS.....	XIV
CHAPTER 1.....	1
INTRODUCTION.....	1
CHAPTER 2.....	7
LITERATURE REVIEW.....	7
2.1 Review on Available Gasification Approaches.....	7
2.2 Review on Equilibrium Approaches.....	13
2.3 Review on Hybrid Systems.....	14
CHAPTER 3.....	18
MOTIVATION AND OBJECTIVES.....	18
3.1 Motivation.....	18
3.2 Objectives.....	18
CHAPTER 4.....	20
BACKGROUND.....	20
4.1 Introduction.....	20
4.2 Hydrogen Production Methods.....	20
4.2.1 Natural Gas Steam Reforming.....	21
4.2.2 Water Electrolysis.....	21
4.2.3 Biomass Pyrolysis.....	22
4.2.4 Gasification.....	22
4.2.4.1 Coal Gasification.....	24

4.2.4.2	Biomass Gasification	24
4.2.4.2.1	Char	24
4.2.4.1.2	Tar.....	27
4.2.5	Flow Through The Gasifier	27
4.2.6	Approaches of Gasification Modelling.....	28
4.2.6.1	Kinetic Approach.....	28
4.2.6.1.1	Reaction Kinetics.....	29
4.2.6.2	Equilibrium Approach	30
4.2.6.2.1	Stoichiometric Equilibrium Approach.....	31
4.2.6.2.2	Non-Stoichiometric Equilibrium Approach	32
4.2.6.3	Neural Network Approach.....	32
4.2.6.3.1	Network Training	34
4.2.6.3.2	Back Propagation.....	34
4.2.7	Strategies to Solve the Different Approaches.....	34
4.2.7.1	Kinetic Approach.....	34
4.2.7.2	Equilibrium Approach	35
4.2.7.3	Neural Network Approach.....	35
CHAPTER 5	37
SYSTEMS DESCRIPTION	37
5.1	System I	37
5.2	System II.....	39
5.2.1	Fuel Cell.....	41
5.2.1.1	The Solid Oxide Fuel Cell (SOFC).....	41
5.3	System III.....	43
5.3.1	Solid Oxide Electrolysis Cell (SOEC).....	45
CHAPTER 6	47
MODELING AND ANALYSIS	47
6.1	Introduction.....	47
6.2	Assumptions.....	47
6.3	Reaction Mechanism.....	47

6.4	Biomass Equations.....	49
6.5	Mass Analysis	50
6.6	First Law of Thermodynamics.....	50
6.6.1	Gasifier Energy Efficiencies	53
6.7	Second Law of Thermodynamics	53
6.7.1	Gasifier Exergy Efficiencies	54
6.7.2	Irreversibility.....	55
6.7.2.1	Internal Irreversibility	55
6.7.2.2	External Irreversibility	55
6.8	System II Components	56
6.8.1	Compressor 5-6.....	56
6.8.2	Gas Turbine 7-8	60
6.8.3	Heat Exchanger 17-18-9-10.....	63
6.8.4	Heat Exchanger 20-21-3-4.....	65
6.8.5	The Steam Reforming Reactor.....	66
6.8.6	Water Gas Shift Reactor	69
6.8.7	SOFC Equations.....	70
6.8.8	Burner	75
6.8.9	System II Energy Efficiencies	77
6.8.10	System II Exergy Efficiencies	78
6.9	System III Components.....	79
6.9.1	Solid Oxide Electrolyse Cell.....	79
6.9.2	Lumped SOFC-SOEC.....	81
6.9.3	System III Energy Efficiencies	84
6.9.4	System III Exergy Efficiencies	84
6.10	Systems Exergoeconomic Analysis	85
CHAPTER 7		90
RESULTS AND DISCUSSION		90
7.1	Introduction.....	90
7.2	Data Utilization.....	92

7.2.1	Data for Biomass and Thermodynamics Properties.....	92
7.2.2	Data for Gasifier	92
7.2.3	Data for Gas Turbine	94
7.2.4	Data for Air Compressor.....	94
7.2.5	Data for SOFC and SOEC	94
7.3	Results for System I.....	95
7.3.1	Results for Gasification Process	96
7.3.1.1	Parameters Affecting Hydrogen Production.....	96
7.3.1.1	Effect of Biomass Quantity on Hydrogen Product	96
7.3.1.2	Effect of Supplied Steam	97
7.3.1.3	Effect of Gasification Temperature	99
7.3.1.4	Effect of Operating Parameters on Process Irreversibility	99
7.3.1.5	Process Energy and Exergy Efficiencies	99
7.3.2	Evaluation of the Gasification Process Efficiency.....	102
7.3.2.1	Effect of Steam-Biomass Ratio on Hydrogen Production	103
7.3.2.2	Effect of Steam-Biomass Ratio on Energy Efficiency	104
7.3.2.3	Effect of Steam-Biomass Ratio on Exergy Efficiency	105
7.3.2.4	Effect of Gasifier Temperature on Hydrogen Production.....	106
7.3.2.5	Effect of Gasifier Temperature on Energy Efficiency	107
7.3.2.6	Effect of Gasifier Temperature on Exergy Destruction and Exergy Efficiency	107
7.3.3	System I Energy Efficiency	109
7.3.4	Exergy Destruction in System I	110
7.3.5	System I Exergy Efficiency	112
7.3.6	System I Exergoeconomic Analysis Results.....	112
7.4	Results for System II.....	115
7.4.1	Effect of Current Density.....	115
7.4.2	Effect of Hydrogen Flow Rate	117
7.4.3	Effect of Preheated Air	119
7.4.4	Effect of Pressure Ratio	123
7.4.5	Electrical Efficiency for System II	124

7.4.6	Exergy Destruction in System II Components.....	124
7.4.7	System II Exergy Efficiencies	126
7.4.8	System II Exergoeconomic Results	128
7.5	Results for System III	134
7.5.1	Effect of Gasification Temperature on Hydrogen Yield.....	135
7.5.2	Effect of Preheated Air in System III	136
7.5.3	System III Electrical Energy Efficiency	138
7.5.4	System III Exergy Destruction.....	141
7.5.5	System III Exergy Efficiencies	141
7.5.6	System III Exergoeconomic Results	142
7.6	Systems Optimization Results	147
7.7	Comparisons and Comments	149
7.7.1	Introduction.....	149
7.7.2	Gasification Process.....	150
7.7.3	Systems I, II, III	151
CHAPTER 8	155
CONCLUSIONS AND RECOMMENDATIONS	155
8.1	Conclusions.....	155
8.2	Recommendations.....	158
REFERENCES	160
APPENDICES	172
APPENDIX A.....	172
APPENDIX B.....	182
EES to simulate the systems	182
B1. System I	182
B2. System II.....	194
B3. System III.....	215
B4. EES for SOFC and SBG calculations	237

List of Table Captions

Table 2.1 Different gasifiers with their used approaches	10
Table 2.2 Summary of investigations on hydrogen production from typical biomass gasification.....	11
Table 4.1 Kinetic coefficient (R_1, R_2, \dots, R_{16} as defined above).....	26
Table 7.1 Ultimate and proximate analysis of sawdust wood	92
Table 7.2 Standard chemical exergy for different components	93
Table 7.3 The coefficients used in constant specific heat empirical equation.....	93
Table 7.4 SOFC geometries and material related data	95
Table 7.5 Cell material resistivity and its dependence on temperature	95
Table 7.6 Economic analysis related data.....	96
Table 7.7 Temperature and mass through system I for a gasification temperature of 1023 K.....	109
Table 7.8 Unit exergy cost and cost rate for flow material through system I.....	115
Table 7.9 Temperature and mass through system II for a gasification temperature of 1023 K.....	122
Table 7.10 Unit exergy cost and cost rate for flow material streams in system II.....	134
Table 7.11 Mass flow per kg of biomass and temperature through system III when the gasification temperature is 1023 K.....	138
Table 7.12 Unit exergy cost and cost rate for flow material streams in system III	145
Table 7.13 Efficiencies of the different systems at 1023 K.....	153
Table 7.14 Unit hydrogen cost from different studies	153
Table A.1 Annualized costs of system I components	172
Table A.2 System II annualized costs of system components	173
Table A.3 Annualized costs of system III components	174
Table A.4 System I cost balance equations	175
Table A.5 System II cost balance equations	177
Table A.6 System III cost balance equations.....	180

List of Figure Captions

Figure 4.1 Schematic diagram of a multilayer feed forward neural network.	33
Figure 4.2 Processing information in a neural network.	33
Figure 4.3 Algorithm for developing a neural network solution.	36
Figure 5.1 System I layout	38
Figure 5.2 System II layout.....	40
Figure 5.3 A Schematic diagram of SOFC	42
Figure 5.4 System III layout	44
Figure 5.5 A schematic diagram of SOEC.....	45
Figure 6.1 Schematic diagram of a system for study	50
Figure 6.2 A schematic diagram of compressor 5-6.	56
Figure 6.3 A schematic diagram of turbine 7-8.	61
Figure 6.4 A schematic diagram of heat exchanger 17-18-9-10.....	63
Figure 6.5 A schematic diagram of heat exchanger 20-21-3-4.....	65
Figure 6.6 A Schematic diagram of steam reforming reactor.....	67
Figure 6.7 A schematic diagram of water gas shift reactor.	69
Figure 6.8 A schematic diagram of burner.	75
Figure 6.9 A schematic diagram of lumped SOFC-SOEC subsystem.....	82
Figure 6.10 Schematic diagram showing exergoeconomic analysis for a component.	87
Figure 7.1 Flow-diagram for analysis steps.....	91
Figure 7.2 Hydrogen production from different quantities of wood sawdust.....	97
Figure 7.3 Produced hydrogen and gasification ratio from different quantities of wood sawdust.	98
Figure 7.4 Hydrogen production from 20 kg/s of wood sawdust at 1000 K versus injected steam.....	98
Figure 7.5 Gases concentration versus gasification temperatures for 32 kg/s from wood sawdust and 4.5 kg/s from steam.....	99
Figure 7.6 Exergy destruction and exergy flows with wood sawdust at 1000 K and 4.5 kg/s steam.	100
Figure 7.7 Exergy efficiency versus gasified wood sawdust at a gasifier temperature of 1500 K.	101

Figure 7.8 Specific entropy generation at a gasification-temperature of 1500 K.....	101
Figure 7.9 Energy efficiency versus fed wood sawdust.	102
Figure 7.10 Concentration of gases from gasification at different steam-biomass ratios and hydrogen yield from different steam-biomass ratios and at 1023 K.....	103
Figure 7.11 Energy efficiencies for different steam-biomass ratios.	104
Figure 7.12 Exergy efficiencies and specific entropy generation for different steam- biomass ratios.	105
Figure 7.13 Hydrogen production and hydrogen yield at different gasification temperatures for 14.5 kg/s from wood sawdust and 6.3 kg/s from steam.	106
Figure 7.14 Energy efficiencies at different temperatures.....	107
Figure 7.15 Exergy destruction and improvement potential in exergy for 14.5 kg/s from wood sawdust and 6.3 kg/s from steam.	108
Figure 7.16 Exergy efficiency and specific entropy generation versus gasification temperature.	108
Figure 7.17 System I energy efficiency with hydrogen and hydrogen yield versus gasification temperature.	110
Figure 7.18 Exergy destruction in system I components at gasification temperature of 1023 K.	111
Figure 7.19 System I exergy efficiency with hydrogen and hydrogen yield versus gasification temperature.	111
Figure 7.20 Hydrogen yield from system I and its unit exergy cost versus gasification temperature.	112
Figure 7.21 Hydrogen yield from system I and its temperature versus gasification temperature.	113
Figure 7.22 Cost of hydrogen yield and its temperature at different gasification temperatures.....	114
Figure 7.23 Overpotential losses for the used SOFC.....	116
Figure 7.24 SOFC volts versus current densities and at different utilization factors.	117
Figure 7.25 AC power produced by SOFC at different utilization factors.	117
Figure 7.26 Variation of SOFC efficiency with voltage at current density of 750 mA/cm ²	118

Figure 7.27 Hydrogen uses and hydrogen yield in system II at different gasification temperatures.....	118
Figure 7.28 Power produced from hydrogen yield at different gasification temperatures.	119
Figure 7.29 System II energy efficiencies versus preheated air flows to the burner.	120
Figure 7.30 System II energy efficiencies versus preheated air flows to the SOFC.	121
Figure 7.31 System II energy efficiencies versus preheated air temperature at different gasification temperatures.	121
Figure 7.32 System II energy efficiencies versus burner temperature.....	122
Figure 7.33 SOFC Power at different pressures and current densities.	123
Figure 7.34 SOFC efficiency at different pressures and current densities.	124
Figure 7.35 System II energy efficiencies versus gasification temperature.	125
Figure 7.36 Exergy destruction in system II components at 1023 K.....	125
Figure 7.37 Exergy destruction in system II components versus gasification temperature.	126
Figure 7.38 System II exergy efficiencies versus gasification temperature.	127
Figure 7.39 Energy efficiencies at the operating pressure of 2 bars.	127
Figure 7.40 Exergy efficiencies at the operating pressure of 2 bars.	128
Figure 7.41 System II primary hydrogen yield and its cost of versus gasification temperature.	129
Figure 7.42 System II primary hydrogen yield and its temperature versus gasification temperature.	129
Figure 7.43 System II primary hydrogen cost and its temperature versus gasification temperature.	130
Figure 7.44 System II secondary hydrogen yield and its cost at different gasification temperatures.....	131
Figure 7.45 System II secondary hydrogen yield and its temperature versus gasification temperature.	131
Figure 7.47 Produced steam in system II and its cost versus gasification temperature..	133
Figure 7.48 Excess steam in system II and its cost versus gasification temperature.	133

Figure 7.49 System III gasification ratio and hydrogen yield at different gasification temperatures.....	135
Figure 7.50 System III efficiencies versus burner preheated air flow.	137
Figure 7.51 System III efficiencies versus preheated air flows in the lumped SOFC-SOEC.....	137
Figure 7.52 System III energy efficiencies at different preheated air temperatures.	139
Figure 7.53 System III energy efficiencies versus burner temperature.	139
Figure 7.54 System III energy efficiencies at different gasification temperatures.	140
Figure 7.55 Exergy destruction in system III components at a gasification temperature of 1023 K.	140
Figure 7.56 System III exergy efficiencies at different gasification temperature.....	141
Figure 7.57 Hydrogen yield from System III and its cost at different gasification temperatures.....	142
Figure 7.58 Hydrogen yield in System III and its temperature at different gasification temperatures.....	143
Figure 7.59 Hydrogen cost in System III and its temperature at different gasification temperatures.....	144
Figure 7.60 Excess steam available in System III and its cost at different gasification temperatures.....	144
Figure 7.61 Excess steam from system III and its temperature at different gasification temperatures.....	145
Figure 7.62 Temperature of excess steam and its cost in system III versus gasification temperature.	146
Figure 7.63 Systems I, II, III objective functions versus gasification temperature.	147
Figure 7.64 System I objective function convergence versus generation.....	148
Figure 7.65 System II objective function convergence versus generation.	149
Figure 7.66 System III objective function convergence versus generation.	149
Figure 7.67 Hydrogen concentrations from this study and others.	151

List of Symbols

a	hydrogen moles (kmol/s)
a_1, \dots, a_6	coefficients in entropy equation
A	gasifier area in m^2 or pre-exponential constant in s^{-1} or min^{-1}
b	carbon monoxide moles (kmol/s)
c	concentration (kg m^{-3}) or cost per exergy unit ($\$/\text{kwh}$)
C	carbon content in biomass (w %) or cross plane resistance ($\Omega\text{-cm}^2$)
\dot{c}	cost of stream ($\$$)
d	methane moles (kmol/s)
$D_{a\text{eff}}$	effective gaseous diffusivity through the anode (cm^2/s)
$D_{c\text{eff}}$	effective gaseous diffusivity through the cathode (cm^2/s)
e	char product (kmol/s)
E	activation energy (kJ mol^{-1}) or ohmic symmetry factor (-)
Ex	exergy (kJ/kg or kJ/kmol)
Ex_o	standard exergy (kJ/kmol)
\dot{Ex}	exergy rate (kW)
f	tar yield (kmol/s)
F	Faraday constant (96,485 coulombs/g-mole)
h	specific enthalpy (kJ/kg or kJ/kmol)
H	hydrogen content in biomass (w %) or total enthalpy (kJ)
i	current density (A/cm^2)
i_o	apparent exchange current density (A/cm^2)
I	current (A) or irreversibility (kW)
K	equilibrium constant (-)
k	rate constant or kinetic constant (s^{-1})
L	characteristic length of SOFC (cm)
LHV	lower heating value (kJ/kg or kJ/kmol)
\dot{m}	mass flow rate (kg/s)
MW	molecular weight (kg/kmol)
N	nitrogen content in biomass (w%)
$n_1\text{-}n_5$	number of moles (kmol)

\dot{n}	molar flow rate (kmol/s)
\dot{n}_{o_2}	molar oxygen flow from SOEC (kmol/s)
O	oxygen content in biomass (w %)
P	pressure or partial pressure (Pa or atm)
PI	improvement potential (kW)
\dot{q}	heat transferred to ambient (kW)
R	universal gas constant (8.314 kJ kmol ⁻¹ K ⁻¹) or resistance (Ω)
T	gasification temperature (K)
T_0	reference temperature (298 K)
s	specific entropy (kJ kmol ⁻¹ K ⁻¹ or kJ kg ⁻¹ K ⁻¹)
\dot{s}	entropy (kW/K)
S	total entropy (kJ)
t	time (s) or thickness (cm)
U_0	wind velocity (m/s)
U	overall heat transfer coefficient (W m ⁻¹ K ⁻¹)
U_f	utilization factor (-)
V	circuit or over potential volts (Volt)
x	thickness (m)
\dot{W}	work rate (W or kW)
X	molar fraction of component (-)

Subscripts

a	anode
act	activation
$Burner$	burner
c	cathode or compressor
ch	chemical
$char$	char
des	exergy destroyed
$deswa$	exergy loss
e	exit

en energy
en,el electrical energy
en,H₂ considers energy content of producer hydrogen
ex exergy
ex,H₂ considers exergy of producer hydrogen
ex,el considers exergy of electricity production
gen generation
gas gas
H₂ hydrogen
H₂O steam
i inlet
ins insulation
lostwa lost from gasifier wall to ambient
o at reference or ambient
O₂ oxygen
ohm ohmic
osf ohmic symmetry factor
pol polarization
ph physical
res resistance
s supply
steam steam
SOFC solid oxide fuel cell
SOEC solid oxide electrolyse cell
SR steam reforming
t turbine
tar tar
w wall
WGS water gas shift
wa from gasifier wall to ambient

Greek Letters

α	quantity of biomass (kmol/s)
β	coefficient (-)
ΔG	standard Gibbs function of reaction (kJ per kg or kJ per kmol)
ε	gasifier wall emissivity (-)
ε_b	bubble phase fraction(-)
η	efficiency (-)
γ	supplied steam (kmol/s) or Pre-exponential factor (A/m^2)
ρ	resistivity (Ω -cm)

Chapter 1

INTRODUCTION

Thermo-conversion processes are combustion, pyrolysis and gasification. Combustion produces gases at a temperature range of 800-1000 °C while the pyrolysis process produces gases, liquids and solids [1]. It is feasible to combust a biomass that has a moisture content of less than 50% while a conventional biomass pyrolysis produces equal fractions of gases, liquids and solids. Modern studies upgrade liquid fraction to produce hydrogen but they have not yet been fully developed [1, 2]. Gasification is an attractive thermo-chemical process and has a higher efficiency than combustion [2]. Gasification adds value to low or negative-value feed stocks in terms of usefulness by converting them to marketable fuels and products. Typical feedstock materials used in gasification are biomass, coal, and agricultural and industrial residuals etc. Gasification converts biomass to gas and diminishes the content of char and tar. The gasification of biomass falls under the scope of this study.

Gasification is one of the most efficient ways to extract energy from fuel sources and convert it into a usable form by partial or total transformation of solids to gases. It is the energy conversion process that has been studied as an alternative solution to environmental issues associated with energy production. By this process, biomass can be broken down to H₂, CH₄, CO, CO₂ and others in the presence of a gasification agent(s). The agent may be oxygen, air, steam or a combination of them. Steam gasification produces a gas rich in hydrogen [3]. It gives a medium heating value gas of ~15–20 MJ m⁻³ which is higher than that from air gasification and costs less compared to oxygen gasification [4].

Hydrogen production by gasification of biomass is a complex process that is influenced by a number of factors, such as: feedstock composition, moisture content, gasifier temperature, gasifier pressure, amount of oxidant present, gasifier geometry and mode of gas-solid contact.

The contact between the solid fuel particles and gases can be obtained through a reactor or gasifier. Entrained suspension, fixed bed and fluidized bed have been explored to gasify fuels. The first type was developed for coal gasification, but the need for

feeding material made fibrous materials like wood unsuitable for gasification by this type of technology; the process has not been considered further. To achieve a higher thermal capacity of $> 5\text{MW}_{\text{th}}$, a fluidized bed gasifier is considered [3]. Fluidized bed gasifiers are considered to be systems with fluidized granular inert materials. The two types are: bubbling fluidized bed (BFB) gasifiers, where the bed material is fluidized or agitated by gases flowing through it; and circulating fluidized bed (CFB) gasifiers, where the bed material circulates between the riser and the down-comer. Depending on the design specification, fuel can be fed to the gasifier into the top, bottom or middle. The choice of the type of gasifier or reactor for gasification depends on the capacity of the unit and its specification has to suit the end use or down-stream gasifier utilization systems. The end-use includes co-firing, firing, stirling engines, gas engines, gas turbines, fuel cells, hydrogen, the Fischer-Tropsch synthesis [5] and others.

Gasification is an endothermic process; therefore, heat is needed to sustain the gasification process. The process could be either auto-thermal or all-thermal depending on how this heat is provided. In the case of auto-thermal gasification, the necessary heat is generated directly by partial oxidation in the gasifier itself while during indirect heating by combusting some of the feedstock, char or clean syngas separate and transfer heat through exchangers using preheated bed material [6].

The hydrodynamic regime in the bed promotes high quality mixing and efficient heat transfer. The product gas exits the reactor at a high temperature and it may contain alkali salts and tar amounts depending on the reactor design specifications. Updraft moving bed gasifiers suffer from high tar yields in the product gas and the inability to maintain uniform radial temperature profiles to avoid local slugging problems [7].

Fluidized bed gasifiers have found wide application in solid fuel gasification; however, a single BFB gasifier cannot achieve high solid gasification due to the degree of solid mixing as well as particle entrainment [8]. Circulating fluidized bed (CFB) gasifiers use cyclone(s) to capture and recycle the solids increasing their residence time, and thus obtaining a higher degree of gasification. The riser of the CFB operates in either the fast or turbulent fluidization flow regime.

For many years, development of thermal fuel gasification processes were going on [9], but it faced two main disadvantages: low gas yields and corrosion of downstream equipment caused by the high concentration of tar vapor contained in the gas phase.

The effort to overcome the problems associated with gasification has continued for many years, but some major problems still remain. The product gas exiting a gasifier contains some particles, alkali compounds, tars, and nitrogen-containing components. The formation of tar (complex mixture of organic liquid constituents) and char (solid carbonaceous materials) during the gasification process are the most severe of all problems [10-12], and because of these problems, none of the processes currently available are universally accepted for commercialization [13-15]. The tar causes mechanical problems in the gasification components and the char causes catalyst deactivation in the catalytic conversion of syngas to useful chemicals and some liquids. The quantity of these components depends on the gasifier design specifications and the type of fuel fed.

The gasifier product has to suit the end use or downstream gasifier utilization systems. The end-uses require clean product gas to include co-firing systems, stirling engines, gas engines, gas turbines, fuel cells [5]. Cyclone filters, barrier filters and electrostatic filters are technologies used to clean the product gas. Wet scrubbers are used to remove particles and alkali at a low temperature. Catalytic destructive and wet scrubbing technologies are used to remove the condensed tars [9]. Also, particles and tars can be removed by catalytic and thermal cracking. The tar from solid gasification and especially biomass gasification is volatile and difficult to coalesce even under iced conditions [16]. Bed particles and finer char particles which are entrained by the product gas are separated in the cyclone. Its composition in the product gas depends on residence time, gasifier design and reaction temperature.

The worldwide increase in energy consumption will have an impact on carbon emission and depletion of fossil fuel. For a feasible solution, efforts were made to use substantial resources and renewable energy. Biomass is classified as the third energy source after coal and oil [17]. It is renewable and neutral with respect to the carbon dioxide emission issue. The level of utilization of biomass to produce hydrogen depends on the economics and the availability of the necessary technology. The gasification of

biomass to produce hydrogen as an energy carrier is part of the effort to combat this threat. The gasification process consists of the following steps: pre-heating, drying, pyrolysis, char-gasification, char-oxidation and ash formation. The gasification steps are theoretically modeled in series, but there is no discrete boundary between them and they often overlap. Hydrogen is expected to be the most important energy carrier in a sustainable energy system. Turn et al. [18] reported there was no emphasis on hydrogen production in past experimental work done on steam gasification of biomass, but the present work is theoretical and will emphasize hydrogen production.

The proper approach will find the optimum conditions which lead to an appreciable hydrogen product from the gasified biomass. A parametric study in the used biomass and steam range will help in identifying the more sensitive parameters to the hydrogen yield and feasibility of hydrogen production via biomass gasification from the first and second laws of thermodynamics' views. This study applies to a self-heated gasifier in order to study the characteristics of hydrogen production from biomass gasification.

The gasifier is considered to be the heart of the gasification process. Recently and in addition to what is mentioned above, Mahishi et al. [19] reported that until their research, no study had addressed hydrogen production by theoretical analysis of the gasifier.

Vlaswinkel et al. [20] and Ptasinski et al. [21] demonstrated that the gasifier is one of the least efficient unit operations in technology of gasification, thereby calling for an improvement of overall efficiency (energy and exergy) of gasifiers.

Past research focused on the effect of process parameters such as temperature, pressure, steam-biomass ratio, air to biomass ratio and biomass type on the hydrogen yield and total gas and tar yields [18, 22, 23]. Focus on the thermodynamics of biomass gasification has been relatively limited [22].

Efficiency evaluation of hydrogen production from biomass gasification through a parametric study aims to calculate the overall efficiency (energy and exergy) for hydrogen production from steam biomass gasification. From the results obtained, one can investigate the optimum conditions which have a higher efficiency rate, or avoid inefficient conditions in the studied range of temperature and steam-biomass ratio. A

performed parametric study will help in identifying the more efficient condition of hydrogen production via biomass gasification from first and second laws of thermodynamics' views.

In addition to this research and the available literature, none of the studies has addressed hydrogen production performance through exergy and energy efficiency. Studying energy efficiency is quite common, for example, Mahishi et al. [19] studied energy efficiency for biomass gasification in existing air-steam mediums.

In the absence of models addressing gasification regarding hydrogen production, it is useful as a first step to discuss approaches that are used to model the gasification process. Mathematically, approaches of fluidized bed gasifiers (FBG) may be classified into three levels [24]. The first is the macroscopic approach. It considers, for example, the coupled momentum equations for individual particles and gases as well as the mass and heat transfer equations approach [25]. The second approach describes the bed hydrodynamics and transport phenomena with empirical relations and functions of the local state. It requires the determination of parameters from simple experiments and allows consideration of the coupled mechanisms with less calculation time than the previous approach. The modeled approaches of [24, 26, 27] are examples of this class. The third approach is simpler and based on curve fitting from experimental data. As those data are not based on universal expressions, this class of models cannot extend to units with different situations.

Modeling an approach to produce hydrogen via biomass gasification enables the designers to predict the effects of many parameters even without any experimental data on the hydrogen product. The validity of this approach can be confirmed only through experimental verification. A good approach can optimize the effects of many parameters in the form of the produced hydrogen per unit fuel intake. The optimization of hydrogen production from the gasification process evaluates hydrogen production regarding efficiency and cost.

This study explores the influence of different parameters on hydrogen production from biomass steam gasification as well as evaluating its energy and exergy efficiencies in conventional and integrated system fashion. In the present study a comprehensive

parametric study is carried out to investigate numerous factors influencing the overall efficiency of hydrogen production from biomass gasification.

Chapter 2

LITERATURE REVIEW

2.1 Review on Available Gasification Approaches

Modeling of wood gasification in a circulating fluidized bed was developed by Jennen et al. [28]. In the model, the riser was divided vertically into cells. The dense bed (0.2 m x 0.5 m height) hydrodynamics was similarly treated as that of a bubbling bed where it was based on a two-phases module: the bubble and emulsion phases. The bubble included most of the gas and modeled as plug flow without back mixing. The emulsion phase included the remaining gas and all the solids and modeled as ideally back mixed. The dilute bed hydrodynamics was assumed in core annulus structure. The core contained dilute gas-solid mixture moving upwards while the annulus contained solid moving downwards. They assumed the gasification reactions take place in the core. They found that the predicted pressure and the temperature along the riser (0.3 m x 8 m height) fit well with the experimental results. They reported that the maximum deviation between the calculated and measured temperature was 5°C. Also, the difference between the calculated and the measured volume fraction of the product gases was ± 1 %. In case of hydrogen it was 1.7 %. They attributed these deviations to the inaccuracy of the measurements.

Hamel et al. [29] developed mathematical model to simulate a BFB gasifier. They built a model from sub-models available in literature. In this model, the gasifier was divided into cells where each cell was modeled based on a two-phase theory: the bubble free solid phase and the emulsion phase. The homogeneous reactions only took place inside the bubbles and both homogeneous and heterogeneous reactions took place in the emulsion phase. They concluded that carbon conversion, concentration of different species and freeboard temperature from the model results were comparable to the results from the experimental work.

De Souza-Santos [26] presented a comprehensive model to simulate a steady state operation of a fluidized bed gasifier. He assumed conditions change in vertical direction. A hydrodynamics of bed was represented by a two-phase theory: a bubble free solid

phase and an emulsion phase. Gas in the two phases was assumed in plug flow. The model results were compared with results from commercial and pilot plants and a small deviation was observed. Specifically, he reported that the predicted gas leaving the freeboard was within a 5% deviation.

Mansray et al. [30] used the ASPEN PLUS process simulator to develop a model that predicted the performance of a dual-distributor fluidized bed gasifier under a steady state condition. The gasifier was used to gasify rice husk and its riser treated as one compartment or two compartments (core and annulus). They predicted the model at the equilibrium state and under various operating conditions include: temperature, gas composition, higher heating value and carbon conversion. The used distributor limits the model's usefulness.

A two-phased model was developed by Sadaka et al. [31] to predict the performance of air-steam biomass gasification in a fluidized bed. The model combined different approaches to derive the system equations and therefore would not be classified under any specific approach. The riser was divided into three zones from bottom to top: jetting, bubbling and slugging. Each zone constitutes two phases: bubble and dense. The model considered non-equilibrium higher hydrocarbons products like C_2H_2 , C_2H_4 and C_2H_6 , contrary to that of other models. The derived equations can predict bed temperature, gas mole fraction and gas higher heating value but they did not present the model validation.

Li et al. [8] developed a non-stoichiometric equilibrium model based on minimizing Gibbs free energy to predict the performance of CFB gasifier. Steady state distribution of parameters was considered. They considered 42 gaseous and 2 solids species including C, H, O, N, and S while the other elements were considered inert. They investigated profiles of temperature and gas composition, and the effects of air ratio, O/C molar ratio, operating temperature, secondary air, suspension density, fly ash re-injection, and steam injection. The model results were compared with results from a pilot plant of 6.5 m height and 0.1 m diameter using biomass fuel. They found an air ratio of 0.15-0.25 and a temperature range of 1100-1300 K were preferred for rich hydrogen production at atmospheric pressure. They reported that the equilibrium model deviated from a real

gasification process and a modified equilibrium model was necessary to take into consideration of the deviation.

Chen et al. [32] presented a model involving hydrodynamics, chemical reaction kinetics and energy balance. The model investigated product gas from biomass by a process that combines pyrolysis, gasification and combustion. The hydrodynamics of a gasifier riser was divided into three sections: a dense section on the bottom, transition section in the middle, and dilute section in the freeboard. They assumed too short a transition section and therefore it was merged into the dilute section. Chemical reactions were focused on the kinetic behaviour of biomass char particles. The gas heating value and the gas yield predicted by the model were not so accurate compared to the published data. They attributed that to the physical constraints regarding the used CFB gasifier such as low preheating capacity which led to a relatively low temperature level in the riser, unsatisfactory separator efficiency and particle size was not ideal. They concluded that the solution to improving the results was to remove those constraints and only after that could the experimental results be used to validate the model.

Corella et al. [33] presented a one-dimensional model for CFB gasifier using air to gasify biomass under a steady state condition. They considered a gasifier which had a bottom dense bed, a transition or splash zone and an upper dilute zone. The kinetic approach was used to describe the chemical reactions. They introduced correction factors in kinetic equations in order to take into account the catalytic effects on reactions. All species were considered in plug flow. The temperature profile along the riser height was modeled on a heat balance basis. The gasifier was represented by four contours: one of them includes the whole gasifier and the other three inside the riser. They found the axial temperature profile was confirmed by the measurements but they did not report the deviation.

Srinivas et al. [34] developed thermo-chemical model to predict gas composition of biomass gasification in a pressurised CFB gasifier. They studied the effect of parameters that included relative air fuel ratio, steam fuel ratio and gasifier pressure, gasifier temperature, gasifier exergy efficiency and lower heating value of the gas on mole gas fraction. They found that the pressure had a slight effect on gas composition and

affected the heating value of produced gas, temperature, and exergy efficiency of the gasifier.

Table 2.1 Different gasifiers with their used approaches

Reference	Gasifier type	Fuel	A	B	C	Condition
[37]	BFB	Carbon	I	b	II	$A=1.17 \text{ m}^2$ $H_{mf}=0.6 \text{ m}$
[25]	BFB	Not Considered	NA	NA	NA	$P=2.5 \text{ Mpa}$ $ER=0.23-0.44$
[38]	CFB	Not Considered	III	NA	NA	$H=8.4,3,12.5 \text{ m}$ $d_B=0.4,0.05,0.304 \text{ m}$
[39]	BFB	A&B Particles	I	c	II	$d_B=3 \text{ m}$, $T=723 \text{ K}$ $P=1 \text{ bar}$
[24]	BFB	Wood Wood/plastic	III	NA	I, II	$T=1040 \text{ K}$
[40]	BFB	Char	III	c	II	$T=1123 \text{ K}$, $H=0.169 \text{ m}$ $C:O_2:H_2O = 1:0.26:0.25$
[28]	CFB	Wood	III	c	I, II	$H=8 \text{ m}$, $d_B=0.3 \text{ m}$
[12]	BFB	Char	NA	NA	II	$T=700-900^\circ\text{C}$ $ER=0.15,0.25,0.35$
[41]	CFB	Char	III	c	II	$d_B=0.048 \text{ m}$, $H=3.56 \text{ m}$ $T=900-950^\circ\text{C}$ $H_2:CO:CH_4$ $3:1:1$
[32]	CFB	Biomass	III	NA	NA	$d_B=0.083 \text{ m}$, $H=6 \text{ m}$ $ER=0.3$, $T=733^\circ\text{C}$
[33]	CFB	Pine wood chips	III	c	I, II	$P=1 \text{ atm}$, $T=750-980^\circ\text{C}$ $ER=0.2-0.45$
[42]	BFB	Biomass	I	a	II	$A=1 \text{ m}^2$ $T=300-600^\circ\text{C}$
[43]	BFB	Coke	II	NA	II	$0.2 < d_p < 2 \text{ mm}$

A: bed cross sectional area; d_p : particle diameter; d_B : bed diameter; ER: equivalence ratio; H: bed height; NA: not available

A. Gasifier modeling approach

- I. Two-phase model: bubble and emulsion phases.
- II. Three-phase model: bubble, cloud and emulsion phases.
- III. Fluidized bed divided into sections.

B. Flow type

- a. Plug flow in bubbling phase, ideally mixed gas in emulsion phase.
- b. Ideally mixed gases in both phases.
- c. Plug flow in both phases, there is exchange between phases.
- d. Plug flow through the bed.
- e. Plug flow in emulsion phase.

C. Gasification approach

- I. Equilibrium consideration.
- II. Kinetic approach.
- III. Neural network.
- IV. Mixing of combination from the above.

Guo et al. [35] developed a hybrid neural network to predict gas yield and composition from gasification of four biomasses: bagasse, cotton stem, pine sawdust and poplar. Multilayer feed forward neural networks were used to approximate the function.

Due to the physical properties of biomass, it was found that fluidized bed gasifiers can handle different biomass types and can provide gases with a degree of purity suitable to end uses. Approaches used, along with their basic characteristics are listed in Table 2.1. From the data available in Table 2.2 one can draw a conclusion that steam gasification has the highest hydrogen yield. Hanaoka et al. [36] gasified wood to produce hydrogen in the presence of CO₂ sorbent. Their experiments showed that the results were affected by the pressure. However, they reported higher atmospheric pressure results in a lower H₂ yield. Therefore, the present study is performed on steam biomass gasification operating near atmospheric pressure, in view of the two laws of thermodynamics.

Table 2.2 Summary of investigations on hydrogen production from typical biomass gasification.

Reference	Inside Diameter, m	Height, m	Fuel Used	Gasification Medium	Operating Pressure	Operating Temperature, K	H ₂ yield (%)
[24]	0.300	2.90	Wood Wood/Plastic	Air	P _{atm}	1016	9.20
[32]	0.083	6.00	Miscanthus	Air	NA	1026	6
[33]	Variable	14.80	Biomass	Air	P _{atm}	1123	25
[44]	0.040	1.400	Pine sawdust	Air	P _{atm}	1073	32.22
[45]	0.06	0.700	Pinewood chips	Air	P _{atm}	1053-1103	22
[28]	0.300	8	Wood	Air/Steam	NA	NA	9
[31]	NA	NA	Wheat straw	Air/Steam	P _{atm}	970	20.96
[31]	NA	NA	Wheat straw	Air/Steam	P _{atm}	933	18.7
[31]	NA	NA	Wheat straw	Air/Steam	P _{atm}	882	21.1
[31]	NA	NA	Wheat straw	Air/Steam	P _{atm}	1039	18.27
[31]	NA	NA	Wheat straw	Air/Steam	Patm	1013	18.46

Table 2.2 (Contiued)

[31]	NA	NA	Wheat straw	Air/Steam	P_{atm}	1089	20.80
[31]	NA	NA	Wheat straw	Air/Steam	P_{atm}	1065	19.06
[31]	NA	NA	Wheat straw	Air/Steam	P_{atm}	992	21.07
[46]	0.070	0.500	Pine and eucalyptus wastes	Steam	P_{atm}	1153	41
[47]	0.089	NA	Sawdust	Steam	P_{atm}	1073	57.4
[48]	0.150	NA	Pine sawdust and wood	Steam	P_{atm}	1023	40
[49]	0.700	0.500	Sawdust wood	steam	P_{atm}	1023	62.5
[50]	NA	NA	Biomass	Steam	P_{atm}	1050	59
[51]	0.04	0.75	Cynara cardunculus L	Steam	$0.53 P_{atm}^a$	923	52.1
[51]	0.04	0.75	Cynara cardunculus L	Steam	$0.53 P_{atm}^a$	973	58.7
[51]	0.04	0.75	Cynara cardunculus L	Steam	$0.53 P_{atm}^a$	1023	60.0
[51]	0.04	0.75	Cynara cardunculus L	Steam	$0.53 P_{atm}^a$	1073	60.4
[27]	0.060	NA	Crushed almond shells	Steam	NA	1093	47.5
[46]	0.070	0.500	Pine	Steam	P_{atm}	1073	34.4
[46]	0.070	0.500	Helm oak	Steam	P_{atm}	1073	42.13

NA: not available.

a: water partial pressure is used

The kinetic approach uses empirical relations that make results from the developed approach accurate and applicable in the range of the applied relation. On the other hand, an equilibrium approach is ideal and gives the predicted hydrogen at gasifier exit.

Finding a way that combines the features available in different approaches could lead to having a flexible approach that can drive the parametric study. The approach is necessary for optimization and scale up of hydrogen production and can predict the effect of different parameters on hydrogen production from biomass. It is an important step forward in the understanding of the efficient hydrogen production from biomass gasification. Parameters like steam-biomass ratio and gasification temperature can be varied to address the hydrogen product from the steam biomass gasification process.

2.2 Review on Equilibrium Approaches

Li et al. [52] developed a non-stoichiometric equilibrium model to predict the performance of a CFB coal gasifier. The model was flexible to simulate gasification of different materials. The results show that high pressure serves to concentrate the gas phase, accelerates reaction and reduces the reactor volume that is required to achieve equilibrium. It has a lesser effect on the chemical equilibrium. Also, the carbon conversion in a gasifier depends on thermodynamic chemical kinetics, hydrodynamics, heat and mass transfer, residence time and particle size distribution. Li et al. [8] developed a non-stoichiometric equilibrium model to simulate gasification of sawdust in a CFB gasifier. This was based on the minimization of Gibbs free energy to predict the performance of the gasifier in a temperature range of 700-850°C. The model results were deviated from the experimental results. This gave them the evidence to modify the equilibrium model to a model so that the results fit well with the real condition.

Altafini et al. [53] developed an equilibrium model to simulate a wood waste gasification. The model shows some tendencies on the working parameter even at a relatively high temperature. Ruggiero et al. [35] described a simple equilibrium model which considered chemical species encountered by biomass gasifiers. They found the data which included gas composition, gas lower heating value; gross efficiency of the gasifier and exergy efficiency were quite different from the experimental data. They

attributed that to perfect gas assumption which described the behaviour of reactants and products. Zainal et al. [54] used the equilibrium modeling to predict the gasification process in a down draft gasifier. The model investigated effects of the wood moisture content and temperature in the gasification zone on the calorific value of the producer gas. They found that the predicted values were similar to the experimental values.

Natarajan et al. [55] presented an overview on gasification of rice husk in a fluidized bed reactor. They reported that the tar content of the produced gas strongly depends on the gasifier operating temperature and they recommended using a deeper bed and or catalytic cracking for further reduction of tar. They found concentrations of H₂ and CO increase and the concentrations of CO₂, N₂ and CH₄ decrease with a temperature increase for a given equivalence ratio.

Turn et al. [18] performed an experimental study by using a bench-scale fluidized bed gasifier. The parametric study investigated the effects of gasifier temperature, equivalence ratio, and steam-biomass ratio on the hydrogen yield. They found that the hydrogen yield potential was more sensitive to equivalence ratio and the highest hydrogen yield was 128 g H₂/kg of dry-ash free sawdust when the gasifier temperature, steam-biomass ratio and equivalence ratio are 850, 1.7 and zero, respectively.

Lv et al. [56] conducted air-steam biomass gasification experimental studies. The experiments were performed in a fluidized bed reactor on pine dust with a size of 0.2–0.3 mm with an emphasis on hydrogen production. They found that the highest hydrogen yield was at a gasification temperature of 900 °C, equivalence ratio of 0.22 and steam-biomass ratio of 2.7.

2.3 Review on Hybrid Systems

Hybrid systems were developed to perform co-duties or multi-duties instead of single-duty systems. This will be considered with more attention as the developed systems successfully show high potential from assessment studies and as hybrid systems effectively show interaction between each other, enabling one system to utilize products from the other system.

The hybrid systems can differ from each other by including different numbers of components or by the way of interaction between them which enables the system to

perform different duties. The existence of these devices in the same system encourages the utilization of products from one system by the other which could improve system efficiency and lower hydrogen production costs.

In general, efficient power generation and improvement in overall performance are the two main aims that are expected when combining different energy systems. It is possible to increase power production with a biomass based integrated gasification combined cycle [57], or solid oxide fuel cells (SOFC) [58]. Research and development efforts continue to investigate different combinations like those which incorporate gasification and internal combustion engines, micro gas turbines or fuel cells to produce fuel, aiming towards efficient small scale systems [59].

SOFC can utilise the gasification derived hydrogen as a fuel where it has a higher inherent tolerance regarding derived gas contaminants. Furthermore, superheated steam leaving the SOFC's anode after combustion of hydrogen can be fed directly to external water gas shift and steam reforming reactions. Also, the excess depleted air and fuel can be combusted and the released energy in the burner can be partially or totally used to cover heat demands of the downstream processes. The reaction that takes place in external reforming SOFC is exothermic; therefore its existence in a system provides an opportunity to supply energy and thus reduce a deficiency in energy that happens internally in the hybrid system.

Steam gasification exhibits enhanced conversions to hydrogen, and it is considered to be superior to the conventional agents in gasification methods. Also, it is reported that the system that belongs to this combination can bypass the capital costs of the intermediate biogas reforming stage [60]. A gasifier and SOFC operate at the same level of temperature, making a conjugation of them in a hybrid system that could lead to appreciable efficiency. Cycle combinations have been recognized as suitable options for efficient power generation [61]. Also, the simultaneous production of power and useful heat from a single plant, i.e. cogeneration or combined heat and power plant, is a very useful option for improving the overall performance of the energy conversion system [62]. In addition, one could avoid the transportation cost of transporting fuel from production site to utilization site. The energy efficiency of biomass gasification could be enhanced if coupled with high efficiency power generation systems like SOFC. While a

biomass gasification combined cycle is a proven technology [63], a fully integrated biomass gasification fuel cell is yet to be established [64].

The most typical hybrid configuration suggested in the literature is a recuperated gas turbine process with a SOFC as the core unit of the system [65]. Baravsad [65] reported that electrical efficiency predictions for the system which combines the two units are in a range of 58–65%. Costamagna et al. [66] energetically investigated a small size hybrid system which combines a ~50 kWe gas turbine and a tubular SOFC.

Omosun et al. [61] explored the possibility of combining SOFC and biomass gasification for the generation of power and heat using the gPROMS modelling tool. They considered a hot gas cleanup process and a cold gas cleanup process in their system. They found that the electrical and the total overall efficiency are 23 and 60 % in the hot process and 21 and 34 % in the cold process. The difference between the two cases was attributed to the complete usefulness of the heat content in the later case. Although energy is a useful parameter in the system analyzed, it treats all forms of energy as equivalent and does not consider the quality of energy.

Zhang et al. [67] reviewed different concepts/strategies for a SOFC based integration systems. Among the systems were SOFC-combined heat and power (CHP) and SOFC-biomass gasification (BG) configurations. They reported that a SOFC-BG configuration operates at the same temperature level, therefore a SOFC is compatible with BG. They reported that a small size 1 kW class SOFC-CHP scheme can achieve an average efficiency of 44 %.

Ni et al. [68] developed a thermodynamic–electrochemical model to analyse a single generation plant to produce hydrogen by a solid oxide steam electrolyser. They found that the SOEC was the major source of exergy destruction and to achieve maximum energy/exergy efficiency, they must regulate the current density, the flow rate of steam or operate the cell at a high temperature.

Thus, research is needed in order to achieve even higher efficiency rates and a greater consensus of such systems, for small scale as well as large scale biomass hybrid system applications.

Balli et al [69] studied the exergetic performance assessment of a combined heat and power (CHP) system installed in Eskisehir, a city in Turkey. The system did not

include a gasifier or SOFC. They found from the performed exergy analysis along essential system components that the highest exergy consumption between the components occurs in the combustion chamber.

Many researchers mentioned that there was limited research performed concerning the exergetic performance of SOFC/GT hybrid systems, for example [65, 70, 71]. Akkaya et al [72] reported that the available studies did not sufficiently research the effects of design and operating parameters affecting final specification of the SOFC/Gas-Turbine as a combined heat and power (CHP) generation system in connection with exergy analysis. In order to improve this hybrid CHP system, it is essential to understand the parametric impacts on the exergetic efficiency and hence enhanced evaluation of the system. Specially, those parameters are related to different components that constitute the system.

Fryda et al. [73] investigated a combination of an air blown fluidised bed biomass gasifier with a high temperature SOFC and/or micro gas turbine in a cogeneration power and heat system of less than 1 MWe, which could operate at two pressure levels, near atmospheric and ~4 bar, respectively. They used Aspen Plus software to simulate the integrated system. They found that the efficiency of the pressurised SOFC operation is greatly improved and with power from a micro gas turbine achieves efficiencies $\geq 35\%$ when the current density value was $400 \text{ mA}\cdot\text{m}^{-2}$.

Akkaya et al. [72] analysed exergy performance by an exergetic-performance coefficient which would give the maximum total exergy output possible for a given entropy-generation rate. The analysis was conducted on a combination of a methane-fed SOFC and gas turbine in a combined heat-power system. They used lumped control volumes to thermodynamically study the system components.

Baravsad [65] analyzed a methane-fed internal reforming solid oxide fuel cell–gas turbine power generation system based on the first and second law of thermodynamics. They found that an increase in the fuel flow rate does not have a satisfactory effect on system performance. Also, they found cycle efficiency increased when fuel or air flow rates were decreased.

An assessment of the developed systems via thermodynamics laws possesses their ability to stand competitively against other systems in single or hybrid forms.

Chapter 3

MOTIVATION AND OBJECTIVES

3.1 Motivation

Hydrogen is expected to play an important role in the near future as an energy carrier. From a review of the literature, it can be seen that none of the studies have addressed a hydrogen production by a theoretical analysis of the gasifier nor addressed the hydrogen production performance through exergy efficiencies in addition to energy efficiencies. With this proposed study, it is intended that this gap will be filled. This study will provide a comprehensive thermodynamic analysis of two different innovative systems that produce and utilize hydrogen as a fuel. It is proposed to merge conventional steam biomass gasification (SBG) in two different hybrid systems. The first system combines SBG with a solid oxide fuel cell (SOFC) and the second system combines SBG with lumped SOFC and a solid oxide electrolyse cell (SOEC). It is expected that the study will contribute to an assessment of by-product steam biomass gasification hydrogen. The study shows the effects of key parameters on efficiencies (energy and exergy) and the cost of different components which constitute the proposed innovative systems. Furthermore, calculating destroyed exergy of different components will enable us to avoid running them under inefficient or higher exergy destruction situations.

3.2 Objectives

The depletion of fossil fuels and the emissions that accompany a conventional conversion technology create the need for alternative resources that can produce environmentally friendly products. Hydrogen plays a role where it can be derived from sustainable and environmentally friendly resources. Biomass is a neutral resource regarding carbon dioxide emissions and biomass-based hydrogen does not emit harmful gases when it is combusted. This study investigates hydrogen production from biomass and aims to achieve the following objectives:

- To define the proposed systems and their components to perform thermodynamic and exergoeconomic analyses.

- To perform comprehensive thermodynamic analyses using energy and exergy to assess the feasibility to produce and use the by-product steam biomass gasification hydrogen.
- To evaluate the produced hydrogen by merging the steam biomass gasification approach in System I, System II and System III.
- To identify components which have a higher exergy destruction for the different systems.
- To perform thermo-economic or exergo-economic analyses to investigate the cost formation on produced hydrogen.
- To perform optimization analyses of the systems in order to investigate the optimum operating conditions.

The changing of the key parameters that affect the hydrogen production from steam biomass gasification and the system performance will be studied in both conventional and hybrid modes of operation. These parameters include: gasification temperature, steam-biomass ratio, temperature of SOFC preheated air in System II, turbine inlet temperature in System II, turbine inlet temperature in System III, SOFC preheated air flows in System II, and burner preheated air flows in System II, burner preheated air flows in system III and SOFC-SOEC preheated air flows in system III.

In this thesis, a background on gasification is presented and the different approaches of modeling the gasification process are reviewed. This is followed by a description of the proposed systems. The different components of the systems are thermodynamically and exergoeconomically analyzed. Finally, results from the hydrogen production and its cost via conventional biomass steam gasification, as well as hybrid systems, are discussed and analyzed. The results are focused on the influence of the gasification temperature, fed biomass and injected steam on the hydrogen yield, and evaluation of energy efficiency and exergy efficiency of hydrogen and power production from the systems.

Chapter 4

BACKGROUND

4.1 Introduction

Hydrogen is an energy carrier, not an energy source, and is a clean-burning fuel. It is colorless, tasteless, odourless, the lightest element with a density of 0.0695 kg/m^3 at standard atmospheric conditions and can exist in different phases. It appears as the most challenging fuel for the future as [74]:

- It is derived from a variety of raw materials such as natural gas, coal, biomass, waste and water.
- It can be transported over large distances through pipelines or via tankers which are more efficient than electricity.
- It can be stored in different phases: a gaseous phase which is convenient for large scale storage, in a liquid phase which is convenient for air and space transportation or in the form of metal hydrides to be convenient for small scale storage requirements.
- It can be efficiently converted into other forms, for example, through catalytic combustion, electro-chemical conversion and hydriding, as well as through flame combustion.
- It can be used with fuel cell technology at the transport sector in cars, ships, etc.
- It can be fed in combustion engines and yields low levels of pollutant emissions.

4.2 Hydrogen Production Methods

Hydrogen can be produced by different ways and using a wide range of technologies. The technologies use sources related to fossil fuel or alternative resources. The most widely applied technologies with potential to be commercially feasible technologies are discussed in the following sections.

4.2.1 Natural Gas Steam Reforming

Hydrogen can be produced from steam forming out of natural gas. It takes place in the presence of steam medium and it is an endothermic process. Hydrocarbon steam reforming turns hydrocarbons into their compounds. Natural gas, coal, petroleum and biofuels undergo this method and the process can be endothermic or exothermic through partial oxidation.

4.2.2 Water Electrolysis

This method uses electrochemical technology to produce hydrogen from water. In this technology, electrical energy is used to perform the chemical reactions. Three major technologies are currently under consideration for electrolytic hydrogen production: alkaline; polymer membrane and ceramic oxide electrolyte; and water electrolysis, one of the most important industrial processes for hydrogen production [75]. Konstantopoulou [76] reported that at present, water electrolysis is the most expensive process of producing hydrogen but cost declines are expected over the course of the next decade as the technology improves and more efficient and easily scalable electrolyzers are manufactured at lower costs.

Biochemical hydrogen is an advanced method used for the biomass-based hydrogen production. Bio-hydrogen production technology includes: photolytic hydrogen production from water by green algae or cyanobacteria, dark-fermentative hydrogen production during the acidogenic phase of anaerobic digestion of organic material, photo-fermentative processes, two stages dark/fermentative, and hydrogen production by water-gas shift reaction [77]. The feeds for biological hydrogen are water for photolysis processes and biomass for fermentative processes [78]. Both technologies were not considered mature enough [75].

Hydrogen via supercritical water extraction and liquefaction are classified under the thermo-chemical process. Water at the supercritical condition method (properties > critical point properties) is used to convert biomass into gases [79]. Liquefaction is the low temperature high pressure thermo-chemical process in the presence of a catalyst [80]. Complexity and higher costs of liquefaction makes pyrolysis more interesting [81].

4.2.3 Biomass Pyrolysis

The biomass pyrolysis is a thermo-chemical conversion process that is used to produce based biomass hydrogen. Pyrolysis is similar to gasification; however, pyrolysis takes place in the absence of the gasification agent at a lower temperature. The three main components left after the pyrolysis process are bio-oil, char and gas. To maximize the gas yield from the pyrolysis process, low heating rate, long residence time and high temperature are preferred [80]. The biomass pyrolysis process produces less hydrogen and the amount of hydrogen can be increased by three methods: steam reforming of the obtained pyrolysis liquid, use tar removal for tar content of the the pyrolysis gas and carried the pyrolysis process around 700 °C and in the third method catalyst will be incorporated to the products in the same reactor at temperature below 750 °C [79].

4.2.4 Gasification

Gasification is a technology that deals with the conversion of a carbon-rich solid fuel into a gaseous fuel in a gasifier. The produced gas has a calorific value of 3-5 MJ/m³ [54] in the case of air blown processes, and 10-18 MJ/m³ in the case of oxygen and steam-blown processes [82]. The gasification of biomass consists of processes including pre-heating, drying, pyrolysis, char gasification, char oxidation and ash formation. The cleaned gas can be used for heat and power applications. Biagini et al. [83] reported that biomass fuels consist of cellulose, lignin and hemi-cellulose. Cellulose has a molecular structure with various molecular weights. The molecular structure of hemi-cellulose is not defined and its molecular weight is lower than that of cellulose. This leads to it having lower thermal stability and higher reactivity [24]. Lignin has a molecular structure similar to low rank coal and it is difficult to extract it from biomass without a chemical modification.

The gasification reaction is the result of chemical reactions between carbon in the char and steam, carbon dioxide and hydrogen in the reactor, as well as chemical reactions between the evolved gases. The gasification process, in principle, involves a wet basis, carbon, carbon monoxide, carbon dioxide, hydrogen, water and methane from the following reactions:

Combustion reactions:



Boudouard reaction:



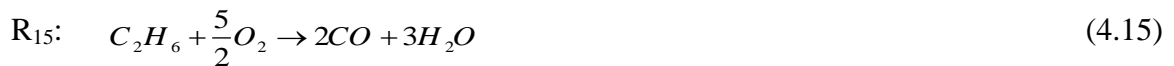
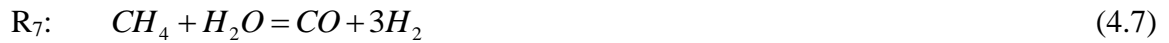
Water gas reaction:



Methanation reaction:



In addition, there are reactions implicit in the above reactions which influence the conversion products like:



In biomass gasification at high temperatures, the amount of heavy hydrocarbons is diminished (R₁₂-R₁₆) and therefore one can expect that the reactions involving the high hydrocarbons could be ignored in the modeling of an approach of the gasification process. Also, biomass in a range of temperature >1000 °C produces insignificant amount

of tar [33].

4.2.4.1 Coal Gasification

Gasification is a technology of hydrogen production that can be self-heated or externally heated. It uses air, steam and oxygen or a mixture of them as agents for an oxygen source and produces syngas which contains hydrogen. Economic studies show that biomass gasification plants can be as economical as conventional coal fired plants [84]. Gasification of coal is the oldest method for hydrogen production, and in the presence of oxygen at 900 °C. It produces synthetic gas which contains large hydrogen concentration.

4.2.4.2 Biomass Gasification

Biomass gasification is a thermo-chemical method that can be used to produce hydrogen based biomass. Gasification is a thermo-chemical process where the organic compounds of biomass are broken down at high temperatures in an oxygen-deficient environment. Biomass gasification is the most likely near-term method to produce hydrogen from biomass [85]. Hydrogen production from biomass gasification exhibits an economy of scale in that larger facilities have lower costs per unit of capacity [85].

The gasification process can be performed with or without a catalyst depending on gasifier downstream use, and can take place in a fixed bed or fluidized bed gasifier and under atmospheric or super atmospheric pressure. For cost effective hydrogen production using this technology, large fuel resources are needed which requires development of smaller, efficiently distributed gasification plants [78]. Biomass gasification-based hydrogen production is under the scope of this study. The gasification technology is studied in more detail in the following sections.

4.2.4.2.1 Char

Char is combustible matter that is left after pyrolysis of the particle. Char gasification is the slowest reaction in the gasification process and governs the overall conversion rate. Williams et al. [86] reported that there are several models describing the Boudouard and water gas reactions, for example, [87] which suggests a two-step process

model for the Boudouard reaction, wherein the first step CO_2 dissociates at a carbon free active site (C_{fas}), releasing carbon monoxide and forming an oxidized surface complex, $C(O)$. In the second step, the carbon-oxygen complex produces a molecule of CO and a new free active site.

Step 1



Step 2



Also, the model for the steam reaction is a two-step reaction wherein the first step H_2O dissociates at a carbon-free active site releasing hydrogen and forming an oxidized surface complex. In the second step, the carbon-oxygen complex produces a molecule of CO and a new free active site.

Step 1



Step 2



Some other models include the possibility of hydrogen inhibition by the inclusion of one of the following steps:



or



The gasification process results in a continuous change in char composition and according to that its reactivity continuously varies. Cetin et al. [96] investigated kinetics of chars from different biomasses in the temperature range of 800-900°C. They used a quartz wall matrix technique to simulate the gasification of char particles in the atmospheric CFB reactor. They found that the total pressure has little effect on reactivity for temperature and pressure up to 900°C and 20 bar respectively.

The temperature dependency of the mass-related reaction rate constant can be expressed in Arrhenius form as:

$$k = A \exp\left(-\frac{E}{RT}\right) \quad (4.23)$$

where A is a pre-exponential constant and E is the activation energy for the reaction.

Table 4.1 Kinetic coefficient (R_1, R_2, \dots, R_{16} as defined above)

Reference	Fuel	Reaction	Equation	Comment
[88]	Biomass	R_2	$k = 4.8 \times 10^8 \exp\left(\frac{-16000}{RT_{gas}}\right)$	$s^{-1} \left(\frac{m^3}{kmol}\right)^{0.8}$
[89]	Biomass	R_3	$k = 4.9 \times 10^{10} \exp\left(\frac{-21500}{RT_{gas}}\right)$	
[90]	Biomass	R_8	$k = 0.03 \exp\left(\frac{-7249}{T_{gas}}\right)$	Dependent
[91, 92]	Biomass	R_7	$k_e = 3.1005 \exp\left(\frac{-15000}{T_{gas}}\right)$	kmol/(m ³ s)
[93, 94]	Biomass	R_8	$k_e = 0.0027 \exp\left(\frac{-3960}{T_{gas}}\right)$	$T_b > 1123K$
	Biomass	R_8	$k = 10^6 \exp\left(\frac{-6370}{T_{gas}}\right)$	$T_b < 1123K$
[40]	NA	R_8	$k_e = 0.0265 \exp\left(\frac{39585}{T_{gas}}\right)$	$\frac{kmol^{-1}}{ms}$
			$k = 2780 \exp\left(\frac{-1510.7}{RT_{gas}}\right)$	NA
[95]	NA	R_1	$k = 0.667 \exp\left(\frac{-16000}{R_{gas} T_{gas}}\right)$	s^{-1}
		R_2	$k = 13 \times 10^{13} \exp\left(\frac{-30000}{R_{gas} T_{gas}}\right)$	s^{-1}
		wood → Char	$k = 7.38 \times 10^5 \exp\left(\frac{106.5}{RT}\right)$	s^{-1}
[33]	Biomass	R_9	$k = 7 \times 10^{11} \exp\left(\frac{-30200}{T_{gas}}\right)$	NA

Kinetic coefficients used by several references for gasification of biomass are given in Table 4.1. The assumption made by Fryda et al. [97] to treat un-reacted char will be applied, such that un-reacted char is 5 % of the biomass carbon content or;

$$e = 0.05\alpha l \quad (4.24)$$

where α is the quantity of used biomass and l is the biomass carbon content.

4.2.4.1.2 Tar

Tar is an undesirable product from biomass gasification due to the various problems of fouling and slugging in the process equipment. There are hundreds of species in the tar sample but in order to simplify the analysis, all the species are treated as a single lump [98]. Currently, three methods are available to minimize tar formation [99]: (i) proper design of a gasifier, (ii) proper control and operation; and (iii) additives/catalysts. Tar is modeled as a benzene compound [93, 100] with the chemical formula C_6H_6 and its yield is assumed to obey the empirical relation developed by [101] as follows:

$$Tar = 35.98 \exp(-0.0029T) \quad (4.25)$$

where T is used as a gasifier temperature in K . Its content in the flow gas has to be estimated with a good model so the product gas becomes more useful.

4.2.5 Flow Through The Gasifier

The cases of plug flow and complete mixing or continuously stirred tank concepts were originally developed to account for the behaviour of reactors [102]. The plug flow gasifier is characterized by the following properties:

1. There is a continuous flow through the reactor.
2. There is no radial gradient.
3. There is no axial mixing.
4. The gasifier operates under steady state condition.

For first order kinetics, the fractional conversion of a reactant after time t is:

$$\frac{c}{c_o} = \exp(-kt) \quad (4.26)$$

The continuously stirred tank gasifier has the following characteristics:

1. There is a continuous flow through the gasifier.
2. The reactor contents are ideally mixed; therefore the inside of the reactor has the same conditions.

The conversion of a component after an average residence time t in the reactor is given by:

$$\frac{c}{c_o} = \frac{1}{1+kt} \quad (4.27)$$

where c_o is the initial concentration of a reactant in kmol m^{-3} , c is the concentration of a reactant in kmol m^{-3} after residence time t in s and k is generalized first rate coefficient in s^{-1} .

4.2.6 Approaches of Gasification Modelling

The modeling is a useful tool for design and optimization of a gasifier. Kinetic, equilibrium and neural networks are the developed models for gasification technology. Modeling of a gasifier riser varies from homogeneous; gas-gas, to heterogeneous; gas-solid modeling, from single to multiple region modeling, and from zero to three dimensional modeling [103].

Many models of biomass gasification used relations similar to that used in coal gasification, but thermo-chemical processing of biomass has some important differences. Corella et al. [33] mentioned three of them: (1) biomass is more reactive than coal, it pyrolyses very quickly and its ash content is usually very low. (2) Gasification of biomass below 1000°C always produces an important amount of tar. In addition to that, coal is predominantly ormatic material whereas the ormatic component of biomass is a relatively minor constituent and biomass has a high oxygen content which decomposes during the pyrolysis process to produce oxygenated gases like CO, CO₂, and H₂O [24]. Also, biomass has low nitrogen and sulfur content which has a very low tendency to form SO_x and NO_x components.

4.2.6.1 Kinetic Approach

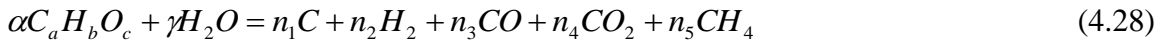
This type of modeling involves parameters such as reaction rate and residence time of particles, and it is very complex to execute computationally. Under certain

operating conditions and gasifier configuration, the kinetic model can predict the profiles of gas composition and temperature inside the gasifier and gasifier performance. The model combines hydrodynamics of a fluidized bed and kinetic schemes of reactions inside the gasifier. At low reaction temperatures, the reaction rate is smaller than that at higher reaction temperatures while the residence time is higher, therefore the kinetic theory is more suitable to use in modeling [53].

Tsui et al. [38] reported that Wen's kinetic model describes the gasification rate of char as a function of the gasifier temperature and the concentration of steam, carbon monoxide and hydrogen. Fiaschi et al. [104] modeled the kinetics of biomass gasification in a bubbling fluidized bed. Bed hydrodynamics treated as one dimension two-phase in a piston motion reactor. Vertically the riser was divided into compartments and the freeboard area was considered chemically inert. The temperature was evaluated from energy balance around each compartment. The model predicted temperature and gas composition along the bed height.

4.2.6.1.1 Reaction Kinetics

In kinetic models, a simultaneous solution of mass and heat balances with kinetics and hydrodynamic aspects are carried out to obtain gas yield, tar and char contents and others at different operating conditions. Assuming low sulfur and nitrogen content fuel, and CH_4 is the only hydrocarbon accounted for in the product gas, the reaction of a quantity of virgin biomass, α , with an amount of steam, γ , steam gasification can be represented by the following reaction equation:



where $C_a H_b O_c$ is the chemical representation of biomass and a , b and c are molar numbers determined from the ultimate analysis of biomass. The stoichiometric coefficients are calculated by mass balance of the species:

$$C: \quad n_1 + n_3 + n_4 + n_5 = a\alpha \quad (4.29)$$

$$H: \quad 2n_2 + 4n_5 = 2\gamma + b\alpha \quad (4.30)$$

$$O: \quad n_3 + 2n_4 = c\alpha + \gamma \quad (4.31)$$

Wang et al. [105] suggested using additional relations to solve the above equations in a way to solve their kinetic model in air-steam biomass gasification. They assumed a relation combines the initial amount of CO_2 , H_2O and moisture. This relation is also used later in the model developed by Sharma [106]. Wang et al. [105] derived equations to govern the gasification reactions which relate reaction rates and number of moles. The rate constant, k_{ai} of a reaction i is given by Arrhenius expression as:

$$k_{ai} = A_i \exp\left(-\frac{E_{ai}}{RT}\right) \quad (4.32)$$

where A_i , is pre-exponential constant, R is the universal gas constant, E_{ai} is the activation energy and T is the absolute temperature. Similar reactions in addition to steam reforming of methane reaction were used by Bilodeau et al. [24] to simulate biomass gasification in a fluidized bed. They considered only the emulsion phase in freeboard and it was treated in a similar way as that in the bed. The same gasification reactions were considered by Fiaschi et al. [104] in modeling a two-phase one-dimensional gasification process. They suggested that total mole concentration of specie i , c_i which has fraction, c_{ib} in the bubble phase. Both have the same concentration at the distributor plate where at a higher level the following relation applies:

$$\varepsilon_b c_i = c_{ib} \quad (4.33)$$

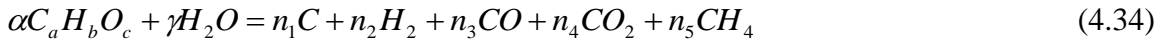
where ε_b is bubble phase fraction.

4.2.6.2 Equilibrium Approach

From a thermodynamic point of view, at equilibrium state, the system is at a stable condition. The reaction is considered to be zero-dimensional and there are no changes with time because all forward and reverse reactions have reached chemical equilibrium [8]. Altafini et al. [53] concluded that the equilibrium models do not represent the reactions that occur at high temperatures very well, but they can show useful tendencies on variations of the working parameters. Ginsburg et al. [107] found evolved nitrogen and sulphur from the reactor that gasifies biomass are negligible, and this was in agreement with that found by Schusteret al. [82]. Most of the equilibrium models considered major product species like H_2 , CO , CO_2 , and CH_4 . Two approaches have developed for equilibrium modeling: stoichiometric and non-stoichiometric.

4.2.6.2.1 Stoichiometric Equilibrium Approach

In the stoichiometric approach, reaction mechanism incorporates chemical reactions and involved species. It usually starts by selecting from all species containing C, H and O only those species which are in the greatest amounts i.e. those that have the lowest value of the free energy of formation. The reaction of a quantity of biomass, α , with an amount of steam, γ (either injected to the gasifier or as fuel content) can be represented as:



where $C_a H_b O_c$ is the chemical representation of biomass and a , b and c are C, H, and O mole determined from the ultimate analysis of biomass. If biomass is considered to have low nitrogen and sulfur content, the atom balance of carbon, hydrogen and oxygen gives:

$$\text{C:} \quad n_1 + n_3 + n_4 + n_5 = a\alpha \quad (4.35)$$

$$\text{H:} \quad 2n_2 + 4n_5 = 2\gamma + b\alpha \quad (4.36)$$

$$\text{O:} \quad n_3 + 2n_4 = a\alpha + \gamma \quad (4.37)$$

During the gasification process the side reactions (R4-R7) take place. The water gas shift reaction can be considered as a result of the subtraction of the steam gasification and Boudouard reactions. For example if R_4 , R_5 and R_6 were considered, equilibrium constants are given by:

$$K_{e1} = \frac{X_{CO}^2 P}{X_{CO_2}} \quad (4.38)$$

$$K_{e2} = \frac{X_{CO} X_{H_2} P}{X_{H_2O}} \quad (4.39)$$

$$K_{e3} = \frac{X_{CH_4}}{X_{H_2}^2 P} \quad (4.40)$$

Also, the equilibrium constant is given by:

$$K_e = \exp\left(-\frac{\Delta G}{RT}\right) \quad (4.41)$$

where X_i is the mole fraction for species i , P is the gasifier pressure, ΔG is the standard

Gibbs function of reaction, R is the universal gas constant and T is the gasification temperature. These equations are solved simultaneously with the atom balance equations.

4.2.6.2.2 Non-Stoichiometric Equilibrium Approach

In the non-stoichiometric formulation approach, no particular reaction mechanism is involved to solve the model and the method based on minimizing the total Gibbs free energy of a system.

$$\Delta G = 0 \tag{4.42}$$

It uses scalar parameters which reduce to an optimization problem where specific Gibbs energy must be expressed as a function of species moles [22]. Then moles of species which minimize specific Gibbs function must be obtained. The approach does not rely on the identification of any stoichiometric equations [50]. It requires composition of biomass and reactant gas stream.

Jarunghammachote et al. [108] pointed out to minimize the Gibbs free energy, where constrained optimization methods are generally used, requires an understanding of complex mathematical theories. The system consists of a set of equations for all chemical species that are involved in the analysis including the equation of atomic balance for each element, the equation of the total number of moles, the equations of variation of the standard Gibbs free energy of formation of the species and the energy balance around the gasifier.

4.2.6.3 Neural Network Approach

Some models use differential equations and to solve them analytically by programming requires time and power to achieve accurate predictions. In addition, commercial system modeling programs are time-consuming and also their cost is high compared to small research establishments [109]. Therefore, there is need of an alternative approach. An artificial neural network (ANN) may be used as an alternative approach of modeling. ANN was developed to predict fluidization and gasification parameters. It determines how a network transforms its input by computation operation into output. ANNs offer an alternative way to model the gasification process, but they can

process only numeric values. Once they are trained, they can perform predictions and generalization at high speed using multiple hidden layer architecture [109].

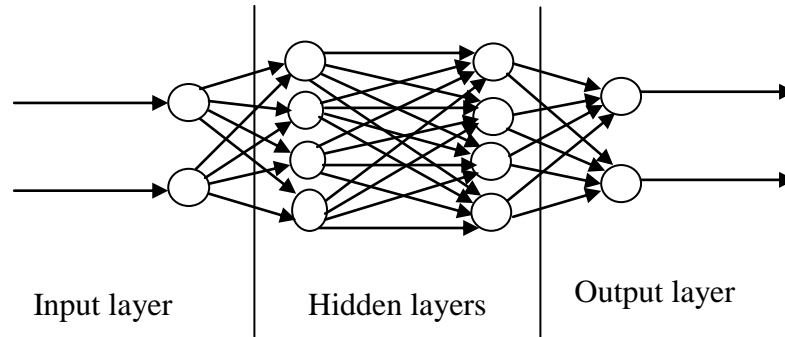


Figure 4.1 Schematic diagram of a multilayer feed forward neural network.

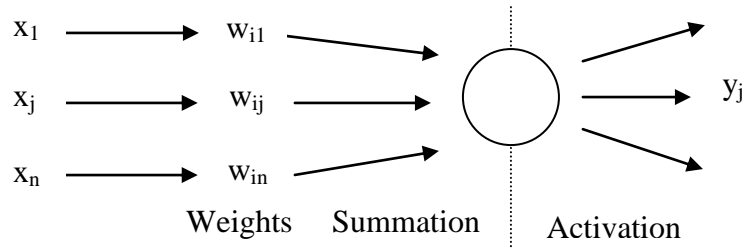


Figure 4.2 Processing information in a neural network.

The ANN architecture is composed of layers of neurons to receive the input(s) and process them to deliver output(s), see Figure 4.1. It refers to the arrangement of neurons into layers and the connection of patterns between layers, activation functions and learning methods. The relationship between the input and the output is learned by studying previously recorded data from experiments and models. Kalogirou [109] suggested the following empirical formula to estimate the number of hidden neurons:

$$\text{Number of hidden neurons} = \frac{1}{2}(\text{inputs} + \text{outputs}) + \sqrt{\text{number of training patterns}} \quad (4.43)$$

The inputs layer has two values associated with them: inputs and weight values. Weights are used to transfer data from layer to layer. Kalogirou et al. [110] suggested the equation below to find the value of each neuron in each layer. Function, y is a result of non linear transfer function, x with argument weighted sum overall the nodes in the previous layer

plus a constant term, b referred as the bias:

$$y_i = \sum_j w_{ij} x_{pj} + b \quad (4.44)$$

where j refers to summation of all nodes in the previous layer, i refers to the node position in the present layer and w_{ij} are weights to connect hidden layers with external layers. The information is processed through nodes where it receives weighted activation of other nodes through its connections and activates them by specific weight (Figure 4.2).

4.2.6.3.1 Network Training

Training is the process which modifies the connection weights in some orderly fashion using learning methods [111]. Kalogirou et al. [110] recommended that to train a network begins with a set of training data that have input and output targets, then adjust weights until the sum of difference between neural network output and the corresponding target is minimum. Once the training process satisfies the required tolerance, the network holds the weights constant and can use it to predict output. After training, the weights contain meaningful information whereas before training they have no meaning.

4.2.6.3.2 Back Propagation

Back propagation algorithm is used to perform the learning of a network. It is adjusted by the iteration method to reduce the error between the actual and the desired output [110]. A neural network is used to predict inside or outside trained data range. More accurate results are expected in the trained data range, although poor results can occur from data that differs from that which is found in the trained data. That sometimes happens because only a small number of calibration data are available to evaluate many constants of model [112].

4.2.7 Strategies to Solve the Different Approaches

4.2.7.1 Kinetic Approach

- 1- Use ultimate analysis and proximate analysis of biomass to calculate moles of produced gases like CO, CO₂, H₂, CH₄ and others.
- 2- Find the hydrodynamic parameters using hydrodynamic relations of a fluidized bed.

- 3- Find the excess gas generation and composition of gases in the emulsion phase.
- 4- Use mass balance of the bubble phase to estimate the changing of bubble properties at a specified height for a certain carbon conversion.
- 5- Use mass balance of the emulsion phase to calculate the generated volume and the composition of gases. Check the assumed carbon conversion by calculating the product gas and the fuel feed rate. If it does not satisfy the convergence criteria, repeat steps 4-6.
- 6- Once the converging criterion is satisfied, the produced hydrogen is determined.

4.2.7.2 Equilibrium Approach

- 1- Write the overall reaction of biomass with used gasification medium.
- 2- Taking atom balances based on elements evolved in the reaction like C, O₂, H₂, etc.
- 3- Write the equilibrium relations for gasification reactions like steam gasification, Boudouard, and methanation reactions.
- 4- Solve the obtained system of algebraic equations simultaneously in order to determine the product hydrogen.

4.2.7.3 Neural Network Approach

After structuring the neural network, information starts to proceed from input layer to output layer according to the concepts that were mentioned above. The algorithm showing the steps that can follow to solve the neural network is given in Figure 4.3.

Experimental data under the same operating conditions are necessary to use ANN in hydrogen production prediction. The kinetic model predicts composition at different heights along the gasifier while the equilibrium model predicts maximum product yield from the gasifier when it is unsafe to reproduce experimentally or in commercial operation [8].

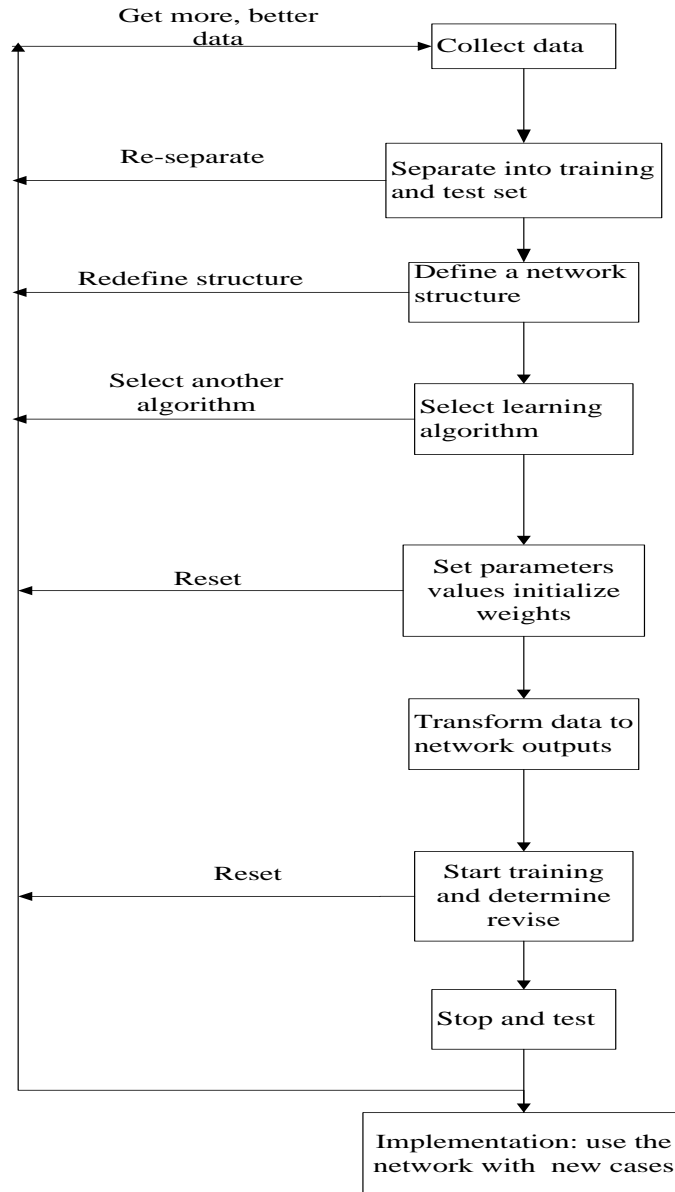


Figure 4.3 Algorithm for developing a neural network solution.

Chapter 5

SYSTEMS DESCRIPTION

5.1 System I

The study aims to produce hydrogen from steam biomass gasification with low emissions of air pollutants, particulates and hydrocarbons as well as no greenhouse gas emissions. Gasification technology and hydrogen from renewable sources are expected to play a significant role in the reduction of CO₂ emission and the realization of a hydrogen energy society [113]. Hydrogen is produced from a thermo-chemical process by processing biomass in a high temperature gasifier first to produce syngas mainly composed of H₂, CO, CO₂ and CH₄. These gases are further processed in the steam reforming and water gas shift reactors to increase the hydrogen yield. The hydrogen is separated at the desired degree of purity using devices like pressure adsorption system (PAS).

This system constitutes different components. The main components are: gasifier, compressor and heat exchangers. The analysis conducted on the system components is used to investigate how competitive the system is to produce hydrogen. The analysis is performed by applying mass conservation, energy conservation, exergy balance and cost balance equations on the system components and under the following general assumptions: steady state with negligible change in kinetic and potential energies and the gases obey the ideal gas relations. The specific cost of water from the main supply (state 7 and state 28 in Figure 5.1) is negligible. The cost of steam everywhere in the system is assumed the same as electricity cost.

The products are allowed to pass through a separator unit to separate char and tar from the products. Methane is gasified to carbon monoxide and hydrogen in the reforming reactor. The hot derived syngas coming from the gasifier and from the steam reforming reactor is then cooled. Next, this carbon monoxide, and that which is in the gas product, are completely oxidised into carbon dioxide and hydrogen in the water gas shift reactor. The hot derived gas coming from the water gas shift reactor is then cooled. The relative cool gas is compressed in the compressor 5-6. In the next step, the gas is filtered to purify the hydrogen and the derived hydrogen is stored.

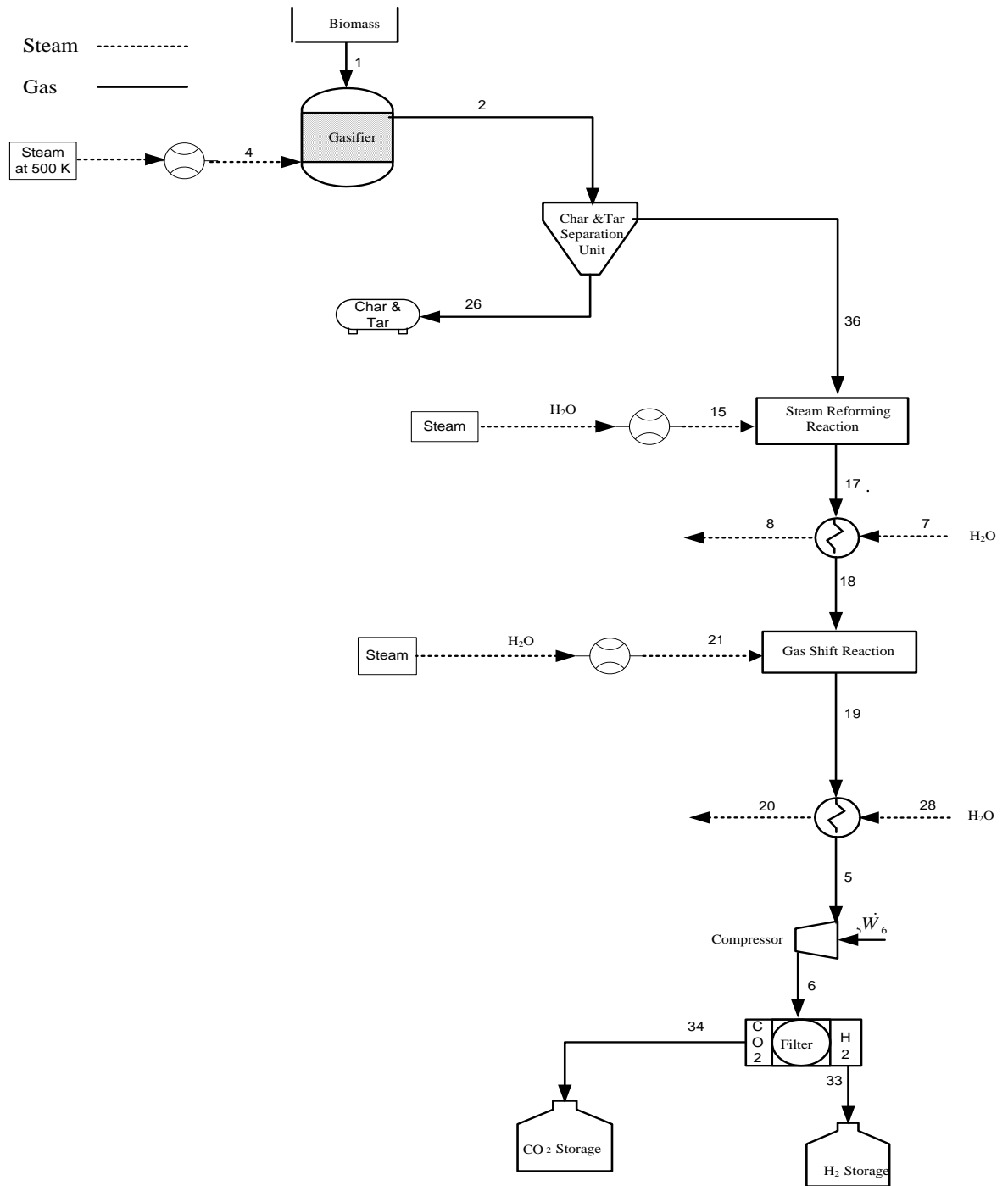


Figure 5.1 System I layout

The gasifier was analysed in the previous section while the steam reforming, water gas shift reactors, heat exchangers and compressor will be analyzed under System II in the next section. For more details regarding applying mass conservation, energy

conservation and exergy balance on processes taking place in these components, follow the same procedure. The same principles are applied for the same components, but properties could be different from system to system as will be seen in the next chapter.

5.2 System II

This system aims to utilize the derived biomass steam gasification hydrogen (primary hydrogen) in producing power and to increase hydrogen yield by further processing of the other gasification by products in steam reforming and water gas shift reactors. The main components of the system are: gasifier, solid oxide fuel cell, compressors, turbine and heat exchangers. Figure 5.2 shows the flow diagram of the system. The system is based on steam biomass gasification combined with a solid oxide fuel cell (SOFC) and gas turbine. The gasifier operates at the same operating conditions of System I. Also, the sawdust reacts in the gasifier with the steam under the same conditions.

The produced gas is separated from the tar and char in the separation unit. The tar and char are sent to the burner to burn, where more energy is extracted. The gas is cooled to approximately 498 K. The cooling process is modelled by heat exchanger 36-5-25-35. The relative cool gas is compressed in the compressor 5-6. The gas is filtered to have pure hydrogen and the rest of the product gas. The pure hydrogen is known as primary hydrogen and is fed to the SOFC; the remaining product gas is further processed in gasifier bottoming reactors. Similar to System I, methane is gasified to carbon monoxide and hydrogen in the reforming reactor. Then, the hot derived syngas coming from the reforming reactor is cooled. This carbon monoxide and that which is in the gas product are completely oxidized to carbon dioxide and hydrogen in the water gas shift reactor. In the next step, the gas is sent to a filtration process to purify the hydrogen and this hydrogen is known as secondary hydrogen, and at the end of the process, is stored.

The SOFC is an external reforming SOFC. It operates at 1000 K and a pressure of 1.2 bar. The hydrogen from the filter enters the anode side of the SOFC through state point 13. Most of the primary hydrogen is oxidized to water. In the fuel cell the hydrogen is converted into electricity and steam. The steam will be used in steam reforming and

water gas shift reactors, while the rest of the steam is available for external use. The unused hydrogen which leaves the anode and the cathode off gas are sent to the burner.

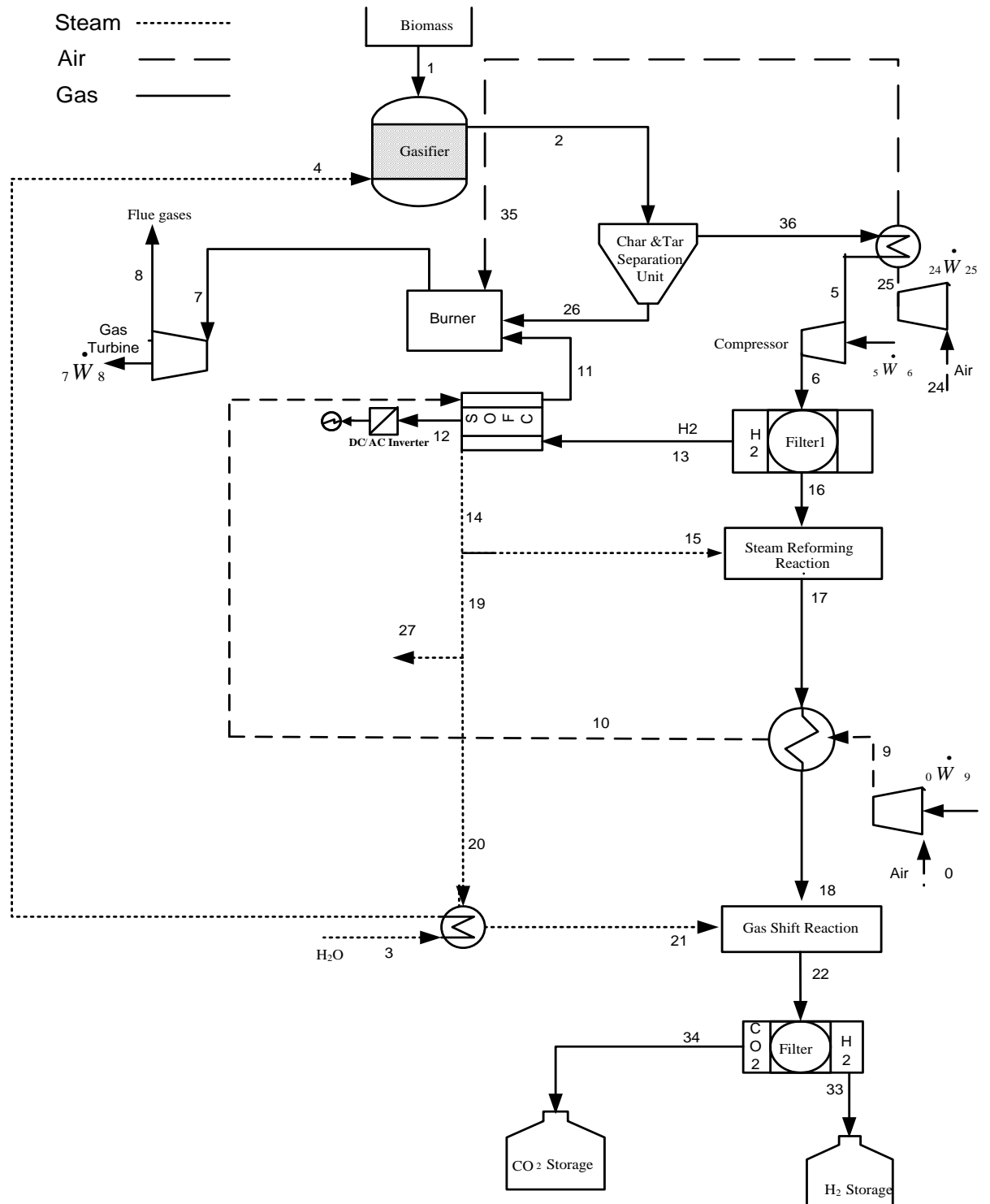


Figure 5.2 System II layout.

In the burner, the unused hydrogen, char and tar are burned. The excess air required in the burning process is compressed in compressor 24-25 and is preheated by passing through the heat exchanger 36-5-24-25. The flue gas results from the burning are expanded in the turbine. In this system, the residual heat from the flue gas is assumed to be further unutilized.

The gasifier is the common component between this system and the previous system (System I), however, the previous system is single duty for conventional steam biomass gasification while this system is a multi-duty system. To have a reasonable basis of comparison between the two systems, operating parameters that drive the parametric study are common for the two systems. To obey that, the analyses are conducted within a gasification temperature range of 1023-1423 K and a steam-biomass ratio of 0.8 kmol steam per kmol biomass.

5.2.1 Fuel Cell

The most common classification of fuel cells is by the type of electrolyte used in the cells, operating temperatures, and the mechanism by which charge is conducted in it [114]; the available fuel cell and its operating temperature range are:

- Direct Methanol Fuel Cell (DMFC), around a temperature of ~ 60 °C;
- Proton Exchange Membrane Fuel Cell (PEMFC), around a temperature of ~ 80 °C;
- Alkaline Fuel Cell (AFC), around a temperature of ~ 100 °C;
- Phosphoric Acid Fuel Cell (PAFC), around a temperature of ~ 200 °C;
- Molten Carbonate Fuel Cell (MCFC), around the temperature ~ 650 °C;
- Solid Oxide Fuel Cell (SOFC), in the temperature range ~ 650 -1000 °C.

The study of all types is out of scope of this study. However, detailed study for the solid oxide fuel cell (SOFC) becomes necessary as it is used in a hybrid system proposed in this study.

5.2.1.1 The Solid Oxide Fuel Cell (SOFC)

A fuel cell is a device that converts the energy released from a reaction of matter, in this case hydrogen, with oxygen directly into electricity without the intermediate step that is seen in conventional thermal cycles where the chemical energy converts first into

thermal and then into electrical. Because of inherent properties that tolerate well with contaminants from the gasification process and operating in a temperature range similar to that of biomass gasification, the solid oxide fuel cell is used in the proposed system. The depleted air at the SOFC temperature from the SOFC's cathode chamber fed directly to the burner (Figure 5.3).

The most common classification of fuel cells is by the type of electrolyte used in the cells, operating temperatures, and the mechanism by which a charge is conducted in it; SOFC operates in a temperature range of 650-1000 °C [114]. SOFC is the device that converts chemical energy available in matter to electric. The oxygen from air reacts with gasification hydrogen by product according to the following reactions and produces electrical and thermal energy and water:

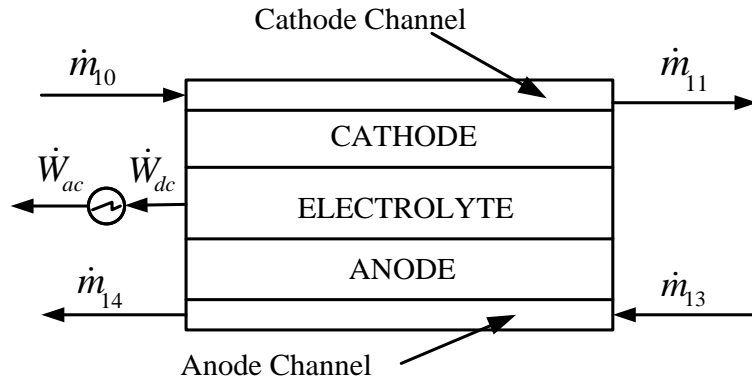


Figure 5.3 A Schematic diagram of SOFC



As a result of ionization of oxygen, the cathode will release two ions which will react with hydrogen and form water and liberated electrons, which are then conducted through the external circuit to close the complete circuit. The current in the circuit is utilized in gas oxidation.

5.3 System III

This system aims to utilize the derived biomass gasification residues in producing electrical power and increasing hydrogen yield by further processing of the other gas by-products in steam reforming and steam shift reactors. The main components of the system are: gasifier, solid oxide fuel cell (SOFC), solid oxide electrolyser cell (SOEC), compressors, turbine and heat exchangers. Figure 5.4 shows the layout of the system. The system is based on steam biomass gasification, lumped SOFC-SOEC and gas turbine.

The gasifier and the SOFC modules are the same as those in System II. The produced gas is separated from the tar and char in the separator unit and is then cooled to 398 K. The cooling process is modelled by the heat exchanger 36-16-25-35. Methane is gasified to carbon monoxide and hydrogen in the reforming reactor. In the next step, the gases are cooled to 311 K to preheat the air needed in the SOFC-SOEC lumped system. The gas is sent to the water gas shift reactor where all derived carbon monoxide is completely oxidized to carbon dioxide and hydrogen. In the last step, the gas is sent to a filtration process to purify the hydrogen and then stored.

The lumped SOFC-SOEC operates at a pressure of 1.2 bar and a temperature of 1000 K. The SOFC model is the same as the one in System II. The SOFC converts the hydrogen into electricity and steam. In this system, the SOEC totally decomposes by SOFC product steam, and the SOFC is totally consumed by SOEC product hydrogen.

The SOFC oxidizes derived SOEC hydrogen to water (steam) which decomposes to hydrogen and oxygen in the SOEC. At the cathode side of the SOFC, preheated and pressurized air enters the cathode of the SOFC (state point 10) and excess depleted air and nitrogen flows out from the cell at the cathode exit (state point 11). The SOFC utilizes by-product SOEC hydrogen to produce heat, steam and power. On the anode side from the SOFC cell, hydrogen is fed in at the anode inlet (state point 13) and steam and excess depleted hydrogen flow out at the anode exit (state point 14).

The SOEC utilizes by-product SOFC power to decompose by-product SOFC steam to hydrogen and oxygen. Steam is fed in at the cathode inlet (state 14) and steam and excess depleted hydrogen flow out from the cathode exit (state 13). The by-product SOEC oxygen flows out at the anode exit (state 12). The excess depleted gas and the

produced oxygen flow out through the lumped SOFC-SOEC system exit (state 27), and are then fed to the burner.

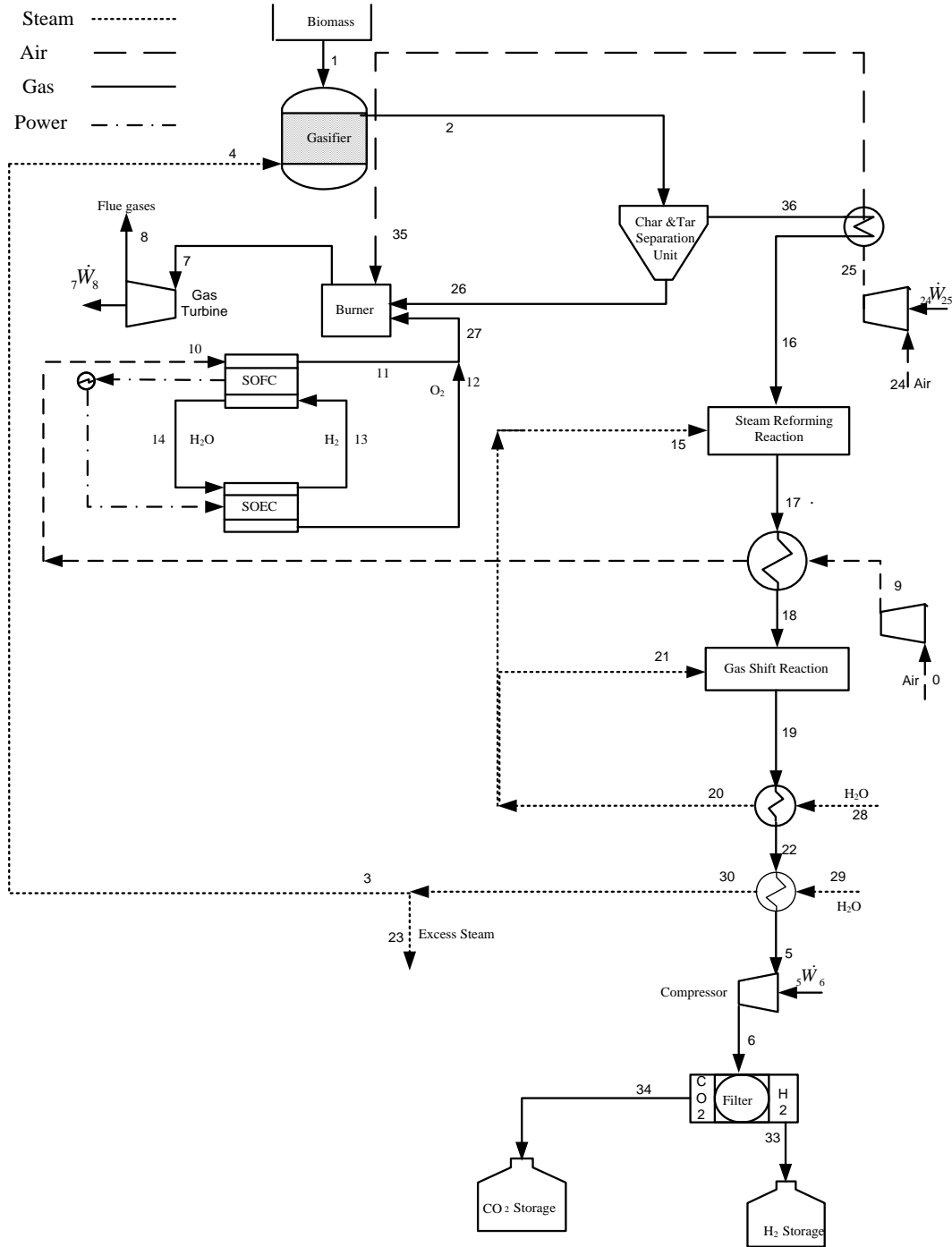


Figure 5.4 System III layout

The gasifier operating conditions are used to perform a parametric study by including those of the conventional gasification system (System I) and those of the hybrid System I (System II). The gasifier and the SOFC are the common components between this system and the previous system (System II).

5.3.1 Solid Oxide Electrolysis Cell (SOEC)

To analyze this system, it is necessary to introduce the SOEC. The SOEC involves separating the atoms of hydrogen and oxygen from water molecules by charging water with an electrical current in SOEC (Figure 5.5). This technology produces hydrogen and is free from greenhouse gas emissions. 5% of the world's hydrogen is produced via water electrolysis [115].

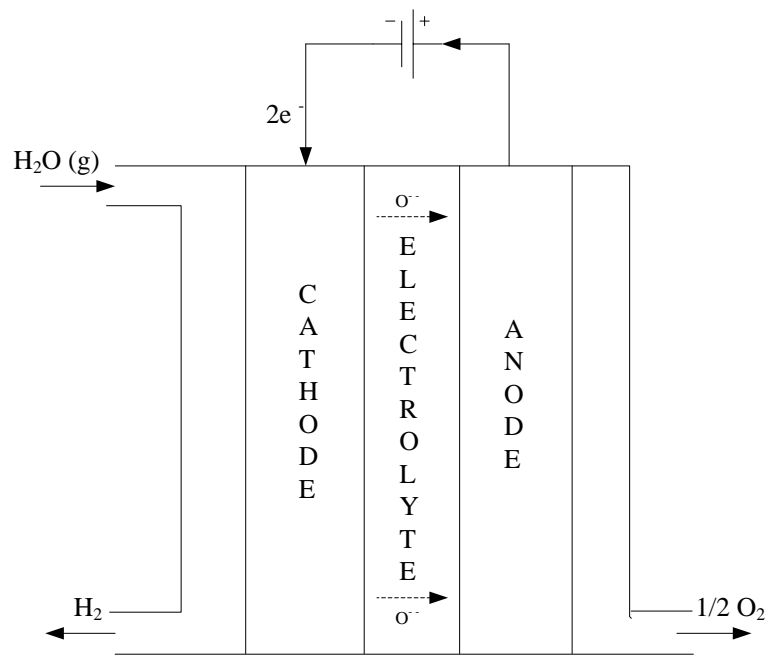


Figure 5.5 A schematic diagram of SOEC.

SOEC works in reverse to that of SOFC to produce hydrogen, and consumes power to perform the electrolysis process. In SOEC, a part of the electrical energy replaces the thermal energy and uses electricity to electrochemically decompose water through electrodes and across an ion conducting electrolytes according to the following reactions [116]:



Chapter 6

MODELING AND ANALYSIS

6.1 Introduction

The use of gasification technology that is fuelled by feed stocks which have a neutral carbon dioxide life cycle, making the technology friendly regarding global warming. Different gasifiers and different approaches of modeling have been proposed, and none of them has theoretically addressed the hydrogen production. The proposed approach in this study is solely aimed to fill that gap. The approach of the gasifier has been applied to the hydrogen production from steam sawdust wood gasification, and has emerged in three innovative systems. This study is performed for different steam-biomass ratios and different gasification temperatures, as well as from a thermodynamic point of view.

6.2 Assumptions

The main assumptions for the analysis are:

- Processes take place at a steady state.
- Potential and kinetic energy changes are negligible.
- Environment and reference state at $T_o = 298$ K and $P_o = 1$ atm.
- H_2 , CO, CO_2 and CH_4 are the product gases.
- Ash residue behind the gasification process is negligible.
- The gases obey the ideal gas relations.
- The gasifier is isothermal and at an equilibrium state.
- The gasifier accepts biomass moisture content.
- The product gases at the gasifier exit are at the gasifier temperature.
- The residence time is sufficient to operate the gasifier under the equilibrium mode.

6.3 Reaction Mechanism

Carbon, hydrogen and oxygen are the major components in biomass. These

elements and negligible elements like sulfur and nitrogen represent the biomass ultimate analysis. The chemical formula of biomass is represented by $C_lH_mO_n$. Biomass is gasified at high temperatures where its particles undergo partial oxidation that results in gas, tar and char products. Finally, it is reduced to form H_2 , CO , CO_2 and CH_4 . This conversion process can be expressed in a global reaction which is given by the following reaction:



l , m and n are the number of atoms of carbon, hydrogen and oxygen in the feedstock respectively determined from the ultimate analysis of biomass; α is the amount of biomass; and γ is the amount of supplied steam. a , b , c , d , e and f are the number of moles of H_2 , CO , CO_2 , CH_4 , C and tar respectively. The number of moles is found from the following atomic balance equations and proposed models for tar and char:

$$C : \alpha l = b + c + d + e + 6f \quad (6.2)$$

$$H : \alpha m + 2\gamma = 2a + 4d + 6f \quad (6.3)$$

$$O : \alpha n + \gamma = b + 2c \quad (6.4)$$

$$N = a + b + c + d + e + f \quad (6.5)$$

The gasification process is applicable to biomass having moisture content less than 35% [117]. In the case of higher moisture content, the biomass undergoes a drying or pre-heating process. This; however, increases the energy required for the gasification process as well as decreases the gasification efficiency.

In addition to the above global reaction, the following side reaction (methanation reaction) is assumed at equilibrium;



The equilibrium constant for the reaction is:

$$K = \frac{a^2 N}{d} \quad (6.7)$$

Also in the equilibrium state and for the ideal gas, the equilibrium constant can be found in terms of free Gibbs function, G from the following equation;

$$K = \exp\left(\frac{-\Delta G}{RT}\right) \quad (6.8)$$

where R is the universal gas constant. The system of equations is solved simultaneously to find the unknowns, a , b , c and d .

6.4 Biomass Equations

The energy flows in a gasified biomass is calculated in terms of the heating value. It is the amount of heat produced by combustion of a unit quantity of a biomass. The heating value is two types: low and high heating value. The lower or net heating value is obtained by subtracting the latent heat of vaporization of the water vapor formed in the combustion. The high or gross heating value is the amount of heat produced by the complete combustion of a unit quantity of fuel. The gross heating value is obtained when all products of the combustion are cooled down to the temperature before the combustion and condensing any water vapor formed during the combustion process. Therefore, the efficiency based on lower heating value is higher.

The energy flows in a gasified biomass; $En_{Biomass}$ is calculated in terms of its lower heating value and its mass flow rate, $\dot{m}_{Biomass}$ as follows:

$$En_{Biomass} = \dot{m}_{Biomass} LHV_{Biomass} \quad (6.9)$$

where the biomass lower heating value is given by Shieh et al. [118]:

$$LHV_{Biomass} = 0.0041868(1 + 0.15[O])(7837.667[C] + 33888.889[H] - [O]/8) \quad (6.10)$$

and C, H and O are carbon, oxygen and hydrogen elements, respectively, in wood sawdust and are obtained from wood sawdust ultimate analysis.

In this experiment, the exergy of used biomass is calculated from the method of Szargut et al. [119] as follows:

$$Ex_{biomass} = \beta LHV_{biomass} \quad (6.11)$$

where the coefficient β is given in terms of oxygen-carbon and hydrogen-carbon ratios and according to the following equation:

$$\beta = \frac{1.0414 + 0.0177[H/C] - 0.3328[O/C]\{1 + 0.0537[H/C]\}}{1 - 0.4021[O/C]} \quad (6.12)$$

Prins et al. [120] developed an equation to find the coefficient β , but it contains nitrogen and the used biomass has negligible nitrogen content. For this reason, this equation will not be used in this work.

6.5 Mass Analysis

At a steady state condition, a mass flow into the component is equal to the mass flow out from it. The mass balance around a component under study is calculated from the following equation (Figure 6.1):

$$\sum_{i=1}^N \dot{m}_i = \sum_{e=1}^M \dot{m}_e \quad (6.13)$$

where N is the total number of streams that enter the control volume occupied, the component under study, and M is the total number of streams that exit the control volume. The mass flow rate at inlets and exits of the control volume can be calculated in terms of molar flow rate from the following equation:

$$\dot{m} = \dot{n}MW \quad (6.14)$$

where MW is the molecular weight. Accordingly, the mass conservation equation becomes:

$$\sum_{i=1}^N \dot{n}_i MW_i = \sum_{e=1}^M \dot{n}_e MW_e \quad (6.15)$$

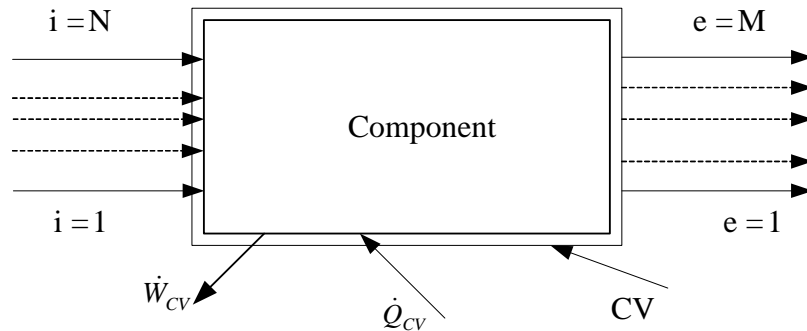


Figure 6.1 Schematic diagram of a system for study

6.6 First Law of Thermodynamics

The first law of thermodynamics is also known as the law of energy conservation. This law governs the energy around the component that occupies the control volume. Its general form is given by the following equation:

$$\sum_{i=1}^N \dot{m}_i h_i + \dot{Q}_{net} = \sum_{e=1}^M \dot{m}_e h_e + \dot{W}_{net} \quad (6.16)$$

where net stands for the net heat and the net power cross the component boundaries.

The gasification process does not need work to take place, but it is an endothermic process. However, as the process is assumed to be self-heated, only the heat lost from the gasifier wall will substitute for the heat transfer from the control volume. The gasification process is similar to any process and it has to satisfy the first law of thermodynamics which describes energy conservation and it is given by:

$$\sum_R H_i - \sum_P H_j = \dot{Q}_{lostwa} \quad (6.17)$$

where \dot{Q}_{lostwa} is the energy lost during the gasification process and H is the enthalpy of products and reactants and is given by:

$$H_i = \dot{m}_i h_i \quad (6.18)$$

$$H_j = \dot{m}_j h_j \quad (6.19)$$

Here, subscripts i and j stand for reactants and products respectively, and sub-symbols R and P refer to the number of reactants and number of products, respectively. Enthalpy and entropy are necessary to perform analysis of the first and second laws of thermodynamics. Gases obey the ideal gas behaviour and their respective enthalpies and entropies are as follows:

$$h = h_f^o + \Delta h \quad (6.20)$$

The enthalpy rise due to temperature is:

$$\Delta h = \int_{T_o}^T C_p dT \quad (6.21)$$

Enthalpy of formation, h_f^o for the product gases is given in Table 6.2. Entropy changes due to temperature rise according to the following equation:

$$\Delta s = \int_{T_o}^T \frac{C_p}{T} dT \quad (6.22)$$

In the case of processes at super atmospheric pressure, the term of pressure needs to be considered. C_p is constant pressure specific heat in kJ/kmol-K and for gases it is the function of the gasifier temperature and is given by the following empirical equation:

$$C_p = a' + b'T + c'T^2 + d'T^3 \quad (6.23)$$

The coefficients, a' , b' , c' and d' of different gases are summarized in Table 7.3. The specific heat of tar in coal gasification was developed by Hyman et al. [121] and

modified by Lowry [122]. The same equation is used for derived tar from biomass gasification and in $\text{kJ/kg}_{\text{tar}}\text{K}$:

$$C_p = 0.00422T \quad (6.24)$$

Eisermann et al. [123] proposed the following equation to calculate the enthalpy and the entropy of tar. The term related to sulfur is omitted where the used biomass has negligible sulfur content:

$$h_{\text{tar}} = h_{\text{tar}}^o + \int_{T_o}^T C_p dT \quad (6.25)$$

$$h_{\text{tar}}^o = -30.980 + X_{\text{CO}_2} h_{\text{CO}_2}^o + X_{\text{H}_2\text{O}} h_{\text{H}_2\text{O}}^o \quad (6.26)$$

where X_i is the mole fraction and h_i^o is the standard enthalpy of formation for specie i .

The tar entropy is given by:

$$s = s_{\text{tar}}^o + \int_{T_o}^T \frac{C_p}{T} dT \quad (6.27)$$

The standard tar entropy, s_{tar}^o in kJ/kmol-K is given by:

$$s_{\text{tar}}^o = a_1 + a_2 \text{EXP} \left[-a_3 \left(\frac{H}{C} + N \right) \right] + a_4 \left(\frac{O}{C+N} \right) + a_5 \left(\frac{N}{C+N} \right) + a_6 \left(\frac{S}{C+N} \right) \quad (6.28)$$

where the coefficients a_1 - a_6 : $a_1 = 37.1635$, $a_2 = -31.4767$, $a_3 = 0.564682$, $a_4 = 20.1145$, $a_5 = 54.3111$ and $a_6 = 44.6712$. C, H, N, O and S are, respectively, carbon, hydrogen, nitrogen, oxygen and sulfur weight fractions in the used biomass. The system consists of a set of equations for all chemical species involved in the analysis including the equation of atomic balance for each element, the equation of the total number of moles, the equations of a variation of the standard Gibbs free energy of formation of the species and the energy balance around the gasifier.

Most researchers assume losses from the gasifier to the ambient are negligible compared to the energy entering or leaving the gasifier. De Souza-Santos [124] reported these losses are around 1 to 2% of the power input into the biomass. However, to maintain more accurate results from this study, these losses are taken into consideration.

The energy lost due to transferred heat to the environment, \dot{Q}_{lostwa} is calculated from:

$$\dot{Q}_{\text{lostwa}} = U_{\text{wa}} A (T_w - T_o) \quad (6.29)$$

The overall heat transfer coefficient, U_{wa} between the external gasifier wall at temperature T_w and the ambient temperature T_o estimated by the following empirical relation given by Isachenko et al. [125]:

$$U_{wa} = 1.9468(T_w - T_o)^{1/4} (2.8633U_o + 1)^{1/2} + 5.75 \times 10^{-8} \varepsilon_{ins} \frac{T_w^4 - T_o^4}{T_w - T_o} \quad (6.30)$$

where U_o is the average wind velocity and a value of 2 m/s is used in this study. T_w is estimated from the energy balance made around the gasifier wall by assuming the wall is insulated with material that has thickness, x_{ins} and thermal conductivity, k_{ins} as follows:

$$U_{wa}(T_w - T_o) = \frac{k_{ins}}{x_{ins}}(T - T_w) \quad (6.31)$$

6.6.1 Gasifier Energy Efficiencies

Gasifier energy efficiencies are also called the first law efficiencies. Three forms of energetic efficiencies, η_{en1} , η_{en2} and η_{en3} are applied as follows:

$$\eta_{en1} = \frac{En_{H_2}}{En_{Biomass} + En_{steam}} \quad (6.32)$$

$$\eta_{en2} = \frac{En_{gas}}{En_{Biomass} + En_{steam}} \quad (6.33)$$

$$\eta_{en3} = \frac{En_{gas} + En_{tar} + En_{char}}{En_{Biomass} + En_{steam}} \quad (6.34)$$

where En_{H_2} is the energy content in the producer hydrogen, En_{gas} is the energy flow-out with gases, En_{tar} is the energy flow-out with tar, En_{char} is the energy flows out with char, En_{steam} is the energy flows in with the injected steam.

6.7 Second Law of Thermodynamics

In the gasification system, the second law of thermodynamics governs the exergy or energy available around the system under the study. The exergy flow rate is primarily calculated from the following equation:

$$\dot{Ex}_i = \dot{m}_i Ex_i \quad (6.35)$$

where the subscript i represents fuel or agent or product, Ex is the specific exergy. The exergy depends on matter composition known as chemical exergy, Ex_{ch} and for a mixture

is given by:

$$Ex_{ch} = \sum_i (X_i Ex_{o,i}) + RT_o \sum_i (X_i \ln X_i) \quad (6.36)$$

Here, X_i is the mole fraction of component i and Ex_o is standard exergy and for different compounds is summarized in Table 6.2. The other part of exergy depends on the matter temperature and matter pressure. It is known as physical exergy, Ex_{ph} and is given by:

$$Ex_{ph} = (h - h_o) - T_o (s - s_o) \quad (6.37)$$

where h and s are specific enthalpy and specific entropy of a specie when a gasifier operates at T and P and h_o and s_o are enthalpy and entropy at standard state ($T_o = 289$ K and $P_o = 1$ atm). Therefore, the total exergy, Ex is:

$$Ex = Ex_{ch} + Ex_{ph} \quad (6.38)$$

The physical exergy is related to the entropy. The entropy balance is represented by the following equation:

$$\sum_i \dot{S}_i + \dot{S}_{gen} = \sum_e \dot{S}_e + \Delta \dot{S}_{CV} \quad (6.39)$$

$\Delta \dot{S}_{CV}$ is the entropy accompanied by heat transfer that crosses the system boundary, and it is given in terms of heat transfer that crosses the system boundary and the temperature at the system boundaries. Accordingly, the above equation becomes:

$$\sum_i \dot{S}_i + \dot{S}_{gen} = \sum_e \dot{S}_e + \frac{\dot{Q}_{lostwa}}{T_w} \quad (6.40)$$

where entropy rate is given in terms of specific entropy, s and mass flow rate, \dot{m} at inlets and exits respectively as follows:

$$\dot{S}_i = \dot{m}_i s_i \quad (6.41)$$

$$\dot{S}_e = \dot{m}_e s_e \quad (6.42)$$

The exergy accompanied by heat transfer is $\dot{Q}_{lostwa} (1 - T_o/T_w)$. The transferred exergy by work is simply equal to the work itself.

6.7.1 Gasifier Exergy Efficiencies

Performing exergy analysis is an effective method using conservation of both mass and energy with the second law of thermodynamics to design and analyze the conversion of biomass by gasification. The exergy efficiency for a system under study is

defined as the ratio between useful exergy outputs from the system to the necessary exergy input to the system. For a gasifier, three forms of rational exergetic efficiencies, η_{ex1} , η_{ex2} and η_{ex3} are applied as follows:

$$\eta_{ex1} = \frac{\dot{E}x_{H_2}}{\dot{E}x_{Biomass} + \dot{E}x_{steam}} \quad (6.43)$$

$$\eta_{ex2} = \frac{\dot{E}x_{gas}}{\dot{E}x_{Biomass} + \dot{E}x_{steam}} \quad (6.44)$$

$$\eta_{ex3} = \frac{\dot{E}x_{gas} + \dot{E}x_{tar} + \dot{E}x_{char}}{\dot{E}x_{Biomass} + \dot{E}x_{steam}} \quad (6.45)$$

where total exergy rate leaves gasifier is exergy rate of all gases, tar and char. $\dot{E}x_{H_2}$ is the exergy flow rate of the produced hydrogen, $\dot{E}x_{gas}$ is the exergy flows with the produced gas, $\dot{E}x_{tar}$ is the exergy flows with tar, $\dot{E}x_{char}$ is the exergy flows with char, $\dot{E}x_{steam}$ is the exergy flows with steam and $\dot{E}x_{biomass}$ is the exergy flows with biomass.

6.7.2 Irreversibility

Prins et al. [120] reported there is a loss of equality of materials due to entropy production, heat and mass transfer and chemical reactions and that was represented by irreversibility. In order for any process to be applicable from a thermodynamics point of view, it has to satisfy both the first and the second laws of thermodynamics.

6.7.2.1 Internal Irreversibility

Internal irreversibility represents the internal exergy lost as the quality of material and energy is lost due to dissipation. It is calculated in terms of the generated entropy during the gasification process as a result of the flow of substances, heat and mass transfer and chemical reactions. It is given by the following equation:

$$\dot{E}x_{destin} = T_o \dot{S}_{gen} \quad (6.46)$$

6.7.2.2 External Irreversibility

Exergy loss due to the energy lost from the system component wall is:

$$\dot{E}x_{destwa} = \dot{Q}_{lostwa} \left(1 - \frac{T_0}{T_w} \right) \quad (6.47)$$

The total exergy destruction is:

$$\dot{E}x_{des} = \dot{E}x_{desin} + \dot{E}x_{destwa} \quad (6.48)$$

A potential to improve the exergy efficiency of the hydrogen production from biomass gasification is analyzed by using the concept of potential improvement. It investigates how much available energy can be redirected towards hydrogen production. The potential improvement in exergy can be calculated from the following equation [126]:

$$PI = \dot{E}x_{des} (1 - \eta_{exl}) \quad (6.49)$$

6.8 System II Components

The main components of the system are described in the following sections. However, a description of the gasifier was done under analysis of System I and any information regarding gasification and gasifiers used here will refer to the above sections for more details. The analysis is conducted by applying mass conservation; energy conservation and entropy balance on processes that take place in the system components.

6.8.1 Compressor 5-6

This component is used to increase the pressure required in the filtration process and to increase the gas temperature to the temperature that is preferred in order to make a reformation reaction take place. The component is also used to prevent the gasifier from potential back flow. The continuity equation is given by (Figure 6.2):

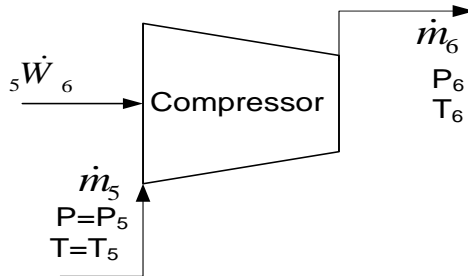


Figure 6.2 A schematic diagram of compressor 5-6.

$$\dot{m}_5 = \dot{m}_6 \quad (6.50)$$

where i and e refer to H₂, CO, CO₂ and CH₄, and the mass flow rate at the two states is given as follows:

$$\dot{m}_5 = \sum_{i=1}^4 \dot{m}_i \quad (6.51)$$

$$\dot{m}_6 = \sum_{i=1}^4 \dot{m}_e \quad (6.52)$$

The mass flow rate at the compressor inlet and exit is given in terms of the molar flow rate of the species, \dot{N} and their molecular weight as follows:

$$\sum_{i=1}^4 \dot{m}_i = \sum_{i=1}^4 \dot{N}_i MW_i \quad (6.53)$$

Where H₂, CO, CO₂ and CH₄ are the species left to compress after a separation of the char and the tar. The energy conservation for the adiabatic compressor that is under study is given by:

$${}_i\dot{W}_e = \sum_{e=1}^4 \dot{m}_e h_e - \sum_{i=1}^4 \dot{m}_i h_i \quad (6.54)$$

The temperatures of the gas at the compressor exit and inlet are given in terms of the pressures at the inlet and exit and compressor isentropic efficiency, η_c as follows:

$$T_e = T_i \left[1 + \eta_c^{-1} \left(\left(\frac{P_e}{P_i} \right)^{\frac{\gamma_{gas}-1}{\gamma_{gas}}} - 1 \right) \right] \quad (6.55)$$

In the isentropic compression process, the pressure and the temperature of the compressor upstream are related to the pressure and the temperature of the compressor downstream by the following equation:

$$\frac{T_{es}}{T_i} = \left(\frac{P_e}{P_i} \right)^{\frac{\gamma_{gas}-1}{\gamma_{gas}}} \quad (6.56)$$

where γ_{gas} is the specific heats ratio of the compressed gas and is given by:

$$\gamma_{gas} = \frac{Cp_{gas}}{Cv_{gas}} \quad (6.57)$$

The constant pressure specific heat of the ideal gas is a function of temperature only. The specific heat of specie, i in kJ/kmol-K, is assumed a polynomial of 3rd degree [127].

$$\overline{Cp}_i = a + bT_i + cT_i^2 + dT_i^3 \quad (6.58)$$

where a , b , c and d are constants. The specific heat in [kJ/kg-K] is simply calculated from:

$$Cp_i = \frac{\overline{Cp}_i}{MW_i} \quad (6.59)$$

where MW_i is the specie molecular weight. The specie constant volume specific heat in [kJ/kg-K] is given by:

$$\overline{Cv}_i = \overline{Cp}_i - \overline{R} \quad (6.60)$$

Similarly, the gas constant volume specific heat in kJ/kg-K is:

$$Cv_i = \frac{\overline{Cv}_i}{MW_i} \quad (6.61)$$

where the specific heat and the molecular weight of the mixture of gases at a state point are calculated respectively from:

$$Cp_{gas} = \sum_i x_i Cp_i \quad (6.62)$$

$$Cv_{gas} = \sum_i x_i Cv_i \quad (6.63)$$

The second law governs the entropy balance and for the compressor under the study is:

$$\sum_{i=1}^4 \dot{m}_{i,i} s_{i,i} - \sum_{i=1}^4 \dot{m}_{e,i} s_{e,i} + \dot{S}_{gen,5-6} = 0 \quad (6.64)$$

where the subscripts i and e refer to inlet to and exit from the compressor streams respectively. The entropy generation from the process takes place in the compressor is:

$$\dot{S}_{gen,5-6} = \sum_{i=1}^4 \dot{N}_{i,i} \overline{s}_{i,e} - \sum_{i=1}^4 \dot{N}_{e,i} \overline{s}_{e,i} \quad (6.65)$$

The exergy loss in the compression process is given by:

$$\dot{Ex}_{des,5-6} = T_o \dot{S}_{gen,5-6} \quad (6.66)$$

Compression of gases everywhere in the system is similarly treated. The compression process is also needed to compress air required for the electrochemical reaction that takes

place in the SOFC. The same principles applied above can be used here with properties related to air. The continuity equation is:

$$\dot{m}_0 = \dot{m}_9 \quad (6.67)$$

The amount of air that will compress is that air which is necessary to make the electrochemical reaction takes place in the SOFC which is related to fuel with a hydrogen-air ratio of two. The energy conservation of the compression process is given by:

$${}_0\dot{W}_9 = \dot{m}_0 (h_0 - h_9) \quad (6.68)$$

The pressure and the temperature of the compressor upstream are the same as the ambient. The temperature of the preheated air that is fed to SOFC is calculated from the energy balance that is conducted on the SOFC former heat exchanger. The temperature and pressure of the other streams are known. Streams exit SOFC have a temperature and pressure of the SOFC and the fuel (H₂) stream has the properties after the filtration process: temperature after gases compression process and pressure increases a pressure of SOFC by 5%. Applying the second law for the compression process leads to the following equation:

$$\dot{m}_0 s_0 - \dot{m}_9 s_9 + \dot{S}_{gen,0-9} = 0 \quad (6.69)$$

From which the entropy generation rate is:

$$\dot{S}_{gen,0-9} = \dot{m}_9 s_9 - \dot{m}_0 s_0 \quad (6.70)$$

Therefore, the exergy loss in the compression process 0-9 is given by:

$$\dot{E}x_{des,0-9} = T_o \dot{S}_{gen,0-9} \quad (6.71)$$

The energy required for the preheating process is extracted from by-product gases when passing in the SOFC former heat exchanger installed after the steam reforming reactor.

The compression process is also needed to compress air that is required for the burner. This air is also used to control burner temperature. The same principles applied to the above air compressor can be applied where the compressed air is preheated by passing through the heat exchanger that is installed after the separation process. The continuity equation is:

$$\dot{m}_0 = \dot{m}_{25} \quad (6.72)$$

The amount of air that will compress is the amount used to control the burner temperature on one hand and on the other hand to make sure there is a sufficient amount of air that can be used to completely burn the residuals sent to the burner from the SOFC and the gasifier. This amount of air can be investigated by performing an iterative process through the energy conservation equation of the burner to have a burner with a reasonable operating temperature. The power that drives this compressor is calculated from the energy conservation of the compression process. The energy conservation of the compression process is given by:

$${}_0\dot{W}_{25} = \dot{m}_{24}(h_0 - h_{25}) \quad (6.73)$$

The pressure and the temperature of this compressor upstream are the same as the ambient condition. The air temperature after the preheating process is assumed 430 K and a pressure equal to the SOFC pressure. Applying the second law for the compression process of the burner preheated air leads to

$$\dot{m}_0 s_0 - \dot{m}_{25} s_{25} + \dot{S}_{gen,0-25} = 0 \quad (6.74)$$

The entropy generation during the compression process is:

$$\dot{S}_{gen,0-25} = \dot{m}_{25} s_{25} - \dot{m}_0 s_0 \quad (6.75)$$

Therefore, the exergy loss in the compression process 0-25 is given by:

$$\dot{E}x_{des,0-25} = T_o \dot{S}_{gen,0-25} \quad (6.76)$$

The preheated air temperature is found based on the sufficient amount of air and the temperature needs at the burner.

6.8.2 Gas Turbine 7-8

The flue gas which leaves the burner is expanded in the turbine to extract its energy content and use it as power (Figure 6.3). Properties of the stream at the turbine inlet are the same as those of the burner exit. According to the analysis that was done on the burner; the gas at the burner exit or the turbine inlet (state 7) constitutes steam, carbon dioxide, air and nitrogen. Properties of the stream at the turbine exit (state 8) are given such that it obeys the environmental constraints and to flow against the environment conditions (P_0 and T_0). The continuity equation is:

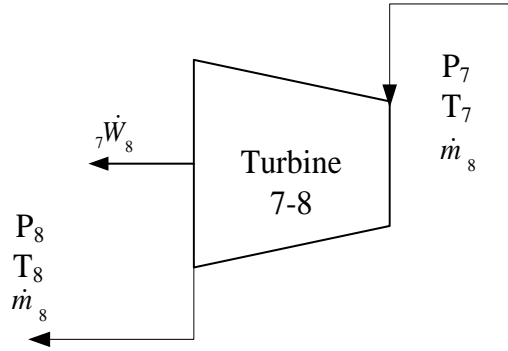


Figure 6.3 A schematic diagram of turbine 7-8.

$$\dot{m}_7 = \dot{m}_8 \quad (6.77)$$

where the mass flow rates at the two states are given as follows and i and e refer to water, air, nitrogen and carbon dioxide:

$$\dot{m}_8 = \sum_{e=1}^4 \dot{m}_e \quad (6.78)$$

$$\dot{m}_7 = \sum_{i=1}^4 \dot{m}_i \quad (6.79)$$

The mass flow rate is calculated from the molar flow rate of the species, \dot{N} and their molecular weight as follows:

$$\sum_{i=1}^4 \dot{m}_i = \sum_{i=1}^4 \dot{N}_i MW_i \quad (6.80)$$

One can look to the expansion process that takes place in the turbine and describe it as an opposite process to the compression process that happens in the compressor. The produced power when flue gases expand in the turbine is found by applying the first law or from the energy conservation of the expansion process which gives:

$${}_7\dot{W}_8 = \dot{m}_7 h_7 - \dot{m}_8 h_8 \quad (6.81)$$

Where the gas energy content at the two states are:

$$\dot{m}_7 h_7 = \sum_{i=1}^4 \dot{N}_i \bar{h}_i \quad (6.82)$$

$$\dot{m}_8 h_8 = \sum_{e=1}^4 \dot{N}_e \bar{h}_e \quad (6.83)$$

All species behave like an ideal gas at both states and therefore their enthalpies are a function of temperature only, and they are given in terms of constant pressure specific heat. In addition to the above equations, the turbine isentropic efficiency, η_t can be used to determine the unknown properties of an ideal gas from:

$$T_8 = T_7 \left[1 - \eta_t \left(1 - \left(\frac{P_7}{P_8} \right)^{\frac{\gamma_{fgas}-1}{\gamma_{fgas}}} \right) \right] \quad (6.84)$$

The temperature and pressure at the turbine exit state and those at the turbine inlet state in the isentropic expansion process are related according to the ideal gas equations:

$$\frac{T_8}{T_7} = \left(\frac{P_8}{P_7} \right)^{\frac{\gamma_{fgas}-1}{\gamma_{fgas}}} \quad (6.85)$$

The flue gas specific heat ratio, γ_{fgas} is given in terms of constant pressure specific heat and constant volume specific heat by:

$$\gamma_{fgas} = \frac{\overline{Cp}_{fgas}}{\overline{Cv}_{fgas}} \quad (6.86)$$

The specific heats of the flue gas are calculated from:

$$\overline{Cp}_{fgas} = \sum_{i=1}^4 x_i \overline{Cp}_i \quad (6.87)$$

$$\overline{Cv}_{fgas} = \sum_{i=1}^4 x_i \overline{Cv}_i \quad (6.88)$$

where the specific heats of specie i that constitutes the flue gas, \overline{Cp}_i and \overline{Cv}_i are calculated as above and is \overline{R} the universal gas constant.

The net power from the system is given by the following equation:

$$\dot{W}_{net} = \dot{W}_8 - \dot{W}_9 - \dot{W}_{25} \quad (6.89)$$

The temperature of the flue gas at the turbine exit is assumed such that obeying the environmental restraints. The entropy balance of the adiabatic turbine 7-8 is performed by applying the second law for the expansion process from state 7 to state 8 as follows:

$$\dot{m}_7 s_7 - \dot{m}_8 s_8 + \dot{S}_{gen,7-8} = 0 \quad (6.90)$$

From which the entropy generation in the process is:

$$\dot{S}_{gen,7-8} = \dot{m}_8 s_8 - \dot{m}_7 s_7 \quad (6.91)$$

where the entropy for the inlet and exit states are calculated from:

$$\dot{m}_7 s_7 = \sum_{i=1}^4 \dot{N}_i \bar{s}_i \quad (6.92)$$

$$\dot{m}_8 s_8 = \sum_{e=1}^4 \dot{N}_e \bar{s}_e \quad (6.93)$$

The exergy loss corresponds to the expansion process that takes place in the turbine 7-8 is:

$$\dot{E}x_{des,7-8} = T_o \dot{S}_{gen,7-8} \quad (6.94)$$

6.8.3 Heat Exchanger 17-18-9-10

The first two symbols, 17, 18 indicate the hot stream while the second one, 9, 10 indicate the cold stream (Figure 6.4). The existence of this heat exchanger aims to extract heat from the by-product gasification gas to preheat the air that passes through the heat exchanger and is utilized in the SOFC. The continuity equation for the heat exchanger is given for the hot and cold streams, respectively, by the following equations:

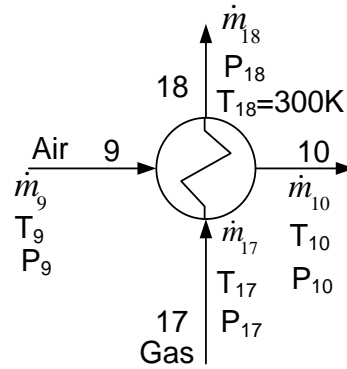


Figure 6.4 A schematic diagram of heat exchanger 17-18-9-10.

$$\dot{m}_{17} = \dot{m}_{18} \quad (6.95)$$

$$\dot{m}_9 = \dot{m}_{10} \quad (6.96)$$

The energy conservation of the process in the heat exchanger says that the energy removed from the gas line is absorbed by the air line; this can be expressed by the following equation:

$${}_{17}\dot{Q}_{18} = {}_9\dot{Q}_{10} \quad (6.97)$$

or

$$\dot{m}_{17}h_{17} - \dot{m}_{18}h_{18} = \dot{m}_9h_9 - \dot{m}_{10}h_{10} \quad (6.98)$$

Three species constituting the gas stream are: H₂, CO and CO₂. Therefore, the energy content of the gas at the heat exchanger inlet and exit is:

$$\dot{m}_{17}h_{17} = \sum_{i=1}^3 \dot{N}_i \bar{h}_i \quad (6.99)$$

$$\dot{m}_{18}h_{18} = \sum_{e=1}^3 \dot{N}_e \bar{h}_e \quad (6.100)$$

while the cold stream is air with an energy content at state 9 as

$$\dot{m}_9h_9 = \dot{N}_9 \bar{h}_9 \quad (6.101)$$

and

$$\dot{m}_{10}h_{10} = \dot{N}_{10} \bar{h}_{10} \quad (6.102)$$

at state 10. In this system, the temperature of the hot stream at state 17 is obtained from the energy balance of the steam reforming reactor, while at state 18, the temperature is assumed equal to the ambient temperature and the pressure is decreased by 5% of that which state 17 has. Therefore, the parameters of the hot line are known. Also, the properties of air at the heat exchanger inlet are known from the compressor 0-9 analysis and those of air at the heat exchanger outlet is known from the energy balance of the all heat exchangers. Accordingly, a number of cells in the SOFC stack are known from SOFC analyses. The entropy balance around the heat exchanger leads to:

$$\dot{m}_{17}h_{17} + \dot{m}_9h_9 + \dot{S}_{gen,17-18-9-10} = \dot{m}_{18}h_{18} + \dot{m}_{10}h_{10} \quad (6.103)$$

The entropy of the hot stream at the heat exchanger inlet and exit are:

$$\dot{m}_{17}s_{17} = \sum_{i=1}^3 \dot{N}_i \bar{s}_i \quad (6.104)$$

$$\dot{m}_{18}s_{18} = \sum_{e=1}^3 \dot{N}_e \bar{s}_e \quad (6.105)$$

while for the cold stream, the entropy is:

$$\dot{m}_9 s_9 = \dot{N}_9 \bar{s}_9 \quad (6.106)$$

and

$$\dot{m}_{10} s_{10} = \dot{N}_{10} \bar{s}_{10} \quad (6.107)$$

Therefore, the exergy loss as a result of the process in the heat exchanger is:

$$\dot{E}x_{des,17,18-9,10} = T_o \dot{S}_{gen,17-18-9-10} \quad (6.108)$$

6.8.4 Heat Exchanger 20-21-3-4

Similarly, first two symbols, 20 and 21, indicate the states on the hot stream while the second two symbols, 3 and 4 indicate the states on the cold stream (Figure 6.5). The existence of this heat exchanger aims to produce steam and use it as a gasification agent in the gasification process by extracting heat from the high temperature steam stream (20, 21) that is produced by electrochemical reaction in SOFC. Applying the continuity equation on the heat exchanger gives the following equations:

$$\dot{m}_{20} = \dot{m}_{21} \quad (6.109)$$

$$\dot{m}_3 = \dot{m}_4 \quad (6.110)$$

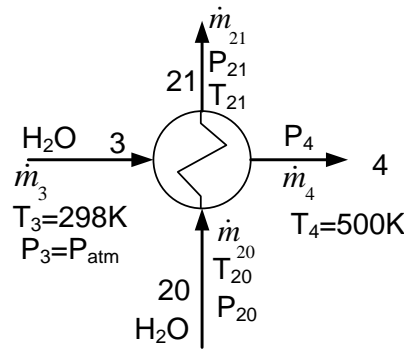


Figure 6.5 A schematic diagram of heat exchanger 20-21-3-4.

In this study, an amount and properties of the steam that delivers to the gasifier (state 4) is known, and the properties of water from the main supply are known (state 3). Also, the amount and properties of the hot stream steam at state 20 are known from the SOFC

analysis. Only the temperature of the hot stream at state 21 is unknown, which is calculated from the performed energy balance on the heat exchanger. The energy balance of the heat exchanging process simply says that energy removed from the hot stream line is absorbed by the steam flow in the cold line; this can be expressed by the following equation:

$${}_{20}\dot{Q}_{21} = {}_3\dot{Q}_4 \quad (6.111)$$

or

$$\dot{m}_{20}(h_{20} - h_{21}) = \dot{m}_4(h_4 - h_3) \quad (6.112)$$

Applying of the entropy balance or the second law for this heat exchanger gives:

$$\dot{m}_{20}s_{20} + \dot{m}_3s_3 + \dot{S}_{gen,20-21-3-4} = \dot{m}_{21}s_{21} + \dot{m}_4s_4 \quad (6.113)$$

From which, the entropy generation is:

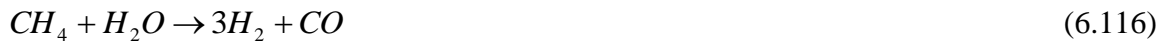
$$\dot{S}_{gen,20-21-3-4} = \dot{m}_4(s_4 - s_3) + \dot{m}_{20}(s_{21} - s_{20}) \quad (6.114)$$

Therefore, the exergy loss accompanied with this process is:

$$\dot{E}x_{des,20,21-3,4} = T_o\dot{S}_{gen,20-21-3-4} \quad (6.115)$$

6.8.5 The Steam Reforming Reactor

As a way to increase the hydrogen yield from the system, the producer gas from the gasification process is further processed to the steam reforming reactor (Figure 6.6). The reaction in the reactor is governed by the following reaction equation:



According to this reaction, H₂-CO ratio of three is used in the analyses. The process can be simulated by the gasification process using methane as fuel and steam as an agent. Part of the steam of the SOFC electrochemical reaction by-product is used as a gasification medium. The amount of steam that is required for the steam reforming reaction is calculated based on the mole balance of the reaction equation, and no excess steam is required. It is clear from the reaction equation that a ratio of the number of methane moles to that of used steam is one. The molar flow rate of methane is known from the gasification process analyses, while the molar flow rates of both the steam needed to perform the steam reforming reaction, and that of the reaction products are known from

the molar balance of the reaction equation.

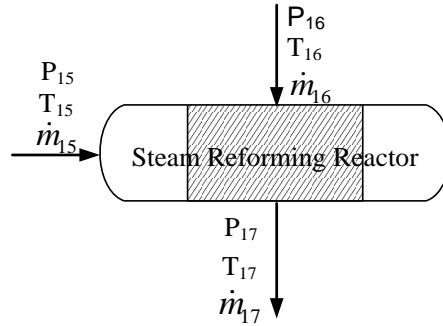


Figure 6.6 A Schematic diagram of steam reforming reactor.

The steam reforming reaction is an endothermic reaction, because no external heating is supplied; the products from the reaction are expected to have a lower heat content compared to the reactants and thus lower temperature. Also, the producer gas in the gasifier has small methane content; therefore, a small quantity of steam is sufficient for the reaction to take place. For the adiabatic steam reforming reactor, the first law of thermodynamics gives:

$$\sum_i \dot{m}_{i,SR} h_{i,SR} = \sum_e \dot{m}_{e,SR} h_{e,SR} \quad (6.117)$$

The mass flow rate of the reactants is calculated in terms of their molar flow rates and their molecular weights. On mole basis, the terms of the above equation can be rewritten as follows:

$$\sum_i \dot{m}_{i,SR} h_{i,SR} = \sum_e \dot{N}_{i,SR} \bar{h}_{i,SR} \quad (6.118)$$

$$\sum_e \dot{m}_{e,SR} h_{e,SR} = \sum_e \dot{N}_{e,SR} \bar{h}_{e,SR} \quad (6.119)$$

where the subscripts i refers to the reactants of the steam reforming reactor and those are H₂O, CH₄, CO and CO₂ and e refers to the products of the steam reforming (SR) reactor and those are H₂, CO and CO₂. For the shown states on the schematic diagram which represents the steam reforming reactor, the above equations can be rewritten as follows:

$$\sum_i \dot{N}_{i,SR} \bar{h}_{i,SR} = \dot{N}_{CH_4,16} \bar{h}_{CH_4,16} + \dot{N}_{CO,16} \bar{h}_{CO,16} + \dot{N}_{CO_2,16} \bar{h}_{CO_2,16} + \dot{N}_{H_2O,15} \bar{h}_{H_2O,15} \quad (6.120)$$

$$\sum_e \dot{N}_{e,SR} \bar{h}_{e,SR} = \dot{N}_{H_2,17} \bar{h}_{H_2,17} + \dot{N}_{CO,17} \bar{h}_{CO,17} + \dot{N}_{CO_2,17} \bar{h}_{CO_2,17} \quad (6.121)$$

Mole rates of carbon monoxide, methane and carbon dioxide flowing to the steam reforming reactor are known from the gasification analysis (system I), while the steam is used according to the steam reforming reaction equation. Thermodynamic properties at the steam reforming reactor inlet states (state 15 and state 16) are known and the mole flow rates of species at the steam reforming exit (state 17) are known. Only a temperature at the reactor downstream is unknown, and can be calculated from the energy balance equation of the reactor.

The entropy balance for the reforming process is found from the second law of thermodynamics as follows: rate of entropy of gases at the inlet states plus a rate of the entropy generation in the reactor is equal to the rate of entropy of gases at the exit state. Mathematically, it can be expressed by the following equation:

$$\sum_i \dot{m}_{i,SR} s_{i,SR} + \dot{S}_{gen} = \sum_e \dot{m}_{e,SR} s_{e,SR} \quad (6.122)$$

On mole basis, the terms of the above equation can be written as follows:

$$\sum_i \dot{m}_{i,SR} s_{i,SR} = \sum_e \dot{N}_{i,SR} \bar{s}_{i,SR} \quad (6.123)$$

$$\sum_e \dot{m}_{e,SR} s_{e,SR} = \sum_e \dot{N}_{e,SR} \bar{s}_{e,SR} \quad (6.124)$$

For the shown states on the schematic diagram which represents the steam reforming reactor, the above equation can be written as:

$$\sum_i \dot{N}_{i,SR} \bar{s}_{i,SR} = \dot{N}_{CH_4,16} \bar{s}_{CH_4,16} + \dot{N}_{CO,16} \bar{s}_{CO,16} + \dot{N}_{CO_2,16} \bar{s}_{CO_2,16} + \dot{N}_{H_2O,15} \bar{s}_{H_2O,15} \quad (6.125)$$

$$\sum_e \dot{N}_{e,SR} \bar{s}_{e,SR} = \dot{N}_{H_2,17} \bar{s}_{H_2,17} + \dot{N}_{CO,17} \bar{s}_{CO,17} + \dot{N}_{CO_2,17} \bar{s}_{CO_2,17} \quad (6.126)$$

After rearranging the above equation, the entropy generation is given by the following equation:

$$\dot{S}_{gen,SR} = \sum_e \dot{N}_{e,SR} \bar{s}_{e,SR} - \sum_i \dot{N}_{i,SR} \bar{s}_{i,SR} \quad (6.127)$$

And the exergy loss rate is calculated from:

$$\dot{Ex}_{des,SR} = T_o \dot{S}_{gen,SR} \quad (6.128)$$

The producer gas from the steam reforming reactor is further processed in the steam water shift reactor after undergoing a heat exchanging process in the heat exchanger.

6.8.6 Water Gas Shift Reactor

A further processing of the gases to the water gas shift reactor (WGS) also aims to increase a hydrogen yield of the system (Figure 6.7). In this process, carbon monoxide from the gasification process as well as that from the steam reforming reaction will shift by steam to hydrogen and carbon dioxide according to the following reaction:

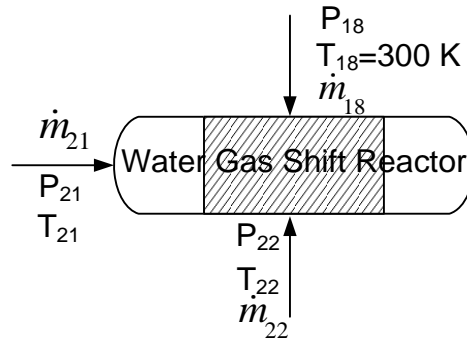
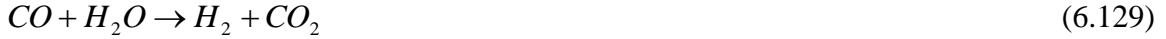


Figure 6.7 A schematic diagram of water gas shift reactor.

The properties for state 21 are known from the SOFC analysis, while the thermodynamic properties of the state 18 are known from the performed analysis on the heat exchanger 17-18-9-10. From the thermodynamic point of view, the water gas shift reactor will be treated in a manner similar to that of the steam reforming reactor. However, in this case, the reaction is exothermic and it takes place at a lower temperature. The process is assumed to take place adiabatically and with no excess steam. Therefore, the energy conservation is given by the following equation:

$$\sum_i \dot{m}_{i,WGS} h_{i,WGS} = \sum_e \dot{m}_{e,WGS} h_{e,WGS} \quad (6.130)$$

The mass flow rate of the species is calculated in terms of their molecular weights and their molar flow rates. The molar flow rate of the carbon monoxide will be the sum of the one from the gasification process and the one from the steam reforming reaction, while the molar flow rate for the other species are known from the mole balance of the reaction equation.

$$\sum_i \dot{m}_{i,WGS} h_{i,WGS} = \sum_e \dot{N}_{i,WGS} \bar{h}_{i,WGS} \quad (6.131)$$

$$\sum_e \dot{N}_{e,WGS} h_{e,WGS} = \sum_e \dot{N}_{e,WGS} \bar{h}_{e,WGS} \quad (6.132)$$

By applying the above equation to the states on the shift reactor control volume gives:

$$\sum_i \dot{N}_{i,WGS} \bar{h}_{i,WGS} = \dot{N}_{H_2,17} \bar{h}_{H_2,17} + \dot{N}_{CO,17} \bar{h}_{CO,17} + \dot{N}_{CO_2,17} \bar{h}_{CO_2,17} + \dot{N}_{H_2O,21} \bar{h}_{H_2O,21} \quad (6.133)$$

$$\sum_e \dot{N}_{e,WGS} \bar{h}_{e,WGS} = \dot{N}_{H_2,22} \bar{h}_{H_2,22} + \dot{N}_{CO_2,22} \bar{h}_{CO_2,22} \quad (6.134)$$

By applying the second law for the water gas shift reactor gives:

$$\dot{S}_{gen,WGS} = \sum_e \dot{N}_{e,WGS} \bar{s}_{e,WGS} - \sum_i \dot{N}_{i,WGS} \bar{s}_{i,WGS} \quad (6.135)$$

For the states on the water gas shift reactor control volume, the equation becomes:

$$\sum_i \dot{N}_{i,WGS} \bar{s}_{i,WGS} = \dot{N}_{H_2,17} \bar{s}_{H_2,17} + \dot{N}_{CO,17} \bar{s}_{CO,17} + \dot{N}_{CO_2,17} \bar{s}_{CO_2,17} + \dot{N}_{H_2O,21} \bar{s}_{H_2O,21} \quad (6.136)$$

$$\sum_e \dot{N}_{e,WGS} \bar{s}_{e,WGS} = \dot{N}_{H_2,22} \bar{s}_{H_2,22} + \dot{N}_{CO_2,22} \bar{s}_{CO_2,22} \quad (6.137)$$

Finally, the exergy loss in the steam shift gas reaction is calculated from:

$$\dot{E}x_{des,WGS} = T_o \dot{S}_{gen,WGS} \quad (6.138)$$

The hydrogen in this case is called secondary hydrogen and is stored after it undergoes a filtration process, while the hydrogen from the gasification process is called primary hydrogen and is used to fuel the SOFC after it is purified from the contaminants.

6.8.7 SOFC Equations

The open circuit voltage of the SOFC is calculated at the average temperature between the mixed anode and cathode inlet flow and the outlet of the SOFC from Nernst's equation as follows:

$$V_{SOFC} = -\frac{\Delta G^o}{2F} - \frac{RT_{SOFC}}{2F} \ln \left(\frac{P_{H_2O}^{SOFC}}{P_{H_2}^{SOFC} \sqrt{P_{O_2}^{SOFC}}} \right) \quad (6.139)$$

where ΔG^o is the standard Gibbs free energy change per mole, R is the universal gas constant (8.314 kJ/kmole-K), and F is the Faraday constant (96,485 coulombs/g-mole). $P_{H_2O}^{SOFC}$, $P_{H_2}^{SOFC}$ and $P_{O_2}^{SOFC}$ are respectively the partial pressure of H₂O and H₂ at the cathode and of O₂ at the anode. The voltage is obtained by subtracting the over potential voltages from the above voltage. The over-potential losses are originated from three

sources: concentration, ohmic and activation. The over potentials due to activation, V_{act} is calculated from general Butler-Volmer equation with a reaction rate constant of 0.5 as follows [128]:

$$V_{act} = \frac{2RT_{SOFC}}{n_{H_2}F} \sinh^{-1}\left(\frac{i}{2i_o}\right) \quad (6.140)$$

This equation is applied for the electrodes, cathode and anode, where i is current density and i_o is apparent exchange current density. The apparent exchange current density is given for cathode by [129]:

$$i_{o,c} = \gamma_c P_{O_2}^{1/4} \exp\left(-\frac{E_{act,c}}{RT_{SOFC}}\right) \quad (6.141)$$

and for anode by:

$$i_{o,a} = \gamma_a P_{H_2} P_{H_2O} \exp\left(-\frac{E_{act,a}}{RT_{SOFC}}\right) \quad (6.142)$$

where the partial pressures are in atmospheric pressure. The ohmic over potential, V_{ohm} obeys ohm's law and is given by:

$$V_{ohm} = iR_{res} \quad (6.143)$$

The resistance of all materials, R_{res} that used in SOFC components is calculated from [129]:

$$R_{res} = CJ \left\{ \coth(J) + B \left[J - 2 \tanh\left(\frac{J}{2}\right) \right] \right\} \quad (6.144)$$

The cross plane resistance area, C is:

$$C = \rho_c t_c + \rho_{ccc} t_{ccc} + \rho_{cca} t_{cca} + \rho_{el} t_{el} + \rho_{cca} t_{cca} + \rho_a t_a \quad (6.145)$$

The ohmic symmetry factor, E_{osf} is:

$$E_{osf} = \frac{t_{ccc}/\rho_{ccc} + t_c/\rho_c}{t_{cca}/\rho_{cca} + t_a/\rho_a} \quad (6.146)$$

The characteristic length, L is:

$$L = \left\{ \frac{\rho_{el} t_{el}}{\left[(t_{cca}/\rho_{cca}) + (t_a/\rho_a) \right]^{-1} + \left[(t_{ccc}/\rho_{ccc}) + (t_c/\rho_c) \right]^{-1}} \right\}^{1/2} \quad (6.147)$$

where the subscripts, *el*, *a*, *c*, *cca*, and *ccc* stand for electrolyte, anode, cathode, current collector anode and current collector cathode respectively.

$$B = E_{osf} (1 + E_{osf})^{-2} \quad (6.148)$$

$$J = \frac{X}{L} \quad (6.149)$$

The respective resistivity, ρ which is a function of temperature is calculated by [130]:

$$\rho = a \exp\left(\frac{b}{T_{SOFC}}\right) \quad (6.150)$$

where *a* and *b* are constants depending on cell material.

The polarization or concentration overpotential, V_{pol} is a summation of overpotential from anode, $V_{pol,a}$ and that from cathode, $V_{pol,c}$ [129]:

$$V_{pol,a} = -\frac{RT_{SOFC}}{2F} \left[\ln\left(1 - \frac{iRT_{SOFC}}{2F} \left(\frac{t_a}{D_{eff,a} P_{H_2}}\right)\right) - \ln\left(1 + \frac{iRT_{SOFC}}{2F} \left(\frac{t_a}{D_{eff,a} P_{H_2O}}\right)\right) \right] \quad (6.151)$$

$$V_{pol,c} = -\frac{RT_{SOFC}}{2F} \ln\left[\frac{P_c - (P_c - P_{O_2}) \exp(iRt_c T_{SOFC} / (4FD_{eff,c} P_c))}{P_{O_2}}\right] \quad (6.152)$$

$$V_{pol} = V_{pol,a} + V_{pol,c} \quad (6.153)$$

where *t* is a thickness of the cell component, *i* is current density, $D_{eff,a}$ is gas diffusivity through anode, $D_{eff,c}$ is gas diffusivity through cathode and P_c is pressure at the cathode.

The output voltage from the cell is given by:

$$V = V_{oc} - V_{act} - V_{ohm} - V_{pol} \quad (6.154)$$

The electric power produced by the fuel cell is:

$$\dot{W}_{SOFC,dc} = VI \quad (6.155)$$

For H_2 fuel, the current *I* is calculated from:

$$I = 2F \cdot \dot{n}_{H_2} \quad (6.156)$$

where 2 is a number of electrons transferred per molecule of fuel and \dot{n}_{H_2} is the H_2 (mol/s) reacting in the hydrogen electrochemical reaction which is solely considered. \dot{n}_{H_2} is calculated in terms of the supplied hydrogen to SOFC, \dot{N}_s and the fuel utilization factor, U_f from the following equation:

$$\dot{n}_{H_2} = U_f \cdot \dot{N}_s \quad (6.157)$$

The fuel cell model developed in this study is based on planer. The preheating air is fed in at the cathode inlet (state 10) and excess depleted air and nitrogen flows out of the cell at the cathode exit (11). On the anode side of the cell, hydrogen is fed in at the anode inlet (state 13) and steam and excess depleted hydrogen flows out at the anode exit (state 14). The SOFC operates in a temperature range near that of the steam biomass gasification which helps to use both of them in the hybrid system. It utilizes by-product gasification hydrogen to produce heat, water (steam) and power. The mass balance equation for SOFC is:

$$\dot{m}_{10} - \dot{m}_{11} + \dot{m}_{13} - \dot{m}_{14} = 0 \quad (6.158)$$

If the fuel cell utilizes fuel by a factor of U_f , the mass flow rate \dot{m}_{13} and \dot{m}_{14} at states of 13 and 14 respectively are related by the following equation:

$$\dot{m}_{14} = (1 - U_f) \dot{m}_{13} \quad (6.159)$$

One mole from water contains a H_2 - O_2 mole ratio of 2. Therefore, it is possible to write a relation between a molar flow rate of oxygen, $\dot{N}_{O_2,10}$ that is used from the supplied air and a molar flow rate of hydrogen that is used from the gasification process as follows:

$$\dot{N}_{13} = 2\dot{N}_{O_2,10} \quad (6.160)$$

That means the consumed oxygen will change according to the utilized hydrogen and both of them will depend on the assumed utilization factor. It is well known that air has approximately a N_2 - O_2 ratio of 79-21 and the nitrogen is treated as an inert substance. Therefore, from the molar flow rate of the utilized oxygen; the total amount of air that supplies to the SOFC can be calculated from:

$$\dot{N}_{10} = 4.762\dot{N}_{O_2,10} \quad (6.161)$$

The supplied air mass flow rate is given in terms of its molar flow rate and its molecular weight, MW_{air} by the following equation:

$$\dot{m}_{10} = MW_{air} \dot{N}_{10} \quad (6.162)$$

The energy balance for the adiabatic SOFC and for the states shown on the schematic diagram of the SOFC is:

$$\sum_i \dot{m}_{i,SOFC} h_{i,SOFC} = \sum_e \dot{m}_{e,SOFC} h_{e,SOFC} + \dot{W}_{SOFC,dc} \quad (6.163)$$

The mass flow rate at the inlet and exit are calculated in terms of their molar flow rates and their molecular weights.

$$\sum_i \dot{m}_{i,SOFC} h_{i,SOFC} = \sum_e \dot{N}_{i,SOFC} \bar{h}_{i,SOFC} \quad (6.164)$$

$$\sum_e \dot{m}_{e,SOFC} h_{e,SOFC} = \sum_e \dot{N}_{e,SOFC} \bar{h}_{e,SOFC} \quad (6.165)$$

where the subscripts i and e refer to inlet and exit states of the SOFC, respectively. For the shown states on the schematic diagram representing the SOFC, the above equations become:

$$\sum_i \dot{N}_{i,SOFC} \bar{h}_{i,SOFC} = \dot{N}_{H_2,13} \bar{h}_{H_2,13} + \dot{N}_{air,10} \bar{h}_{air,10} \quad (6.166)$$

$$\sum_e \dot{N}_{e,SOFC} \bar{h}_{e,SOFC} = \dot{N}_{H_2O,14} \bar{h}_{H_2O,14} + \dot{N}_{O_2,11} \bar{h}_{O_2,11} + \dot{N}_{H_2,11} \bar{h}_{H_2,11} + \dot{N}_{N_2,11} \bar{h}_{N_2,11} \quad (6.167)$$

The entropy balance for the SOFC is obtained by applying the second law of thermodynamics as follows:

$$\sum_i \dot{m}_{i,SOFC} s_{i,SOFC} + \dot{S}_{gen} = \sum_e \dot{m}_{e,SOFC} s_{e,SOFC} \quad (6.168)$$

On mole basis, the terms of the above equation can be rewritten as follows:

$$\sum_i \dot{m}_{i,SOFC} s_{i,SOFC} = \sum_e \dot{N}_{i,SOFC} \bar{s}_{i,SOFC} \quad (6.169)$$

$$\sum_e \dot{m}_{e,SOFC} s_{e,SOFC} = \sum_e \dot{N}_{e,SOFC} \bar{s}_{e,SOFC} \quad (6.170)$$

For the shown states on the schematic diagram of the SOFC, the right side of the above two equations become:

$$\sum_i \dot{N}_{i,SOFC} \bar{s}_{i,SOFC} = \dot{N}_{H_2,13} \bar{s}_{H_2,13} + \dot{N}_{air,10} \bar{s}_{air,10} \quad (6.171)$$

$$\sum_e \dot{N}_{e,SOFC} \bar{s}_{e,SOFC} = \dot{N}_{H_2O,14} \bar{s}_{H_2O,14} + \dot{N}_{O_2,11} \bar{s}_{O_2,11} + \dot{N}_{H_2,11} \bar{s}_{H_2,11} + \dot{N}_{N_2,11} \bar{s}_{N_2,11} \quad (6.172)$$

From which the entropy generation in the SOFC is:

$$\dot{S}_{gen,SOFC} = \sum_e \dot{N}_{e,SOFC} \bar{s}_{e,SOFC} - \sum_i \dot{N}_{i,SOFC} \bar{s}_{i,SOFC} \quad (6.173)$$

The exergy loss in the SOFC is calculated from the following equation:

$$\dot{Ex}_{des,SOFC} = T_o \dot{S}_{gen,SOFC} \quad (6.174)$$

6.8.8 Burner

A burner is used to convert the chemical energy of the unutilized fuel in the SOFC stack, char and tar to heat (Figure 6.8). In this process, more chemical energy is converted to thermal energy. After the SOFC stack, the excess depleted fuel and air, the separated char and tar derived gasification were sent to the burner. It is found from the obtained preliminary results that the air is not sufficient to burn material in the burner; therefore an extra amount of preheated air via stream 35 is fed to the burner to make sure that all materials are completely burned.

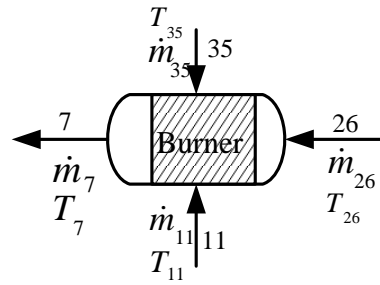


Figure 6.8 A schematic diagram of burner.

Quantity and properties of the excess depleted air and hydrogen (at state 11) are known from the SOFC analyses, quantities and properties of char and tar (at state 26) are found from the gasification module. Therefore, from the energy conservation of the burner, the properties at the burner exit (state 7) can be determined. In the presence of the excess and/or depleted oxygen and oxygen coming from the air, the products of this combustion process contain mainly steam, carbon dioxide and nitrogen according to the following reactions:



where $char_{26}$, tar_{26} and $H_{2,11}$ are respectively the flow rates of char and tar at state 26 and hydrogen at state 11. It is clear from the above reaction equations that hydrogen is oxidized to water (steam), the char (carbon) to carbon dioxide and nitrogen is inert. The

minimum oxygen consumed in the burning process is:

$$O_{2,consumed} = char_{26} + 7.5tar_{26} + 0.5H_{2,11} \quad (6.178)$$

The excess depleted oxygen from the burner former process is the oxygen flows at state 11, $O_{2,11}$ and is known from the SOFC analyses. Therefore, the minimum amount of oxygen that needs the burner is found from the following equation:

$$O_{2,min} = O_{2,consumed} - O_{2,11} \quad (6.179)$$

The oxygen supplied to the burner has to satisfy $O_{2,min}$ at least, and results in a reasonable temperature in the burner. Therefore, preheated burner air, \dot{m}_{35} flows at state 35 on the system flow diagram is found from:

$$\dot{m}_{35} > 4.762O_{2,min} \quad (6.180)$$

The mole flow rates of char and tar are known from the gasifier analyses, while the mole flow rates of unutilized hydrogen, $H_{2,11}$, unutilized oxygen, $O_{2,11}$ and nitrogen, $N_{2,11}$ are known from SOFC analyses. An iteration process is performed with the aid of EES to determine the exact amount of preheating air that is fed to the burner, such that the burner has a reasonable operating temperature and ensures that all the materials sent to the burner are completely burned.

The energy balance for the adiabatic burner and for the states shown on the burner schematic diagram is:

$$\sum_i \dot{m}_{i,Burner} h_{i,Burner} = \sum_e \dot{m}_{e,Burner} h_{e,Burner} \quad (6.181)$$

The mass flow rate at the inlet and exit are calculated in terms of their molar flow rates and their molecular weights.

$$\sum_i \dot{m}_{i,Burner} h_{i,Burner} = \sum_i \dot{N}_{i,Burner} \bar{h}_{i,Burner} \quad (6.182)$$

$$\sum_e \dot{m}_{e,Burner} h_{e,Burner} = \sum_e \dot{N}_{e,Burner} \bar{h}_{e,Burner} \quad (6.183)$$

where the subscripts i and e refer to the inlet and exit states of the burner, respectively. For the shown states on the schematic diagram representing the burner, the above equations become:

$$\sum_i \dot{N}_{i,Burner} \bar{h}_{i,Burner} = \dot{N}_{H_{2,11}} \bar{h}_{H_{2,11}} + \dot{N}_{N_{2,11}} \bar{h}_{N_{2,11}} + \dot{N}_{O_{2,11}} \bar{h}_{O_{2,11}} + \dot{N}_{air,35} \bar{h}_{air,35} \quad (6.184)$$

$$\sum_e \dot{N}_{e,Burner} \bar{h}_{e,Burner} = \dot{N}_{H_2O,7} \bar{h}_{H_2O,7} + \dot{N}_{N_2,7} \bar{h}_{N_2,7} + \dot{N}_{CO_2,7} \bar{h}_{CO_2,7} + \dot{N}_{air,7} \bar{h}_{air,7} \quad (6.185)$$

The properties of states 11, 35 and the mole flow rates at state 7 are known; the only unknown property is the temperature at the burner exit which can be determined from equations 6.184 and 6.185.

The entropy balance for the burner is obtained by applying the second law of thermodynamics as follows:

$$\sum_i \dot{m}_{i,Burner} s_{i,Burner} + \dot{S}_{gen,Burner} = \sum_e \dot{m}_{e,Burner} s_{e,Burner} \quad (6.186)$$

On mole basis, the terms of the above equation can be rewritten as follows:

$$\sum_i \dot{m}_{i,Burner} s_{i,Burner} = \sum_i \dot{N}_{i,Burner} \bar{s}_{i,Burner} \quad (6.187)$$

$$\sum_e \dot{m}_{e,Burner} s_{e,Burner} = \sum_e \dot{N}_{e,Burner} \bar{s}_{e,Burner} \quad (6.188)$$

For the shown states on the schematic diagram representing the burner, a right side of the above two equations expand to the following two equations:

$$\sum_i \dot{N}_{i,Burner} \bar{s}_{i,Burner} = \dot{N}_{H_2,11} \bar{s}_{H_2,11} + \dot{N}_{N_2,11} \bar{s}_{N_2,11} + \dot{N}_{O_2,11} \bar{s}_{O_2,11} + \dot{N}_{air,35} \bar{s}_{air,35} \quad (6.189)$$

$$\sum_e \dot{N}_{e,Burner} \bar{s}_{e,Burner} = \dot{N}_{H_2O,7} \bar{s}_{H_2O,7} + \dot{N}_{N_2,7} \bar{s}_{N_2,7} + \dot{N}_{CO_2,7} \bar{s}_{CO_2,7} + \dot{N}_{air,7} \bar{s}_{air,7} \quad (6.190)$$

From which the entropy generation in the burning process is given by:

$$\dot{S}_{gen,Burner} = \sum_e \dot{N}_{e,Burner} \bar{s}_{e,Burner} - \sum_i \dot{N}_{i,Burner} \bar{s}_{i,Burner} \quad (6.191)$$

The exergy loss in the burning process is calculated from the following equation:

$$\dot{E}x_{des,Burner} = T_o \dot{S}_{gen,Burner} \quad (6.192)$$

6.8.9 System II Energy Efficiencies

Three energy efficiencies are defined: electrical efficiency of SOFC, electrical efficiency of gas turbine and hydrogen yield. Hydrogen is used to fuel the SOFC; therefore, its electrical efficiency is given by the following equation:

$$\eta_{el,SOFC} = \frac{\dot{W}_{SOFC}}{\dot{E}n_{Biomass}} \quad (6.193)$$

while the turbine is defined based on the lower heating value of the wood sawdust fed to the system as follows:

$$\eta_{el,t} = \frac{\dot{W}_{t,net}}{\dot{E}n_{Biomass}} \quad (6.194)$$

The overall system electrical efficiency is defined as follows [131]:

$$\eta_{el,overall} = \eta_{el,SOFC} + \eta_{el,t} \quad (6.195)$$

The efficiency based on hydrogen yield from the downstream gasification process is calculated from:

$$\eta_{H_2} = \frac{\dot{E}n_{H_2}}{\dot{E}n_{Biomass}} \quad (6.196)$$

where the subscripts *el* and *t* stand for electricity and turbine, respectively.

6.8.10 System II Exergy Efficiencies

A study of the system exergy efficiency or second law efficiency gives an indication of the potential that the system has to increase the secondary hydrogen yield from gasification via downstream processes; from external steam reforming and external steam shift reactions, and to use the primary hydrogen in producing electricity and heat in different processes through the system. Four exergy efficiencies were defined for this system based on the exergy of the fed saw dust: the exergy efficiency for producing power from SOFC, the exergy efficiency for producing power from the gas turbine, the exergy efficiency that considers production of the secondary hydrogen from the gasification downstream processes and the efficiency considers all power from the system. The exergy efficiency for producing power from SOFC is:

$$\eta_{EX,SOFC} = \frac{\dot{E}x_{SOFC}}{\dot{E}x_{Biomass}} \quad (6.197)$$

The exergy efficiency that considers production of electricity and accompanies an expansion process of gases in the gas turbine is:

$$\eta_{EX,t} = \frac{\dot{E}x_{t,net}}{\dot{E}x_{Biomass}} \quad (6.198)$$

The third exergy efficiency considers the derived gasification downstream reactions and it is called secondary hydrogen:

$$\eta_{EX,H_2} = \frac{\dot{E}x_{H_2}}{\dot{E}x_{Biomass}} \quad (6.199)$$

The overall system exergetic efficiency for electricity production is calculated from:

$$\eta_{EX,Overall} = \eta_{EX,SOFC} + \eta_{EX,t} \quad (6.200)$$

where $\dot{E}x_{H_2}$ is the exergy flow rate of the secondary hydrogen and $\dot{E}x_{biomass}$ is the exergy flow rate of biomass. The exergy flows with species at different states are calculated in a similar way to that used under System I. The exergy of power is equal to the power itself.

6.9 System III Components

Most of these system components were described in System I and System II. However, a gasifier analysis was done under analysis of System I and the description of the rest was done under analysis of System II. For more interesting details it is recommended follow the specific sections. The same gasifier and SOFC modules are used in this system; therefore, the same assumptions under which they were developed are valid for this system.

A reasonable basis of comparison between the three systems requires using common operating parameters to drive the parametric study for the three systems. These are a gasification temperature range and a steam-biomass ratio. In addition, the module that was developed for a component in previous systems will be used for the same component in this system. The SOEC and the lumped SOFC-SOEC will be analyzed in the following sections.

6.9.1 Solid Oxide Electrolyse Cell

Water electrolysis at the SOEC's cathode results in two oxygen ions and one hydrogen ion. The ions will attract at the anode to form oxygen, leaving two free electrons to move from anode to cathode to perform the electrochemical reaction. The total energy demand, ΔH for SOEC hydrogen production can be expressed as:

$$\Delta H = \Delta G + T\Delta S \quad (6.201)$$

where ΔG is the electrical energy demand (free Gibbs energy change) and $T\Delta S$ is the

thermal energy demand (J molH_2^{-1}). The voltage will be derived from the same equation under an assumption that a reaction takes place under the equilibrium condition where the reaction of water decomposing is reverse to the reaction of water product. Similarly, to calculate the open circuit voltage of SOEC, the Nernst equation form is used as follows:

$$V_{SOEC} = -\frac{\Delta G_0}{2F} - \frac{RT_{SOEC}}{2F} \ln \left(\frac{P_{H_2O}^{SOEC}}{P_{H_2}^{SOEC} \sqrt{P_{O_2}^{SOEC}}} \right) \quad (6.202)$$

Iora et al. [132] expected a significant improvement when a steam-electrolyze operating at a higher temperature. In the case of using cells that have the same materials, one can estimate how much auxiliary power is needed for SOEC by calculating the reversible voltage difference in the SOEC-SOFC system from the following equation:

$$V_{SOEC} - V_{SOFC} = \frac{RT}{4F} \ln \left(\frac{P_{O_2}^{SOEC}}{P_{O_2}^{SOFC}} \right) \quad (6.203)$$

where $T_{SOFC} = T_{SOEC} = T$. The consumed power in an existence of current I , is calculated from:

$$W_{rev} = I \frac{RT}{4F} \ln \left(\frac{P_{O_2}^{SOEC}}{P_{O_2}^{SOFC}} \right) \quad (6.204)$$

The current is calculated in terms of oxygen mole flow rate, \dot{n}_{O_2} as follows:

$$I = 4\dot{n}_{O_2} F \quad (6.205)$$

SOFC is always at a exothermic mode of operation while the SOEC mode of operation depends on the operating voltage. The SOEC mode of operation can be neutral at neutral voltage, endothermic at an operating voltage lower than the neutral voltage or exothermic at an operating voltage higher than the neutral voltage. The cycle voltage is neutral at a zero open circuit voltage or at voltage that corresponds to an efficiency of 100 % of hydrogen production [115]. The efficiency is defined as the ratio of a heating value of generated hydrogen to power input to the cell i.e.

$$\eta_{H_2} = \frac{\dot{N}_{H_2} LHV_{H_2}}{IV_{SOFC}} \quad (6.206)$$

In the case of an SOFC-SOEC combination, the hydrogen is consumed and the system produces oxygen and therefore the efficiency becomes:

$$\eta_{O_2} = \frac{\dot{N}_{O_2} LHV_{O_2}}{IV_{SOEC}} \quad (6.207)$$

It is favourable from both the operational and hydrogen production costs to operate SOEC near neutral voltage [115].

6.9.2 Lumped SOFC-SOEC

The lumped SOFC-SOEC module is based on a planar design in which their geometries and material related data are identical. The derived products of the SOFC are utilized in the SOEC such that the steam circulates from the SOFC to the SOEC and the hydrogen circulates from the SOEC to the SOFC (Figure 6.9). The preheating air is fed to SOFC's cathode inlet (state 10) and excess depleted air and nitrogen flows out the SOFC's cathode exit (state 11). On the anode of the SOFC, hydrogen is fed into the anode inlet (state 13) and steam and excess depleted hydrogen flows out at the anode exit (state 14) and circulates to feed into the SOEC's cathode (state 14). Excess depleted steam and hydrogen circulates to the SOFC's anode (state 13). On the SOEC's anode, oxygen flows out from the anode exit. The lumped SOFC-SOEC system operates in a temperature range near to that of the steam biomass gasification which helps to use both of them in the hybrid system. The mass balance equation for the lumped SOFC-SOEC is:

$$\dot{m}_{10} - \dot{m}_{11} - \dot{m}_{12} = 0 \quad (6.208)$$

One mole of water contains O₂-H₂ mole ratio of 2. The hydrogen will circulate to be used in the SOFC while O₂ sends to the burner. Therefore, it is possible to write a relation between a molar flow-rate of the SOEC derived oxygen $\dot{N}_{O_2,12}$ and the circulated hydrogen as follows:

$$2\dot{N}_{H_2,13} = \dot{N}_{O_2,12} \quad (6.209)$$

This means the consumed oxygen will change according to the utilized hydrogen and both of them will depend on the assumed utilization factor. It is well known that air has an approximate N₂- O₂ ratio of 79-21 and the nitrogen is treated as an inert substance. Therefore, from the molar flow rate of the utilized oxygen, the total amount of air supplied to the SOFC can be calculated from:

$$\dot{N}_{air,10} = 4.762\dot{N}_{H_2,13} \quad (6.210)$$

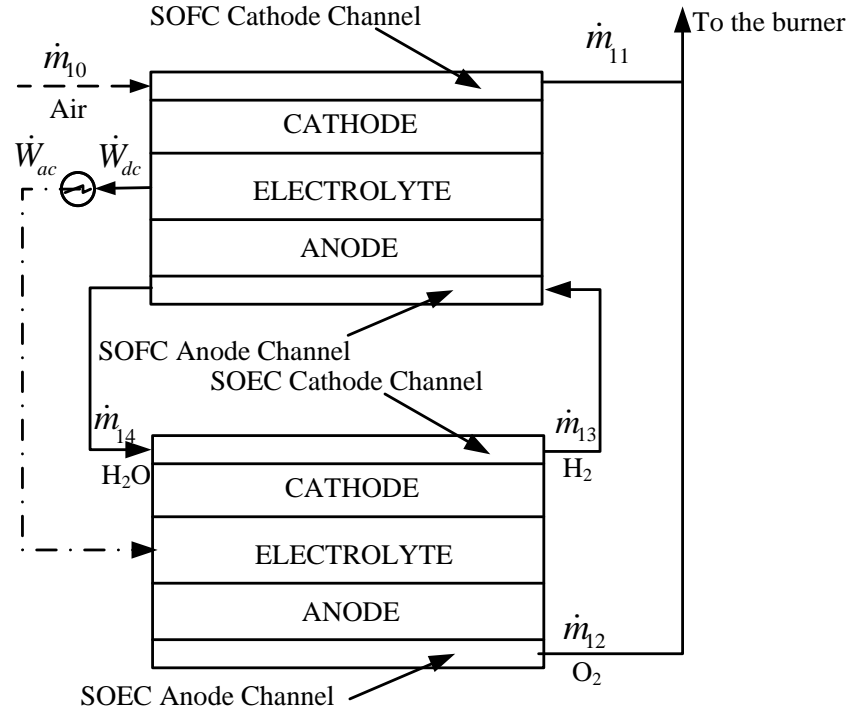


Figure 6.9 A schematic diagram of lumped SOFC-SOEC subsystem.

To simplify the analysis, for this system, it is assumed that the supplied air is equal to that used in the SOFC preheated air in System II. Accordingly, the circulated hydrogen in the lumped system is equal to hydrogen flows at state point 13 in System II. The amount of air is calculated in terms of its molar flow rate and its molecular weight, MW_{air} by the following equation:

$$\dot{m}_{air,10} = MW_{air} \dot{N}_{air,10} \quad (6.211)$$

The energy balance for the adiabatic lumped SOFC-SOEC and for the states shown in the schematic diagram of the SOFC-SOEC is:

$$\sum_i (\dot{m}h)_{SOFC-SOEC,i} = \sum_e (\dot{m}h)_{SOFC-SOEC,e} \quad (6.212)$$

The mass flow rate at the inlet and exit are calculated in terms of their molar flow rates and their molecular weights.

$$\sum_i (\dot{m}h)_{SOFC-SOEC,i} = \sum_i (\dot{N}\bar{h})_{SOFC-SOEC,i} \quad (6.213)$$

$$\sum_e (\dot{m}h)_{SOFC-SOEC,e} = \sum_e (\dot{N}\bar{h})_{SOFC-SOEC,e} \quad (6.214)$$

where the subscripts i and e refer to the inlet and exit states of the lumped SOFC-SOEC,

respectively. For the shown states on the schematic diagram which represents the lumped SOFC-SOEC system, the above two equations can be rewritten as follows:

$$\sum_i (\dot{N}\bar{h})_{SOFC-SOEC,i} = \dot{N}_{air,10} \bar{h}_{air,10} \quad (6.215)$$

$$\sum_e (\dot{N}\bar{h})_{SOFC-SOEC,e} = \dot{N}_{O_2,11} \bar{h}_{O_2,11} + \dot{N}_{O_2,12} \bar{h}_{O_2,12} + \dot{N}_{N_2,11} \bar{h}_{N_2,11} \quad (6.216)$$

As the operating conditions of the SOFC and SOEC are assumed identical, it is possible to rewrite Equation 6.216 as follows:

$$\sum_e (\dot{N}\bar{h})_{SOFC-SOEC,e} = (\dot{N}_{O_2,11} + \dot{N}_{O_2,12}) \bar{h}_{O_2,11} + \dot{N}_{N_2,11} \bar{h}_{N_2,11} \quad (6.217)$$

The entropy balance for the SOFC-SOEC is obtained by applying the second law of thermodynamics as follows:

$$\sum_i (\dot{m}s)_{SOFC-SOEC,i} + \dot{S}_{gen,SOFC-SOEC} = \sum_e (\dot{m}s)_{SOFC-SOEC,e} \quad (6.218)$$

On mole basis, the terms of the above equation can be rewritten as follows:

$$\sum_i (\dot{m}s)_{SOFC-SOEC,i} = \sum_i (\dot{N}\bar{s})_{SOFC-SOEC,i} \quad (6.219)$$

$$\sum_e (\dot{m}s)_{SOFC-SOEC,e} = \sum_e (\dot{N}\bar{s})_{SOFC-SOEC,e} \quad (6.220)$$

For the shown states on the schematic diagram which represents the lumped SOFC-SOEC system, the right side of the above two equations is expanded to state as follows:

$$\sum_i (\dot{N}\bar{s})_{SOFC-SOEC,i} = \dot{N}_{air,10} \bar{s}_{air,10} \quad (6.221)$$

$$\sum_e (\dot{N}\bar{s})_{SOFC-SOEC,e} = \dot{N}_{O_2,11} \bar{s}_{O_2,11} + \dot{N}_{O_2,12} \bar{s}_{O_2,12} + \dot{N}_{N_2,11} \bar{s}_{N_2,11} \quad (6.222)$$

The operating conditions of the SOFC and SOEC are assumed identical; it is possible to rewrite Equation 6.222 as follows:

$$\sum_e (\dot{N}\bar{s})_{SOFC-SOEC,e} = \bar{s}_{O_2,11} (\dot{N}_{O_2,11} + \dot{N}_{O_2,12}) + \dot{N}_{N_2,11} \bar{s}_{N_2,11} \quad (6.223)$$

From which the entropy generation in the SOFC-SOEC is:

$$\dot{S}_{gen,SOFC-SOEC} = \sum_e (\dot{N}\bar{s})_{SOFC-SOEC,e} - \sum_i (\dot{N}\bar{s})_{SOFC-SOEC,i} \quad (6.224)$$

The exergy loss in the SOFC-SOEC is calculated from the following equation:

$$\dot{E}x_{des,SOFC-SOEC} = T_0 \dot{S}_{gen,SOFC-SOEC} \quad (6.225)$$

6.9.3 System III Energy Efficiencies

The SOEC derived hydrogen is used internally in the lumped SOFC-SOEC system to fuel the SOFC. The gasification derived hydrogen and that derived from the processing of by-product gasification gas in a steam reforming reactor and water gas shift reactor are stored. Two energy efficiencies are defined: electrical efficiency of gas turbine and efficiency that considers hydrogen yield. The turbine efficiency is defined based on the LHV of the sawdust wood fed to the system as follows:

$$\eta_{el,t} = \frac{\dot{W}_{t,net}}{\dot{m}_{biomass} \cdot LHV_{biomass}} \quad (6.226)$$

The efficiency that considers the hydrogen yield from the gasification as well as the downstream gasification processes is calculated from:

$$\eta_{en,H_2} = \frac{\dot{E}n_{H_2}}{\dot{m}_{biomass} \cdot LHV_{biomass}} \quad (6.227)$$

where the subscripts t and H_2 stand for turbine and hydrogen, respectively.

6.9.4 System III Exergy Efficiencies

A study of the system exergy efficiency or second law efficiency gives an indication of the potential that the system has to increase the hydrogen yield from steam sawdust gasification and from processing the by-product gasification gas in downstream processes; external steam reforming and external water gas shift reactions. In addition, gasification products in electricity production and heat in different processes inside the system is used. Two exergy efficiencies were defined for this system based on the exergy of the fed sawdust: the exergy efficiency for producing power from the gas turbine and the exergy efficiency that considers the hydrogen yield.

The exergy efficiency that considers electricity production and accompanies an expansion of gases in the gas turbine is:

$$\eta_{ex,t} = \frac{\dot{E}x_{t,net}}{\dot{E}x_{biomass}} \quad (6.228)$$

The second exergy efficiency that considers the system hydrogen yield from the gasification and the gasification downstream reactions is calculated from:

$$\eta_{ex,H_2} = \frac{\dot{E}x_{H_2}}{\dot{E}x_{biomass}} \quad (6.229)$$

where $\dot{E}x_{H_2}$ is the exergy flow rate of the derived hydrogen and $\dot{E}x_{biomass}$ is the exergy flow rate with fed sawdust. The exergy flows with species at different states is calculated in a way similar to that discussed under System I.

6.10 Systems Exergoeconomic Analysis

This type of analysis combines both exergy analysis and cost accounting as a powerful tool for the systematic study and optimization of energy systems [133]. Application of second law costing methods is carried out by assigning costs to exergy. Knowing the cost of the exergy supplied to a component allows an economic analysis of that component and accordingly design, maintenance and operation decisions can be made without contending with the whole system [134].

Exergoeconomic is a precise characterization of an exergy-aided cost-reduction approach. Many names were given to the proposed exergoeconomic approaches, including, for example [135]: Exergy Economics Approach (EEA), First Exergoeconomic Approach (FEA), Specific Exergy Costing Method (SPECOC) etc. It is reported that the main differences among the approaches refer to: the definition of exergetic efficiencies, the development of auxiliary costing equations and the productive structure.

To evaluate hydrogen production from biomass exergoeconomically, the following steps are followed [136]: detailed exergy analysis, economic analysis of each component, calculation of the cost of each stream using an appropriate cost method, and finally evaluation with the aid of some relevant exergoeconomic variables. Once fuel and product definitions are the same, the costs calculated by the various approaches are the same [137]. The capital cost for large biomass gasification systems is about \$700/kW of H₂ [138].

For a system component that has an inlet stream i and or an exit stream e , its exergy cost is:

$$\dot{C} = c\dot{E}x \quad (6.230)$$

where c is the cost per exergy unit in $\$/\text{kWh}$ and \dot{E}_x is the exergy rate $[\text{kW}]$ with the flowing stream. The concept of exergy is also called available energy, availability or useful energy, which is the resource of value or the commodity of value and provides the key to cost accounting [134]. Part of exergy is converted to the desired product(s), part of it is consumed by the process and known as internal loss, and part of it is lost and known as external loss. Exergy analysis aims to identify the sources of thermodynamic inefficiencies (consumptions and losses) in order to make design changes that lead to improved overall system efficiency [136].

Tsatsaronis et al. [139] presented an exergoeconomic analysis methodology and evaluation of energy conversion plants. Tsatsaronis et al. [136] applied that methodology to a coal-fired steam power plant. Kim et al. [140] applied an exergy costing method to 1-MW gas turbine cogeneration with a waste-heat boiler. They found that the unit exergy costs increase as the production process continues. Also, they found that electricity cost increases with the input cost. Balli et al. [141] performed an exergoeconomic analysis for a combined heat and power (CHP) system that was installed in Eskisehir City, Turkey. The obtained results indicate that the produced electrical power cost was 18.51 US\$/GW. Colpan et al. [142] investigated the thermo-economic aspects of the Bilkent combined cycle cogeneration plant in Turkey. Cost balances and auxiliary equations are applied to different components used in the plant; the accounted cost of exergy unit from electrical power was nearly the same (18.89 US\$/GW).

In the present study, the SPECOC approach for calculating costs in thermal systems is followed. It is based on three steps [143]. In the first step, identify the exergy streams by deciding the analysis of the system components should be conducted by using total exergy. In the second step, define the fuel and the products from each component. In the last step, cost equations are built based on exergy by assigning a system of experiences with its surroundings to the sources of inefficiencies within it. A cost balance applies to any component, k , in the system states as (Figure 6.10): the sum of cost rates of entering exergy stream(s), i plus the cost rate due to expenses of investment and operating and maintenance, \dot{Z} equals a sum of the cost rates of exiting stream(s), j . The above expression is mathematically expressed by the following equation [144]:

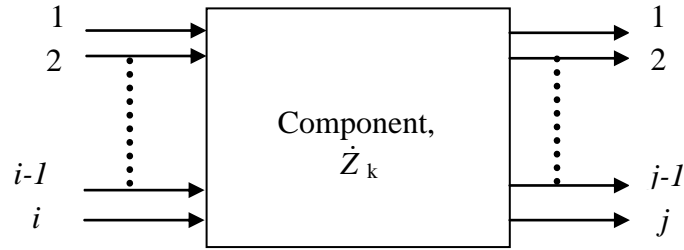


Figure 6.10 Schematic diagram showing exergoeconomic analysis for a component.

$$\sum_i \dot{C}_{i,k} + \dot{Z}_k = \sum_j \dot{C}_{j,k} \quad (6.231)$$

where \dot{C} is exergy costing, and c denotes average cost per unit of exergy. For N exiting streams from a component will have N unknowns and for a system that has K components will have k times N unknowns. To solve the obtained system of equations or to find the unknowns, $N-1$ extra or auxiliary equations are obtained by applying F (Fuel) and P (Product) principles [135]. The formal principle refers to the removal of exergy from an exergy stream within the component under the study. It states that the average specific cost or cost per exergy unit associated with this removal of exergy must be equal to the average specific cost at which the removed exergy has been supplied to the same stream in upstream components, while the latter principle refers to the supplied exergy stream within the component under study. It states that each exergy unit is supplied to any stream associated with the exergetic product of the component at the same cost. The equations describe the balance of exergy of the different components which constitute the systems, and in terms of their cost are given in Table A1-A3. Based on the number of unknowns, the number of extra equation(s) is decided by applying the principle of fuel and product rules. In addition to the principal equations, the extra equations are also developed and included in the same table. By solving the derived equations, exergy costing of the different streams can be defined. The cost of owning and operating the component is [140]:

$$\dot{Z}_k = \left[\frac{\phi \cdot \dot{C}_o}{\tau} \right]_k \quad (6.232)$$

where ϕ is the operating and maintenance factor excluding fuel, \dot{C}_o is the annualized cost of the component and τ is the annual operation time of the component k at the nominal

capacity. The operating and maintenance cost will be taken into consideration through $\phi=1.06$ [140]. The annualized cost is calculated by converting the present worth of the component by using the capital recovery factor, CRF as follows:

$$\dot{C}_o = PW \cdot CRF \quad (6.233)$$

The present worth of a system component can be calculated from the initial investment, C_0 , the present worth factor, PWF and the salvage value at the end of component life n, S_n , as follows:

$$PW = C_0 - S_n \cdot PWF \quad (6.234)$$

The initial investment cost, C_0 for the components is adopted under the criteria such that its operating condition does not go beyond the maximum value obtained by applying the equations of a cost model that was presented in Calise et al. [146] for turbine, compressor and heat exchanger, respectively, and they are as follows:

$$\frac{C_0}{\dot{W}_{t,max}} = 1318.5 - 98.328 \ln(\dot{W}_{t,max}), \dot{W}_{t,max} < 585 \text{ kW} \quad (6.235)$$

$$\dot{W}_{c,max} = 445 \left(\frac{C_0}{91562} \right)^{0.67}, \dot{W}_{c,max} < 1156 \text{ kW} \quad (6.236)$$

$$A_{HE} = 0.093 \left(\frac{C_0}{130} \right)^{0.75}, A_{HE} < 272 \text{ m}^2 \quad (6.237)$$

where $\dot{W}_{t,max}$ is the maximum power that can be achieved by the turbine, $\dot{W}_{c,max}$ is the maximum power that can be applied to the compressor and A_{HE} is the maximum permissible heat transfer area that can be used in the heat exchanger. The restrictions used with the above equations are based on the initial investment cost. The initial cost of the components that are used in the systems is given in Table A4-Table A6. The capital recovery factor is calculated in terms of the interest rate, i and the expected life of the component, n from:

$$CRF = \frac{i(i+1)^n}{(1+i)^n - 1} \quad (6.238)$$

The salvage factor taken is 10 % of the initial investment [140]. The present worth factor is simply calculated from:

$$PWF = (i + 1)^{-n} \quad (6.239)$$

The data related to economic analysis are given in Table 7.6. The exergetic sawdust cost rate \dot{C}_f is calculated in terms of its energetic cost rate, \dot{C}_e , time of operation, τ and the quality coefficient as follows:

$$\dot{C}_f = \frac{\dot{C}_e}{\tau \cdot \beta} \quad (6.240)$$

The energetic cost rate is given by [141]:

$$\dot{C}_e = \frac{Pr \cdot LHV \cdot \tau}{ER} \quad (6.241)$$

where Pr is the sawdust price, ER is the exchange rate in CA\$/US\$ and LHV and τ are as defined above. The purchasing cost of the system components is adopted such that the initial investment of the burner, the steam reforming reactor and the steam shifting reactor are assumed to have the same purchasing cost as the combustion chamber. Also, the gas compressor is assumed to have the same initial investment as the fuel compressor.

The annualized cost of the SOFC is calculated by the costing model that was given in Plazzi et al. [145]. According to this model, the cost of SOFC stack is given by:

$$C_{Stack} = (2.7C_{SOFC}N_{SOFC} + 2.507N_{Stack}A_{SOFC}) \quad (6.242)$$

where the cost of one cell, C_{SOFC} is calculated in terms of its area from the following equation

$$C_{SOFC} = 0.1442A_{SOFC} \quad (6.243)$$

and the number of used stacks is given by

$$N_{Stack} = \frac{\text{Total active surface area}}{\text{Active area of one stack}} \quad (6.244)$$

The costs of owning and operating for the system components and for the three systems are given in Appendix A.

Chapter 7

RESULTS AND DISCUSSION

7.1 Introduction

A good approach can determine the optimum conditions which lead to appreciable hydrogen product from the gasified biomass. A performed parametric study on the used biomass and within steam ranges will help in identifying the more sensitive parameters to the hydrogen yield and feasibility of hydrogen production via biomass gasification from the first and second laws of thermodynamics views. This study applies to a self-heated gasifier in order to analyse the characteristics of hydrogen production from biomass gasification.

The gasifier considers the heart of the gasification process. In this study, a scheme which utilizes equilibrium reactions to describe the gasification process is proposed. It is used to simulate hydrogen production from biomass steam gasification. To model an approach for the biomass gasification, it is important to know biomass properties, specifically, the proximate and the ultimate analysis and its heating value. The biomass has a higher carbon-hydrogen ratio and significantly lower sulfur and nitrogen contents. The low sulfur and nitrogen contents of biomass make potential pollutants which are neutral or very low. The biomass is considered a neutral resource regarding the CO₂ life cycle. The modeling approach for hydrogen production from biomass gasification through a parametric study aims to calculate producer hydrogen from a gasification of biomass amount in the presence of an amount of the gasification agent (steam). To conduct the gasification reaction, heat is required and this is taken into consideration by assuming the gasifier is self-heated.

The Engineering Equation Solver (EES) code for the Microsoft windows operating system is written in order to solve the approach developed to simulate the gasification process, proposed systems and perform a parametric study (B1-B4). The code is able to calculate the gas fraction content, the energy, available energy or exergy and exergy destruction at an amount of steam and biomass as well as at different gasification temperatures. EES has built in thermodynamic properties which prevents errors in calculating the needed thermodynamics properties from occurring. This also

prevents errors from using a code that was written by the others. All of the above-mentioned features eliminate the necessity of validating the results. However, in order to support the results obtained, the author takes into consideration as much of the available literature as possible. The analyses are performed according to the flow chart in Figure 7.1.

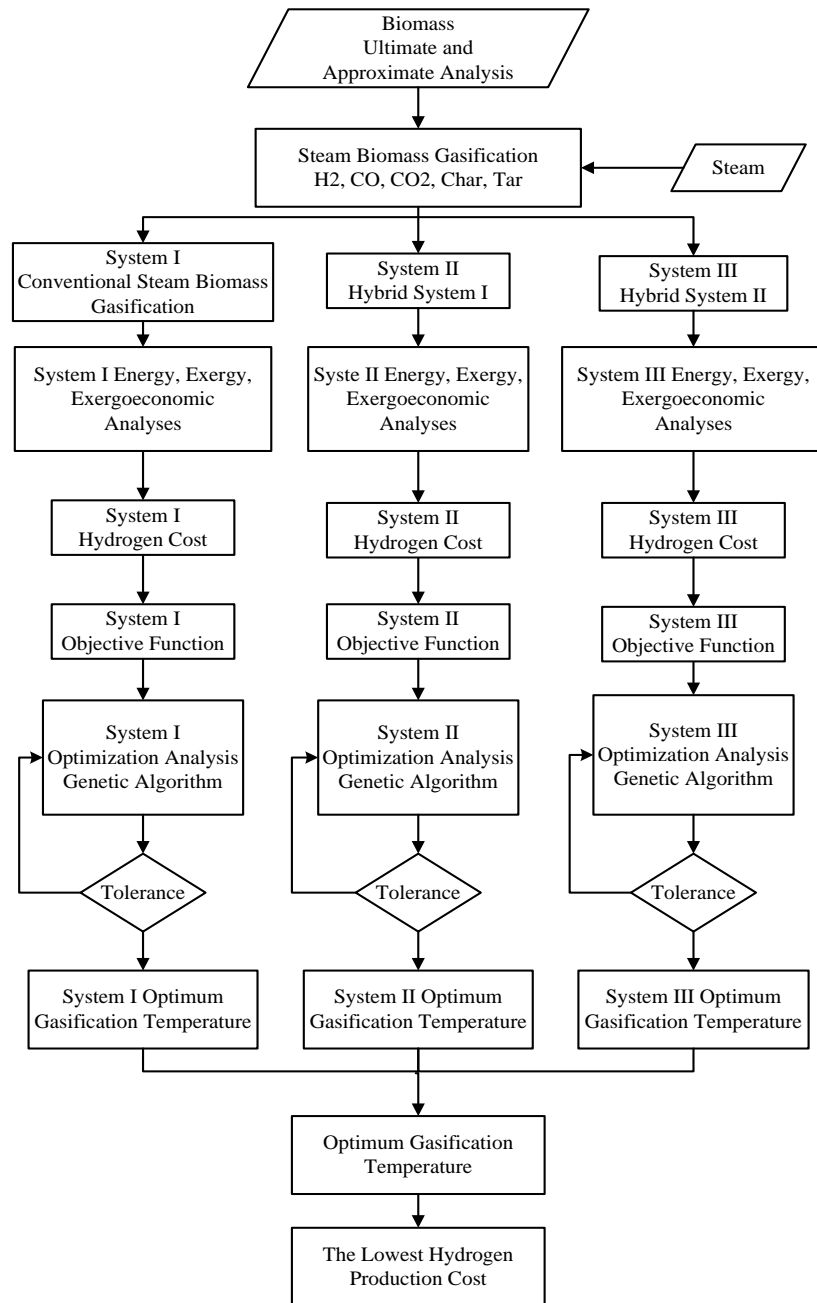


Figure 7.1 Flow-diagram for analysis steps.

The presented results are of the performed parametric study: to study parameters that affect hydrogen production from sawdust steam gasification, to evaluate the overall efficiency (energy and exergy), and to perform exergoeconomic and optimization analyses of the proposed systems. Most of the presented results in the following sections are adopted from the published work in [49, 147, 148].

7.2 Data Utilization

7.2.1 Data for Biomass and Thermodynamics Properties

The ultimate and proximate analysis of the used wood is given in Table 7.1.

Table 7.1 Ultimate and proximate analysis of sawdust wood

Element	Weight on dry basis [%]
C	48.01
H	6.04
O	45.43
N	0.15
S	0.05
Ash	0.32
HHV (MJ/kg)	18.4
Volatile matter	76.78
Fixed carbon	18.7
Ash	0.32

Source: [18]

Standard chemical exergy and enthalpy of formation for different compounds are summarized in Table 7.2. The coefficients, a' , b' , c' and d' of different gases are summarized in Table 7.3.

7.2.2 Data for Gasifier

The analysis used is with respect to the black box gasifier i.e. it assumes the change happens at the inlet and exit.

- Ambient condition $T_0 = 298 \text{ K}$ and $P_0 = 1 \text{ atm}$.
- Gasifier operates in a temperature range of 1000-1423 K and pressure of 1.2 bar.
- Gasifier dimensions are 0.080 m outside diameter and 0.50 m height.
- Gasifier has wall with insulation thickness, $x_{ins} = 5 \text{ mm}$, thermal conductivity, $k_{ins} = 0.06 \text{ w/(m.K)}$ and emissivity, $\varepsilon_{ins} = 0.01$.
- The average wind velocity, $U_o = 2 \text{ m/s}$.
- The feeding biomass, α in a range of 10 to 32 kg/s
- The injected steam, γ in a range of 4.5 to 6.3 kg/s

Table 7.2 Standard chemical exergy for different components

Component	Standard chemical exergy [kJ/kmol]	Enthalpy of formation [kJ/kmol]
CH ₄	831,650	-74,850
CO	275,100	-110,530
CO ₂	19,870	-393,520
H ₂ O	9,500	-241,820
H ₂	236,100	0.0
C	410,260	0.0
C ₆ H ₆	3,303,600	82,930

Source: [144]

Table 7.3 The coefficients used in constant specific heat empirical equation

Gas	a'	b'	c'	d'
CO	28.16	0.1675×10^{-2}	0.5372×10^{-5}	-2.222×10^{-9}
CO ₂	22.26	5.981×10^{-2}	-3.501×10^{-5}	-7.469×10^{-9}
H ₂ O	32.24	0.1923×10^{-2}	1.055×10^{-5}	-3.595×10^{-9}
H ₂	29.11	-0.1916×10^{-2}	0.4003×10^{-5}	-0.8704×10^{-9}
CH ₄	19.89	5.2040×10^{-2}	1.269×10^{-5}	-11.01×10^{-9}

Source: [127]

7.2.3 Data for Gas Turbine

The isentropic efficiency of the gas turbine, η_t is 80%.

The temperature at the gas turbine exit is calculated from the following equation:

$$T_8 = T_7 \left[1 - \eta_t \left(1 - \left(\frac{P_7}{P_8} \right)^{\frac{1-\gamma_{gas}}{\gamma_{gas}}} \right) \right] \quad (7.1)$$

$$\dot{W}_t = \dot{m}_7 h_7 - \dot{m}_8 h_8 \quad (7.2)$$

$$\dot{W}_{net} = \dot{W}_t - \dot{W}_{com} \quad (7.3)$$

7.2.4 Data for Air Compressor

Inlet temperature of the air compressor is T_0

Inlet pressure of the air compressor is P_{atm}

Specific heats ratio of air, $\gamma_{air}=1.4$

Constant pressure specific heat of air, $C_{P,air}=1.004 \text{ kJ kg}^{-1} \text{ K}^{-1}$

Isentropic efficiency of air compressor, η_c is 80%

$$T_e = T_i \left[1 + \eta_c^{-1} \left(\left(\frac{P_e}{P_i} \right)^{\frac{\gamma_{air}-1}{\gamma_{air}}} - 1 \right) \right] \quad (7.4)$$

$$\dot{W}_{com} = \dot{m}_i h_i - \dot{m}_e h_e \quad (7.5)$$

A pressure drop in burner and recuperate are adopted from Palsson et al. [149]:

Pressure drop in burner is 5 %

Pressure drop in recuperator is 5 %

7.2.5 Data for SOFC and SOEC

The fuel cell model developed in this study is based on the planer design in which its geometries and material related data are according to data in Table 7.4. The respective resistivity measures how strongly SOFC's material opposes the flow of electric current and as a function of temperature is summarised in Table 7.5. The data related to economic analysis are given in Table 7.6.

Table 7.4 SOFC geometries and material related data

Parameter	Value	Reference
Utilization factor	0.95	[130]
DC/AC inverter efficiency	0.95	[130]
Temperature of SOFC	1000 K	[130]
Active surface area, A_{SOFC}	100 cm ²	[150]
Effective gaseous diffusivity through the anode	0.2 cm ² s ⁻¹	[150]
Effective gaseous diffusivity through the cathode	0.05 cm ² s ⁻¹	[150]
Thickness of the anode, t_a	0.05 cm	[150]
Thickness of the cathode, t_c	0.005 cm	[150]
Thickness of the electrolyte, t_e	0.001cm	[150]
Thickness of the interconnect, t_{int}	0.3 cm	[150]
Pre-exponential factor, γ_a	5.5×10^8 A/m ²	[129]
Pre-exponential factor, γ_c	7×10^8 A/m ²	[129]
$E_{act,a}$	100 kJ/mol	[129]
$E_{act,c}$	120 kJ/mol	[129]

Table 7.5 Cell material resistivity and its dependence on temperature

Cell material (carrier type)	Resistivity formula Ω -cm
Air electrode (electronic)	$0.008114exp(600/T_{SOFC})$
Electrolyte (ionic)	$0.00294exp(10350/T_{SOFC})$
Fuel electrode (electronic)	$0.00298exp(-1392/T_{SOFC})$
Interconnection (electronic)	$0.1256exp(4690/T_{SOFC})$

Source: [130]

7.3 Results for System I

The gasifier is the heart of this system. Therefore, the main results from this system are of those parameters related to the gasifier that affect hydrogen production like gasifier operating temperature, steam-biomass ratio and gasifier efficiencies.

7.3.1 Results for Gasification Process

In this section, the obtained results from studying the effect of different parameters on hydrogen production and performance of gasification process such as: gasification temperature, amount of fed sawdust, and injected steam are analyzed and discussed.

Table 7.6 Economic analysis related data

Parameter	Value	Reference
Interest rate, i	10%	[140]
Salvage value, S_n	10%	[140]
Life time, n	25 years	Assumed
Exchange rate, ER	1	Assumed
Maintenance factor, \emptyset	1.06	[140]
Cost of electricity	0.1046 \$/kWh	[151]
Cost of biomass, Pr	2 \$/GJ	[61]

7.3.1.1 Parameters Affecting Hydrogen Production

Two sets of analysis are performed. In the first set, 4.5 kg/s of steam is used while in the second set the amount of 6.3 kg/s is used and both at the steam temperature of 500 K. The study done for a black box simulates gasifier. Its temperature is in a range of 1000-1500 K and the fed biomass is in a range of 10-32 kg/s. The performed parametric study simulates steam gasification of biomass process in two ways: one by varying the amount of biomass in the gasifier at a fixed amount of steam and gasifier temperature, while the second by varying the gasifier operating temperature at certain amounts of biomass and steam.

7.3.1.1 Effect of Biomass Quantity on Hydrogen Product

Results from different biomass amounts are shown in Figure 7.2. Biomass quantity, α is increased from 10 to 32 kg/s and holds all other conditions constant: steam quantity is 4.5 kg/s and the gasifier temperature is 1000 K. Hydrogen concentration flow decreases from 59 to 54 %. Carbon monoxide levels in the gases are increased. Methane concentration in gas production shows a little variation over the biomass range. Carbon dioxide concentration shows a decrease over the same biomass range and behaves

opposite to carbon monoxide concentration. Tar is modelled as benzene and its yield is a function of gasification temperature, thus its mole fraction is constant at the specific gasification temperature. Char concentration is given in terms of biomass carbon content and thus increases with increasing in the biomass quantity.

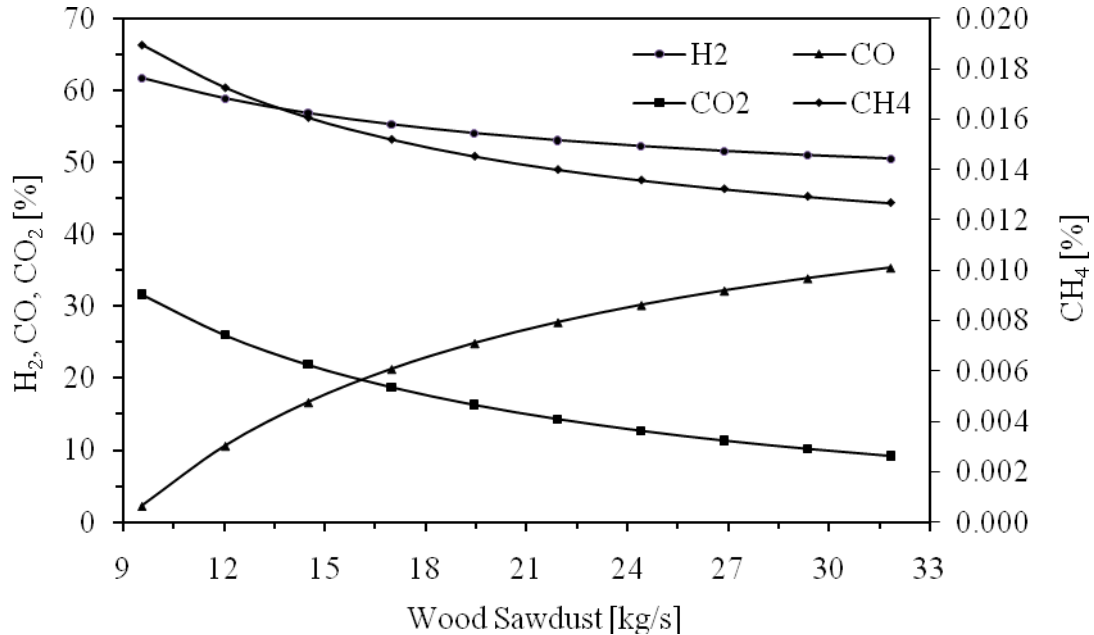


Figure 7.2 Hydrogen production from different quantities of wood sawdust.

Hydrogen content decreases from 62 % to 50 % in the feeding biomass range. This was also observed experimentally by Lv et al. [98]. They found the highly excessive feeding rate was unbeneficial for biomass gasification cracking and reforming reactions because it leads to a reduction of hydrogen content in gases. On the weight basis the graph (Figure 7.3) shows that 7-11% of wood sawdust is converted to hydrogen under the same conditions.

7.3.1.2 Effect of Supplied Steam

Gases concentration versus injected steam is shown in Figure 7.4. Steam is increased from 4.5 to 6.3 kg/s in an increment of ~ 0.18 while the sawdust quantity in the gasifier and gasifier temperature are 20 kg/s and 1000 K, respectively. It is found that hydrogen increases from 54 to 57 % and carbon monoxide concentrations decrease from

25 to 16 %. The carbon dioxide concentration exhibited an opposing trend where it increases from 16 to 22 %. In the studied supplied steam range, the improvement of gas yield from the gasification process results in an increase in hydrogen yield by 3 %.

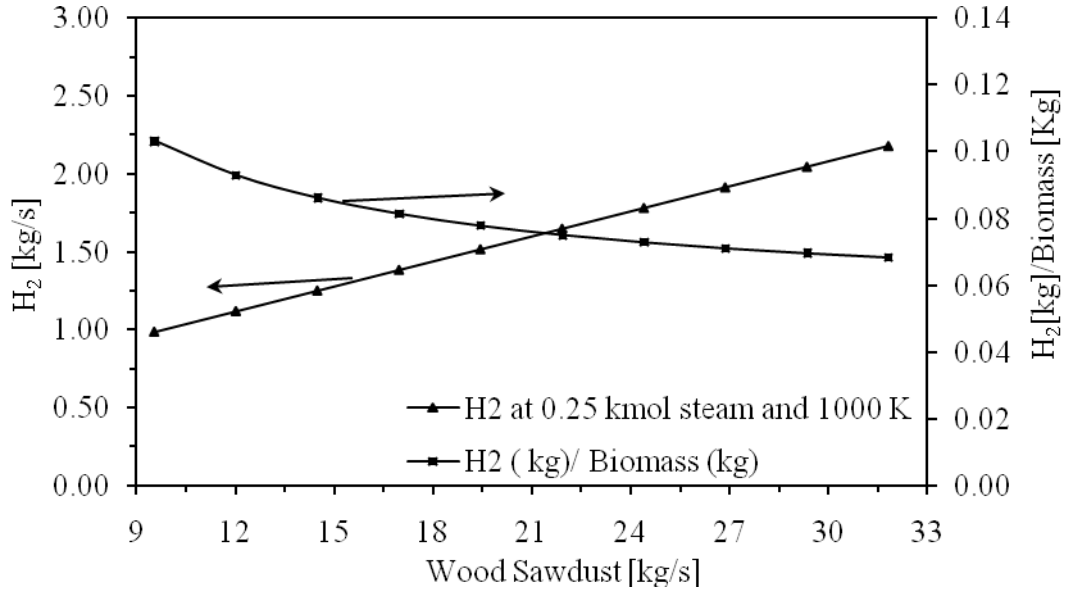


Figure 7.3 Produced hydrogen and gasification ratio from different quantities of wood sawdust.

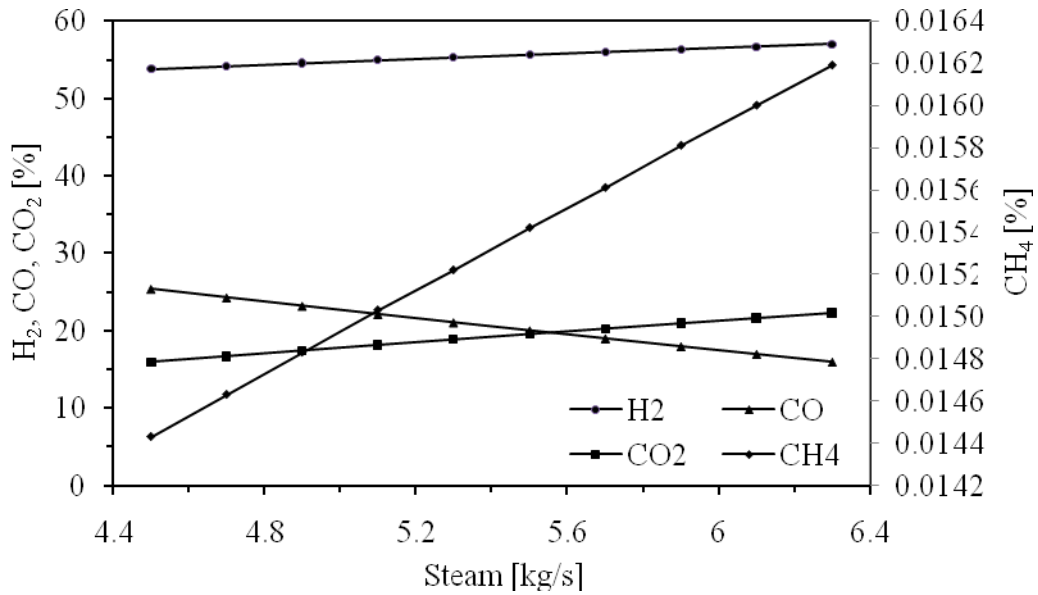


Figure 7.4 Hydrogen production from 20 kg/s of wood sawdust at 1000 K versus injected steam.

7.3.1.3 Effect of Gasification Temperature

The effect of gasification temperature on the hydrogen production from sawdust steam gasification is studied for the sawdust and steam mass flow rates are 32 kg/s and 4.5 kg/s respectively. It is found that an increase in temperature leads to an increase in the hydrogen yield. Over the studied temperature range some differences in gas yield are obtained (Figure 7.5). Hydrogen concentration is in an appreciable amount where the rise in temperature is found to decrease hydrogen concentration from 53 to 51%.

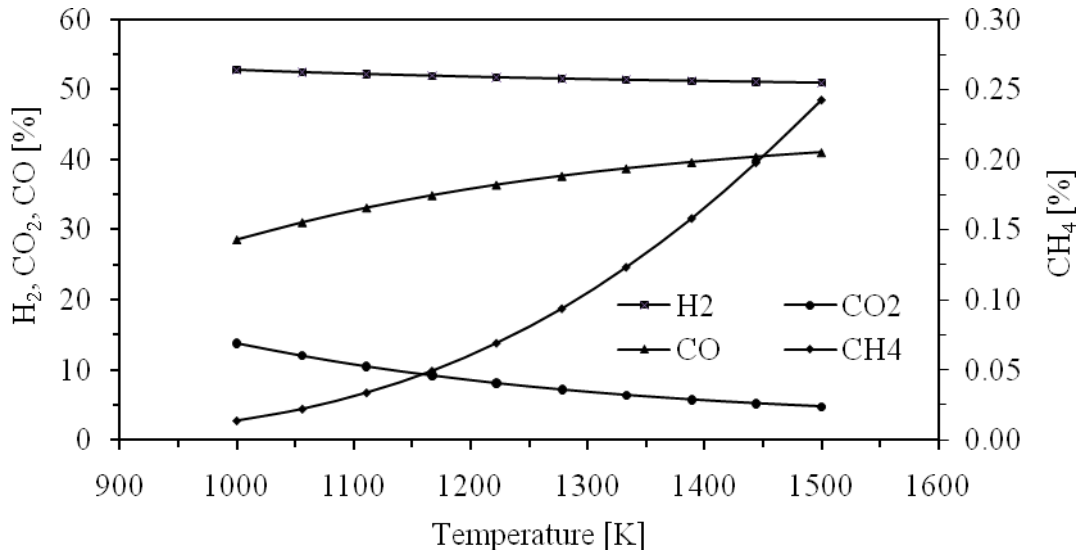


Figure 7.5 Gases concentration versus gasification temperatures for 32 kg/s from wood sawdust and 4.5 kg/s from steam.

7.3.1.4 Effect of Operating Parameters on Process Irreversibility

Figure 7.6 shows the gasification process irreversibility or exergy destruction from exergy flows within sawdust when the gasification temperature is 1000 K and the injected steam is 4.5 kg/s. It is clear that there is an increase in exergy destruction. This is due to an increase in the entropy generation. However, in the studied biomass range, the exergy destruction due to thermal losses is unchanged because the energy lost from the gasifier does not change.

7.3.1.5 Process Energy and Exergy Efficiencies

Three exergetic efficiencies were defined in the analysis section above according to the desired outputs and are plotted in Figure 7.7. The exergy efficiency, η_{ex1} that considers hydrogen production is presented by a dotted line and decreases as mass flow rate of sawdust increases. This is because there is unbeneficial available energy or the efficiency of using the available energy decreases. The other two efficiencies, η_{ex2} and η_{ex3} have similar trends. The exergy efficiency, η_{ex3} has the highest value because it considers all products from the gasification process. It is observed that there is a point where the exergetic efficiencies η_{ex2} and η_{ex3} have minimum values.

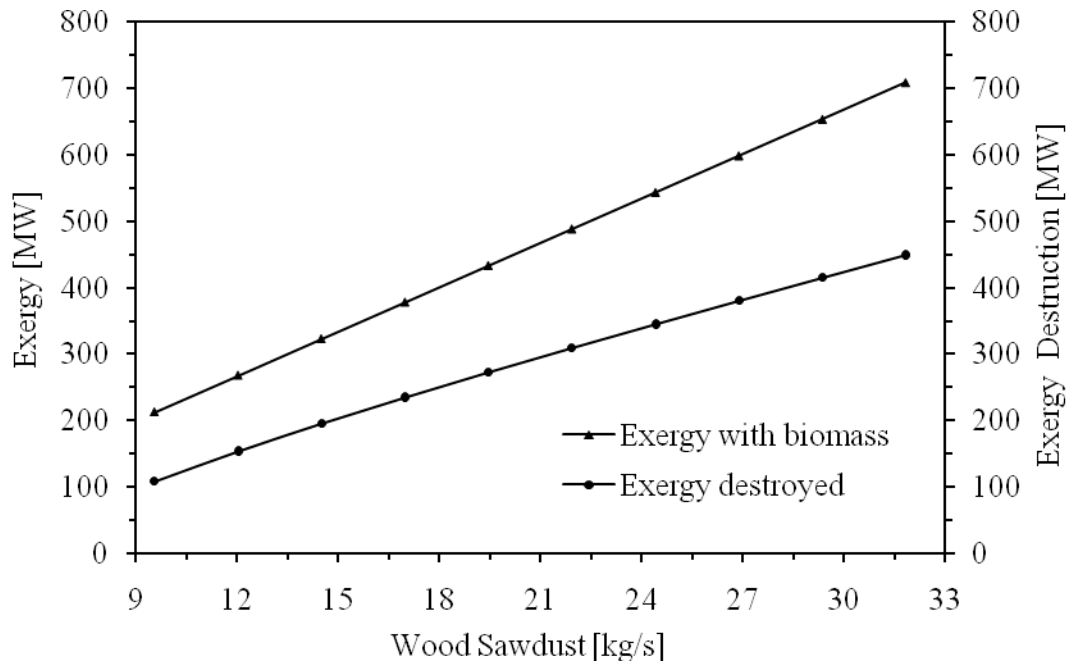


Figure 7.6 Exergy destruction and exergy flows with wood sawdust at 1000 K and 4.5 kg/s steam.

For a declaration considering η_{Ex3} where the gasifier temperature is constant, the irreversibility is either external, which is related to the thermal losses from the gasifier wall, or internal, which is calculated from entropy generation. The former is a function of the gasifier wall temperature and this is constant as the gasifier temperature is kept constant. Therefore, one can attribute that to the internal irreversibility part.

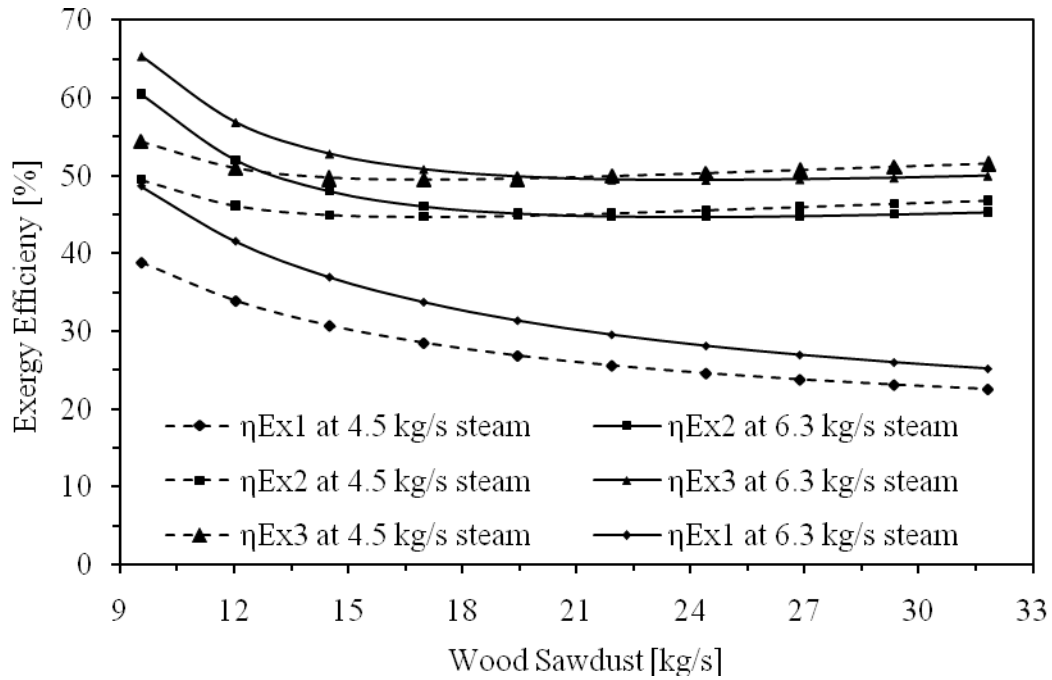


Figure 7.7 Exergy efficiency versus gasified wood sawdust at a gasifier temperature of 1500 K.

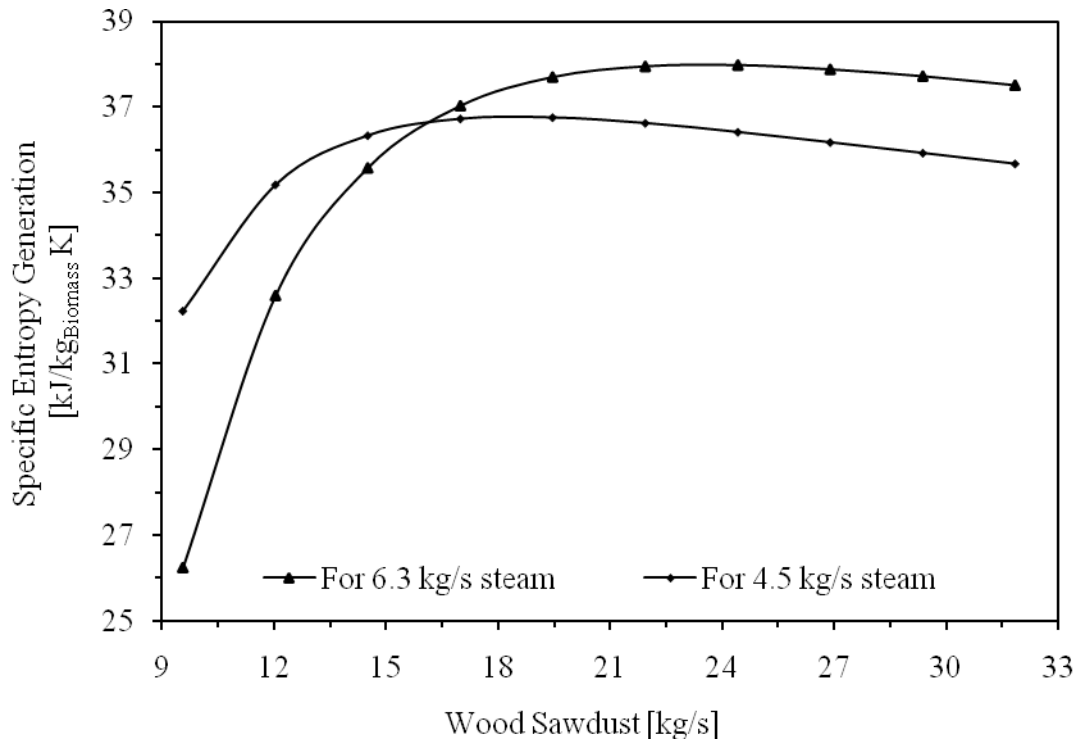


Figure 7.8 Specific entropy generation at a gasification-temperature of 1500 K.

To make that more clear, the entropy generation per unit mass from sawdust is plotted in Figure 7.8. It is obvious from the graph that the specific entropy generation is maximum at the state that corresponds with the minimum exergy efficiency. An increasing of the injected steam amount from 4.5 to 6.3 kg/s shows a similar trend for specific entropy generation, but the minimum exergy state moves towards the right-hand direction. The energetic efficiencies both have similar trends in the studied sawdust mass flow rate range. It can be observed from Figure 7.9 that both energy efficiencies are more sensitive to biomass flow rate than to steam flow rate.

7.3.2 Evaluation of the Gasification Process Efficiency

The study evaluates hydrogen production from a process of biomass steam gasification in two ways. In the first: the amount of steam-biomass ratio is varied while the gasification temperature is kept constant gasification. In the second set, the temperature is varied while the fed biomass and injected steam are 14.5 kg/s and 6.3 kg/s respectively.

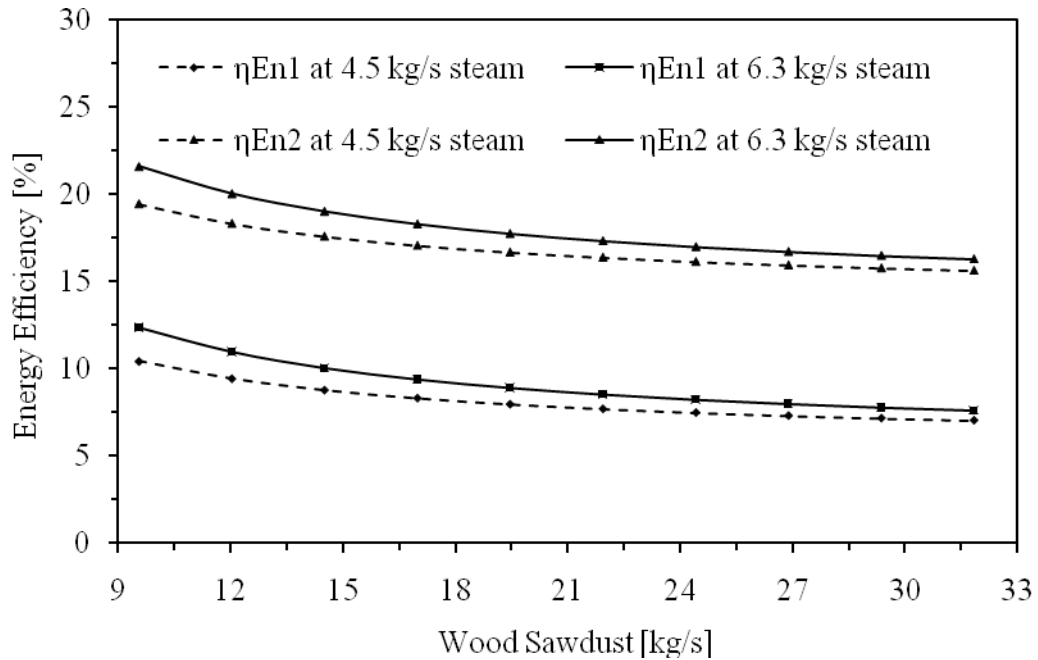


Figure 7.9 Energy efficiency versus fed wood sawdust.

7.3.2.1 Effect of Steam-Biomass Ratio on Hydrogen Production

In this section, a parametric study for the combined effects of steam amount and biomass quantity is performed. Here, the steam-biomass ratio refers to mass of steam injected per mass of biomass fed. The displayed trend in Figure 7.10 shows an increase in H_2 corresponds to an increase in steam-biomass ratio. Such trend was also observed by Mahishi et al. [19] and is consistent with their results. Hydrogen yields range from 70 to 107 g H_2 per kg biomass. This is also consistent with the literature experimental data. For example, Turn et al. [18] reported some hydrogen production results using different gasifier types, namely batch-type reactor, bubbling fluidized beds and dual fluidized bed technologies as ranging from 30 to 80 g H_2 per kg biomass. They did not give a specific reason for such a large difference.

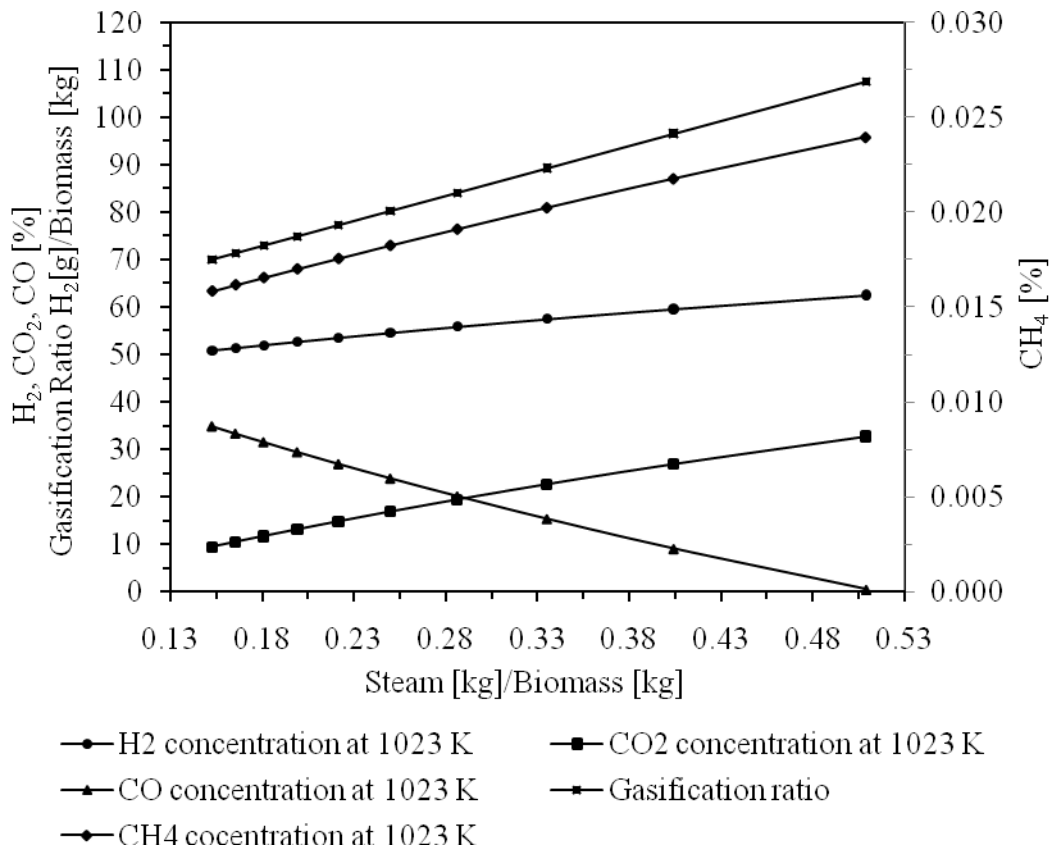


Figure 7.10 Concentration of gases from gasification at different steam-biomass ratios and hydrogen yield from different steam-biomass ratios and at 1023 K.

To predict potentials to increase the gasification ratio, the gas concentration against steam-biomass ratio are plotted in Figure 7.10. From the first look on the graph, one can observe that the hydrogen concentration increases with an increase in the steam-biomass ratio. Also, for this set of results, the CO concentration becomes negligible after a steam-biomass ratio of $\sim 0.50 \text{ kg steam kg}^{-1} \text{ biomass}$. Therefore, theoretically, one can expect enhanced hydrogen will come from the sawdust conversion and side reactions that use other species.

7.3.2.2 Effect of Steam-Biomass Ratio on Energy Efficiency

It is found that the considered energy efficiencies have a low sensitivity to the studied range of steam-biomass ratio. Figure 7.11 shows the efficiencies versus steam-biomass ratio have similar trends. A little variation, $\sim 3\%$ in these efficiencies, appears within the studied steam-a biomass ratio range at a gasification temperature of 1023 K. All the products from the gasification process leave the gasifier at the gasification temperature. Therefore, some improvement in gas efficiency is expected if their energy content is extracted.

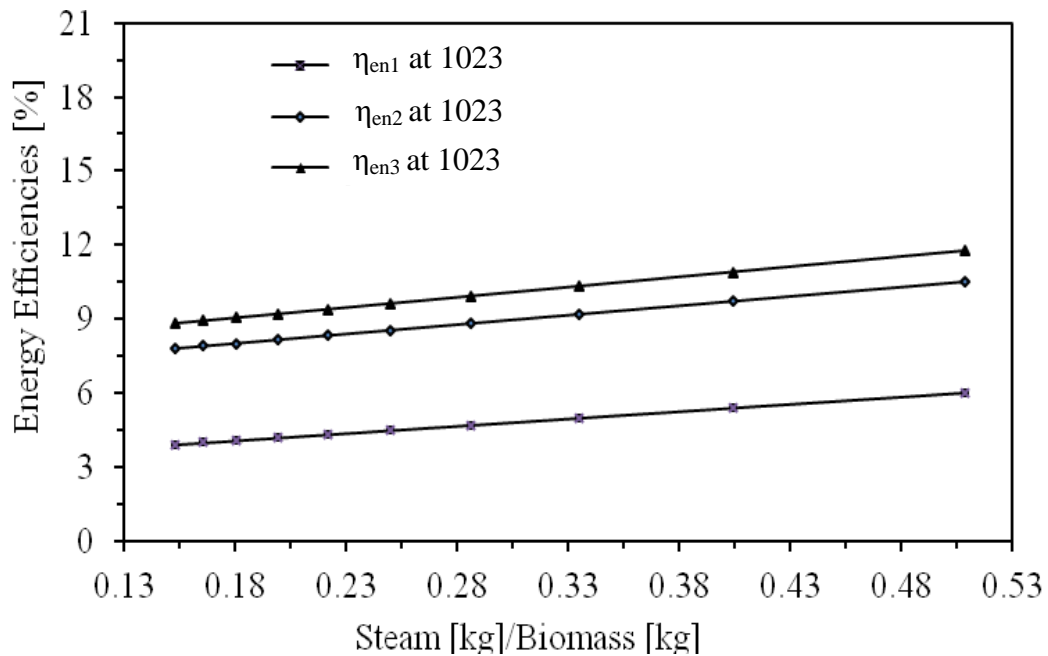


Figure 7.11 Energy efficiencies for different steam-biomass ratios.

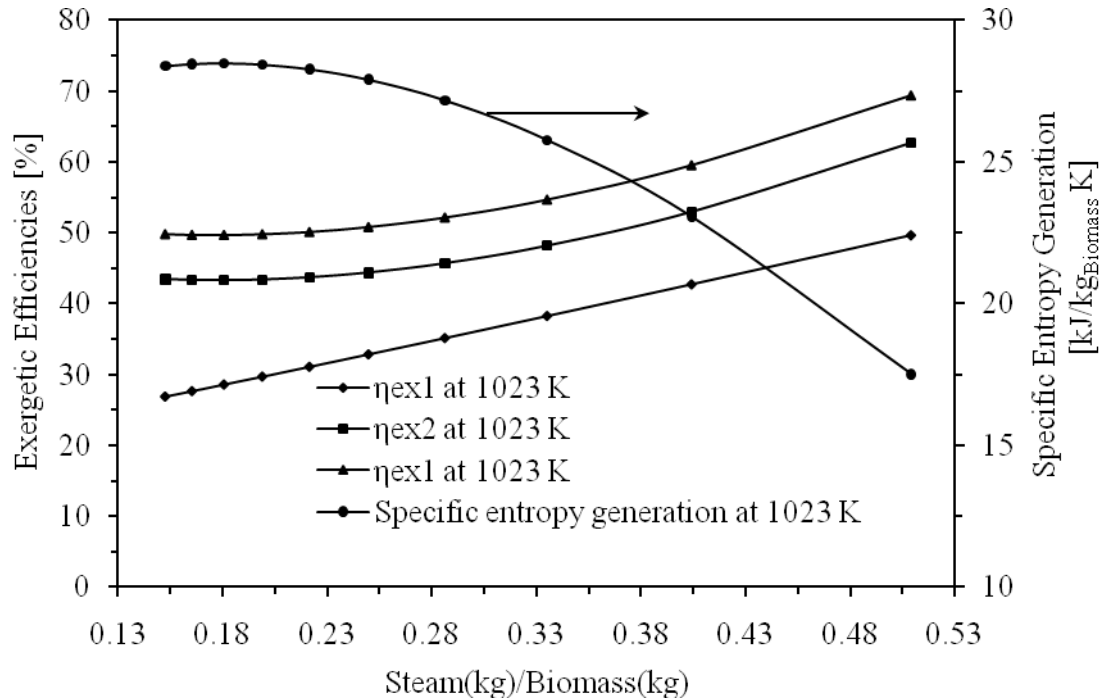


Figure 7.12 Exergy efficiencies and specific entropy generation for different steam-biomass ratios.

7.3.2.3 Effect of Steam-Biomass Ratio on Exergy Efficiency

Three exergy efficiencies were defined in the analysis section earlier according to the desired outputs and plotted in Figure 7.12. The exergy efficiency, η_{ex1} that considers hydrogen production is increasing as steam-biomass ratio increases and that because there is available energy increases as hydrogen increases. The other two efficiencies, η_{ex2} and η_{ex3} have similar trends. The exergy efficiency, η_{ex3} has the highest value because it considers all the products from the gasification process. It is noticed that there is a point where the exergy efficiencies η_{ex2} and η_{ex3} are minimum.

The entropy generation per unit mass of biomass is plotted in Figure 7.12. It is obvious from the graph that the specific entropy generation is maximum at the state corresponding to the minimum exergy efficiency. At a lower steam-biomass ratio there is insignificant change in specific entropy generation. However, the results show that there is a minimum exergy efficiency point that belongs to η_{ex3} curve and corresponds to a maximum specific entropy generation point. For declaration, considering η_{ex3} where the

gasifier temperature is constant, the external irreversibility is related to the thermal losses from the gasifier wall and internal irreversibility that is calculated from entropy generation. The former is a function of the gasifier wall temperature and this is constant as gasifier temperature is kept constant. Therefore, one can attribute that to the internal irreversibility.

5.3.2.4 Effect of Gasifier Temperature on Hydrogen Production

In this section, a parametric study on the effects of gasification temperature is performed. The gasification temperature is a temperature at which the gasification process takes place. The displayed trend in Figure 7.13 shows there is a decrease in H_2 which corresponds to an increase in gasification temperature. This can be attributed to the fact that at higher temperatures, other reactions take place and produce gases from reaction with other species. This is also observed by Florin et al. [50].

In the same temperature range, it is found that the gasification ratio increases and becomes less sensitive to higher temperature (Figure 7.13). The maximum hydrogen that can be produced under this condition is 105 g per kg of biomass gasified.

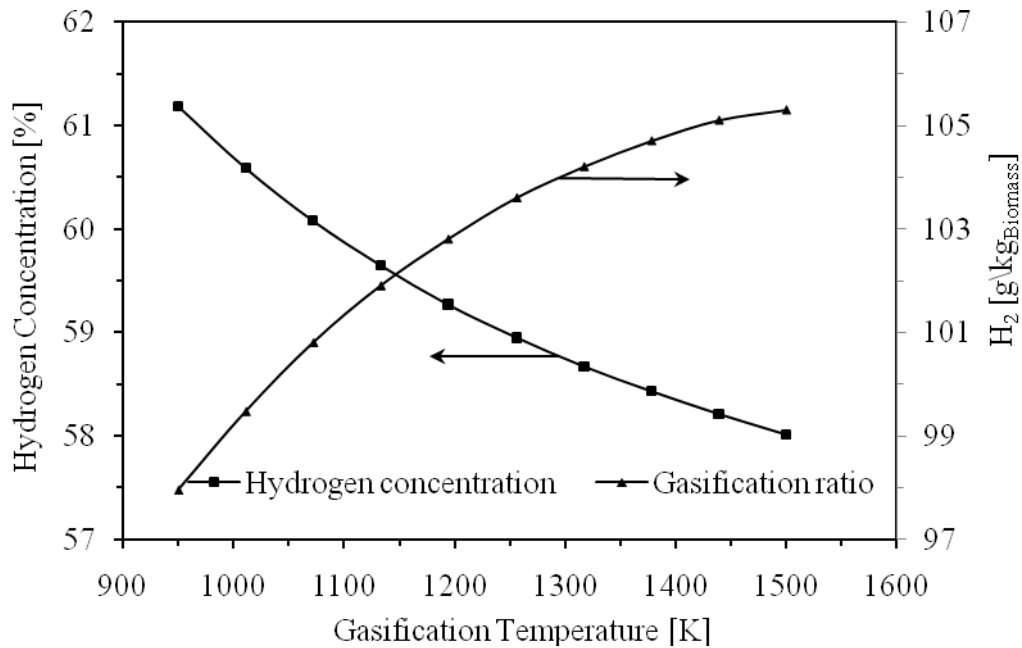


Figure 7.13 Hydrogen production and hydrogen yield at different gasification temperatures for 14.5 kg/s from wood sawdust and 6.3 kg/s from steam.

7.3.2.5 Effect of Gasifier Temperature on Energy Efficiency

Over the studied temperature range it is observed that energy efficiency η_{en1} is less sensitive to temperature, Figure 7.14. This may be attributed to the fact that there is more energy content in products other than hydrogen, and that also can be observed when including more energy by including more products in the case of η_{en2} and η_{en3} .

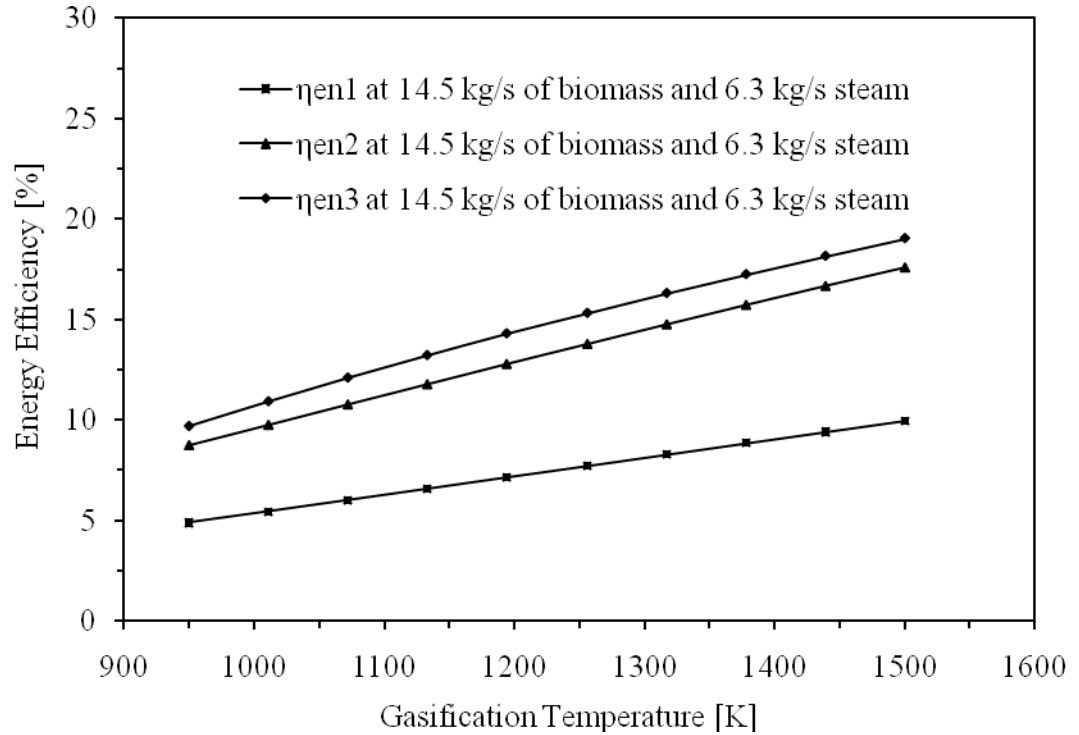


Figure 7.14 Energy efficiencies at different temperatures.

7.3.2.6 Effect of Gasifier Temperature on Exergy Destruction and Exergy Efficiency

The exergy destruction in the gasification process decreases after a temperature of 1000 K. This is because the available energy with gasification process products becomes dominant and this can be also seen from the exergy efficiencies graph where exergy efficiency increases. It is also observed that the potential to improve the exergy efficiency of hydrogen production becomes minimum at 1000 K and it increases beyond that temperature as well as the destruction exergy (Figure 7.15).

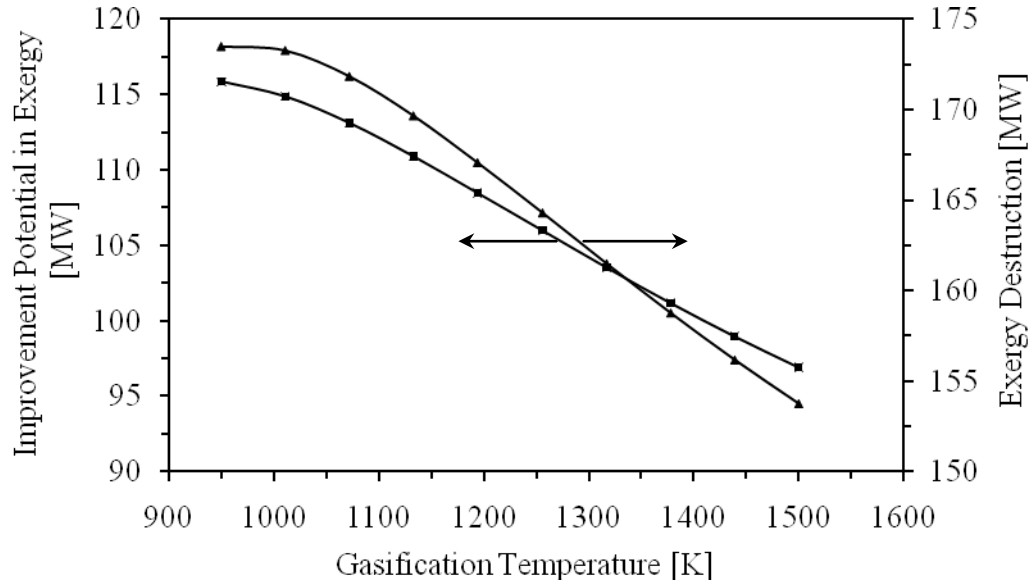


Figure 7.15 Exergy destruction and improvement potential in exergy for 14.5 kg/s from wood sawdust and 6.3 kg/s from steam.

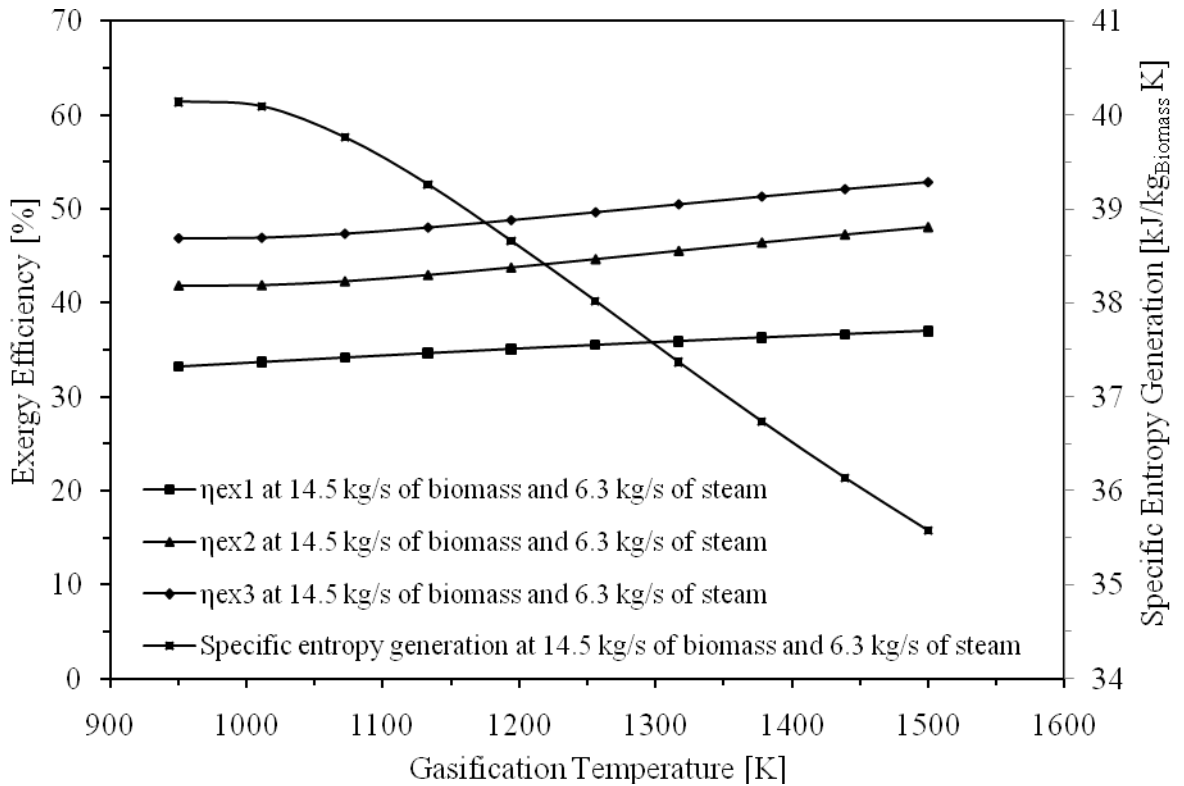


Figure 7.16 Exergy efficiency and specific entropy generation versus gasification temperature.

In the studied temperature range, the same exergy efficiency trend scenario is repeated. There is an improvement in exergy efficiency over the studied temperature range. However, the efficiency is more sensitive to temperature than to steam-biomass ratio. The exergy efficiency when hydrogen is taken into consideration does not exceed ~4% and it is less sensitive to temperature than the other two efficiencies. Also, it is observed from the results that there is a point of minimum exergy efficiency regarding η_{ex2} and η_{ex3} , see Figure 7.16. To discuss that, specific entropy is plotted over the temperature range in Figure 7.16. The same scenario as that of steam-biomass ratio is repeated and the same conclusion is drawn. It is difficult to declare that from the graph, due to an insignificant change of specific entropy in the studied range around a point of maximum entropy generation. There is a more drastic decrease in specific entropy compared to that in the steam-biomass ratio range.

Table 7.7 Temperature and mass through system I for a gasification temperature of 1023 K.

State no.	Temperature [K]	Mass[kg]/Biomass[kg]	State no.	Temperature [K]	Mass[kg]/Biomass[kg]
0	298	-	18	745.7	1.030
2	1023	1.154	19	949.7	1.464
4	500	0.153	20	886.3	1.736
5	298	1.464	21	500	0.444
6	366.3	1.464	26	1023	0.004
7	298	0.153	28	298	1.736
8	1015	0.153	33	366.3	0.119
15	886.3	0.0002	34	366.3	1.345
17	1022	1.030	36	1023	1.030

7.3.3 System I Energy Efficiency

Mass flow rate ratio and temperature at different states through system I are given in Table 7.7. The energy efficiency is studied in a gasification temperature range of 1023-1423 and for steam-biomass ratio of 0.8 kmol-steams per kmol-biomass where the hydrogen yield increases from 13.7 to 16.6 kg/h. In the gasification temperature range, the energy efficiency considers hydrogen yield increases from 59.3 % to 75.2 % (Figure

7.17). Under the same above operating conditions, it is found also that the exergy efficiency with hydrogen yield increases from 62.7 % to 76.1 % (Figure 7.17).

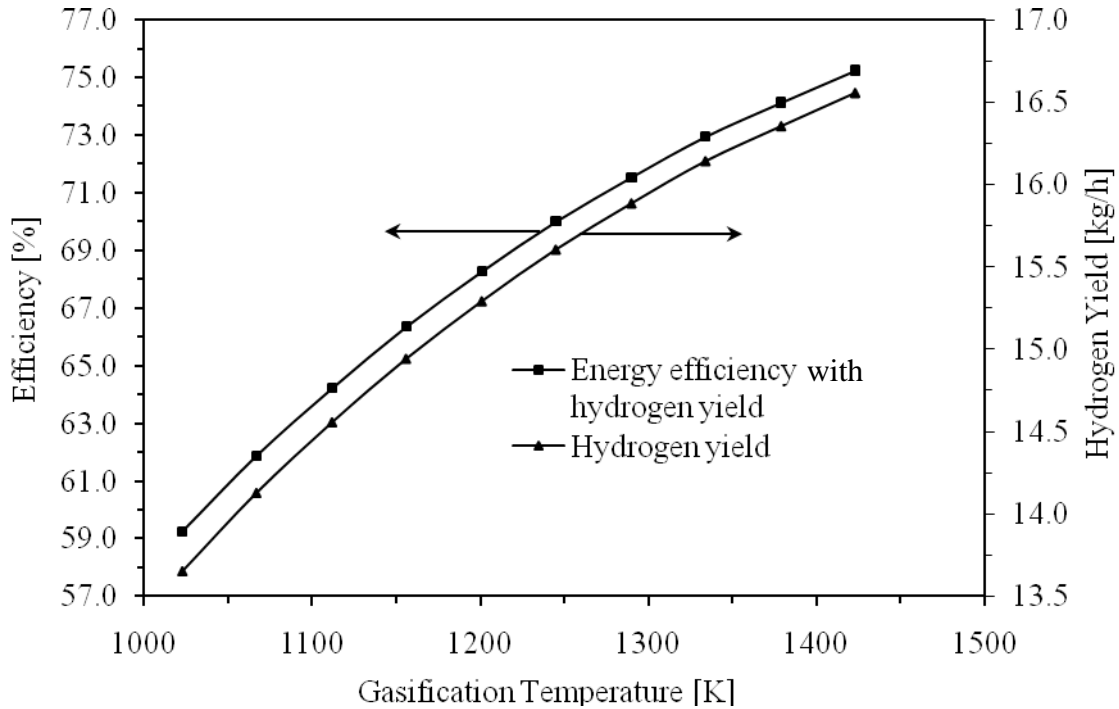


Figure 7.17 System I energy efficiency with hydrogen and hydrogen yield versus gasification temperature.

The hydrogen yield increases with gasification temperature both the energy content and exergy increase which results in an improvement in the system energy and exergy efficiencies.

7.3.4 Exergy Destruction in System I

The rate of exergy destruction for the system components is shown in Figure 7.18. From the destructed exergy results, it is clear that a major part of the exergy destruction occurs in heat exchangers 19-5-28-20 followed by the steam reforming reactor. Also, its exergy destruction increases with the gasification temperature increase.

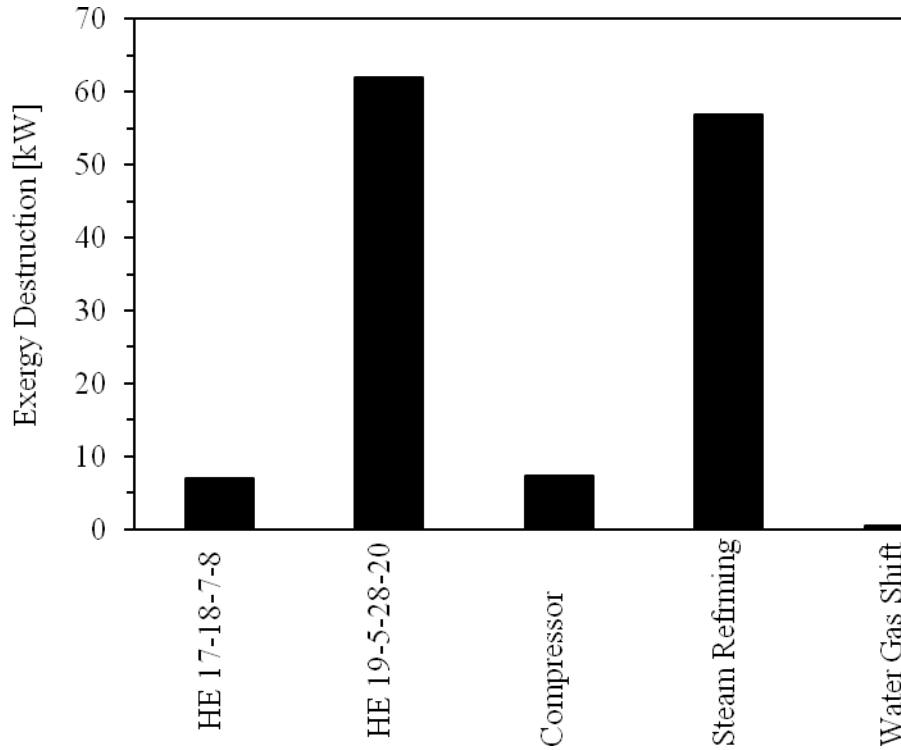


Figure 7.18 Exergy destruction in system I components at gasification temperature of 1023 K.

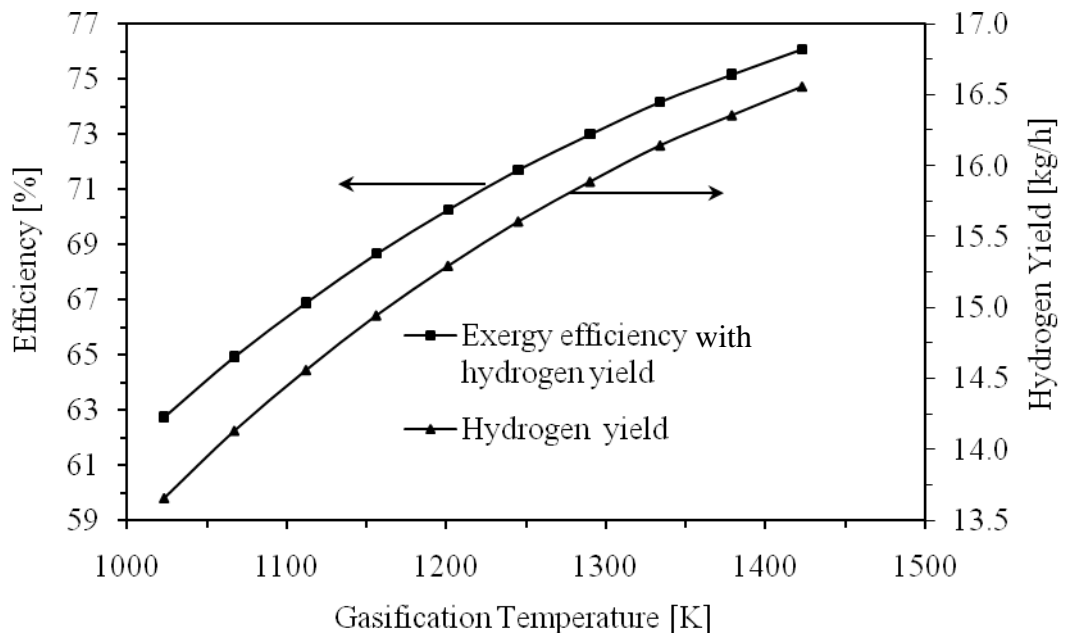


Figure 7.19 System I exergy efficiency with hydrogen and hydrogen yield versus gasification temperature.

7.3.5 System I Exergy Efficiency

In the gasification temperature range, the exergy efficiency with the hydrogen yield based on exergy of biomass throughput versus gasification temperature is shown in Figure 7.19. The efficiency increases from 62.7 to 76.1 % in the studied gasification temperature range because of an increase in the exergy of the hydrogen yield.

7.3.6 System I Exergoeconomic Analysis Results

The results from the exergoeconomic analysis by applying the SPECO method and within the studied gasification temperature range of 1023-1423 K show how much the by-product gasification hydrogen influences the cost of its exergy unit. It is found that within the studied gasification temperature range and with the steam-biomass ratio, the by-product steam gasification hydrogen increases with increasing gasification temperature (Figure 7.20).

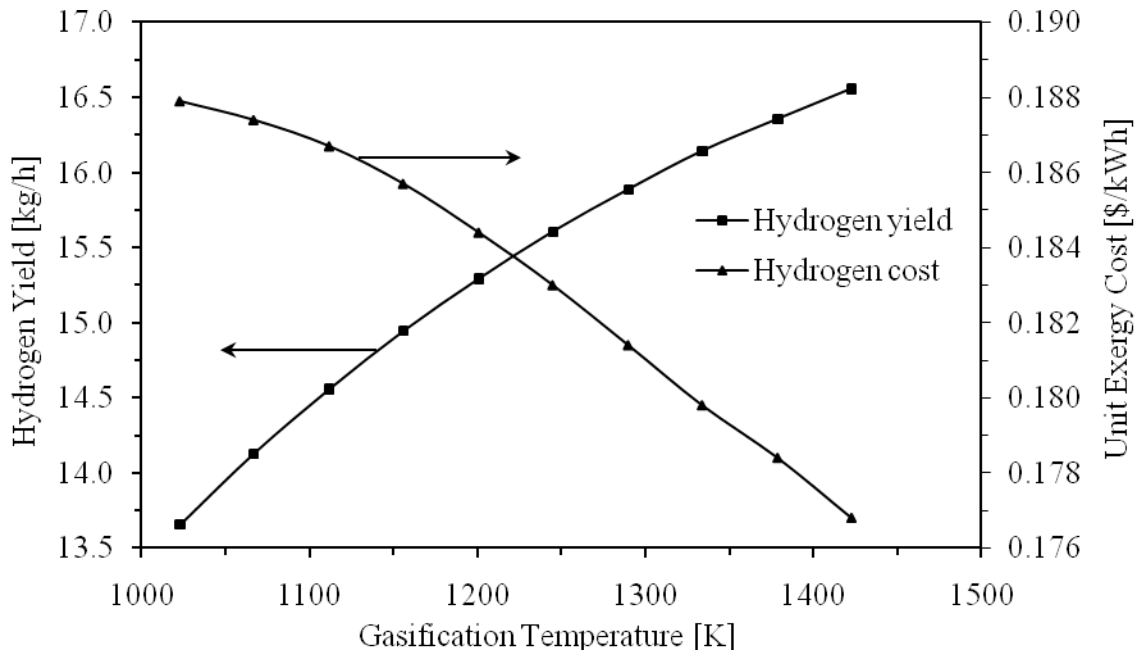


Figure 7.20 Hydrogen yield from system I and its unit exergy cost versus gasification temperature.

The cost of unit exergy from this hydrogen decreases with the increasing gasification temperature. Also, the hydrogen yield or the hydrogen derived from the

gasifier bottom processes increases within the studied gasification temperature range and this enhances the total hydrogen yield from the system. It is observed from the results that there is a drastic decrease in the cost per unit exergy of the hydrogen at a higher gasification temperature. This is attributed to the increasing hydrogen yield which results in the decrease in the specific cost (Figure 7.20). At a higher gasification temperature, it is found that the hydrogen yield increases and this is due to more hydrogen product in both the gasifier and bottom processes.

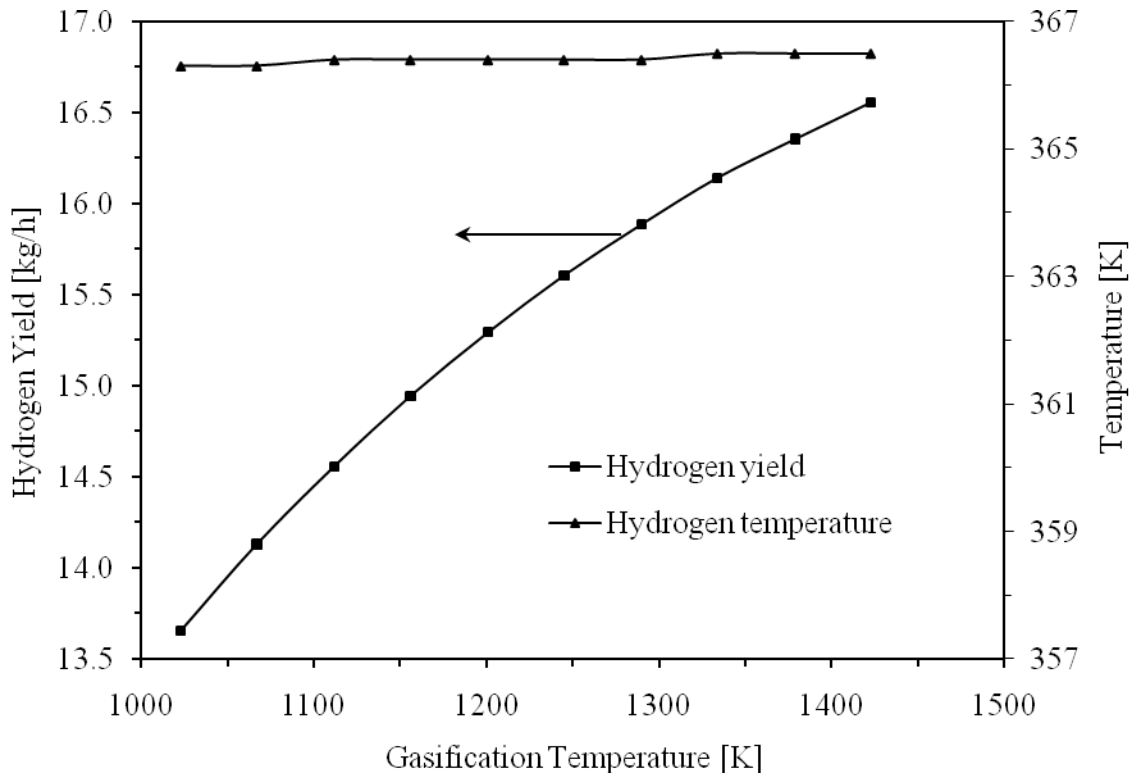


Figure 7.21 Hydrogen yield from system I and its temperature versus gasification temperature.

As the gasification temperature increases, more gases are produced and thus more steam is needed to perform the water gas shift and steam reforming reactions. According to the exergoeconomic model, the steam unit cost is equal to the unit cost of electricity and they are constant.

More hydrogen is produced in the system and thus its energy content is higher which results in hydrogen with a higher temperature (Figure 7.21). Although the hydrogen yield is increased, its temperature is almost constant. However, more energy content is available with more flow of the gasification products at a higher gasification temperature. Contrary, it is found that there is an insignificant increase in the produced hydrogen temperature (Figure 7.21). This is due to the cooling process that takes place in the gas compressor former heat exchanger to produce steam, the low compressor ratio and the low upstream temperature of the compressor. Therefore the hydrogen yield in this case influences the specific cost and the hydrogen temperature does not.

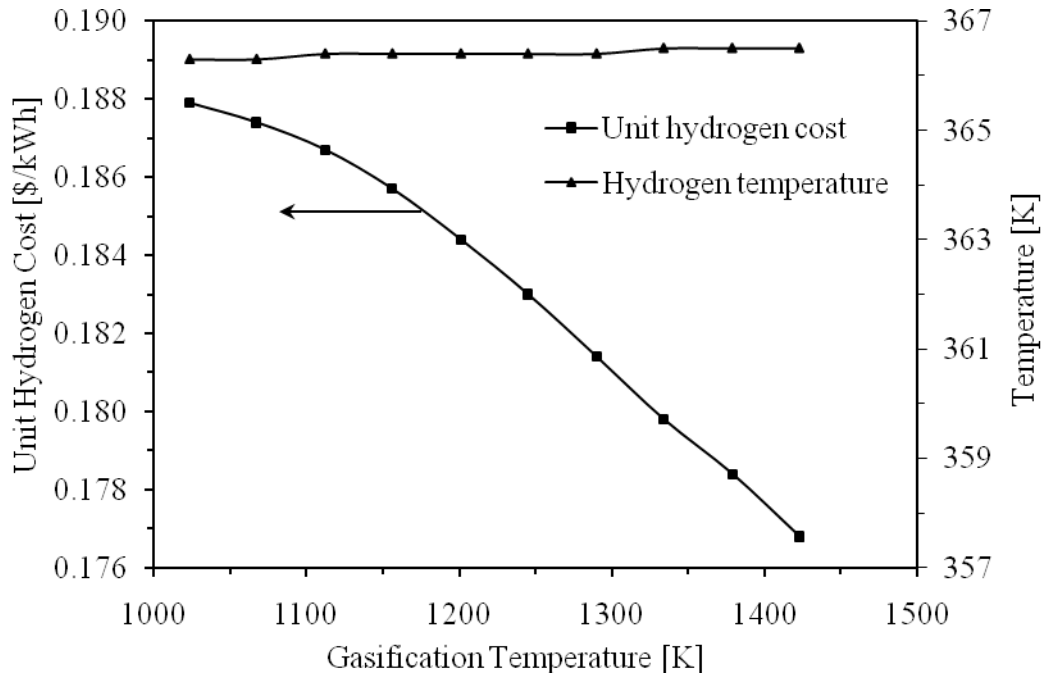


Figure 7.22 Cost of hydrogen yield and its temperature at different gasification temperatures.

Similarly, it is found that the unit hydrogen cost decrease and hydrogen temperature is almost constant with an increasing of the gasification temperature (Figure 7.22). The decreasing of the specific cost of the hydrogen is attributed to the fact that the hydrogen unit cost is affected by the increasing of the hydrogen yield in both the gasifier and in the bottom processes. At a gasification temperature of 1023 K, the specific cost of

the other flow material streams can be found in Table 7.8. The cost from this study does not consider other costs from the calculated cost to the delivered cost.

Table 7.8 Unit exergy cost and cost rate for flow material through system I

State no.	C [\$/kWh]	\dot{C} [\$/h]	State no.	C [\$/kWh]	\dot{C} [\$/h]
1	0.0002	116.7	18	0.3899	87.19
2	0.3841	118.3	19	0.2729	88.55
4	0.1046	0.5663	20	0.1046	6.239
5	0.2839	83.06	21	0.1046	0.0195
6	0.2866	85.3	26	0.3852	27.49
7	0.0000	0.0000	28	0.0000	0.0000
8	0.6712	5.761	33	0.1879	83.65
15	0.1046	0.0004	34	0.0987	1.905
17	0.3899	92.2	36	0.3841	90.86

7.4 Results for System II

The analysis was performed under the following general assumptions: steady state and the gases obey the ideal gas relations with negligible potential and kinetic energies. The system under investigation is simulated at a steady state condition and the results are obtained from the conducted analyses on sawdust steam gasification and its downstream processes to perform multiple duties: heat and power generation. The sawdust ultimate and approximate analyses were discussed in System I.

To follow a strategy regarding the gasification module of System I, its operating conditions and a range of parameters' analysis are considered. Accordingly, it is decided to perform the analysis of this system within an operating temperature range of 1023-1423 K and a steam-biomass ratio of 0.8 kmol steam per kmol biomass which fall in the range that was studied in System I. In addition, the products from the gasifier in this model are found by using the same module developed there.

7.4.1 Effect of Current Density

Over potentials against current density are plotted in Figure 7.23. Results show

that at SOFC's operating temperature of 1000 K, activation overvoltage is dominant at a lower current density, while at a higher current density, ohmic overvoltage becomes important. This was also observed by Bavarsad [65]. However, in this study, a lower current density, different geometric and material related data are used. Also, analyses show that in a current density range of 750-900 mA/cm² and for a cell with a specific utilization factor that operates at a pressure of 1.20 bar and a temperature of 1000 K, there is an increase in cell voltage as current density decreases as shown in Figure 7.24.

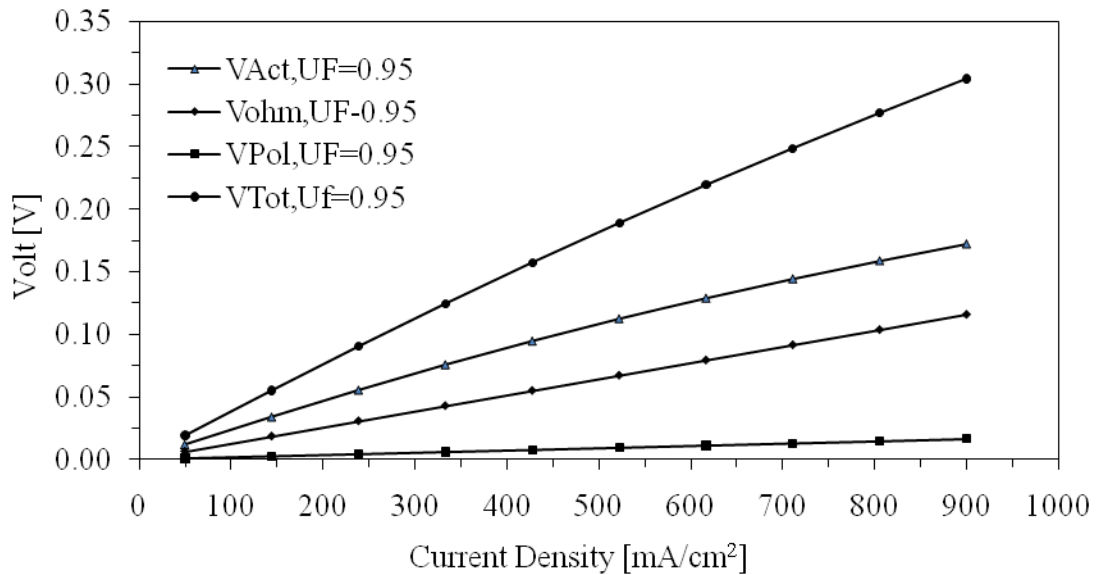


Figure 7.23 Overpotential losses for the used SOFC

At a specific current density, an increase in utilization factor results in lower cell voltage. Analyses show that there is an improvement in cell power as its current density varies from 750 to 900 mA/cm² (Figure 7.25). For a specific factor of fuel utilization and for a cell that operates at a pressure of 1.20 bars and a temperature of 1000 K, an increase in cell current density improves the power of the cell. Figure 7.26 shows there is an improvement in cell efficiency as its voltage increases. At a specific current density and utilization factor, and under the same operating conditions, an increase in cell voltage improves the cell efficiency.

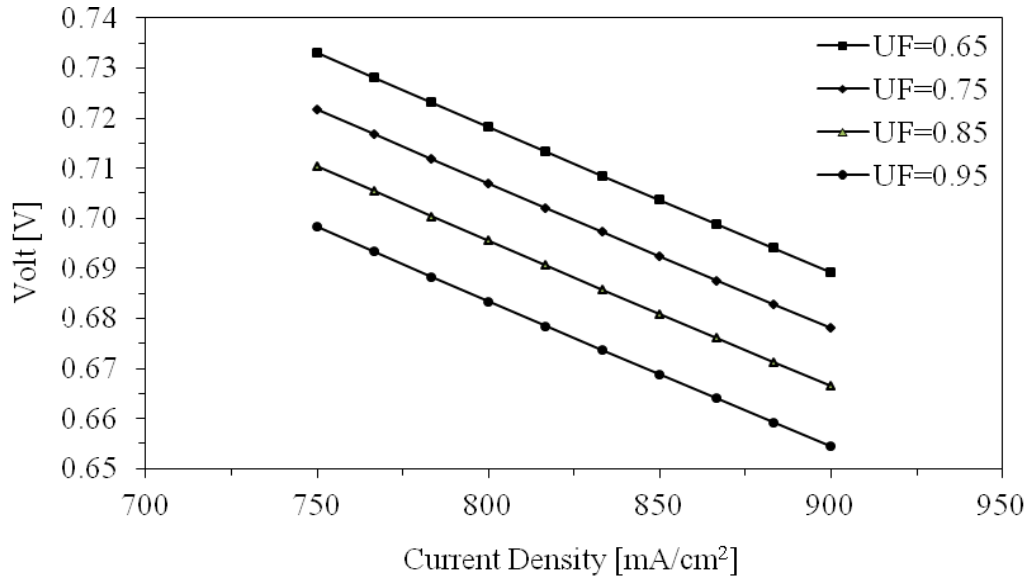


Figure 7.24 SOFC volts versus current densities and at different utilization factors.

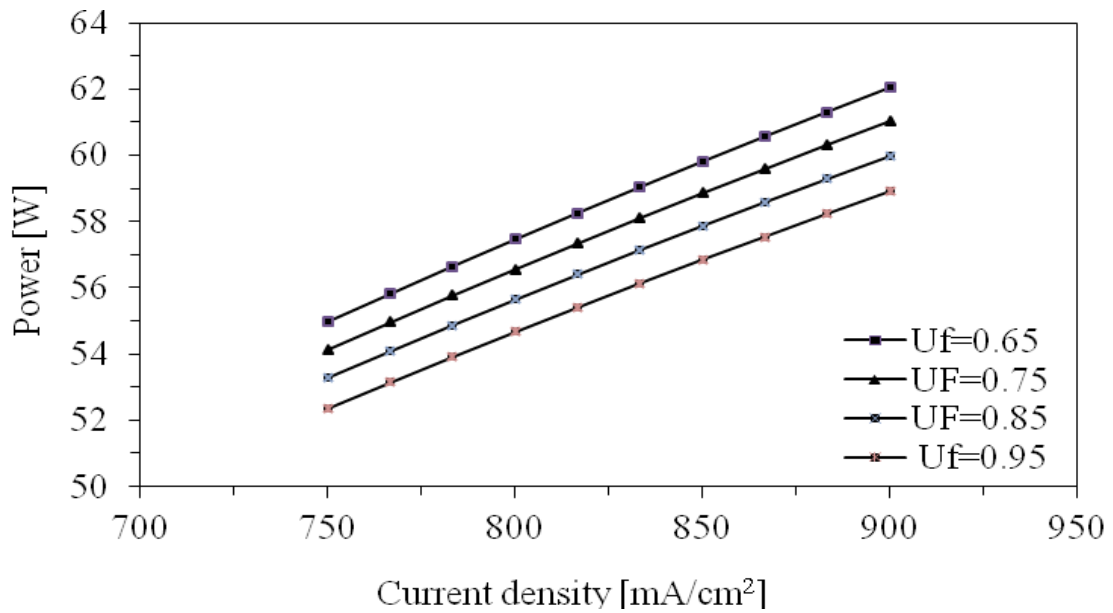


Figure 7.25 AC power produced by SOFC at different utilization factors.

7.4.2 Effect of Hydrogen Flow Rate

Hydrogen yield from gasified biomass that is consumed in the SOFC are plotted on Figure 7.27. From the SOFC module and for the specified cell, the consumed hydrogen by one cell is known. From the gasifier module, the hydrogen yield increases with the gasification temperature increasing from 1023 to 1423 K. At a fuel utilization of

0.95, it is found that an increase in hydrogen flow rate results in more current flow, and hence more power production per cell and thus per SOFC stack. This gives an indication that more chemical energy is converted into electrical energy.

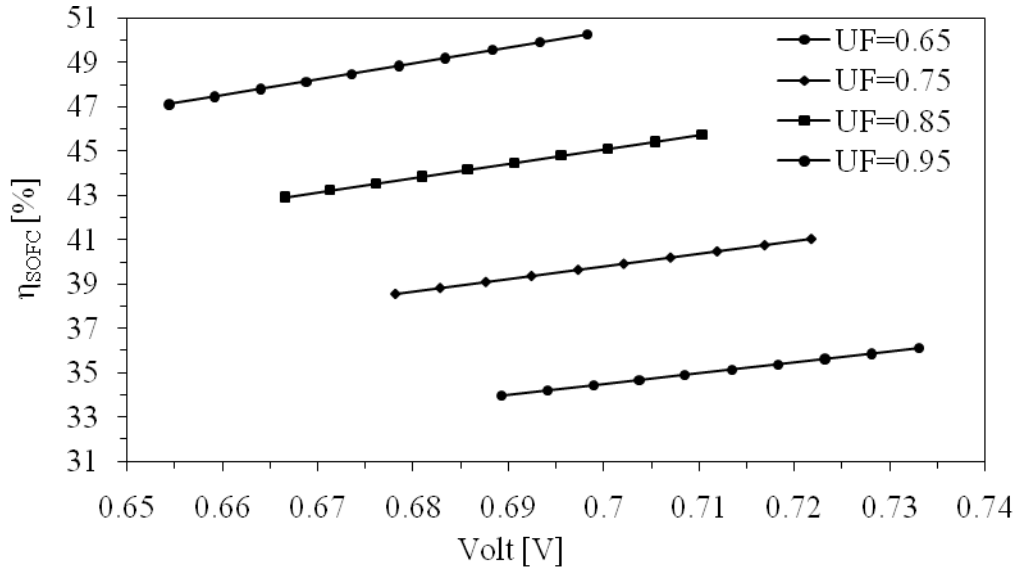


Figure 7.26 Variation of SOFC efficiency with voltage at current density of 750 mA/cm².

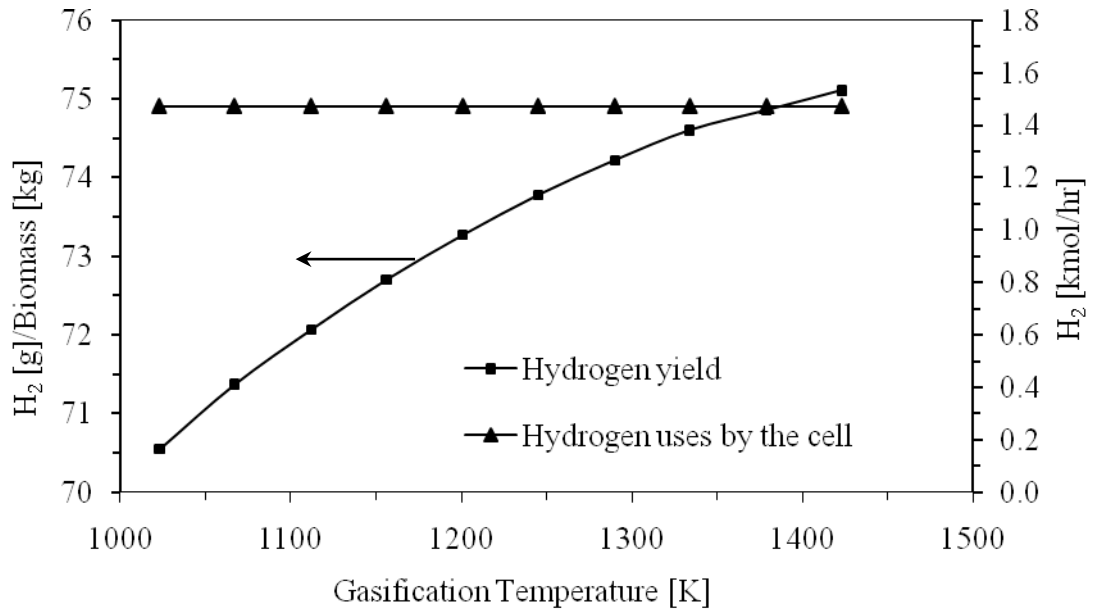


Figure 7.27 Hydrogen uses and hydrogen yield in system II at different gasification temperatures.

The hydrogen yield from the steam sawdust gasification module is utilized with an amount defined by the used utilization factor to produce power via SOFC stack while the unutilized hydrogen is sent to the burner. The hydrogen yield from the gasified biomass and the power produced from the consumed hydrogen is plotted in Figure 7.28.

7.4.3 Effect of Preheated Air

In the gasification temperature range, the utilized hydrogen that stack consumes is known. The power produced from the stack is calculated and from the energy conservation of SOFC, the preheated temperature of air that is fed to SOFC is known. The preheated air flow rate changes such that a hydrogen-oxygen ratio of 2 is required to perform the electrochemical reaction. More preheated air per gasified biomass consumes more hydrogen, and thus produces more power which enhances the system efficiency. Also, air has a cooling effect on the cell Bavarsad [65] and on the downstream stack components like the burner as well. This leads to less power produced and hence less stack power and results in lower electrical efficiency.

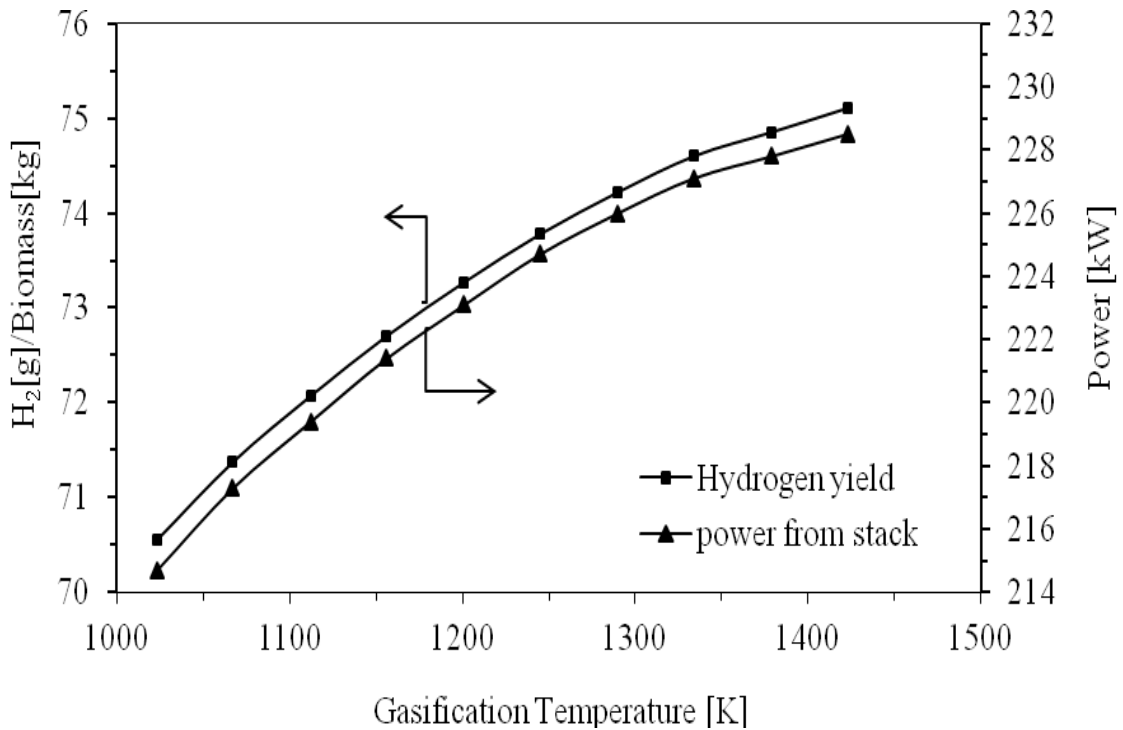


Figure 7.28 Power produced from hydrogen yield at different gasification temperatures.

The burner preheated air temperature is kept constant (430 K) for energy conservation analysis. To keep energy balance around the burner former heat exchanger more air is required to flow. More preheated air fed to the burner lowers the burner temperature. Therefore, the stream at the gas turbine inlet has a lower energy content which leads to lower efficiency. Results show that the air flow rate has the almost same trend; air flow rates in the gasification temperature range are shown in Figures 7.29-7.32 to illustrate variations of the system efficiency against preheated air biomass ratio, preheated air temperature and burner temperature, respectively. Higher preheated air temperature means higher energy available for the burner and less energy hydrogen content, which results in lower efficiency of the system that is based on hydrogen yield.

The mass flow rate ratio and temperature at different states throughout the system are given in Table 7.9.

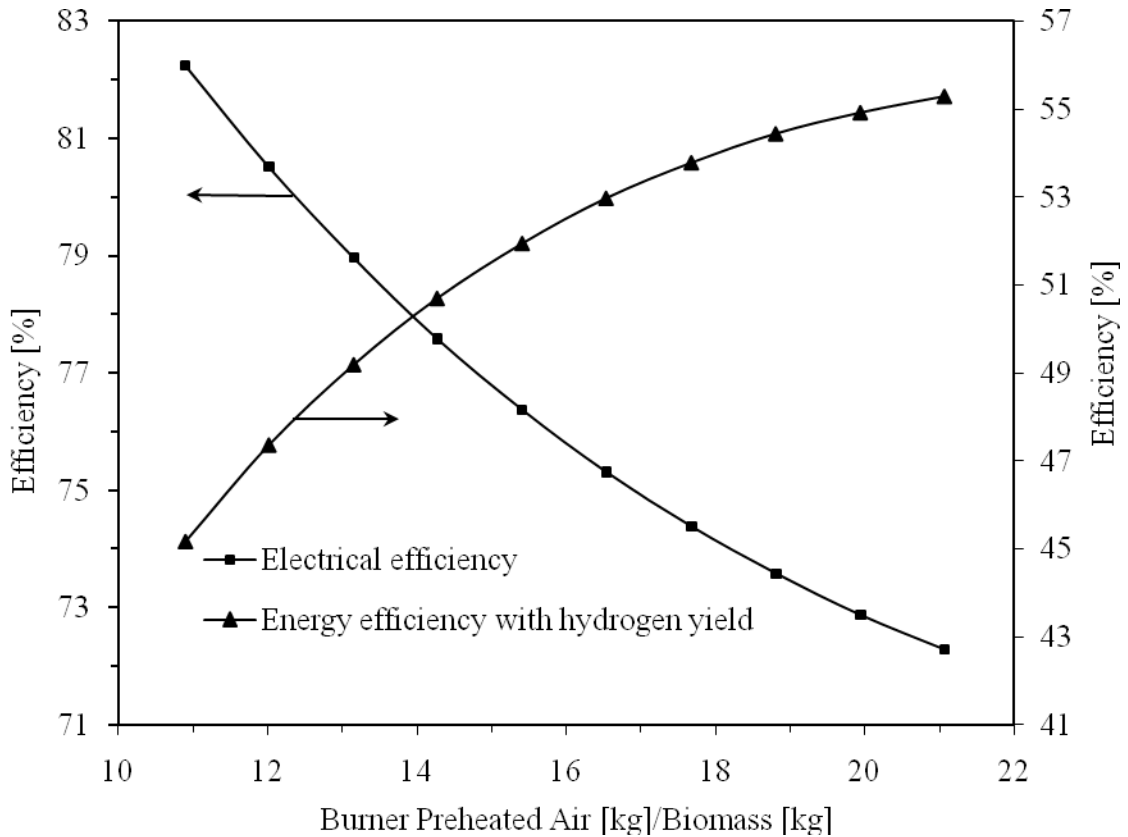


Figure 7.29 System II energy efficiencies versus preheated air flows to the burner.

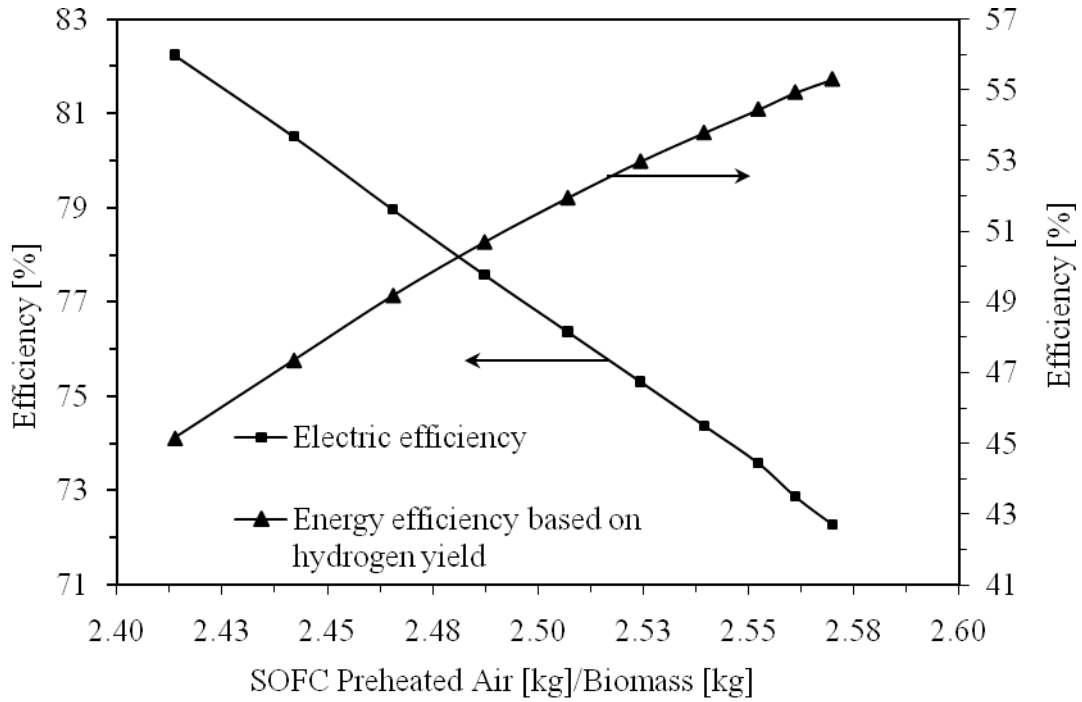


Figure 7.30 System II energy efficiencies versus preheated air flows to the SOFC.

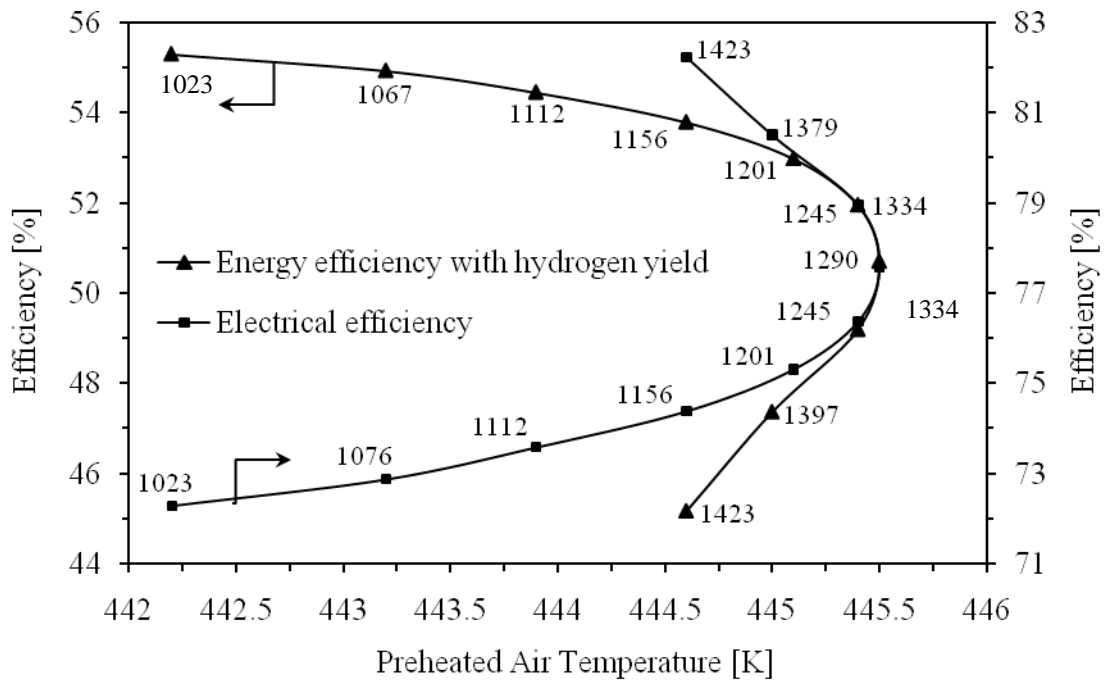


Figure 7.31 System II energy efficiencies versus preheated air temperature at different gasification temperatures.

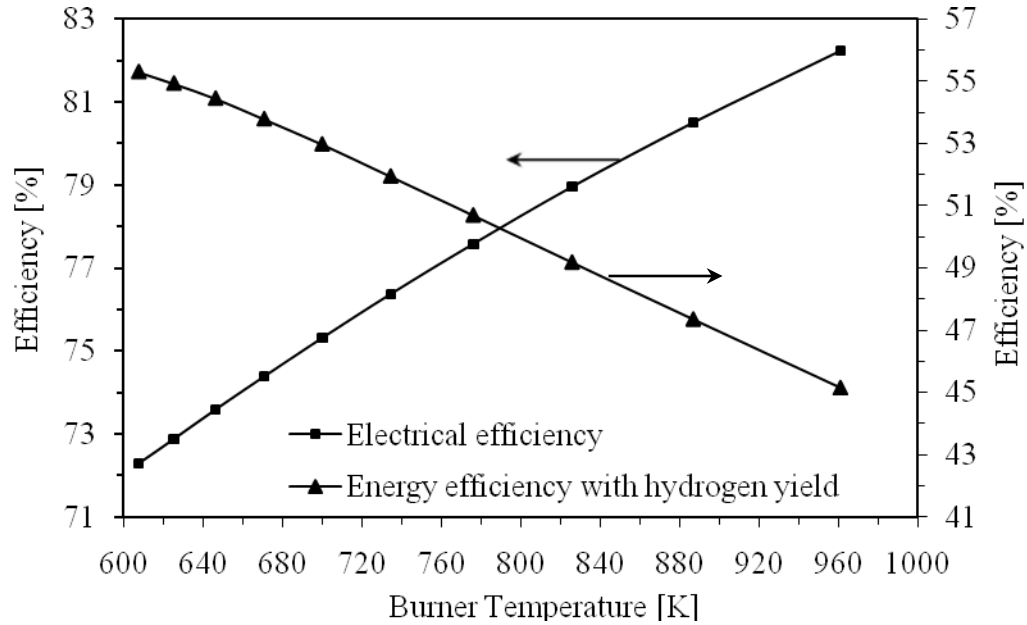


Figure 7.32 System II energy efficiencies versus burner temperature.

Table 7.9 Temperature and mass through system II for a gasification temperature of 1023 K.

State no.	Temperature [K]	Mass[kg]/Biomass[kg]	State no.	Temperature [K]	Mass[kg]/Biomass[kg]
0	298	-	24	298	9.884
10	444.6	2.414	25	322.2	9.884
11	1000	1.904	27	1000	0.196
13	615	0.071	33	889.2	0.049
14	1000	0.631	34	889.2	1.345
15	1000	0.0002	35	430	9.884
16	615	0.959	3	298	0.153
17	612.8	0.960	4	500	0.153
18	289	0.960	5	498	1.030
19	1000	0.630	6	615	1.030
20	1000	0.434	7	961.2	10.899
21	534.3	0.434	8	363	10.899
22	889.2	1.393	9	316.4	2.414
SOFC	1000	-	FG	363	-

7.4.4 Effect of Pressure Ratio

The study was performed at the same pressure where the lower pressure was found to be preferable for hydrogen production from steam biomass gasification. Pressure effect is studying when the SOFC operates at a temperature of 1000 K and different current densities of 600, 750 and 900 mA/cm² and the utilization factor is 0.95. It is found that an increase in cell operating pressure has a diminishing effect on the power produced per cell and cell efficiency as well (Figures 7.33 and 7.34).

However, increasing the pressure ratio will increase the preheated air and its temperature as well. This leads to an increase in the excess depleted fuel and air temperature, and thus more energy is available for the burning process and less preheated air is required for the burning process. A variation in the operating pressure of the used SOFC shows that there is an improvement of ~1% in the efficiency and an improvement of ~1 W in the produced power.

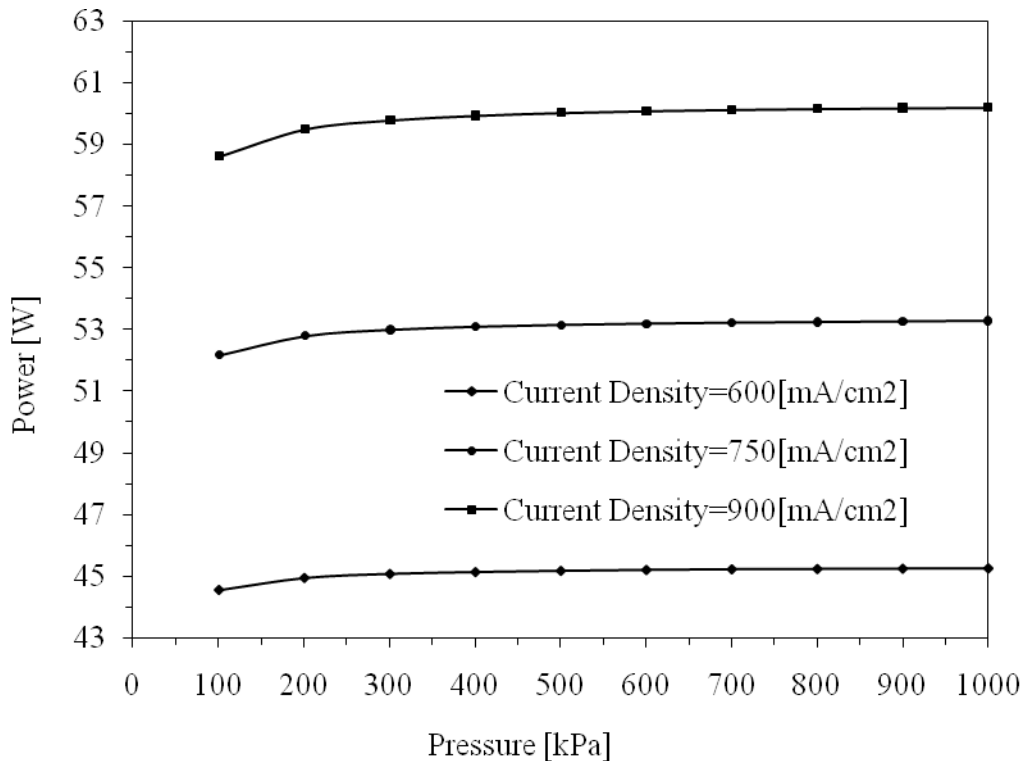


Figure 7.33 SOFC Power at different pressures and current densities.

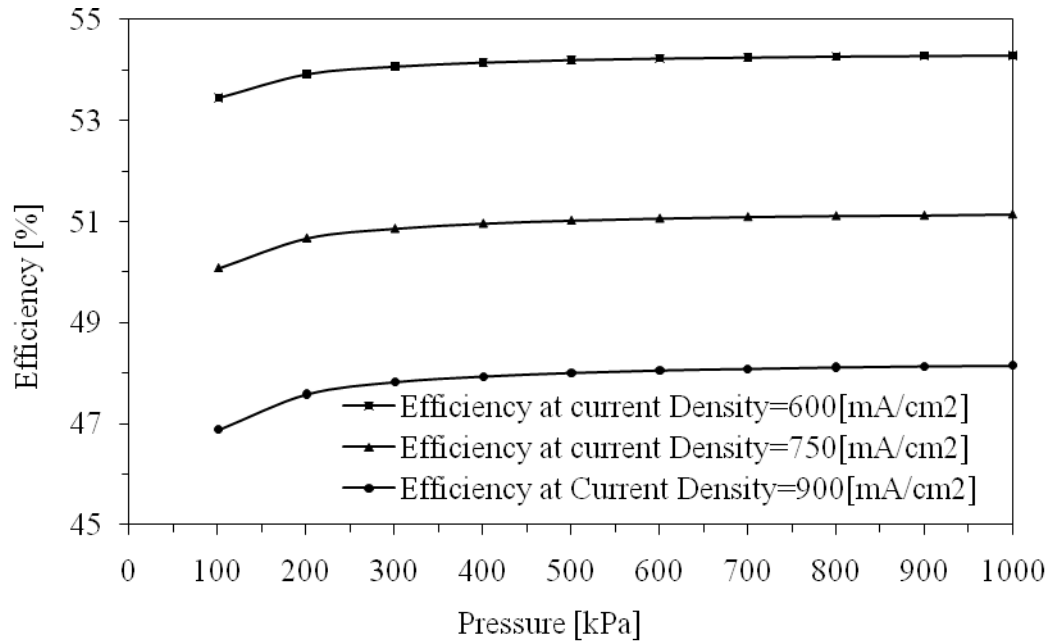


Figure 7.34 SOFC efficiency at different pressures and current densities.

7.4.5 Electrical Efficiency for System II

The electrical efficiency is studied in a gasification temperature range of 1023-1423 where the hydrogen yields are in the range of 70-75 gH₂/kg of biomass. In the gasification temperature range and for the given steam-biomass ratio, the gasification products from gasification are known from the gasifier module. The derived gasification hydrogen is consumed by the SOFC stack while the hydrogen is derived from bottoming processes; methane steam reforming and water gas shift reactions is stored.

The efficiency of the system for hydrogen yields from the later processes as well as that for electrical efficiency is plotted in Figure 7.35. It is found that the electrical efficiency is decreased from 82 to 72 %. The electrical efficiency of the SOFC is the same while the electrical efficiency of the turbine decreases as a result of burner temperature decreasing. In the same range of the gasification temperature, the efficiency of the system considers secondary hydrogen yield increases from 45 to 55.3%.

7.4.6 Exergy Destruction in System II Components

The rate of exergy destruction is calculated for the system components and is shown in Figure 7.36. It is clear from the graph that a major part of the exergy destruction

occurs in the SOFC stack followed by the turbine and the burner. Also, it is found that the total exergy destruction in the system components is at minimum when the gasification temperature is 1175 K, see Figure 7.37.

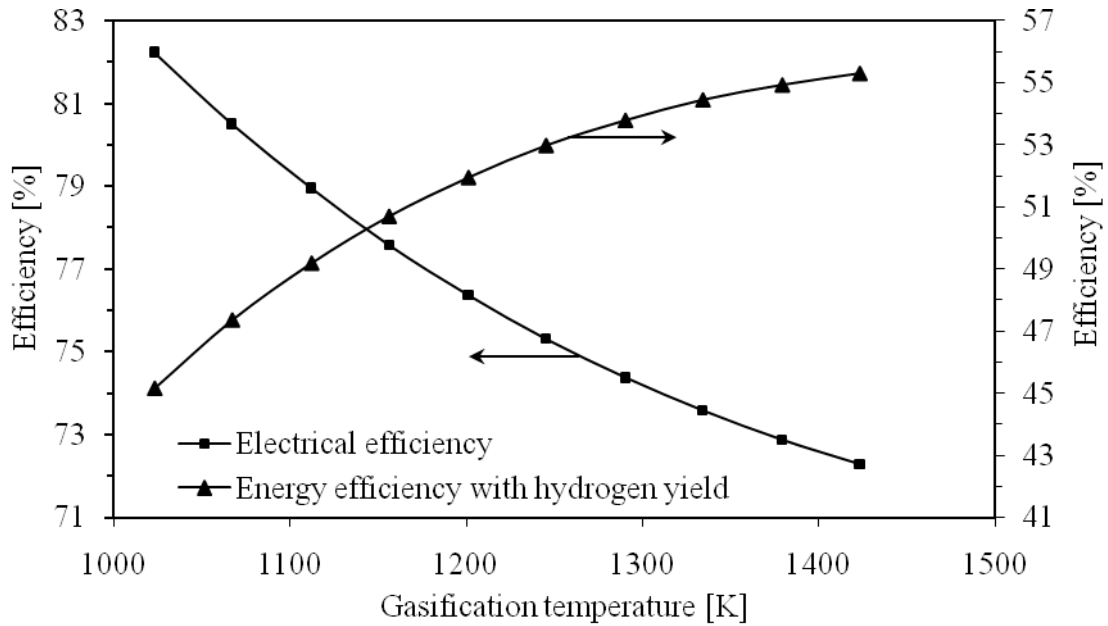


Figure 7.35 System II energy efficiencies versus gasification temperature.

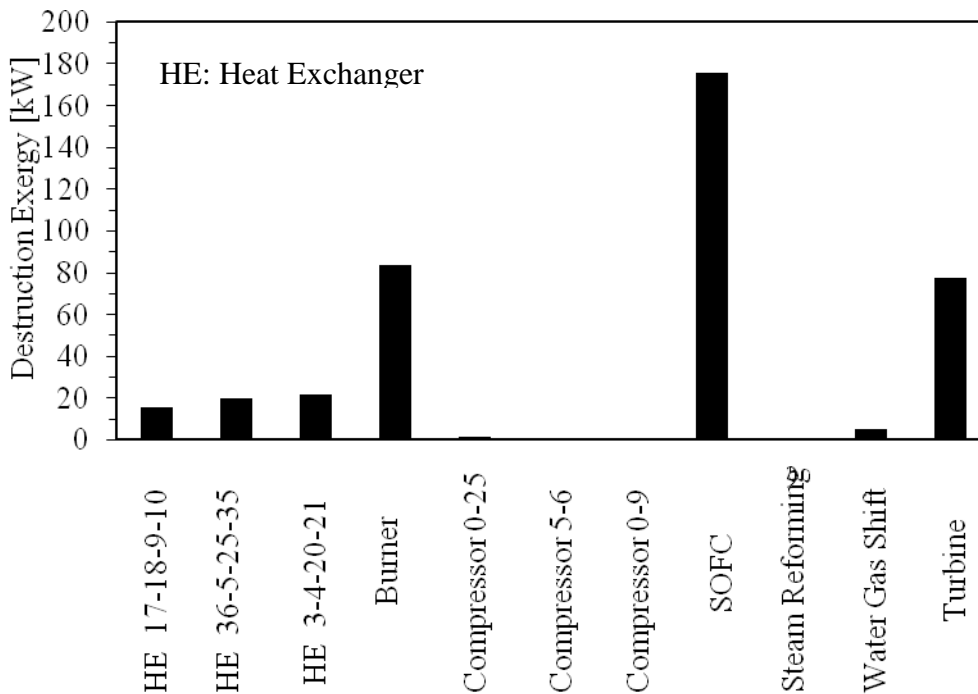


Figure 7.36 Exergy destruction in system II components at 1023 K.

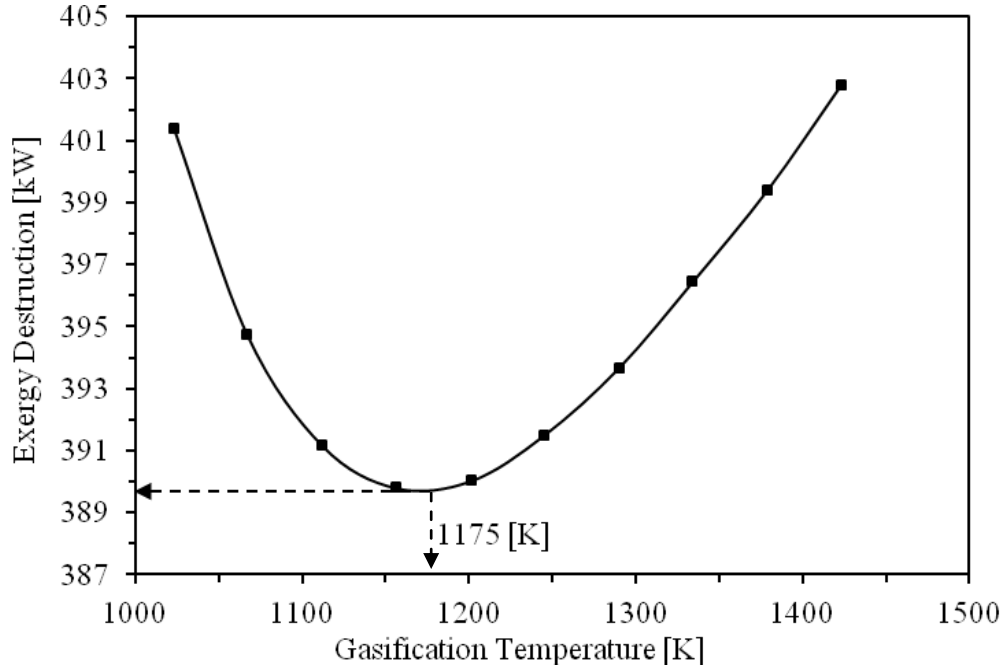


Figure 7.37 Exergy destruction in system II components versus gasification temperature.

7.4.7 System II Exergy Efficiencies

In the gasification temperature range, and for a given utilization factor and steam-biomass ratio, the overall exergy efficiency for electrical production from the system was based on exergy of biomass through put versus gasification temperature as shown in Figure 7.38. The efficiency decreases from 56 to 49.4 % in the studied gasification temperature range because of the decrease in the exergy efficiency of the turbine. From the exergy loss results, it was found that a major part of exergy destruction occurred in the SOFC. Also, its exergy destruction increased with the gasification temperature. Secondary hydrogen yield increases and accordingly, its exergy increases and thus its exergy efficiency increases from 22 to 32 %.

To study the effect of pressure ratio through the gas turbine on the system efficiencies, the system pressure increases to 2 bar and the obtained efficiencies are plotted in Figure 7.39 and Figure 7.40. It is observed that the efficiencies have similar trends; there is also an improvement in both energy and exergy efficiencies for hydrogen production where at 1023 K the energy efficiency increases from 45.16 % to 45.30 % and

the exergy efficiency increases from 21.85 % to 26.20 %. This is attributed to the hydrogen yield from steam reforming and water gas shift reactors increase.

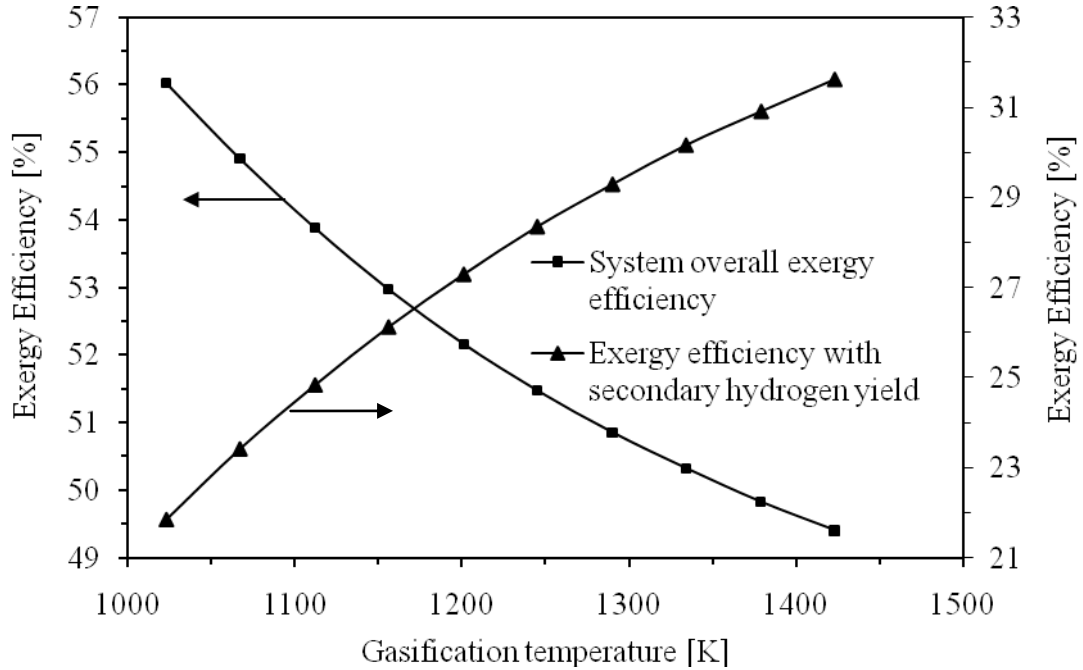


Figure 7.38 System II exergy efficiencies versus gasification temperature.

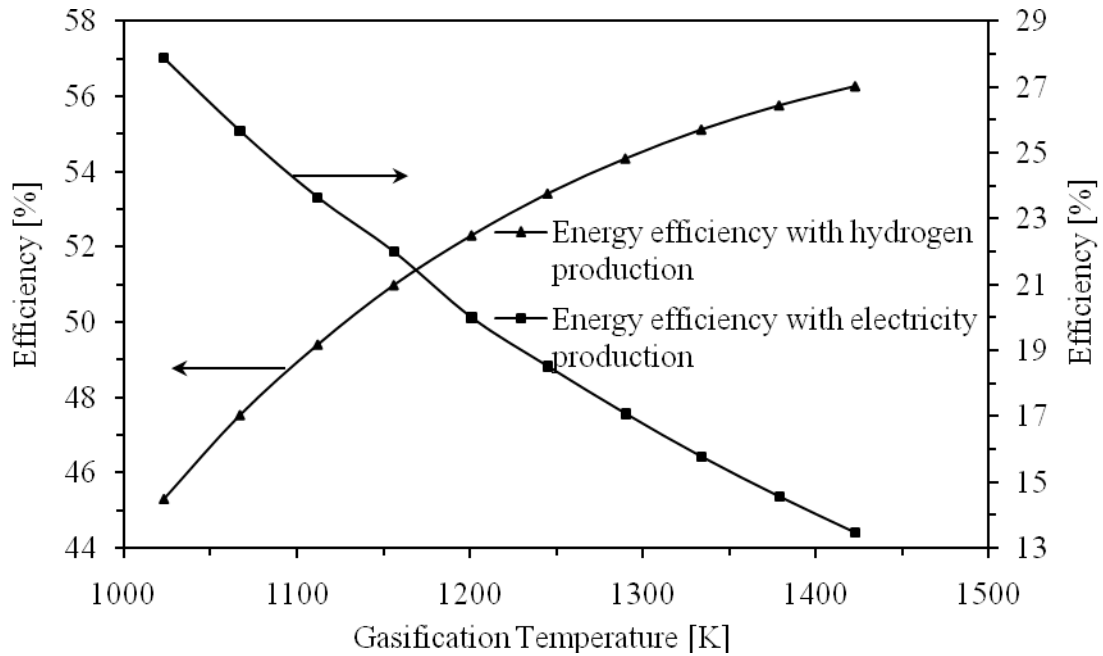


Figure 7.39 Energy efficiencies at the operating pressure of 2 bars.

7.4.8 System II Exergoeconomic Results

The practical system has to satisfy the thermodynamic laws. Energy and exergy analyses are thus first conducted to find the properties of the state points, and the results are then used in the exergoeconomic analysis. In the economic analysis, the system costs are levelized for 25 years. Conducting the study at different gasification temperature requires, according to the used exergoeconomic model, that the SOFC find its owning and operating cost for each gasification temperature where the number of SOFC that utilizes the hydrogen derived by the gasification process is varied.

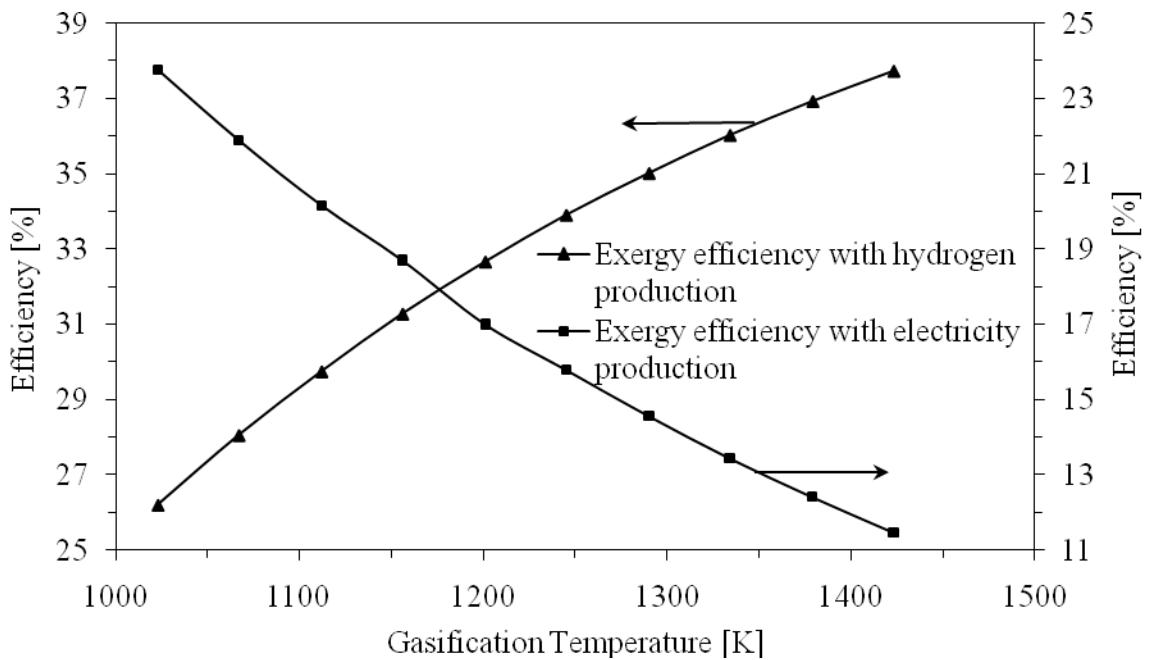


Figure 7.40 Exergy efficiencies at the operating pressure of 2 bars.

The results from the exergoeconomic analysis by applying the SPECO method and within the studied gasification temperature range of 1023-1423 K show how much hydrogen yield influences the cost of its exergy unit. It is found that within the gasification temperature range, the primary or by-product steam gasification hydrogen increases with increasing gasification temperature (Figure 7.41).

The primary hydrogen yield and its temperature have almost the same trend versus the gasification temperature (Figure 7.42) where the results show that there is an increase of 4°C in the primary hydrogen temperature during the studied gasification

temperature range where the exergy is increased and therefore the cost per unit exergy decreases (Figure 7.43).

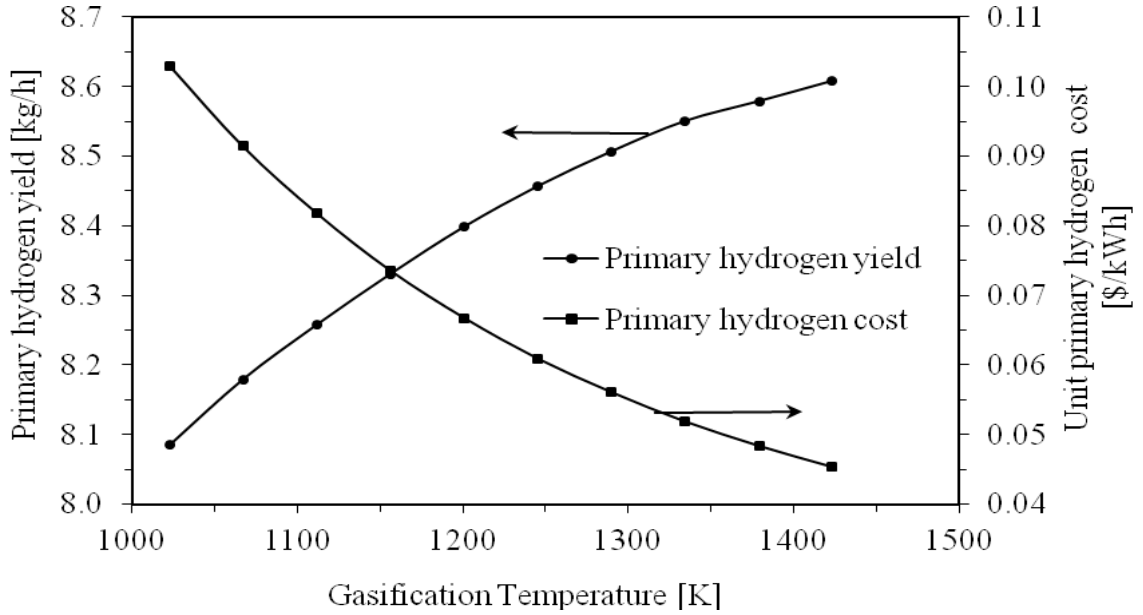


Figure 7.41 System II primary hydrogen yield and its cost of versus gasification temperature.

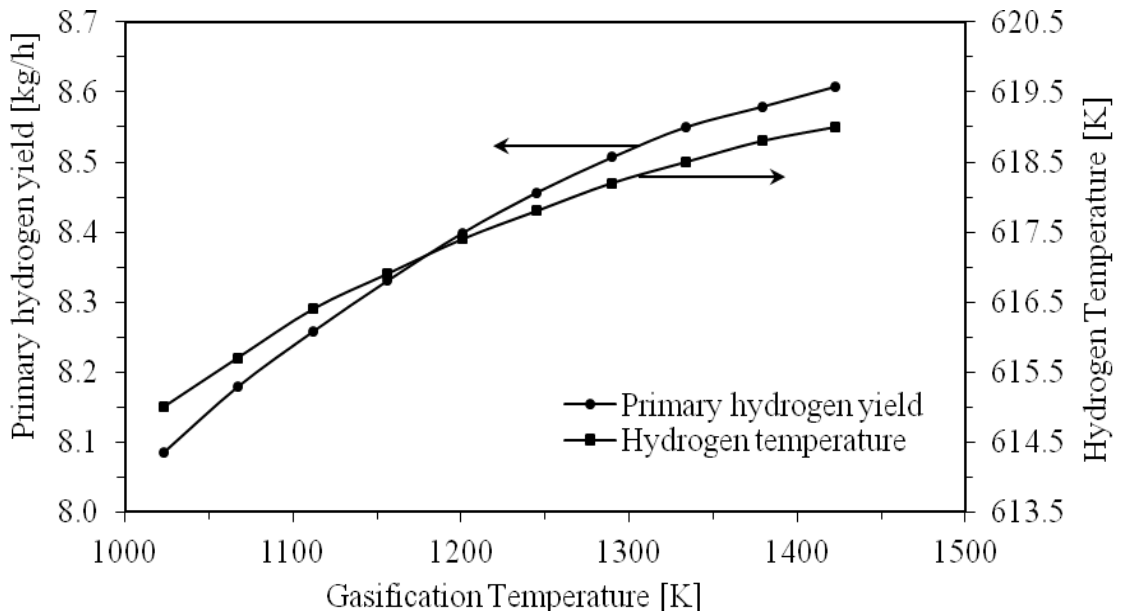


Figure 7.42 System II primary hydrogen yield and its temperature versus gasification temperature.

The secondary hydrogen yield or the hydrogen derived from the further processing of the gas products in the gasifier bottoming processes increases within the studied gasification temperature range. It is observed at a higher gasification temperature that there is a drastic decrease in the cost per unit exergy from the secondary hydrogen. This can be attributed to the hydrogen yield increase with the operating temperature of the gasifier increase which results in a reduction in specific cost by 0.025 \$/kWh (Figure 7.44). This hydrogen has a temperature that varies with a trend similar to that of its yield; however, its temperature is less sensitive at a higher gasification temperature (Figure 7.45). Although there is an increase in hydrogen yield, its temperature continuously increases and this could be due to the increase of hydrogen contribution from reactions that take place in the gasifier bottoming processes (Figure 7.46).

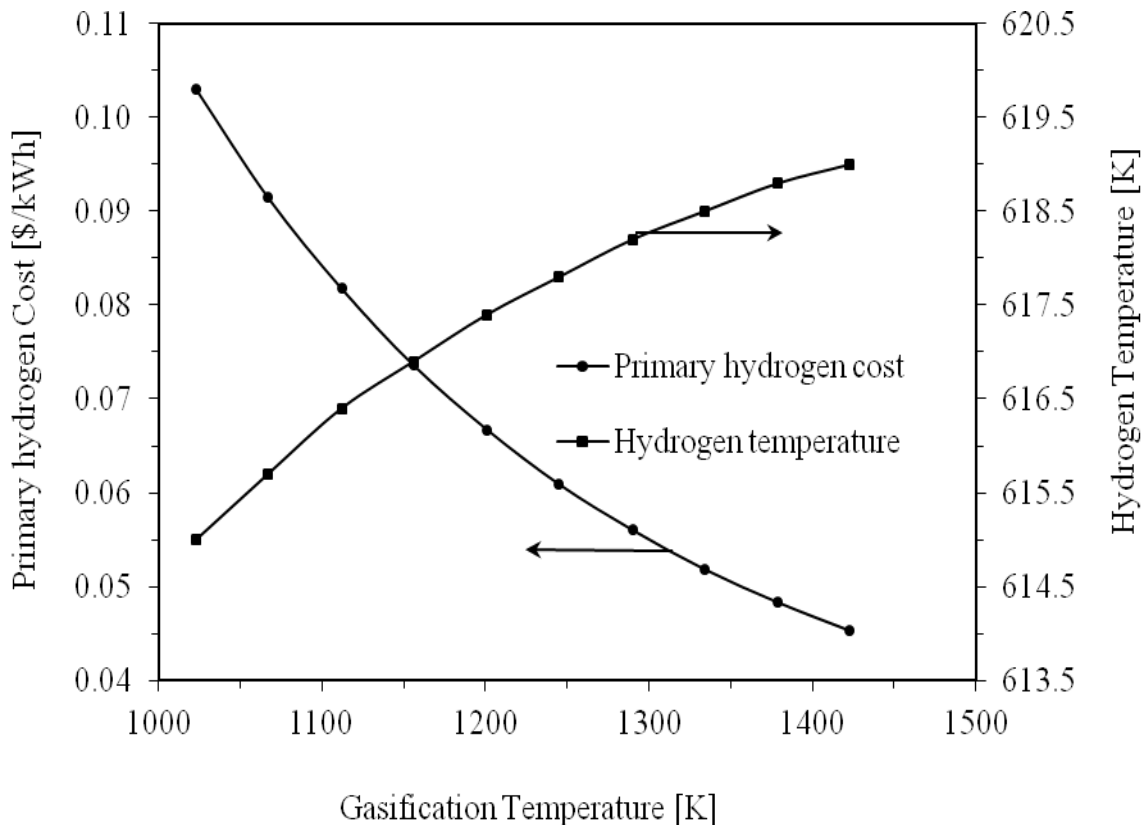


Figure 7.43 System II primary hydrogen cost and its temperature versus gasification temperature.

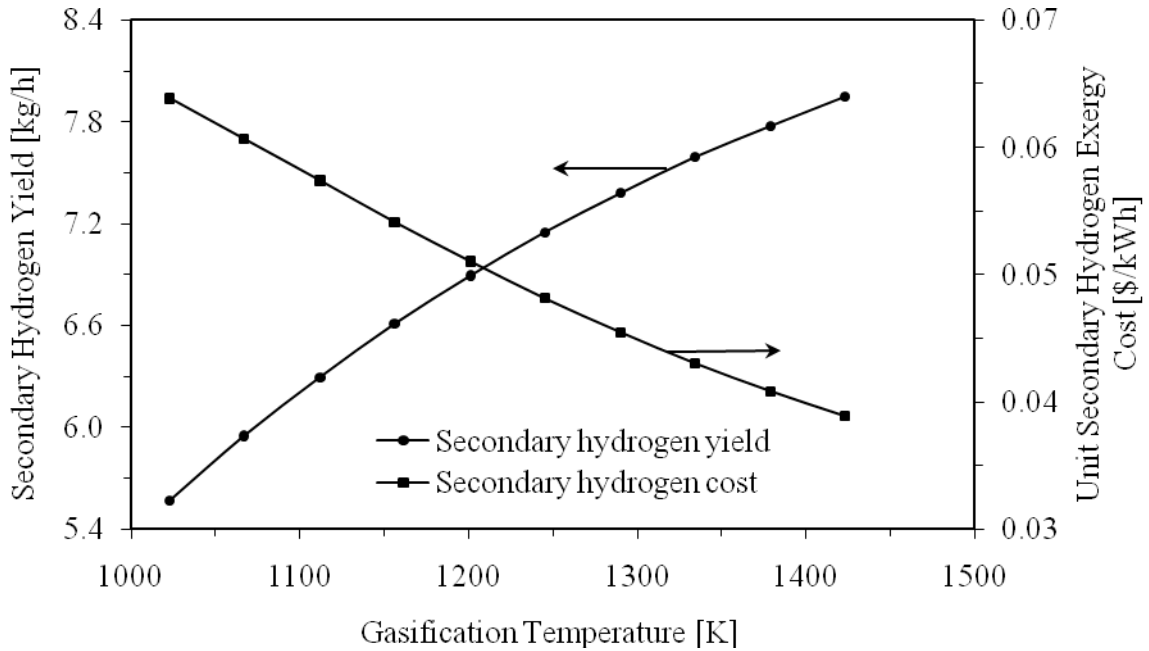


Figure 7.44 System II secondary hydrogen yield and its cost at different gasification temperatures.

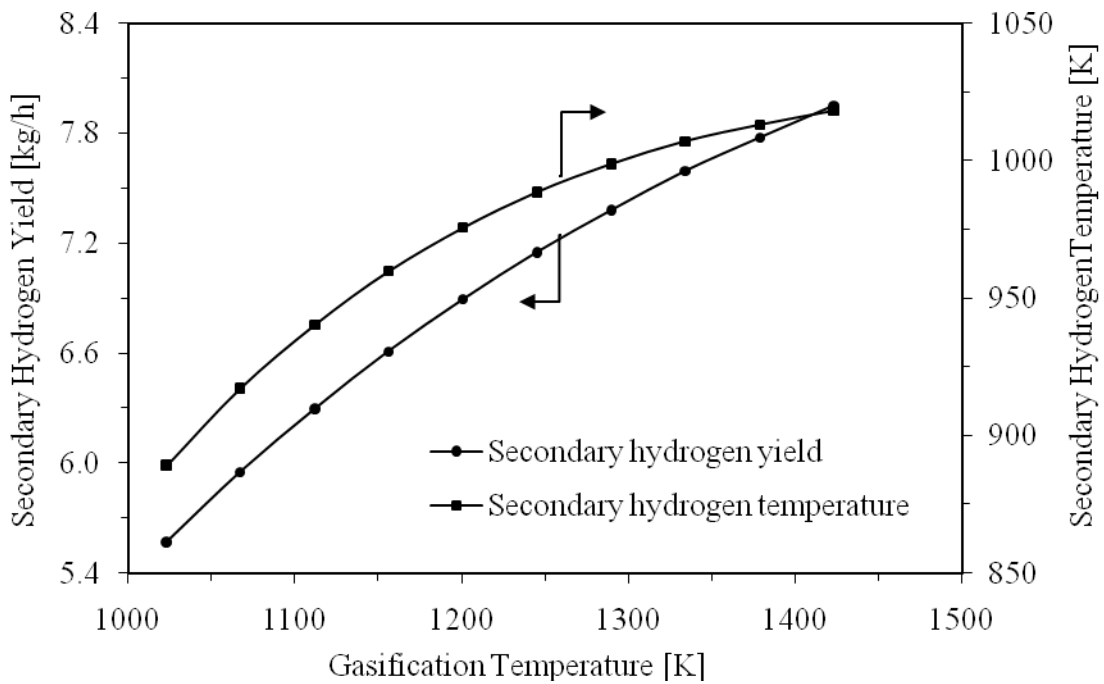


Figure 7.45 System II secondary hydrogen yield and its temperature versus gasification temperature.

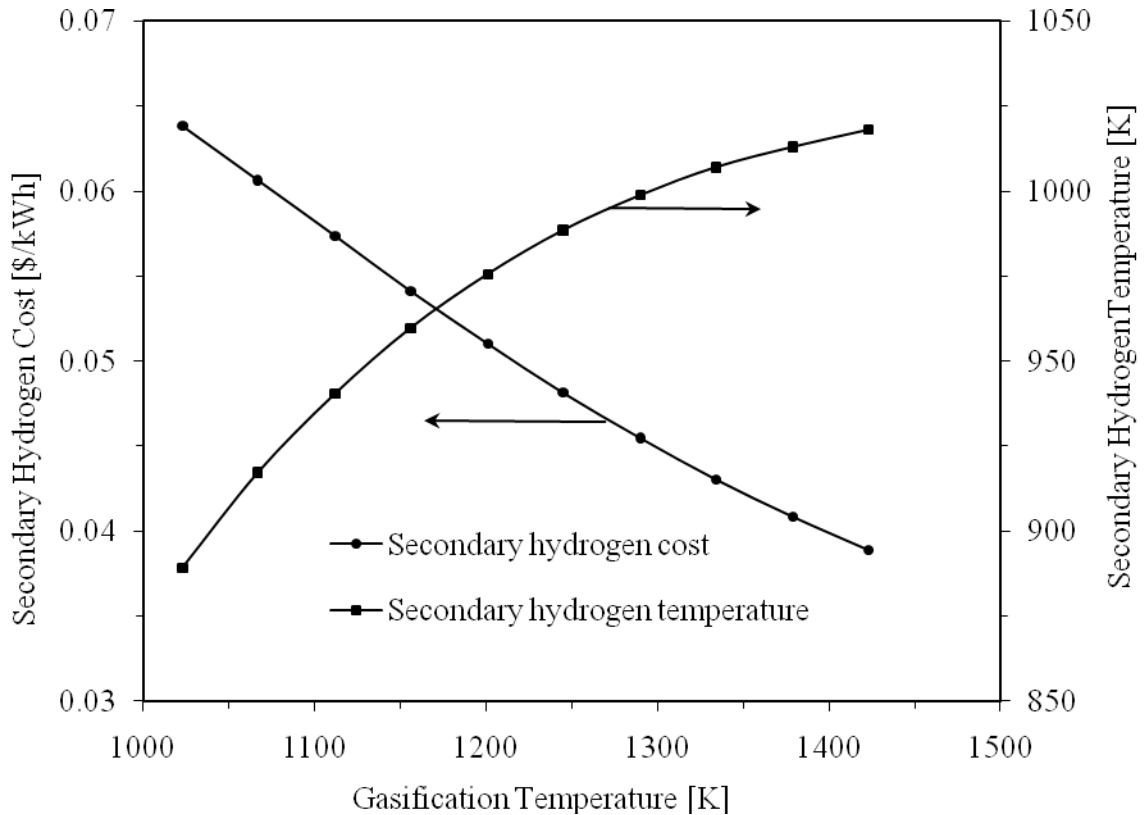


Figure 7.46 System II secondary hydrogen cost and its temperature versus gasification temperature.

In this study, the SOFC stack totally consumes the primary hydrogen. It is found that the primary hydrogen yield increases with increasing gasification temperatures. According to the reaction equation that governs the reaction in the SOFC, the steam will increase as more primary hydrogen is fed (Figure 7.47). On the other hand, more steam is needed to perform the water gas shift and steam reforming reactions which make less excess steam are available for use (Figure 7.48). The decrease in the specific cost at this state point is attributed to the fact that the steam exergy cost is affected by the cost of the SOFC product steam whereas in the exergoeconomic model both are assumed to have the same cost. Therefore, its cost will decrease as the cost of the total steam decreases and vice versa.

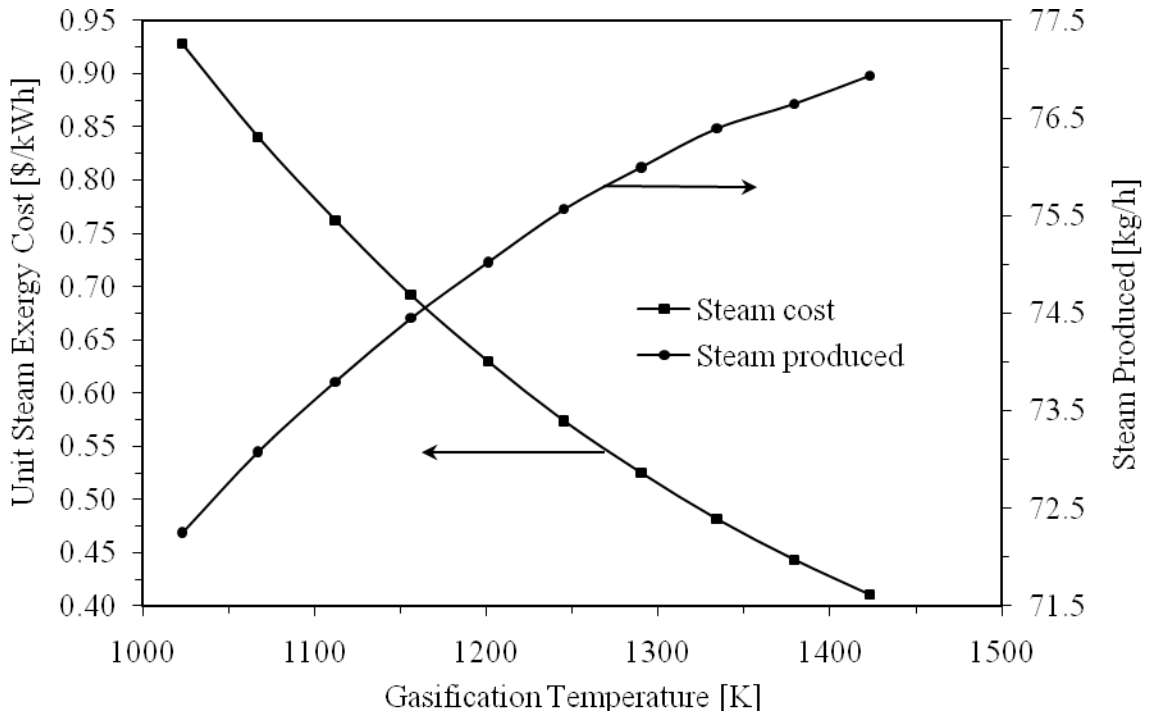


Figure 7.47 Produced steam in system II and its cost versus gasification temperature.

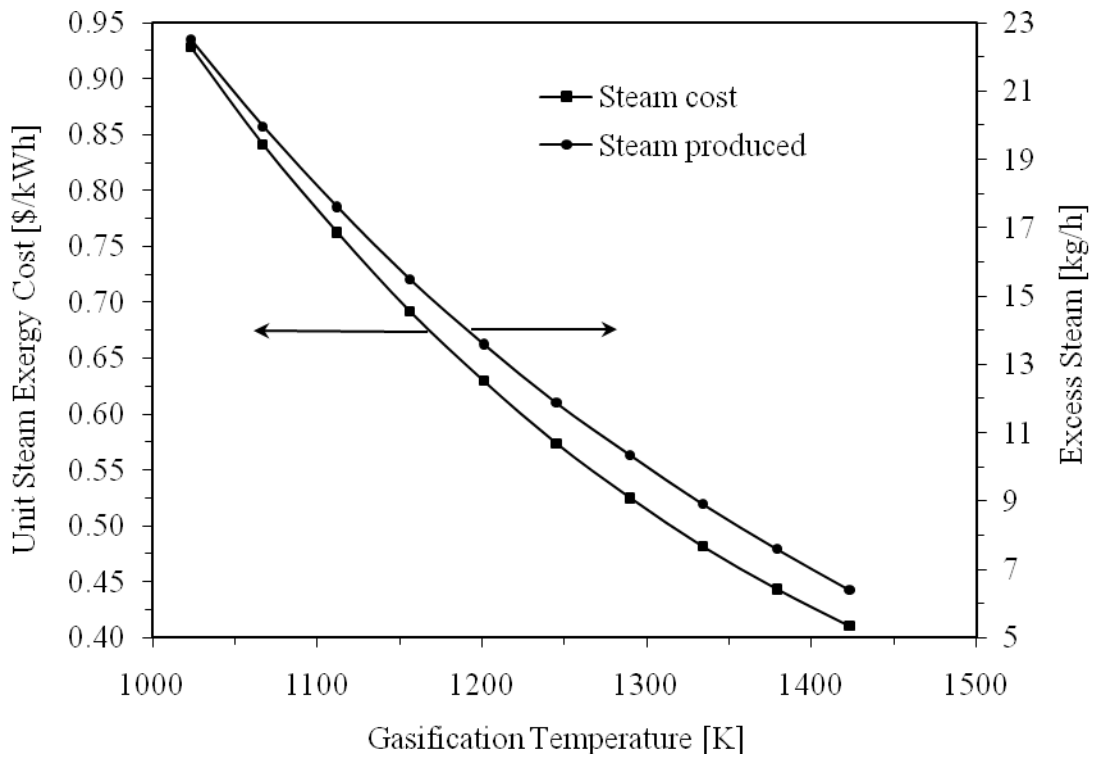


Figure 7.48 Excess steam in system II and its cost versus gasification temperature.

At a gasification temperature of 1023 K, the specific cost of the other flow material streams can be found from Table 7.10.

Table 7.10 Unit exergy cost and cost rate for flow material streams in system II.

State no.	C [\$/kWh]	\dot{C} [\$/h]	State no.	C [\$/kWh]	\dot{C} [\$/h]
0	0.000	0.000	16	0.103	17.390
1	5.2E-06	3.714	17	0.111	18.740
2	0.105	25.170	18	0.111	10.020
3	0.000	0.000	20	0.928	22.300
4	3.769	20.410	21	0.928	2.646
5	0.105	22.720	22	0.135	14.000
6	0.113	25.100	24	0.000	0.000
7	0.161	19.040	25	0.155	3.304
8	0.000	0.000	26	0.137	0.361
9	0.546	2.660	27	0.928	10.100
10	6.175	12.130	33	0.064	11.810
11	0.928	11.120	34	0.071	2.447
13	0.103	7.966	35	0.005	6.220
14	0.928	13.350	36	0.105	24.890
15	0.928	0.004			

7.5 Results for System III

The system under investigation is simulated at a steady state condition and the results are obtained from the conducted analyses on sawdust steam biomass gasification and its downstream reactions to perform multi duties: heat and power generation. To follow the same strategy regarding the gasification module of System I and System II, its operating conditions and a range of parameters analysis are considered. Accordingly, it is decided to perform the parametric study within a gasification temperature range of 1023-1423 K and a steam-biomass ratio of 0.8 kmol steams per kmol biomass which fall in the range that was studied in System I and System II. In addition, the products from the gasifier module in this system are found by using the same module developed there.

The SOFC module was discussed in System II and the results regarding the SOFC showed acceptable trends compared to what is available from literature and what was discussed there. Here the SOFC is coupled with the SOEC in a type of lumped system. The SOEC uses the same operating and related data as that of the SOFC which can be considered, at this stage, satisfactory to a certain extent and a type of support to any results which will be obtained from this system. The same module will be used in this system and under the same operating and related material data.

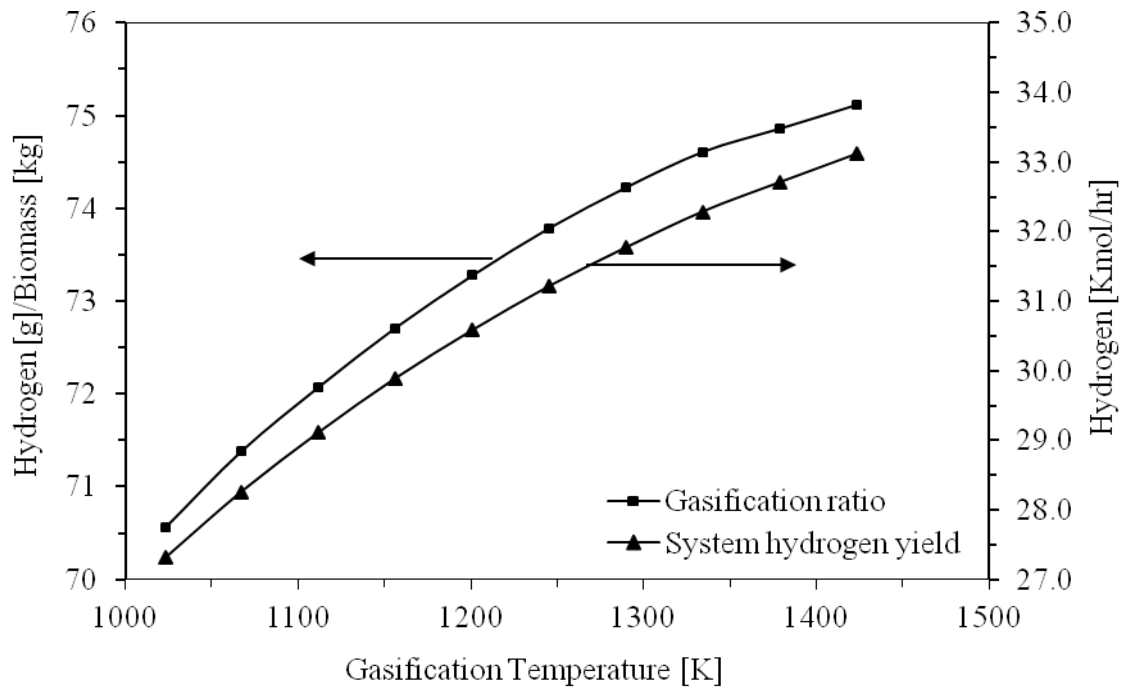


Figure 7.49 System III gasification ratio and hydrogen yield at different gasification temperatures.

7.5.1 Effect of Gasification Temperature on Hydrogen Yield

For the certain amount of sawdust wood and the certain amount of steam, it is found that the hydrogen yield increases as the gasification temperature increases from 1023 to 1423 K. That gives an indication that both the primary hydrogen (derived gasification hydrogen) and the secondary hydrogen (hydrogen from gasifier downstream reactions) from this system contribute to the system hydrogen yield. This contribution increases with an increase in the gasification temperature. In this system, the primary

hydrogen is not utilized in any conversion process. The hydrogen yield from the gasified sawdust and that produced from the processing system are plotted in Figure 7.49.

7.5.2 Effect of Preheated Air in System III

For the specified SOFC, the utilized hydrogen that the cell consumes is known. At the preheated air temperature and by knowing the power produced from the SOFC, the number of cells in the SOFC stack is calculated from energy conservation of the SOFC, and this also will be the number of cells in the SOEC stack. The flow rate of the preheated air changes such that a hydrogen-oxygen ratio of 2 is required to perform the electrochemical reaction in the SOFC. This hydrogen continuously circulates from the SOEC cell to the SOFC cell. More preheated air consumes more hydrogen and produces more steam, which in turn decomposes to circulate more hydrogen to the SOFC and results in more oxygen being sent to the burner which increases the burner temperature.

To keep a common base of comparison between this system and System II, the burner preheated air is kept at the same temperature (430 K). More gases flow through the former burner heat exchanger, resulting in higher energy content in the burner. To keep energy balance around the burner former heat exchanger, more air is required to flow as more gasification products flow. More preheated air feeds to the burner and lowers the burner temperature. Therefore, the stream at the gas turbine inlet has a lower energy content which leads to lower turbine efficiency (Figure 7.50). Also, the same conclusion can be drawn in regard to the SOCF-SOEC preheated air (Figure 7.51). The higher preheated air temperature enhances the electrical efficiency whereas more energy will be available to the burner. The efficiency increasing becomes drastic in the case of the higher preheated burner air temperatures (Figure 7.52) and totally linear in case of the higher preheated SOFC-SOEC air temperatures (Figure 7.53). Higher preheated air temperature means higher energy available for the burner and less energy content in hydrogen which results in lower efficiency of the system that considers hydrogen yield. Mass flow rate ratio and temperature at different states through the system are given in Table 7.11.

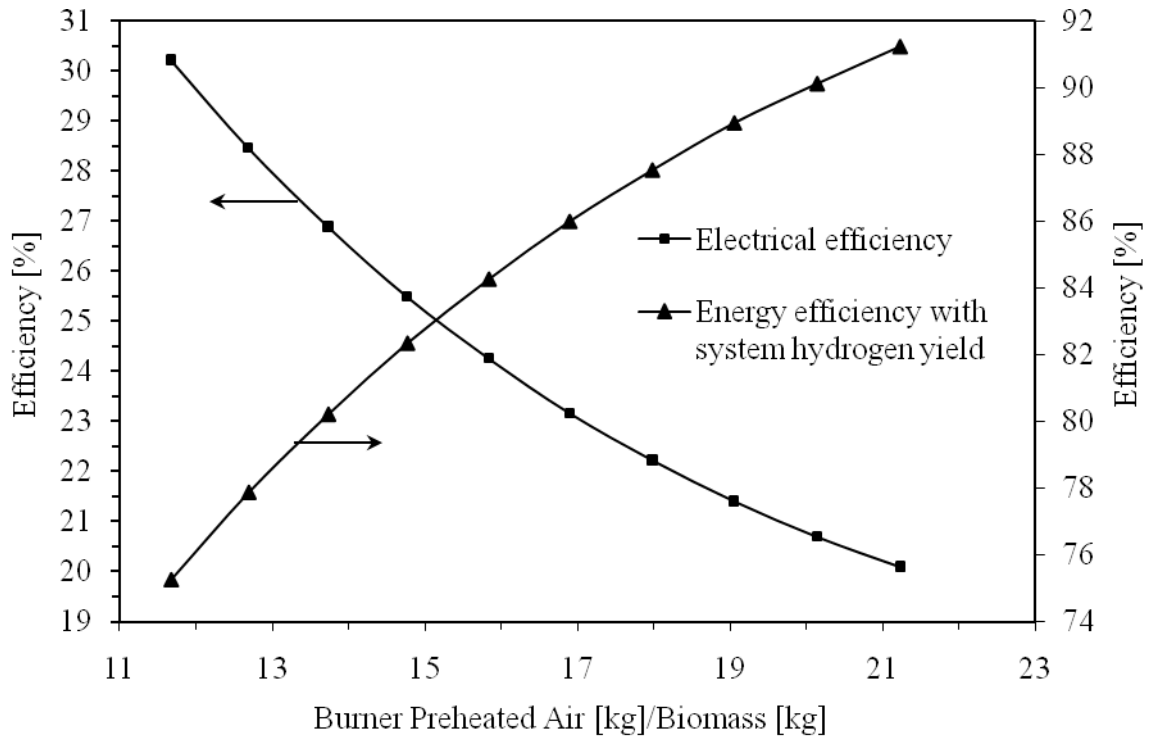


Figure 7.50 System III efficiencies versus burner preheated air flow.

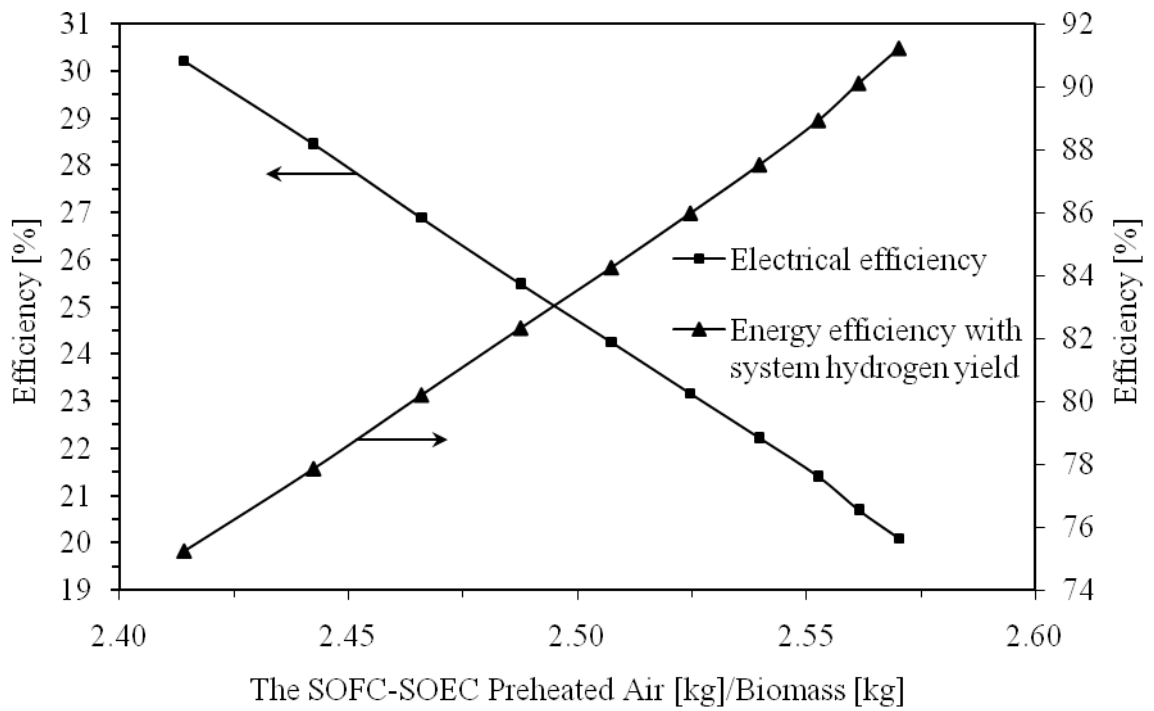


Figure 7.51 System III efficiencies versus preheated air flows in the lumped SOFC-SOEC.

Table 7.11 Mass flow per kg of biomass and temperature through system III when the gasification temperature is 1023 K.

State no.	Temperature [K]	Mass[kg]/Biomass[kg]	State no.	Temperature [K]	Mass[kg]/Biomass[kg]
0	298	-	18	311	1.030
3	298	0.153	19	766	1.464
4	500	0.153	20	759	0.434
5	298	1.464	21	759	0.434
6	366.4	1.464	22	637.7	1.464
7	841.4	13.223	23	759	0.434
8	363	13.223	24	298	11.668
9	316.4	2.414	25	321.9	11.668
10	385.3	2.414	28	298	0.434
11	1000	1.904	29	298	33.710
12	1000	0.133	30	500	33.710
13	1000	0.071	33	366.4	0.119
14	1000	0.158	34	366.4	1.345
15	759	0.0002	35	430	11.668
16	398	1.030	36	1023	1.030
17	396.9	1.030	FG	363	13.223

7.5.3 System III Electrical Energy Efficiency

The electrical efficiency is studied in a gasification ratio range of 70-75 gH₂/kg of biomass which corresponds to a gasification temperature range of 1023-1423 K. For a steam-biomass ratio of 0.8 kmol steam per kmol biomass, the gasification by products are known. The energy efficiency of the system considers hydrogen yield as well as electricity production, as plotted in Figure 7.54. It is found that the electrical efficiency decreases from ~30 to ~20 %. This is attributed to a decrease in the burner temperature. In the same range of the gasification temperature, the efficiency considers hydrogen yield increases from ~75 to ~91%.

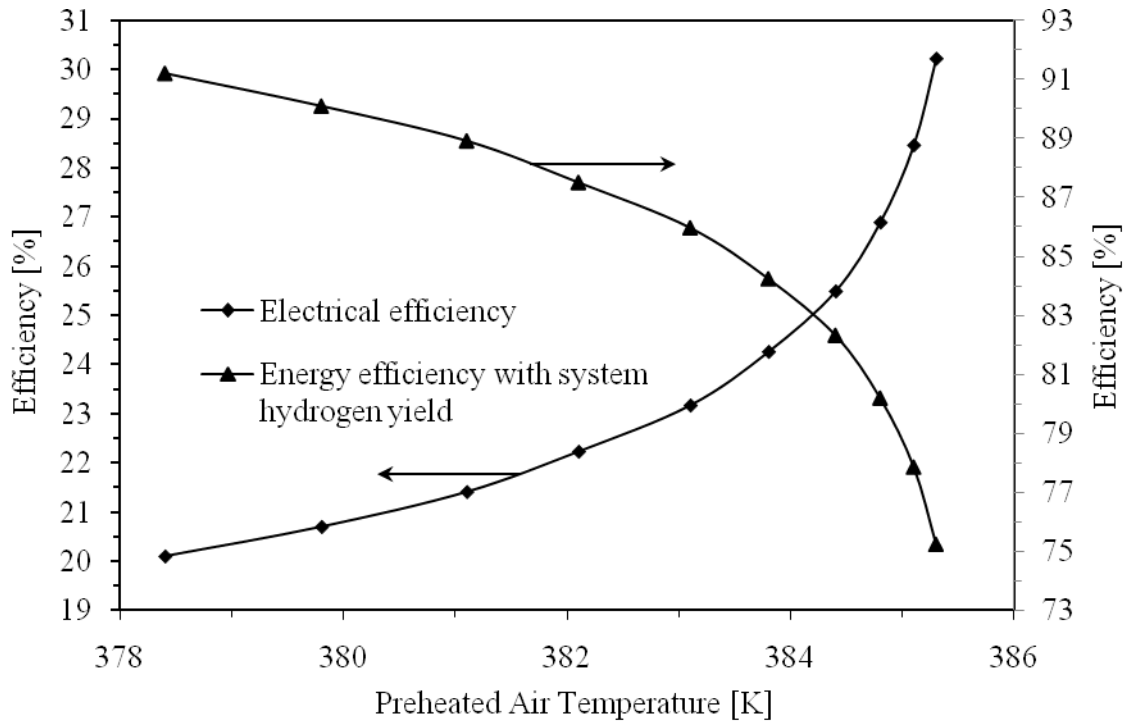


Figure 7.52 System III energy efficiencies at different preheated air temperatures.

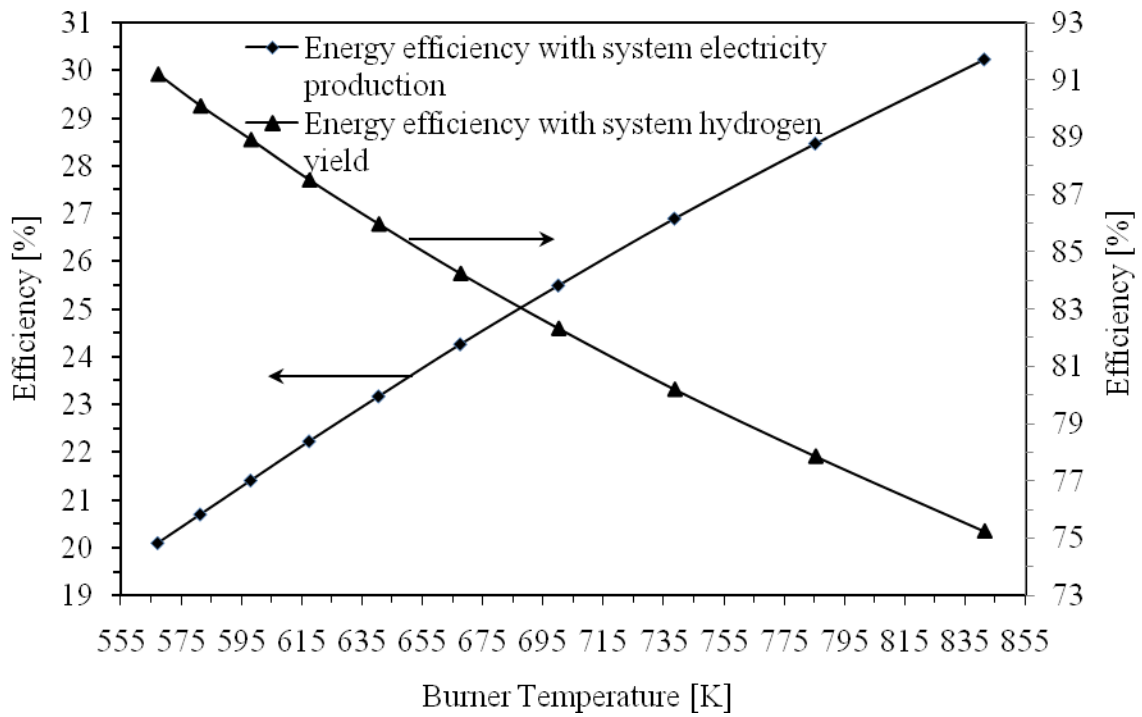


Figure 7.53 System III energy efficiencies versus burner temperature.

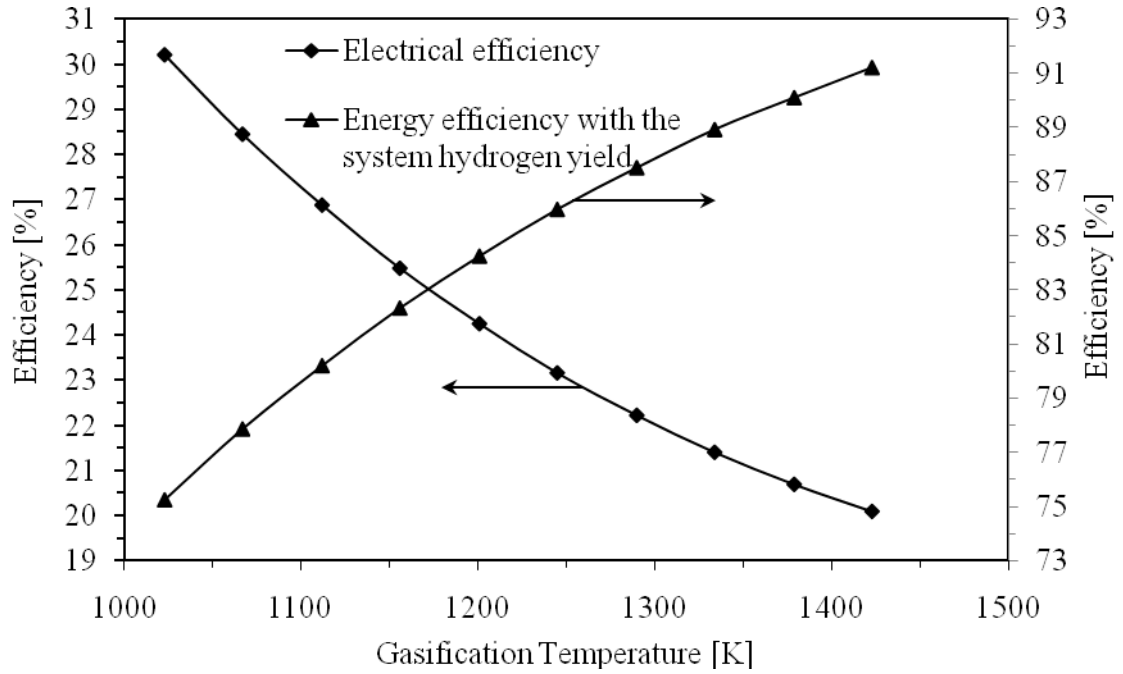


Figure 7.54 System III energy efficiencies at different gasification temperatures.

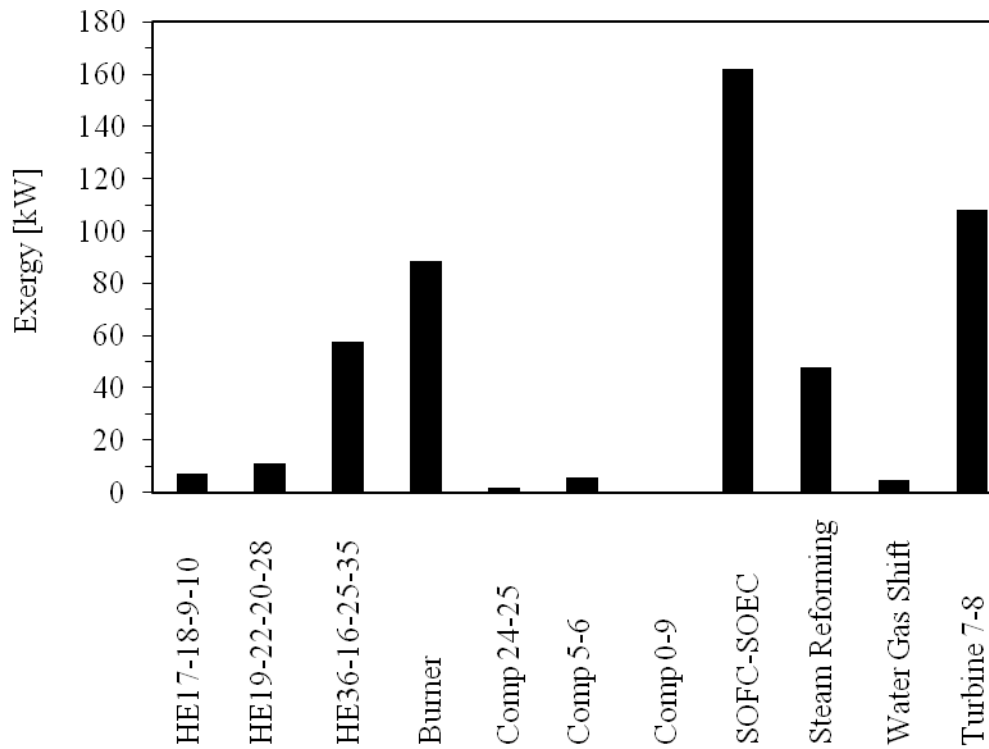


Figure 7.55 Exergy destruction in system III components at a gasification temperature of 1023 K.

7.5.4 System III Exergy Destruction

The rate of exergy destruction is calculated for the system components and is shown in Figure 7.55. From the graph, it is clear that a major part of the exergy destruction occurs in the SOFC-SOEC stack followed by the turbine and the burner.

7.5.5 System III Exergy Efficiencies

In the same gasification temperature range, and for the same steam-biomass ratio, the system exergy efficiency that considers electricity production versus the gasification temperature is shown in Figure 7.56. The efficiency decreases from 26 to 17 %. Under the same conditions, the system hydrogen yield increases and accordingly, its exergy increases and thus its exergy efficiency increases from ~63 to ~76 %. The exergy efficiency that considers electricity production from System III is lower than that of System II because only electricity from the turbine is considered, whereas that from the SOFC stack is internally consumed by the SOEC stack.

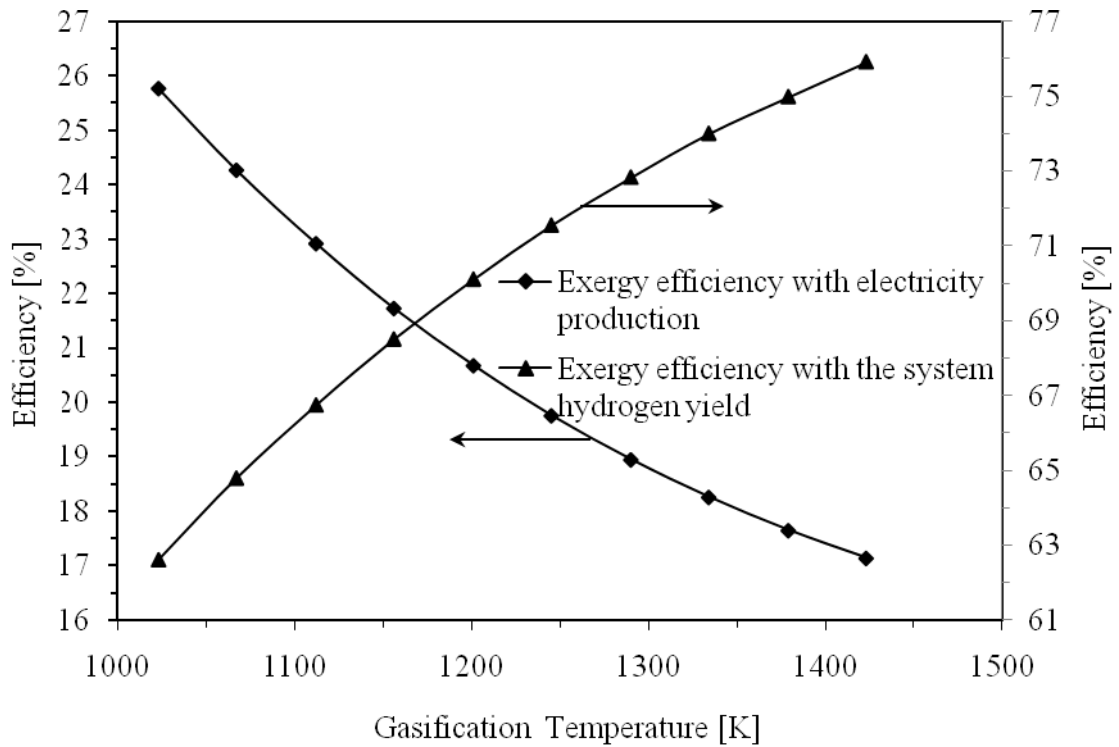


Figure 7.56 System III exergy efficiencies at different gasification temperature.

7.5.6 System III Exergoeconomic Results

In order for the system to be applicable, it has to satisfy the thermodynamic laws. The energy and exergy analyses were conducted to find the properties of the state points and the results are used in the exergoeconomic analysis.

The results from the exergoeconomic analysis after applying the SPECO method and within the studied gasification temperature range of 1023-1423 K show that the by gasification hydrogen product influences the cost of its unit exergy. It is found that within the studied gasification temperature range, by-product gasification hydrogen increases with increasing gasification temperature (Figure 7.57) while the cost of the unit exergy from this hydrogen decreases as the gasification temperature is increased.

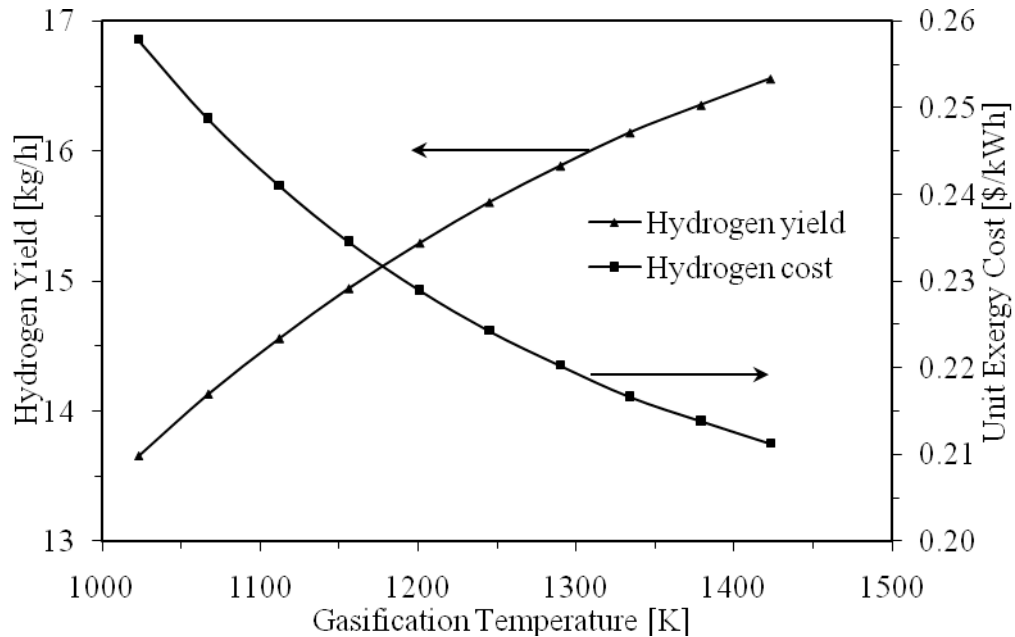


Figure 7.57 Hydrogen yield from System III and its cost at different gasification temperatures.

Conducting the study at different gasification temperatures requires the used exergoeconomic model to calculate the owning and operating cost for the lumped SOFC-SOEC, and it is considered twice that of the SOFC. In this system, the SOEC totally decomposes the by SOFC steam product and the SOFC totally consumes the by SOEC hydrogen product. More hydrogen is produced in the system and thus its energy content

is higher which results in hydrogen with higher temperature. Contrary, it is found that there is an insignificant increase in the hydrogen temperature versus the gasification temperature increase (Figure 7.58). This is due to the cooling process that takes place in the gas compressor former heat exchanger to deliver the gas at the compressor upstream temperature. Therefore, the hydrogen yield in this case influences the specific cost and the hydrogen temperature does not (Figure 7.59).

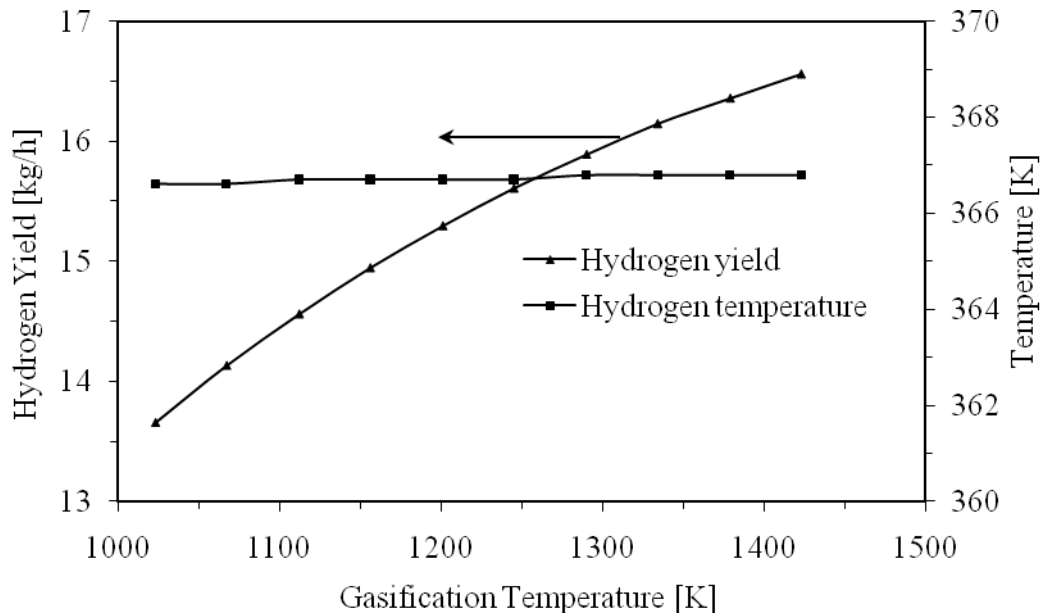


Figure 7.58 Hydrogen yield in System III and its temperature at different gasification temperatures.

More steam is needed to perform the water-gas shift and the steam reforming reactions. The decreasing of the specific cost of the delivered steam at these reactors is attributed to the steam exergy cost and is affected by the cost of the excess steam whereas in the exergoeconomic model it is assumed that the unit exergy cost of steam is the same. Therefore, its specific cost decreases as the specific cost of the excess steam decreases and vice versa (Figure 7.60). The excess steam temperature is 500 K. It is found that the produced steam at this temperature increases versus the gasification temperature increase (Figure 7.61). This is attributed to the fact that the product gas has higher energy content at a higher gasification temperature, and in order to deliver the gas at the upstream

compressor temperature, more steam needs to flow to extract the excess energy. The steam amount increases and therefore its unit cost will decrease (Figure 7.62).

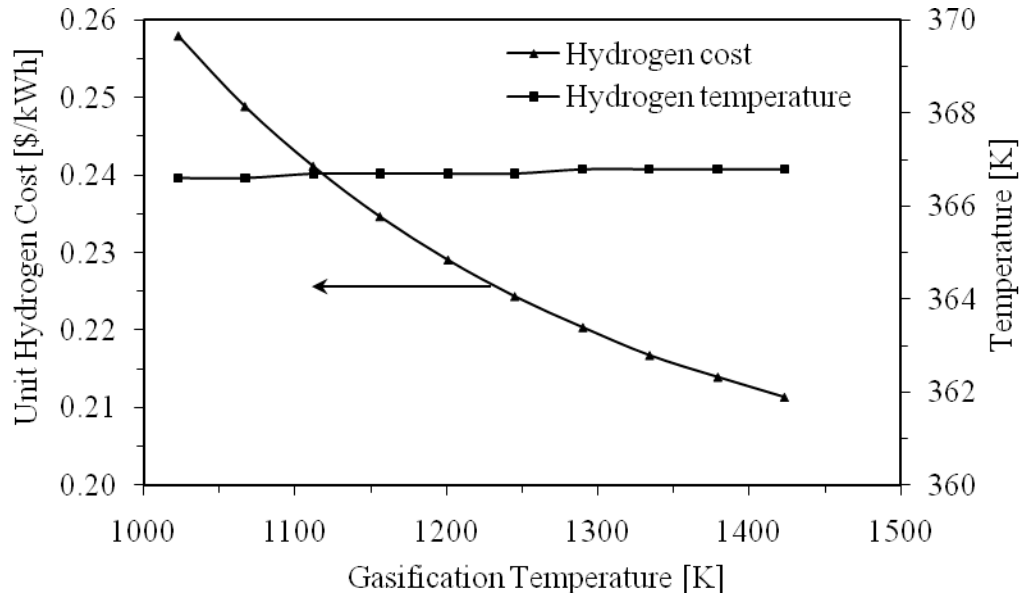


Figure 7.59 Hydrogen cost in System III and its temperature at different gasification temperatures.

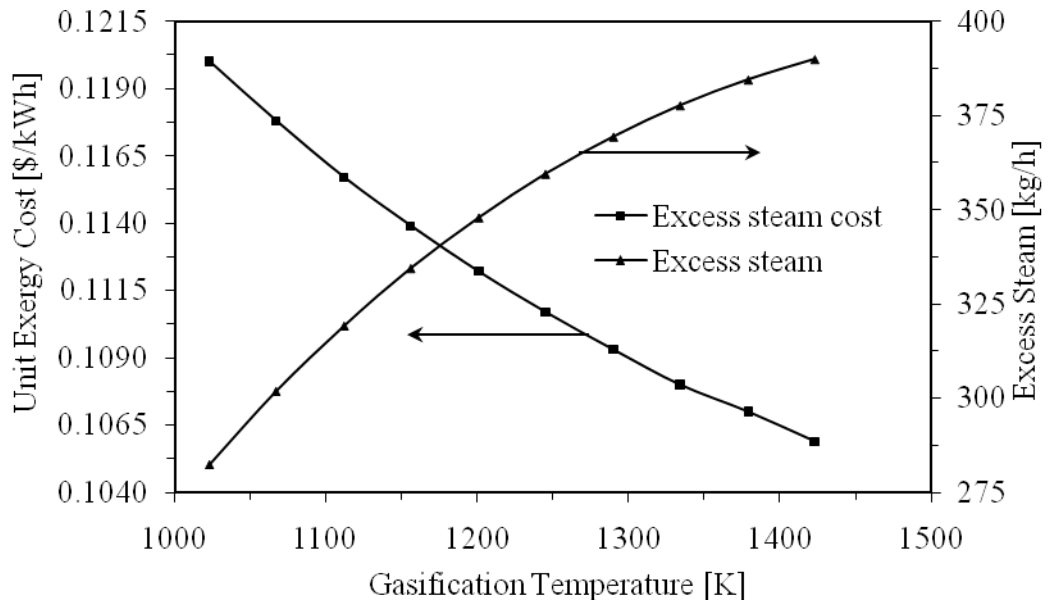


Figure 7.60 Excess steam available in System III and its cost at different gasification temperatures.

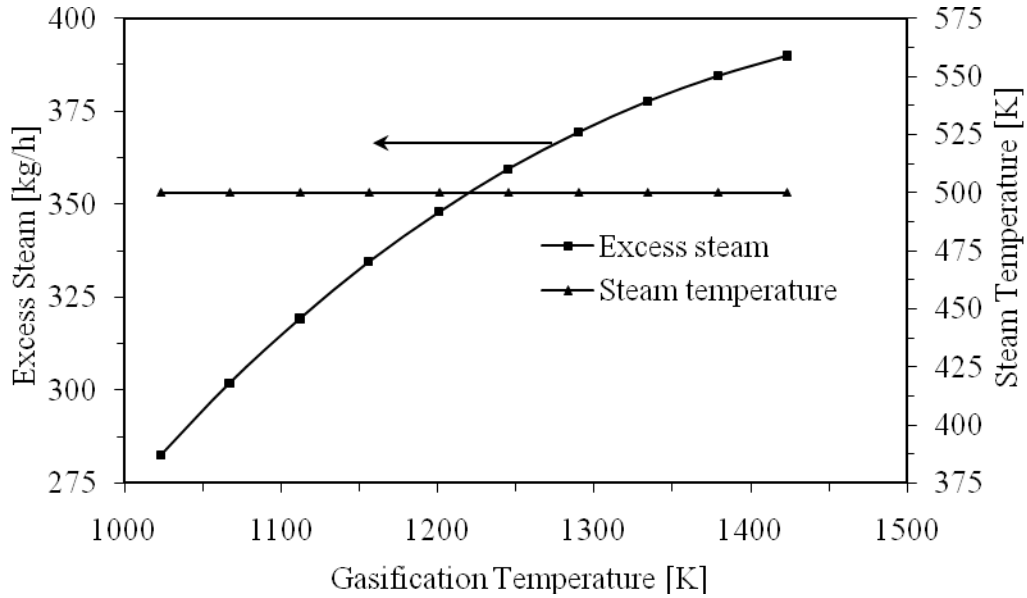


Figure 7.61 Excess steam from system III and its temperature at different gasification Temperatures.

Table 7.12 Unit exergy cost and cost rate for flow material streams in system III

State no.	C [\$/kWh]	\dot{C} [\$/h]	State no.	C [\$/kWh]	\dot{C} [\$/h]
0	0.000	0.000	20	0.120	1.499
1	0.000	116.700	21	0.120	0.479
2	0.496	118.400	22	0.504	120.300
4	0.120	0.650	23	0.120	5.921
5	0.504	114.700	24	0.000	0.000
6	0.392	117.000	25	0.137	3.449
7	0.170	17.370	26	0.529	1.329
8	0.000	0.000	27	0.393	10.490
9	0.546	2.660	28	0.000	0.000
10	0.467	2.650	29	0.000	0.000
15	0.120	0.0003	30	0.120	6.288
16	0.549	117.100	33	0.258	114.600
17	0.555	118.400	34	0.135	2.610
18	0.785	119.200	35	0.003	4.210
19	0.389	121.000	36	0.496	117.100

At a gasification temperature of 1023 K, the specific cost of the other flow material streams can be found from Table 7.12.

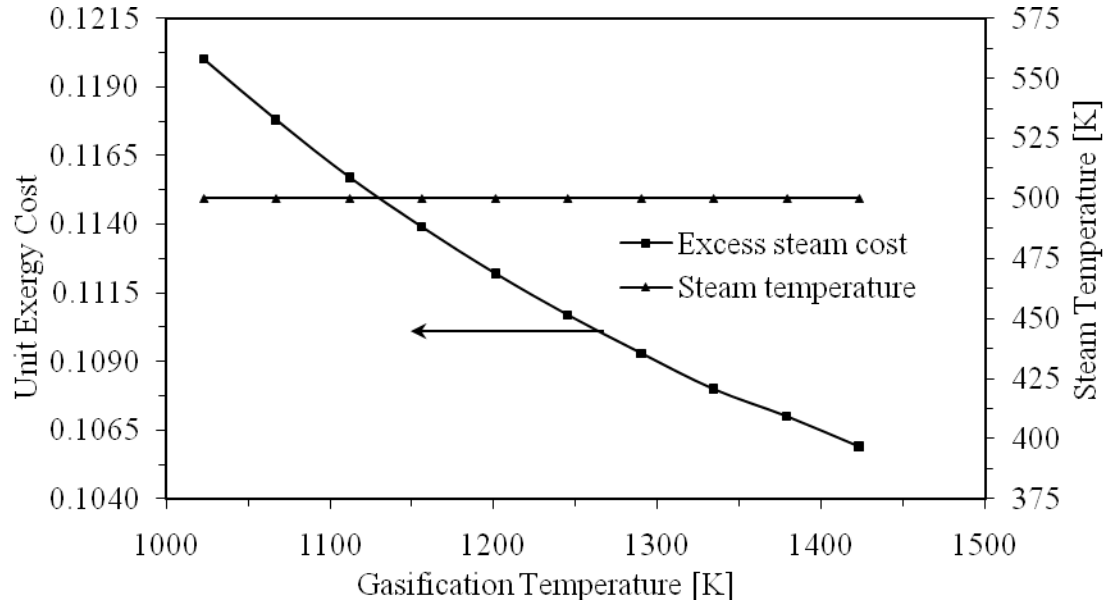


Figure 7.62 Temperature of excess steam and its cost in system III versus gasification temperature.

Cost of unit products from this system does not consider other costs from the calculated cost to the delivered cost. The results show that the unit exergy cost of hydrogen from this system is in good agreement with that obtained from the electrolyzed hydrogen, and this will be discussed in the next section. Therefore, from an exergoeconomic analysis point of view, developing a system that has similar configurations and does not include electrolyze could produce hydrogen with lower unit exergy cost.

The system potential to emissions is determined based on a ratio of wood sawdust that gasified to CO_2 in $\text{g}_{\text{CO}_2}/\text{kg}_{\text{Biomass}}$ after it performs its duties. It is found that for System I, System II and System III, respectively, the potentials to emission are: 0.694, 0.913 and $0.983 \text{ g}_{\text{CO}_2}/\text{kg}_{\text{Biomass}}$.

7.6 Systems Optimization Results

An optimization has been done in order to have good insight into this project. For this reason, an objective function is introduced and a summation of the purchase cost of each component in the systems and the cost of their exergy destruction has been considered. Objective functions of System II and System III versus gasification temperature have similar trends, and the three functions have good fitting with 3rd degree polynomial (Figure 7.63).

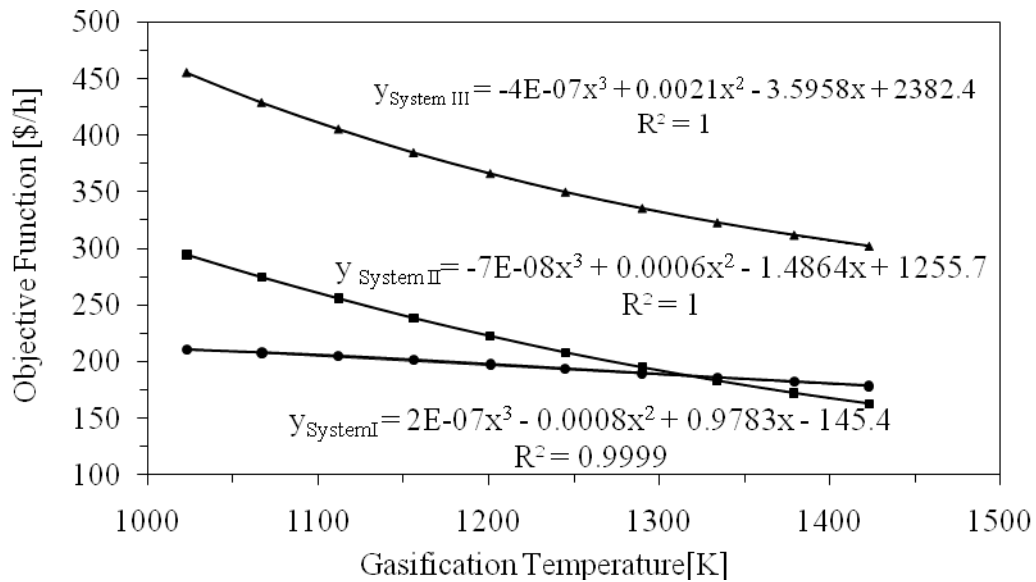


Figure 7.63 Systems I, II, III objective functions versus gasification temperature.

The decision variables are selected as the gasification temperature. By considering a set of constraints, the objective functions have been optimized using genetic algorithm. The genetic algorithm can solve an optimization of systems that are not well suited by standard algorithm. It starts with a set of solutions called population.

The genetic algorithm creates the next generation from the current population which satisfies a certain criteria. Usually the number of generation and fitting tolerance are criteria used to terminate the optimization process. Over successive generations, the population evolves toward the optimal solution. The following steps are followed to perform the systems optimization:

1. Calculation of exergy destruction cost.
2. Calculation of operation and maintenance cost.
3. Definition of objective function and its constrains.

$$\text{Objective Function} = \dot{C}_{\text{des},k} + \dot{Z}_k \text{ and } 1023 \text{ K} \leq \text{Gasification Temperature} \leq 1423 \text{ K}$$

The Objective Function is the function that solvers attempt to minimize. The cost rates in the objective function equation are known from exergo-economic analysis.

4. Matlab is used to perform the optimization.
5. The genetic algorithm is used to solve systems optimization.

The optimization code is developed in the Matlab software program for System I, System II and System III. The objective function convergence is shown in Figures 7.64, 7.65, 7.66.

Respectively for System I, System II and System III, the optimum gasification temperatures which correspond to the optimum objective functions are 1139 K, 1245 K and 1205 K. The optimization studies have shown that one can decrease the cost of exergy destruction and cost due to operation and maintenance considerably by adjusting the gasification temperature.

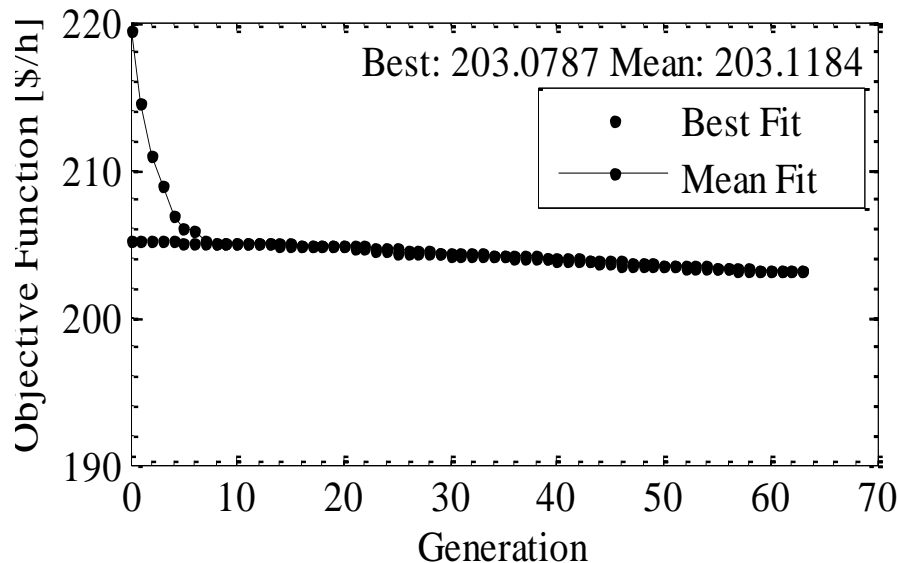


Figure 7.64 System I objective function convergence versus generation.

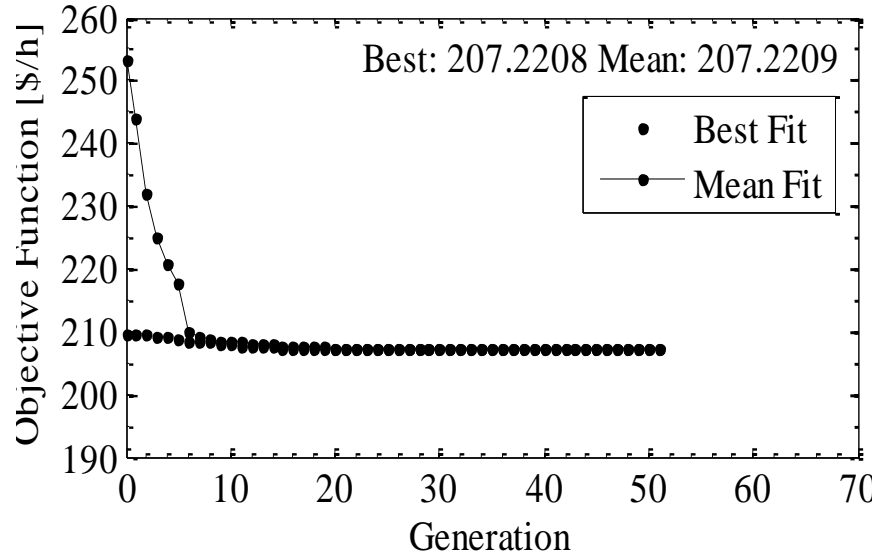


Figure 7.65 System II objective function convergence versus generation.

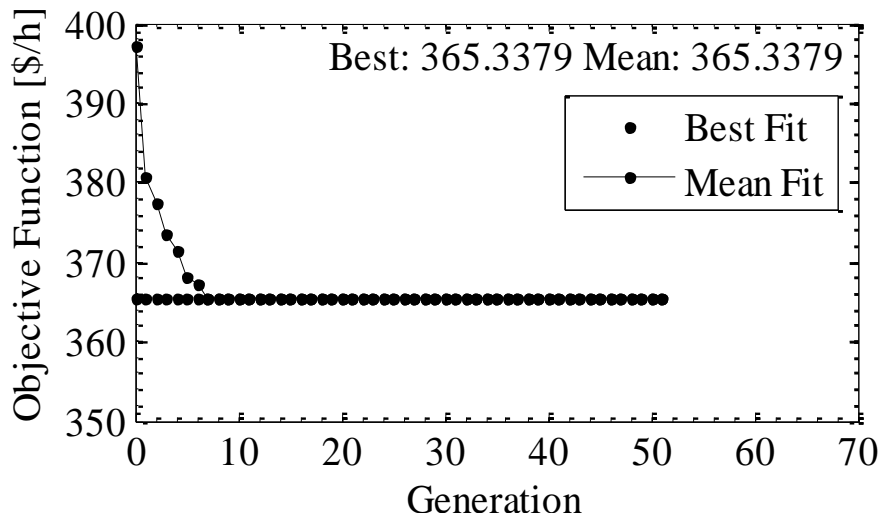


Figure 7.66 System III objective function convergence versus generation.

7.7 Comparisons and Comments

7.7.1 Introduction

Recent available investigations used different gasifier designs and a variety of biomasses in addition to different operating conditions. The gasifier approach did not completely agree with the investigated conditions by the others, but it can predict the range that was covered by their investigations. The modeled approach has a feature

where it is more flexible and easily predicts different parameters and gives reasonable results.

In the absence of the experimental and theoretical results obtained from a study that was performed under the same conditions, it is difficult to show how accurate this study results are. In addition, the interaction between system components is different from system to system. Therefore throughout this section, one will notice comparison is made on a system component basis, whereas on a system basis, it is done between systems from the present study.

7.7.2 Gasification Process

Florin et al. [152] reported that there is an increase in H₂ concentration corresponding to an increase in steam-biomass ratio. This is due to hydrogen enhancement from steam reforming and gas-shift reactions. These are side reactions and are included in the proposed systems. It is also found there is an increase in hydrogen yield corresponding to an increase in gasification temperature. Although methane concentration in the studied range was low, at high temperatures it decomposes and is accompanied by increasing CO. The production of CO is enhanced by a decreasing CO₂. This agrees with the Herguido et al. [48] results at 1023 K. Such comparison cannot be considered realistic because they used different biomass (pine sawdust and wood) with different hydrogen content, different gasification agent (90% H₂O), different pressure, and a gasifier with different geometries. Specific details are not available to make a comparison using a gasification ratio, the ratio between the H₂ product and the biomass fed. This result is also true as observed by Turn et al. [18] at a different temperature (1073 K). It is noticed from the results that hydrogen production at 1073 K is less sensitive to steam-biomass ratio than at 1023 K, and the same conclusion can be drawn from this study where the hydrogen production at a higher temperature is less sensitive to steam-biomass ratio.

Although Herguido et al. [48] used a wide range of steam-biomass ratio (0.50-2.50), the hydrogen concentration was 40-60 % and after 0.70 did not show significant change (55-59 %). If this study neglects the difference in conditions under which they reached their results and at a low steam-biomass ratio, hydrogen product from this study

approach fall in the narrow range 51 to 63 % in the steam-biomass ratio of 0.15 to 0.51 and with same degree of sensitivity to change in hydrogen yield.

Hydrogen produced by a gasification process in this study and in other studies, with a gasification temperature range of 1023-1153 K and atmospheric pressure, are plotted in Figure 7.67. The gasification process was conducted for different biomasses and took place under the same pressure and temperature. The hydrogen concentration from other studies is similar to that from this study. It is this type of validation that encourages using the same gasification module in the proposed systems.

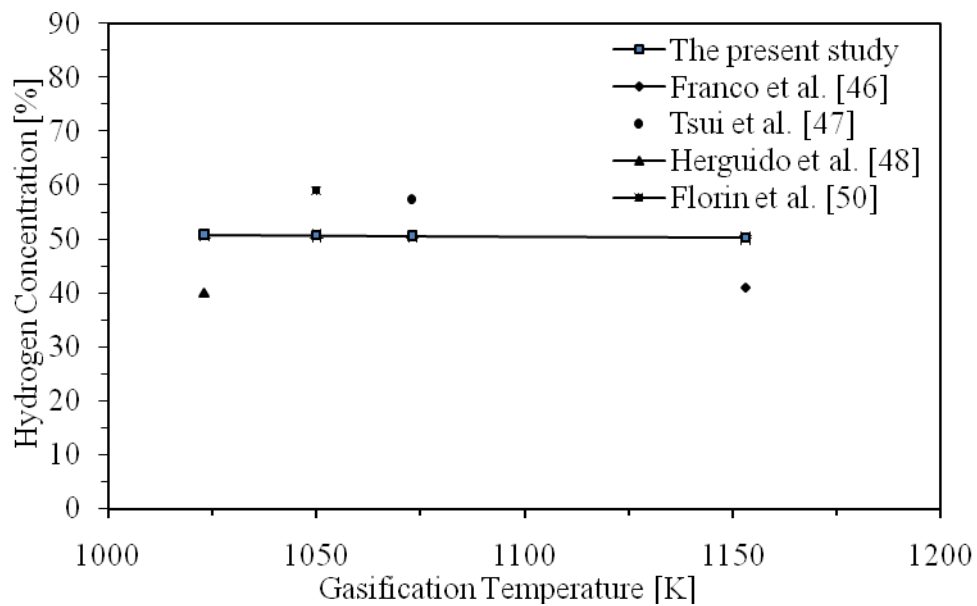


Figure 7.67 Hydrogen concentrations from this study and others.

7.7.3 Systems I, II, III

In this section Systems I, II and III are compared to determine the influence of the system configuration on the hydrogen yield and overall system performance. Then, Systems I and II are compared to evaluate the influence of the existence of the SOFC on the system performance and hydrogen cost. Then, Systems I and III are compared to evaluate the system performance and hydrogen cost on the existence of the SOFC-SOEC subsystem. Finally, Systems II and III are compared to see what influence the SOEC has on the system performance and hydrogen cost.

Composition of gas that leaves the gasifier is the same and thus the gas mass flow rate and the gas heating value are equal. The study uses steam in the gasification process which enhances the hydrogen content in the gas product, and thus the gas product has a higher heating value. The gasifier is assumed to have the same operating conditions which lead to have the same exergy losses. System II generates more electricity so its efficiency that considers electricity is higher. System III internally consumes a part of electricity in the SOEC to produce oxygen and therefore has lower efficiency that considers electricity production.

System I is conventional steam biomass gasification. System II conjugates SOFC, steam biomass gasification and gas turbine. The gasification and SOFC products were used in downstream energy equipments. This is one of the system features. In the last system, the steam biomass gasification conjugates SOFC-SOEC and gas turbine. The gasification and lumped SOFC-SOEC residues were used in their downstream energy equipment which is one of the features of the system. The systems are evaluated and assisted exergoeconomically by means of thermodynamics laws.

System I and System II have different components and therefore they have different configurations. The former system performs single duty and the later performs multiple duties. The performance of System II that considers hydrogen is lower than that of System I because System II internally consumes the primary hydrogen and System I efficiency that considers electricity is zero because it does not produce electricity. The unit exergy cost of the hydrogen in System II is lower because it performs more duties.

Systems I and III have different components and therefore they have different configurations. Neither System 1 nor System III internally consumes hydrogen; therefore, their efficiency that considers hydrogen yield is higher than that of System II. System I does not produce electricity and System III does. Part of System III electricity is used to power the SOEC.

System II and System III have different components and therefore they have different configurations. They are hybrid systems and they perform multiple duties. They produce hydrogen, but System II internally consumes part of the hydrogen, therefore its performance that considers hydrogen is lower. Both systems produce electricity, but System III internally consumes part of the electricity in the lumped SOFC-SOEC.

Therefore, its efficiency that considers electricity production is lower than that of System II.

From Table 7.13 and Table 7.14, it is clear that System II has the lowest hydrogen cost and the highest electrical efficiency, and System III has the highest efficiency with hydrogen production and the highest hydrogen cost.

Table 7.13 Efficiencies of the different systems at 1023 K

System configuration	System I	System II	System III
Energy efficiency with H ₂ production [%]	62.07	45.16	75.24
Exergy efficiency with H ₂ production [%]	59.30	21.85	62.62
Efficiency with electricity production [%]	-	31.94	30.22
Exergy efficiency with electricity production [%]	-	34.18	25.77
Overall electrical efficiency [%]	-	82.24	30.22
Overall exergy electrical efficiency [%]	-	56.03	25.77

The exergoeconomic study results are validated such that the cost of unit exergy hydrogen from all systems is compared with the cost of unit exergy hydrogen from different studies that were found from the literature review (Table 7.14). The unit hydrogen cost from this study is compared with the hydrogen fuelling infrastructure cost of the one produced from biomass.

Table 7.14 Unit hydrogen cost from different studies

Unit H ₂ Cost [\$/kg]	Unit H ₂ cost [\$/kWh]	Reference
2.76 ^a	0.067	Ogden [153]
3.70 ^a	0.094	Richards et al. [154]
10 ^b	0.254	Georgi [155]
4.28 ^c	0.108	Iwasaki [113]
7.41	0.188	The present study, system I
4.06	0.103	The present study, system II
10.17	0.258	The present study, system III

a: Forming a hydrogen-based fuelling infrastructure depend on vehicular fuel cell and fuelling infrastructure

b: Electrolyzed hydrogen included capital and operation cost

c: Hydrogen from wood pyrolysis

The cost from this study does not consider other costs from the calculated cost to the delivered cost. Produced hydrogen in System III has a higher unit exergy cost while that from System II has the lowest unit exergy cost. Here one can draw a conclusion that a large number of components constitute the system, and does not necessarily mean higher unit hydrogen cost and vice versa. Therefore, the way to estimate the hydrogen cost is a performing of the exergoeconomic analysis.

Chapter 8

CONCLUSIONS AND RECOMMENDATIONS

8.1 Conclusions

Biomass gasification is the technology that has attracted the attention of researchers for many decades. This is due mainly to lesser or diminished effects regarding emission and pollution issues, and it has potential to be used as one of the energy resources. Steam biomass gasification has the potential to produce gases which have the highest hydrogen content. Studying the steam biomass gasification of hydrogen production received strong attention from this study.

The thesis theoretically addressed the hydrogen production from steam biomass gasification. Also, it investigated ideal hydrogen production conditions by performing a comprehensive sensitivity study with regard to parameters that affect the hydrogen yield from steam biomass gasification. The value of produced hydrogen was investigated by merging the hydrogen production module in the innovated systems. The feasibility of the proposed systems was investigated by conducting energy, exergy exergoeconomic and optimization analyses. The results from the study showed key parameters that are preferable for hydrogen production as well as for the performances of the systems. The present study achieved the following concluding remarks:

- Hydrogen production by steam sawdust gasification appears to be the ultimate option for hydrogen production in terms of the conducted parametric studies and based on the first law and second law efficiencies evaluations. By studying the energy and exergy efficiencies, the performance assessment showed the potential to produce hydrogen from sawdust wood.
- The results showed the predicted gasification ratio by following the proposed approach was in the range of 70-107 g H₂ kg⁻¹ biomass. At the examined operating gasifier temperature, the hydrogen yield range was 97-105 g H₂ kg⁻¹ biomass. The hydrogen yield was consistent with the literature and verified such with reasonable accuracy.

- It can also be concluded from the efficiency evaluation that biomass gasification exhibits good potential for hydrogen production in the range of the studied parameters. Furthermore, the emergence of the steam biomass gasification module in the hybrid systems showed high potential to increase hydrogen yield and produce power and heat.
- The study revealed the potential of System II by the utilization of steam biomass gasification derived hydrogen. The efficiencies of System II were calculated at a particular pressure, operating temperature, current density and fuel utilization factor. The obtained results showed that the highest exergy destruction occurred in the SOFC. The results from System II give strong evidence that SOFC performs well with the steam biomass gasification module.
- System II was studied in terms of thermodynamic laws. It was found that this system has potential in the gasification temperature range to increase the hydrogen yield with energy efficiency increasing from 45 to 55 %. That was accompanied with an efficiency of 51% that considers hydrogen yield when the preheated air temperature was 446 K. At the same temperature, energy electrical efficiency was 78 %. The observed decrease in the electrical energy efficiency within the studied gasification temperature range is attributed to the decrease in turbine energy efficiency.
- The study investigated and assessed the exergy efficiency of System II that considers the hydrogen yield and the electricity production. It was found that System II exergy efficiency that considers secondary hydrogen yield increases from 22 to 32 %. This is attributed to the increase in hydrogen yield from the bottoming reactions that take place in the steam reforming and water gas shift reactors. Also, System II exergy efficiency that considers electricity production decreases from 57.5 to 51 %.
- Effects of the preheated air in System II on exergy efficiency were also studied. It was found that System II electrical exergy efficiency increases and exergy efficiency that considers hydrogen decreases when both SOFC preheated air and burner preheated air flows per biomass throughput decrease.

- System III employs the steam biomass gasification and the lumped SOFC-SOEC system. The steam biomass gasification derived products are sent to further processes in order to increase hydrogen yield and produce electricity. The lumped SOFC-SOEC has the same operating conditions of the SOFC in System II.
- System III was studied in terms of thermodynamic laws. It was found that the system has potential in the studied gasification temperature range to increase the hydrogen yield with an energy efficiency increasing from ~75 to ~91 %. Within the same temperature range, it was found that the system potential for electricity production decreased from ~30 to ~20 %. This decrease in electrical efficiency is attributed to the decrease in gas turbine electrical efficiency.
- System III results showed that the highest exergy destruction occurred in the lumped SOFC-SOEC subsystem. In the studied gasification temperature range, the overall exergy efficiency for electricity production from System III decreased from 26 to 17 %. System III exergy efficiency considers hydrogen yield increases from ~ 63 to ~ 76 %, but it has a lower electrical exergy efficiency which it is attributed to the fact that only electricity from the turbine was considered, whereas that from the SOFC stack was internally consumed by the SOEC stack. System I did not produce electricity.
- From the conducted exergoeconomic analysis on System I, it was found that the unit hydrogen exergy costs 0.188 \$/kWh on the basis of electricity and steam costs of 0.1046 \$/kWh.
- System II primary and secondary hydrogen yields increase. Accordingly, both the primary and secondary hydrogen costs decrease from 0.103 to 0.045 \$/kWh for the former and from 0.064 to 0.039 \$/kWh for the latter. System II product steam increases which resulted in the steam unit cost decreased from 0.928 \$/kWh to 0.410 \$/kWh.
- System III net hydrogen yield increases from 13.7 to 16.6 kg/h which resulted in a decreasing of the unit hydrogen cost from 0.258 to 0.211 \$/kWh. Also, its excess steam production was increased from 282.5 to 389.9 kg/h and accordingly its specific exergy cost decreased from 0.120 to 0.106 \$/kWh. According to the exergoeconomic model, the specific exergy cost of the used steam in the

bottoming gasifier reactions and that available for external use were reduced by the same amount.

- The study results were validated such that unit exergy hydrogen cost compares with hydrogen cost from different studies. The results gave the indication that the unit cost of hydrogen from the present study is reasonable and falls within the favourable margin, and therefore the systems have potential to compete.
- In general, within the studied gasification temperature, the hydrogen yield increases with an increasing gasification temperature which results in a decrease of the unit hydrogen cost and its value of the decreasing depends on the system configuration. The optimization results have shown that one can decrease the cost of exergy destruction and purchase cost considerably by adjusting the gasification temperature. Systems optimization results showed that System II has the highest optimum gasification temperature and therefore the highest optimum hydrogen yield via sawdust steam. System III has the highest potential to emissions.

8.2 Recommendations

It is recommended that the study should be extended by including more parameters which affect hydrogen yield such as including mechanisms treating the catalysts and CO₂ capture both in gasifier downstream and bottoming process downstream. This can be evaluated in detailed studies and compared to the present study.

Heat exchanger19- 5-28-20 has the major contribution in System I exergy destruction, the SOFC has the major contribution in System II exergy destruction, and the lumped SOFC-SOEC has the major contribution in System III exergy destruction. Therefore, one can enhance the performance of the systems by reducing exergy destruction of those components where less exergy destruction results in higher efficiency.

The exergoeconomic results were obtained by considering the total exergy and did not consider its primary components' (physical and chemical exergies) cost which will add a significant number of equations. This will make the way to the results behind the study more tedious. In addition, such a step did not address the purpose of this study which could be dealt with in a future detailed study.

Due to the high potential to use biomass in different applications, this raises the demand of biomass. This could lead to frequent fluctuations in prices and hence difficulties to predict its future expenditure cost and by-products expenditure cost, which could be a source of the error and was not considered in the present study.

The results of the energy, exergy, exergoeconomic and optimization analyses can be considered in building experimental biomass based hydrogen production.

References

- [1] Orecchini, F., Bocci, E., Biomass to hydrogen for the realization of closed cycles of energy resources, *Energy*, 2007, Vol. 32, pp. 1006–1011.
- [2] Jong, W. de., Ünal, Ö., Andriosa, J., Heinb, K.R.G., Spliethoff, H., Thermochemical conversion of brown coal and biomass in a pressurised fluidised bed gasifier with hot gas filtration using ceramic channel filters: measurements and gasifier modelling, *Applied Energy*, 2003, Vol. 74, pp. 425–437.
- [3] Seitarides, T., Athanasiou, C., Zabaniotou, A., Modular biomass gasification-based solid oxide fuelcells (SOFC) for sustainable development, *Renewable and Sustainable Energy Reviews*, 2008, Vol. 12, pp. 1251 –1276.
- [4] Bridgwater, A. V., Renewable fuels and chemicals by thermal processing of biomass, *Chemical Engineering Journal*, 2003, Vol. 91, pp. 87–102.
- [5] Knoef, H., The UNDP/World Bank monitoring program on small scale biomass gasifiers (BTG's experience on tar measurement), *Biomass and Bioenergy*, 2000, Vol. 18, pp. 39-54.
- [6] Rezaian, J., Cheremisinoff, N., P., Gasification technologies a primer for engineers and scientists, Taylor & Francis Group, 2005, CRC Press, USA.
- [7] Beenackers, A., Biomass gasification in moving beds, a review of European technologies, *Renewable Energy*, 1999, Vol. 16, pp 1180-1186.
- [8] Li, X. T., Grace, J. R., Lim, C. J., Watkinson, A. P., Chen, H. P., Kim, J. R., Biomass gasification in a circulating fluidized bed, *Biomass and Bioenergy*, 2004, Vol. 26, pp 171-193,.
- [9] Higman, C., Burgt, M., Gasification, Elsevier Science, 2003, USA.
- [10] Brage, C., Yu, Q., Chen, G., Sjöström, K., Tar Evolution profiles obtained from gasification of biomass and coal, *Biomass Bioenergy*, 2000, Vol. 18, pp. 87-91.
- [11] Caballero, M. A., Corella, J., Aznar, M. P., Gil, J., Biomass gasification with air in fluidized bed. Hot gas cleanup with selected commercial and full-size nickel-based catalysts, *Industrial & Engineering Chemistry Research*, 2000, Vol. 39 (5), pp. 1143-1154.
- [12] Miccio, F., Moersch, O., Soliethoff, H., Hein, K. R. G., Generation and conversion of carbonaceous fine particles during bubbling bed fluidized bed gasification of a biomass fuel, *Fuel*, 1999, Vol. 78, pp. 1473-1481.
- [13] Blasi, C. D., Signorelli, G., Portorico, G., *Industrial Engineering Chemical Research*, 1999, Vol. 38, 2571.
- [14] Narváez, I., Orío, A., Aznar, M. P., Corella, J., Biomass gasification with air in an atmospheric bubbling fluidized bed. Effect of six operational variables on the quality of the produced raw gas, *Industrial & Engineering Chemistry Research*, 1996, Vol. 35 (7), pp. 2110-2120.

- [15] Vriesman, P., Heginus, E., Sjöström, K., Biomass gasification in a laboratory-scale AFBG: influence of the location of the feeding point on the fuel-N conversion, *Fuel*, 2000, Vol. 79, pp. 1371-1378.
- [16] Prasad, S. B., Modeling a charcoal production system fired by the exhaust of a diesel engine, *Energy Conversion*, 1996, Vol. 37, pp. 1535-1546.
- [17] Werther, J., Sanger, M., Hartage, E. U., Ogada, T., Siagi, Z., Combustion of agricultural residues. *Progress Energy Combustion Science*, 2000, Vol. 26, pp. 1-27.
- [18] Turn, S., Kinoshita, C., Zhang, Z., Ishimura, D., Zhou, J., An experimental investigation of hydrogen production from biomass gasification. *International Journal of Hydrogen Energy*, 1998, Vol. 23, pp. 641-648.
- [19] Mahishi, M. R., Goswami, D. Y., Thermodynamic optimization of biomass gasifier for hydrogen production, *International Journal of Hydrogen Energy*, 2007, Vol. 32, 3831-3840.
- [20] Vlaswinkel, E. E., Energetic analysis and optimisation of an integrated coal gasification-combined cycle power plant, *Fuel Process Technology*, 1992, Vol. 32 (1-2), pp. 47-67.
- [21] Ptasiński, K. J., Hamelinck, C., Kerkhof, P. J. A. M., Exergy analysis of methanol from the sewage sludge process. *Energy Conversion and Management*, 2002, Vol. 43 (9-12), pp. 1445-1457.
- [22] Herguido, J., Corella, J., González-Saiz, J. Steam gasification of lignocellulosic residues in a fluidized bed at a small pilot scale. Effect of the type of feedstock. *Industrial and Engineering Chemistry Research*, 1992, Vol.31, pp. 1274-1282.
- [23] Franco, C., Pinto, F., Gulyurtlu, I., Cabrita, I., The study of reactions influencing the biomass steam gasification process, *Fuel*, 2003, Vol. 82, pp. 835-842.
- [24] Bilodeau, J. F., Thérien, N., Proulx, P., Czernik, S., Chornet, E., A mathematical model of fluidized bed biomass gasification, *The Canadian Journal of Chemical Engineering*, 1993, Vol. 71, pp. 549-557.
- [25] Pritchett, J. W., Blake, T. R., Garg, S. K., A numerical model of gas fluidized beds, *AIChE Symposium Series*, 1978, Vol. 74, pp. 134-148.
- [26] De Souza-Santos, M. L., Comprehensive modeling and simulation of fluidized bed boilers and gasifiers, *Fuel*, 1989, Vol. 68, pp. 1507-1521.
- [27] Raman, P., Walawender, W. P., Fan, L. T., Chang, C. C., Mathematical model for the fluid-bed gasification of biomass materials, Application to feed lot manure, *Industrial and Engineering Chemistry Process Design and Development*, 1981, Vol. 20, pp. 686-692.
- [28] Jennen, T., Hiller, R., Koneke, D., Weinspach, P., Modeling of gasification of wood in a circulating fluidized bed, *Chemical Engineering Technology*, 1999, Vol. 22 (10), pp. 822-826.

- [29] Hamel S, Krumm W, Mathematical modelling and simulation of bubbling fluidised bed gasifiers, Powder Technology, 8 October 2001, Vol. 120, Issues 1-2, pp. 105-112.
- [30] Mansaray, K. G., Al-Taweel, A. M., Ghaly, A., E., Hamdullahpur, F. and Ugursal, V. I., Mathematical modeling of a fluidized bed rice husk gasifier: part I- model development, Energy Source, 2000 , Vol. 22, pp. 83-98.
- [31] Sadaka, S. S., Ghaly, A. E., Sabbah, M. A., Two phase biomass air-stream gasification model for fluidized bed reactor: part I-model development, Biomass and Bioenergy, 2002, Vol. 22, pp. 439-462.
- [32] Chen, J., Andries, J., Spliethoff, H., Biomass conversion into fuel gas using circulating fluidized bed technology: the concept improvement and modeling discussion, Renewable Energy, 2003, Vol. 28, pp. 985-994.
- [33] Corella, J., Sanz, A., Modeling circulating fluidized bed biomass gasifiers, A pseudo-rigorous model for stationary state, Fuel Processing Technology, 2005, Vol. 86, pp 1021-1053.
- [34] Srinivas, T., Gupta, A. V. , Reddy, B. V., Thermodynamic equilibrium model and exergy analysis of a biomass gasifier, Journal of Energy Resources Technology, 2009, Vol. 131, pp. 031801-7.
- [35] Ruggiero, M. and Manfrida, G., An equilibrium model for biomass gasification processes, Renewable Energy, 1999, Vol. 16, pp. 1106-1109.
- [36] Hanaoka, T., Yoshida, T., Fujimoto, S., Kamei, K., Harada, M., Suzuki, Y., Hatano, H., Yokoyama, S., Minowa, T. Hydrogen production from woody biomass by steam gasification using a CO₂ sorbent. Biomass and Bioenergy, 2005, Vol. 63, pp. 63-68.
- [37] Gordon, A.L., Amundson, N. R., Modelling of fluidized bed reactors-IV: Combustion of carbon particles, Chemical Engineering Science, 1976, Vol. 33, pp.1163-1178.
- [38] Berruti, F., Kalogerakis, N., Modelling the internal flow structure of circulating fluidized beds, The Canadian Journal of Chemical Engineering, December 1989, Vol. 67, pp. 1010-1014.
- [39] Werther, J., Scale-up modeling for fluidized bed reactors, Chemical Engineering Science, 1992, Vol. 47, No. 9-11, pp. 2457-2462.
- [40] Luo, C., Aoki, K., Uemiya, S., Kojima, T., Numerical modeling of a jetting fluidized bed gasifier and the comparison with the experimental data, Fuel Processing Technology, 1998, Vol. 55, pp. 193-218.
- [41] Fang, Y., Huang, J., Wang, Y., Zhang, B., Experiment and mathematical modeling of a bench-scale circulating fluidized bed gasifier, Fuel Processing Technology, 2001, Vol. 69, pp 29-44.

- [42] Galgano, A., Salatino, P., Crescittelli, S., Scala, F., Maffettone, P. L., A model of the dynamics of a fluidized bed combustor burning biomass, *Combustion and Flame*, 2005, Vol. 140, pp 371-384.
- [43] Gascón, J., Téllez, C., Herguido, J., Jakobsen, H. A., Menéndez, M., Modeling of fluidized bed reactors with two reaction zones, *AIChE Journal*, 2006, Vol. 52, pp. 3911-3922.
- [44] Lv, P. M., Xiong, Z. H., Chang, J., Wu, C. Z., Chen, Y., Zhu, J. X., An experimental study on biomass air-steam gasification in a fluidized bed, *Bioresource Technology*, 2004, Vol. 95, pp. 95-101.
- [45] Gil, J., Corella, J., Aznar, M. P., Caballero, M. A., Biomass gasification in atmospheric and bubbling fluidized bed: effect of the type of gasifying agent on the product distribution. *Biomass Bioenergy*, 1999, Vol. 17, pp. 389-403.
- [46] Franco, C., Pinto, F., Gulyurtlu, I., Cabrita, I., The study of reactions influencing the biomass steam gasification process, *Fuel*, 2003, Vol. 82, pp. 835-842.
- [47] Tsui, H., Wu, C., Operating concept of circulating fluidized bed gasifier from the kinetic point of view, *Powder Technology*, 2003, Vol. 132, pp. 167-183.
- [48] Herguido, J., Corella, J., González-Saiz, J. Steam gasification of lignocellulosic residues in a fluidized bed at a small pilot scale. Effect of the type of feedstock. *Industrial and Engineering Chemistry Research*, 1992, Vol. 31, pp. 1274-1282.
- [49] Abuadala, A., Dincer, I., Naterer, G. F., Exergy analysis of hydrogen production from biomass gasification. *International Journal of Hydrogen Energy*, 2010, Vol. 35, pp. 4981-4990.
- [50] Florin, N. H., Harris, A. T., Hydrogen production from biomass coupled with carbon dioxide capture: The implications of thermodynamic equilibrium, *International Journal of Hydrogen Energy*, 2007, Vol. 32, pp. 4119-4134.
- [51] Encinar, J. M., González, J. F., González, J., Steam gasification of *Cynara cardunculus* L.: influence of variables, *Fuel Processing Technology*, 2002, Vol. 75, pp. 27-43.
- [52] Li, X. T., Grace, J. R., Lim, C. J., Watkinson, A. P., Ergüdenenler, A., Equilibrium modeling of gasification: a free energy minimization approach and its application to a circulating fluidized bed coal gasifier, *Fuel*, 2001, Vol. 80, pp. 195-207.
- [53] Altafini, C. R., Wander, P. R., Barreto, R. M. Prediction of the working parameters of a wood waste gasifier through an equilibrium model. *Energy Conversion and Management*, 2003, Vol. 44, pp. 2763-2777.
- [54] Zainal, Z. A., Ali, R., Lean, C. H., Seetharamu, K. N., Prediction of performance of a downdraft gasifier using equilibrium modeling for different biomass materials, *Energy Conversion and Management*, 2001, Vol. 42, Issue 12, pp. 1499-1515.
- [55] Natarajan, E., Nordin, A., Rao, A. N., Overview of combustion and gasification of rice husk in fluidized bed reactors, *Biomass and Bioenergy*, 1998, Vol. 14, pp. 533-546.

- [56] Lv, P., Chang, J., Xion, Z., Huang, H., Wu, C., Chen, Y., Biomass air-steam gasification in fluidized bed to produce hydrogen rich gas, *Energy Fuels*, 2003, Vol. 17, pp. 677–82.
- [57] Brown, D., Gassner, M., Fuchino, T., Marechal, Francois, Thermo-economic analysis for the optimal conceptual design of biomass gasification energy conversion systems, *Applied Thermal Engineering*, 2009, Vol. 29. pp. 2137–2152.
- [58] Cordiner, S., Feola, M., Mulone, V., Romanelli, F., Analysis of a SOFC energy generation system fuelled with biomass reformat; In: Brown, D., Gassner, M., Fuchino, T., Marechal, Francois, Thermo-economic analysis for the optimal conceptual design of biomass gasification energy conversion systems, *Applied Thermal Engineering*, 2009; Vol. 29, pp. 2137–2152.
- [59] Baron, S., Brandon, N., Atkinson, A., Steele, B., Rudkin, R., The impact of wood-derived gasification gases on Ni-CGO anodes in intermediate temperature solid oxide fuel cells. In: Fryda, L., Panopoulos, k., D., Karl, J., Kakaras, E., Exergetic analysis of solid oxide fuel cell and biomass gasification integration with heat pipes. *Energy*, 2008, Vol. 33. pp. 292-299.
- [60] Athanasiou, C., Coutelieris, F., Vakouftsi, E., Skoulou, V., Antonakou, E., Marnellos, G., Zabaniotou, A. From biomass to electricity through integrated gasification/SOFC system-optimization and energy balance, *International Journal of Hydrogen Energy*, 2007, Vol. 32, pp. 337–342.
- [61] Baron, S., Brandon, N., Atkinson, A., Steele, B., Rudkin, R. The impact of wood-derived gasification gases on Ni-CGO anodes in intermediate temperature solid oxide fuel cells. *J Power Sources* 2004;126(1–3):58–66. In: L. Fryda, K.D. Panopoulos, E. Kakaras Integrated CHP with autothermal biomass gasification and SOFC–MGT, *Energy Conversion and Management*, 2008, Vol. 49, pp. 281–290.
- [62] Omosun, O., Bauen, A., Brandon, N. P., Adjiman, C. S., Hart, D. Modelling system efficiencies and costs of two biomass-fuelled SOFC systems. *Journal of Power Sources* 2004, Vol. 131(1–2), pp. 96–106.
- [63] Bridgwater, A.V., Toft, A.J., Brammer, J.G., 2002, A Techno-economic comparison of power production by biomass fast pyrolysis with gasification and combustion. In: Sadhukhan, J., Zhao, Y., Shah, N., Brandon, N. P., Performance analysis of integrated biomass gasification fuel cell (BGFC) and biomass gasification combined cycle (BGCC) systems, *Chemical Engineering Science* 2010, Vol. 65, pp. 1942-1954.
- [64] Sadhukhan, J., Zhao, Y., Shah, N., Brandon, N. P., Performance analysis of integrated biomass gasification fuel cell (BGFC) and biomass gasification combined cycle (BGCC) systems, *Chemical Engineering Science* 2010, Vol. 65, pp. 1942-1954.
- [65] Bavarsad, P., G., Energy and exergy analysis of internal reforming solid oxide fuel cell–gas turbine hybrid system, *International Journal of Hydrogen Energy*, 2007, Vol. 32, pp. 4591 – 4599.

- [66] Costamagna P, Magistri L, Massardo AF. Design and part-load performance of a hybrid system based on a solid oxide fuel cell reactor and a micro gas turbine. *Journal of Power Sources*, 2001, Vol. 96, pp. 352–68.
- [67] Zhang, X., Chan, S.H., Li, G., Ho, Jun Li, H.K., Feng, Z. A review of integration strategies for solid oxide fuel cells, *Journal of Power Sources*, 2010, Vol. 195, pp. 685–702.
- [68] Ni, M., Leung, M. K. H., Leung, D. Y. C. Energy and exergy analysis of hydrogen production by solid oxide steam electrolyser plant. *International Journal of Hydrogen Energy*, 2007, Vol. 32, pp. 4648–4660.
- [69] Balli, O., Aras, H., Hepbasli, A. Exergetic performance evaluation of a combined heat and power (CHP) system in Turkey, *International Journal of Energy Research*, 2007, Vol. 31, pp. 849–866.
- [70] Calise F, Palombo A, Vanoli L. Design and partial load exergy analysis of a hybrid SOFC-GT power plant. 2006; In: Akkaya, A. V., Sahin, B., Erdem, H. H., An analysis of SOFC/GT CHP system based on exergetic performance criteria, *International Journal of Hydrogen Energy*, 2008, Vol. 33, pp. 2566 – 2577.
- [71] Calise F, Dentice d’Accadia M, Palombo A, Vanoli L. Simulation and exergy analysis of a SOFC-gas turbine system. *Energy*. 2006; In: Akkaya, A. V., Sahin, B., Erdem, H. H., An analysis of SOFC/GT CHP system based on exergetic performance criteria, *International Journal of Hydrogen Energy*, 2008, Vol. 33, pp. 2566–2577.
- [72] Akkaya, A. V., Sahin, B., Erdem, H. H., An analysis of SOFC/GT CHP system based on exergetic performance criteria, *International Journal of Hydrogen Energy*, 2008, Vol. 33, pp. 2566–2577.
- [73] Fryda, L., Panopoulos, k., D., Karl, J., Kakaras, E., Exergetic analysis of solid oxide fuel cell and biomass gasification integration with heat pipes. *Energy*, 2008, Vol. 33, pp. 292-299.
- [74] Midili, A., Ay, M., Dincer, I., Rosen, M. A., On Hydrogen and hydrogen energy strategies I: current status and needs, *Renewable and Sustainable Energy Systems*, 2005, Vol. 9, pp. 255-271.
- [75] Momirlan, M., Veziroglu, T., Current Status of Hydrogen Energy, *Renewable and Sustainable Energy Reviews*, 2002, Vol. 6, pp. 141-179.
- [76] Konstantopoulou, P., Giannopoulos, D., Founti, M., Multicriteria analysis of hydrogen production technologies, *Proceedings International Hydrogen Energy Congress and Exhibition IHEC*, 2005, Istanbul, Turkey, 13-15 July 2005.
- [77] Levin, D.B., Pitt, L., Love, M., *International Journal of Hydrogen Energy*, 2004, Vol. 29, pp. 173–185.
- [78] Holladay, J.D., Hu, J., King, D.L., Wang, Y., An overview of hydrogen production technologies, *Catalysis Today*, 2009, Vol. 139, pp. 244–260.

- [79] Saxena , R.C., Seal, D., Kumar, S., Goyal, H.B., Thermo-chemical routes for hydrogen rich gas from biomass: A review, *Renewable and Sustainable Energy Reviews*, 2008, Vol. 12, pp. 1909–1927.
- [80] Demirbas, A., Biomass resource facilities and biomass conversion processing for fuels and chemicals, *Energy Conversion and Management*, 2001, Vol. 42, pp.1357-1378.
- [81] EUREC Agency. The future for renewable energy, prospects and directions. In: Demirbas, A., Biomass resource facilities and biomass conversion processing for fuels and chemicals, *Energy Conversion and Management*, 2001, Vol. 42, pp.1357-1378.
- [82] Schuster, G., Loffler, G., Weigl, K., Hofnauer, H., Biomass steam gasification-an extensive parametric modeling study, *Bioresource Technology*, 2001, Vol. 77, pp. 71-79.
- [83] Biagini, E., Falcitelli, M. and Tognotti, L., Devolatilisation and pyrolysis of biomasses: development and validation of structural models, <http://www.combustioninstitute.it/download/proc%202006/documenti/Papers/09-06-biagini-050.pdf>, 2007.
- [84] Badin, J., Kirschner, J., Biomass greens US power production. In: Demirbas, A., Biomass resource facilities and biomass conversion processing for fuels and chemicals, *Energy Conversion and Management*, 2001, Vol. 42, pp.1357-1378.
- [85] Hamelinck, C. N., Faaij, A. P.C. Future prospects for production of methanol and hydrogen from biomass, *Journal of Power Sources*, 2002, Vol. 111, pp. 1–22
- [86] Williams, A., Pourkashanian, M., Jones, J. M., Skorupska, N., *Combustion and gasification of coal*, Ed. Taylor and Francis, 2000, New York.
- [87] Ergun, S. B., Kinetics of the reaction of Carbon Dioxide with carbon, *Journal Physics and Chemistry*, 1956, Vol. 60, pp 480-485.
- [88] Hottel, H. C., Williams, G. C., Nerheim, N.M. and Schneider, G.R., *Proc. Combustion Institute*, 1965, Vol. 10, pp 111-121.
- [89] Baldwin, R. R., Jackson, D., Walker, R. W., Webster, S. J., *Proc. Combustion Institute*, 1965, Vol. 10, pp 423-432.
- [90] Weimer, A., Clough, D., Modeling a low pressure steam oxygen fluidized bed coal gasifying reactor, *Chemical Engineering Science*, 1981, Vol. 36(3), pp. 548-567.
- [91] Fletcher, D. F., Haynes, B. S., Christo, F. C., Joseph, S.D., A CFD based combustion model of an entrained flow biomass gasifier, *Applied Mathematical Modelling*, 2000, Vol. 24, pp. 165-182.
- [92] Liu, H., Gibbs, B. M., Modeling NH₃ and HCN emissions from biomass circulating fluidized biomass gasifiers, *Fuel*, 2003, Vol. 82, pp. 1591-1604.

- [93] Simell, P. A., Hirvensalo, E. K., Smolander, S. T., Krause, A. O., Steam reforming of gasification gas tar over dolomite with benzene as a model compound, *Industrial & Engineering Chemistry Research*, 1999, Vol. 38, pp. 1250-1257.
- [94] Xu, J., Froment, G. F., Methane steam reforming, Methanation and water-gas shift: In *Intrinsic Kinetics*, *AIChE Journal*, 1989, Vol. 35(1), pp. 88-96.
- [95] Huilin, L., Guangbo, Z., Rushan, B., Yongjin, C. and Gidaspow, D., A coal combustion model for circulating fluidized bed boilers, *Fuel*, 2000, Vol. 79, pp. 165-172.
- [96] Cetin, E., Moghtaderi, B., Gupta, R. and Wall, T. F., Biomass gasification kinetics: influences of pressure and char structure, *Combustion Science and Technology*, 2005, Vol. 177, pp. 765-791.
- [97] Fryda, L., Panopoulos, k., D., Karl, J., Kakaras, E., Exergetic analysis of solid oxide fuel cell and biomass gasification integration with heat pipes. *Energy*, 2008, Vol. 33, pp. 292-299.
- [98] Lv, P., Yuan, Z., Ma, L., Wu, C., Yong, C., Zhub, J., Hydrogen-rich gas production from biomass air and oxygen/steam gasification in a downdraft gasifier. *Renewable Energy*, 2007, Vol. 32, pp. 2173–2185.
- [99] Ni, M., Leung, D. Y. C., Leung, M. K. H., Sumathy, K., An overview of hydrogen production from biomass, *Fuel Processing Technology*, 2006, Vol. 87, pp. 461-472.
- [100] Hulteberg, P. C., Karlsson, H. T., A study of combined biomass gasification and electrolysis for hydrogen production. *International Journal of Hydrogen Energy*, 2009, Vol. 34, pp. 772-782.
- [101] Corella, J., Herguido, J., Gonzalez-Saiz, J., Steam gasification of biomass in fluidized bed-effect of the type of feed stock. In: Sadaka, S., Ghaly, A., E., Sabbah, M., A. Two phase biomass air-steam gasification model for fluidized bed reactors: part I-model development. *Biomass and Bioenergy*, 2002, Vol. 22, pp. 439-462.
- [102] Yates, J. G., Fluidized bed reactors, *The Chemical Engineer*, November 1975, pp. 671-677.
- [103] Kim, Y. J., Lee, J. M., Kim, S. D., Modeling of coal gasification in an internally circulating fluidized bed reactor with draught tube, *Fuel*, 2000, Vol. 79, p. 69-77.
- [104] Fiaschi, D. and Micheline, M., A two-phase one-dimensional biomass kinetics model, *Biomass and Bioenergy*, 2001, Vol. 21, pp. 121-132.
- [105] Wang, Y., Kinoshita, C. M., Kinetic model of biomass gasification, *Solar Energy*, 1993, Vol. 51, pp. 19-25.
- [106] Sharma, A. K., Equilibrium modeling of global reductions for a downdraft (biomass) gasifier, *Energy Conversion and Management*, 2008, Vol. 49, pp. 832–842.

- [107] Ginsburg, J. and DeLasa, H. I., Catalytic gasification of biomass in a CREC fluidized riser simulator, *International Journal of Chemical Reactor Engineering*, 2005, Vol. 3, Article A38.
- [108] Jarungthammachote, S., Dutta, A., Thermodynamic equilibrium model and second law analysis of a downdraft waste gasifier, *Energy*, 2007, Vol. 32, pp. 1660-1669.
- [109] Kalogirou, S. A., Artificial neural networks in renewable energy systems applications: a review, *Renewable and Sustainable Energy Reviews*, 2001, Vol. 5, pp. 373-401.
- [110] Kalogirou, S. A., Panteliou, S. Dentsoras, Artificial neural networks used for the performance of prediction of a thermosiphon solar water heater, *Renewable Energy*, 1999, Vol. 18, pp. 87-99.
- [111] Guo, B., Li, D., Cheng, C., Lü, Z., Shen, Y., Simulation of biomass gasification with a hybrid neural network model, *Bioresource Technology*, 2001, Vol. 76, pp. 77-83.
- [112] Hajek, M., Judd, M. R., Use of neural networks in modeling the interactions between gas analysers at coal gasifiers, *Fuel*, 1995, Vol. 74, pp. 1347-1351.
- [113] Iwasaki, W., A Consideration of the economic efficiency of hydrogen production from biomass, *International Journal of Hydrogen Energy*, 2003, Vol. 28, pp. 939 – 944.
- [114] Kakaça, S., Pramuanjaroenkij, A., Zhou, X. Y., A review of numerical modeling of solid oxide fuel cells, *International Journal of Hydrogen Energy*, 2007., Vol. 32, pp. 761–786.
- [115] Jones, R. H., Thomas, G. J., *Materials for the hydrogen economy* <http://books.google.ca/books>, 2008.
- [116] Hino, R., Haga, K., Aita, H., Sekita, K., 38. R&D on hydrogen production by high-temperature electrolysis of steam, *Nuclear Engineering and Design*, 2004, Vol. 233, pp. 363–375.
- [117] Demirbas, A., Hydrogen production from biomass by the gasification process, *Energy Sources*, 2002, Vol. 24, pp. 59-68.
- [118] Shieh, J.H., Fan, L. T., Estimation of energy (enthalpy) and Exergy (availability) contents in Structurally complicated materials, *Energy Sources*, 1982, Vol. 6, pp. 1-46.
- [119] Szargut, J., Morris, D. R., Steward, F. R., Exergy analysis of thermal, chemical and metallurgical processes, In: Pellegrini, L. F., Jr, S. O., *Exergy analysis of sugarcane bagasse gasification*, *Energy*, 2007, Vol. 32, pp. 314-327.
- [120] Prins, M. J., Ptasinski, K. J., Janssen, F. J. J. G., Thermodynamics of gas-char reactions: first and second law analysis, *Chemical Engineering Science*, 2003, Vol. 58, pp. 1003-1011.

- [121] Hyman, D., Kay, W. B., 1949, In: Li, C., Suzuki, K. Tar property, analysis, reforming mechanism and model for biomass gasification-An overview, 2009, Vol. 13, pp. 594-604.
- [122] Lowry, H. H., 1963, In: Eisermann, W., Johnson, P., Conger, W., L., Estimating thermodynamic properties of coal, char, tar and ash, Fuel Processing Technology, 1979, Vol. 3, pp. 39-53.
- [123] Eisermann, W., Johnson, P., Conger, W., L. Estimating thermodynamic properties of coal, char, tar and ash, Fuel Processing Technology, 1979, Vol. 3, pp. 39-53.
- [124] De Souza-Santos, M. L., Solid fuels combustion and gasification modeling, simulation, and equipment operation, Marcel Dekker, Inc., 2004, New York.
- [125] Isachenko, V. P., Osipova, V. A., Sukomel, A. S., 1977, In: de Souza-Santos, M., L., Solid fuels combustion and gasification modeling, simulation, and equipment operation, 2004, Marcel Dekker Inc., New York.
- [126] Gool, V., 1997. Energy policy: fairly tales and factualities. In: Kalinci, Y., Hepbasli, A., Dincer, I., 2009. Exergetic assessment of an integrated gasifier/boiler system for hydrogen production with different biomass types, Proceedings of the International Conference on Hydrogen Production, May 03-06, Oshawa, Canada.
- [127] Cengel, Y. A., Boles, M. A., Thermodynamics: an engineering approach, Mc Graw Hill Companies, Inc., Ed. 6, 2008, New York.
- [128] Chan, S. H., Low, C. F., Ding, O. L. Energy and Exergy analysis of simple solid-oxide fuel-cell power systems, Journal of Power Sources, 2002, Vol. 103, pp. 188-200.
- [129] Costamagna, P., Honegger, K., Modeling of solid oxide heat exchanger integrated stacks and simulation at high fuel utilization, In: Costamagna, P., Selimovic, A., Borghi, M. D., Agnewc, G., Electrochemical model of the integrated planar solid oxide fuel cell (IP-SOFC), Chemical Engineering Journal, 2004, Vol. 102, pp. 61–69.
- [130] Bessette II, N. F., Wepfer, W. J., Winnick, J., A Mathematical Model of a Solid Oxide Fuel Cell, Journal of the Electrochemical Society, 1995, Vol. 142(11), pp. 3792-3800.
- [131] Athanasiou, C., Coutelieris, F., Vakouftsi, E., Skoulou, V., Antonakou, E., Marnellos, G., Zabaniotou, A. From biomass to electricity through integrated gasification/SOFC system-optimization and energy balance, International Journal of Hydrogen Energy, 2007, Vol. 32, pp. 337 – 342.
- [132] Iora, P., Chiesa, P., High efficiency process for the production of pure oxygen based on solid oxide fuel cell–solid oxide electrolyzer technology, Journal of Power Sources, 2009, Vol. 190, pp. 408–416.
- [133] Valero, A., Lozano, M. A., Serra, L., CGAM problem: definition and conventional solution, Energy, 1994, Vol. 19, No. 3, pp. 279-286

- [134] Gaggioli, R. A., Wepfer, W. J., Exergy economics, *Energy*, 1960, Vol. 5, pp. 823-437.
- [135] Tsatsaronis, G., Application of thermoeconomics to the design and synthesis of energy plants, *Energy, Energy System Analysis, and Optimization*. [http://www.eolss.net/ebooks/Sample %20 Chapters/C08/E3-19-02-07.pdf](http://www.eolss.net/ebooks/Sample%20Chapters/C08/E3-19-02-07.pdf)
- [136] Tsatsaronis, G., Pisa, J., Eergoeconomic evaluation and optimization of energy systems- application to the CGAM problem, *Energy*, 1994, Vol. 19, No. 3, pp. 287-321.
- [137] Lazzaretto, A., Tsatsaronis, G., SPECO: A systematic and general methodology for calculating efficiencies and costs in thermal systems, *Energy*, 2006, Vol. 31, pp. 1257–1289.
- [138] Ogden, J. M., Prospects for building a hydrogen energy infrastructure, *Annual Reviews Energy Environ*, 1999, Vol. 24, pp. 227–279.
- [139] Tsatsaronis, G., Winhold, M. Eergoeconomic analysis and evaluation of energy-conversion plants-I. Anew general methodology, *Energy*, 1985, Vol. 10, pp. 69-80.
- [140] Kim S M, Doek S, Kwon Y H, Kwak H Y. Exergoeconomic analysis of thermal systems. *Energy*, 1998, Vol. 23, pp. 393–406.
- [141] Balli, O., Aras, H., Hepbasli, A. Exergoeconomic analysis of a combined heat and power (CHP) system, *International Journal of Energy Research*, 2008, Vol. 32, pp. 273–289.
- [142] Colpan CO, Yesin T. Energetic, exergetic and thermoeconomic analysis of Bilkent combined cycle cogeneration plant. *International Journal of Energy Research*, 2006, Vol. 30, pp. 875–894
- [143] Lazzaretto, A., Tsatsaronis, G., SPECO: A systematic and general methodology for calculating efficiencies and costs in thermal systems, *Energy*, 2006, Vol. 31, pp. 1257–1289.
- [144] Moran, M. J., Shapiro, H. N., *Fundamentals of engineering thermodynamics*, 2007, John Wiley, Inc., USA
- [145] Palazzi, F. Autissier, N., Marechal, Francois M.A., Favrat, D., A methodology for thermo-economic modeling and optimization of solid oxide fuel cell systems, *Applied Thermal Engineering*, 2007, Vol. 27, pp. 2703–2712.
- [146] Calise, F., d' Accadia, M. D., Vanoli, L., Spakovsky, M. R. Von. Full load synthesis/design optimization of a hybrid SOFC–GT power plant, *Energy*, 2007, Vol. 32, pp. 446–458.
- [147] Abuadala, A., Dincer, I., Efficiency evaluation of dry hydrogen production from biomass gasification. *Thermochimica Acta*, 2010, Vol. 507-508, pp. 127-134.
- [148] Abuadala, A., Dincer, I., Investigation of a multi-generation system using hybrid steam biomass gasification for hydrogen, power and heat. *International Journal of Hydrogen Energy*, 2010, Vol. 35, pp.13146-13157.

- [149] Palsson, J., Selimovic, A., Sjunnesson, L., Combined solid oxide fuel cell and gas turbine systems for efficient power and heat generation, *Journal of Power Sources*, 2000, Vol. 86, pp. 442–448.
- [150] Colpan, C. O., Dincer, I., Hamdullahpur, F., Thermodynamic modeling of direct internal reforming solid oxide fuel cells operating with syngas, *International Journal of Hydrogen Energy*, 2007, Vol. 32, pp. 787–795.
- [151] Dang, H. D. T., & New Zealand Ministry of Economic Development, 2007. In: Feasibility study into the potential for gasification plant in the New Zealand wood processing industry Penniall, C. L., Williamson, C. J., *Energy Policy*, in press, doi:10.1016/j.enpol.2008.11.046.
- [152] Florin, N., H., Harris, A., T. Enhanced hydrogen production from biomass with situ carbon dioxide capture using calcium dioxide sorbent. *Chemical Engineering Science*, 2008, Vol. 63, pp. 287-316.
- [153] Ogden, J. M. Developing an infrastructure for hydrogen vehicles: a South California case study. *International Journal of Hydrogen Energy* 1999, Vol. 24, pp. 709–30.
- [154] Richards M, Liss M. Reformer-based hydrogen fueling station economics. July 2002. In: Iwasaki, W., A consideration of the economic efficiency of hydrogen production from biomass. *International Journal of Hydrogen Energy*, 2003, Vol. 28, pp. 939-944.
- [155] Georgi D. Hydrogen extraction, more than one way to skin the cat. August 2002. In: Iwasaki, W., A consideration of the economic efficiency of hydrogen production from biomass. *International Journal of Hydrogen Energy*, 2003, Vol. 28, pp. 939-944.

APPENDICES

Appendix A

Table A.1 Annualized costs of system I components

Component, k	C(k)[\$]	Reference	S[\$]	\dot{C}_o [\$/h]	\dot{Z}_k [\$/h]
Gas compressor	110000	[140]	11000	12006.64	1.591
Heat exchanger I	51717	[62]	5171.7	5644.976	0.748
Heat exchanger II	51717	[62]	5171.7	5644.976	0.748
SSR	92600	[140]	9260	10107.41	1.339
SRR	92600	[140]	9260	10107.41	1.339
Filter I	17731	[62]	1773.1	1935.361	0.256
Gasifier	72403	[62]	7240.3	7902.879	1.047
Separator	5726	[62]	572.6	625.0001	0.083
Total	494494	Calculated	49449.4	53974.65	7.152

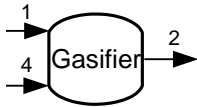
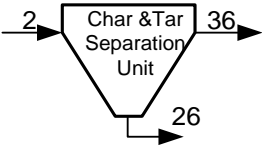
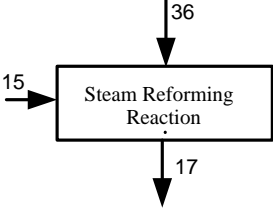
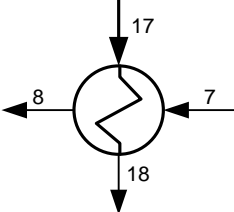
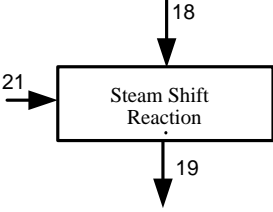
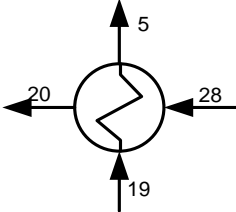
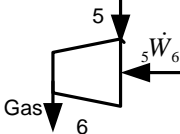
Table A.2 System II annualized costs of system components

Component, k	C(k)[\$]	Reference	S[\$]	\dot{C}_o [\$/h]	\dot{Z}_k [\$/h]
Air compressor I	173600	[140]	17360	18948.66	2.511
Air compressor II	173600	[140]	17360	18928.03	2.511
Burner	92600	[140]	9260	10107.41	1.339
Gas turbine	405100	[140]	40510	44217.18	5.859
Gas compressor	110000	[140]	11000	12006.64	1.591
Heat exchanger I	51717	[62]	5171.7	5644.976	0.748
Heat exchanger II	51717	[62]	5171.7	5644.976	0.748
Heat exchanger III	51717	[62]	5171.7	5644.976	0.748
SOFC stack	169905	[145]	16990.5	18545.35	2.457
SSR	92600	[140]	9260	10107.41	1.339
SRR	92600	[140]	9260	10107.41	1.339
Filter I	17731	[62]	1773.1	1935.361	0.256
Filter II	17731	[62]	1773.1	1935.361	0.256
Gasifier	72403	[62]	7240.3	7902.879	1.047
Separator	5726	[62]	572.6	625.0001	0.083
Total	1578747	Calculated	157874.7	172322.2	22.833

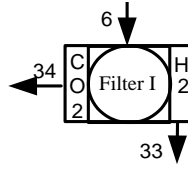
Table A.3 Annualized costs of system III components

Component (k)	C(k)[\$]	Reference	S[\$]	\dot{C}_o [\$]/h]	\dot{Z}_k [\$]/h]
Air compressor I	173600	[140]	17360	18948.66	2.511
Air compressor II	173600	[140]	17360	18928.03	2.511
Burner	92600	[140]	9260	10107.41	1.339
Gas turbine	405100	[140]	40510	44217.18	5.859
Gas compressor	110000	[140]	11000	12006.64	1.591
Heat exchanger I	51717	[62]	5171.7	5644.976	0.748
Heat exchanger II	51717	[62]	5171.7	5644.976	0.748
Heat exchanger III	51717	[62]	5171.7	5644.976	0.748
Heat exchanger IV	51717	[62]	5171.7	5644.976	0.748
SOFC-SOEC stack	339810	[145]	33981	37090.69	4.915
SSR	92600	[140]	9260	10107.41	1.339
SRR	92600	[140]	9260	10107.41	1.339
Filter I	17731	[62]	1773.1	1935.361	0.256
Filter II	17731	[62]	1773.1	1935.361	0.256
Gasifier	72403	[62]	7240.3	7902.879	1.047
Separator	5726	[62]	572.6	625.0001	0.083
Total	1782638	Calculated	178263.8	194577.2	25.781

Table A.4 System I cost balance equations

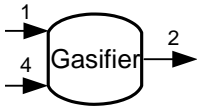
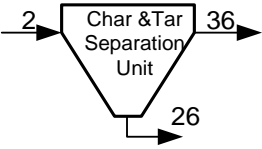
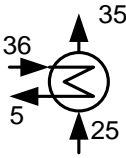
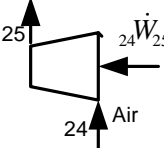
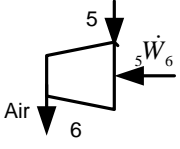
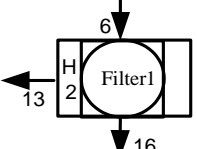
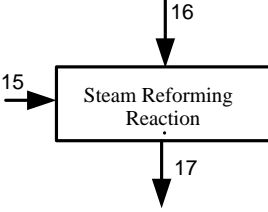
Component name	Component control volume	Cost balance and auxiliary equations
Gasifier		$\dot{C}_1 + \dot{C}_4 + \dot{Z}_{Gasifier} = \dot{C}_2$
Separator		$\dot{C}_2 + \dot{Z}_{Sep} = \dot{C}_{26} + \dot{C}_{36}$ $\frac{\dot{C}_2}{\dot{E}x_2} = \frac{\dot{C}_{26}}{\dot{E}x_{26}}$
Steam reforming reactor		$\dot{C}_{36} + \dot{C}_{15} + \dot{Z}_{SRR} = \dot{C}_{17}$ $\frac{\dot{C}_{15}}{\dot{E}x_{15}} = \frac{\dot{C}_4}{\dot{E}x_4}$
Heat exchanger I		$\dot{C}_7 + \dot{C}_{17} + \dot{Z}_{HE,I} = \dot{C}_{18} + \dot{C}_8$ $\frac{\dot{C}_{17}}{\dot{E}x_{17}} = \frac{\dot{C}_{18}}{\dot{E}x_{18}} ; \dot{C}_7 = 0$
Steam shift reactor		$\dot{C}_{18} + \dot{C}_{21} + \dot{Z}_{SSR} = \dot{C}_{19}$ $\frac{\dot{C}_{21}}{\dot{E}x_{21}} = \frac{\dot{C}_4}{\dot{E}x_4}$
Heat exchanger II		$\dot{C}_{28} + \dot{C}_{19} + \dot{Z}_{HE,II} = \dot{C}_5 + \dot{C}_{20}$ $\dot{C}_{28} = 0 ; \frac{\dot{C}_{20}}{\dot{E}x_{20}} = \frac{\dot{C}_4}{\dot{E}x_4}$
Compressor 5-6		$\dot{C}_5 + \dot{C}_{W5,6} + \dot{Z}_{Comp5,6} = \dot{C}_6$

Filter I

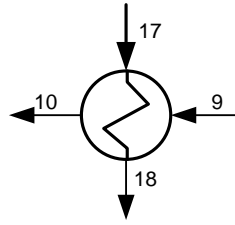


$$\dot{C}_6 + \dot{Z}_{F,I} = \dot{C}_{33} + \dot{C}_{34}$$
$$\frac{\dot{C}_6}{\dot{E}x_6} = \frac{\dot{C}_{33}}{\dot{E}x_{33}} + \frac{\dot{C}_{34}}{\dot{E}x_{34}}$$

Table A.5 System II cost balance equations

Component name	Component control volume	Cost balance and auxiliary equations
Gasifier		$\dot{C}_1 + \dot{C}_4 + \dot{Z}_{Gasifier} = \dot{C}_2$
Separator		$\dot{C}_2 + \dot{Z}_{Sep} = \dot{C}_{26} + \dot{C}_{36}$ $\frac{\dot{C}_2}{\dot{E}x_2} = \frac{\dot{C}_{26}}{\dot{E}x_{26}}$
Heat exchanger I		$\dot{C}_{36} + \dot{C}_{25} + \dot{Z}_{HEI} = \dot{C}_5 + \dot{C}_{35}$ $\frac{\dot{C}_{36}}{\dot{E}x_{36}} = \frac{\dot{C}_5}{\dot{E}x_5}$
Compressor 24-25		$\dot{C}_{24} + \dot{C}_{W24,25} + \dot{Z}_{Comp24,25} = \dot{C}_{25}$ $\dot{C}_{24} = 0$
Compressor 5-6		$\dot{C}_5 + \dot{C}_{W5,6} + \dot{Z}_{Comp5,6} = \dot{C}_6$
Filter 1		$\dot{C}_6 + \dot{Z}_{F1} = \dot{C}_{16} + \dot{C}_{13}$ $\frac{\dot{C}_6}{\dot{E}x_6} = \frac{\dot{C}_{13}}{\dot{E}x_{13}}$
Steam reforming reactor		$\dot{C}_{16} + \dot{C}_{15} + \dot{Z}_{SRR} = \dot{C}_{17}$ $\frac{\dot{C}_{15}}{\dot{E}x_{15}} = \frac{\dot{C}_{14}}{\dot{E}x_{14}}$

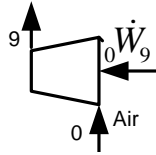
Heat exchanger II



$$\dot{C}_9 + \dot{C}_{17} + \dot{Z}_{HE,II} = \dot{C}_{10} + \dot{C}_{18}$$

$$\frac{\dot{C}_{17}}{\dot{E}x_{17}} = \frac{\dot{C}_{18}}{\dot{E}x_{18}}$$

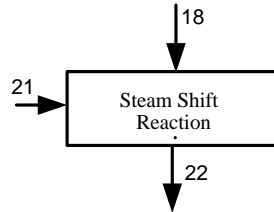
Compressor 0-9



$$\dot{C}_0 + \dot{C}_{W,0,9} + \dot{Z}_{Comp0,9} = \dot{C}_9$$

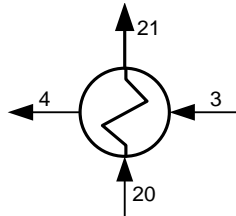
$$\dot{C}_0 = 0$$

Steam shift reactor



$$\dot{C}_{18} + \dot{C}_{21} + \dot{Z}_{SSR} = \dot{C}_{22}$$

Heat exchanger III

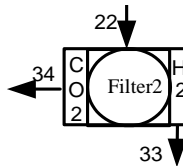


$$\dot{C}_3 + \dot{C}_{20} + \dot{Z}_{HE,III} = \dot{C}_{21} + \dot{C}_4$$

$$\frac{\dot{C}_{20}}{\dot{E}x_{20}} = \frac{\dot{C}_{14}}{\dot{E}x_{14}}$$

$$\dot{C}_3 = 0$$

Filter II



$$\dot{C}_{22} + \dot{Z}_{F,II} = \dot{C}_{33} + \dot{C}_{34}$$

$$\frac{\dot{C}_{22}}{\dot{E}x_{22}} = \frac{\dot{C}_{33}}{\dot{E}x_{33}} + \frac{\dot{C}_{34}}{\dot{E}x_{34}}$$

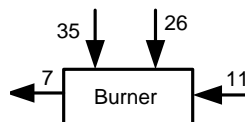
Solid oxide fuel cell



$$\dot{C}_{10} + \dot{C}_{13} + \dot{Z}_{SOFC} = \dot{C}_{11} + \dot{C}_{14} + \dot{C}_{W,SOFC}$$

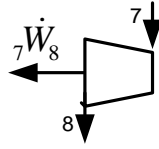
$$\frac{\dot{C}_{14}}{\dot{E}x_{14}} = \frac{\dot{C}_{11}}{\dot{E}x_{11}}$$

Burner



$$\dot{C}_{11} + \dot{C}_{35} + \dot{C}_{26} + \dot{Z}_{Burner} = \dot{C}_7$$

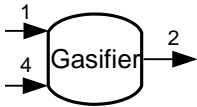
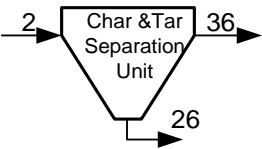
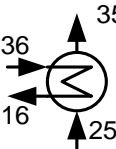
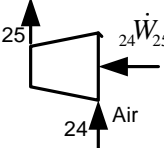
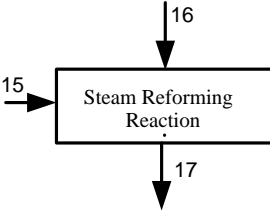
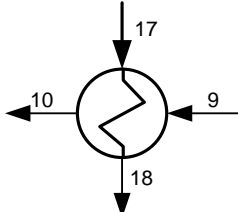
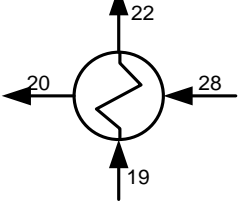
Gas turbine



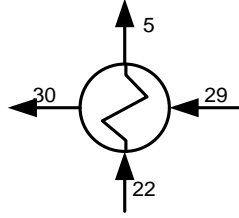
$$\dot{C}_7 + \dot{Z}_{7,8} = \dot{C}_8 + \dot{C}_{W7,8}$$

$$\dot{C}_8 = 0$$

Table A.6 System III cost balance equations

Component name	Component control volume	Cost balance and auxiliary equations
Gasifier		$\dot{C}_1 + \dot{C}_4 + \dot{Z}_{Gasif} = \dot{C}_2$
Separator		$\dot{C}_2 + \dot{Z}_{Sep} = \dot{C}_{26} + \dot{C}_{36}$ $\frac{\dot{C}_2}{\dot{E}x_2} = \frac{\dot{C}_{26}}{\dot{E}x_{26}}$
Heat exchanger I		$\dot{C}_{36} + \dot{C}_{25} + \dot{Z}_{HE,I} = \dot{C}_{16} + \dot{C}_{35}$ $\frac{\dot{C}_{36}}{\dot{E}x_{36}} = \frac{\dot{C}_{16}}{\dot{E}x_{16}}$
Air compressor 24-25		$\dot{C}_{24} + \dot{C}_{W24-25} + \dot{Z}_{C24-25} = \dot{C}_{25}$ $\dot{C}_{24} = 0$
Steam reforming reactor		$\dot{C}_{16} + \dot{C}_{15} + \dot{Z}_{SRR} = \dot{C}_{17}$ $\frac{\dot{C}_{15}}{\dot{E}x_{15}} = \frac{\dot{C}_{20}}{\dot{E}x_{20}}$
Heat exchanger II		$\dot{C}_9 + \dot{C}_{17} + \dot{Z}_{HE,II} = \dot{C}_{10} + \dot{C}_{18}$ $\frac{\dot{C}_{17}}{\dot{E}x_{17}} = \frac{\dot{C}_{18}}{\dot{E}x_{18}}$
Heat exchanger III		$\dot{C}_{28} + \dot{C}_{19} + \dot{Z}_{HE,III} = \dot{C}_{22} + \dot{C}_{20}$ $\dot{C}_{28} = 0$

Heat exchanger IV

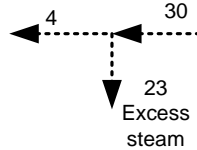


$$\dot{C}_{22} + \dot{C}_{29} + \dot{Z}_{HE,IV} = \dot{C}_{30} + \dot{C}_5$$

$$\dot{C}_{29} = 0$$

$$\frac{\dot{C}_{22}}{\dot{E}x_{21}} = \frac{\dot{C}_5}{\dot{E}x_5}$$

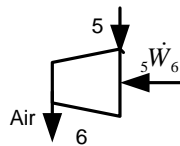
Excess steam



$$\dot{C}_{23} = C_{23} \dot{E}x_{23}$$

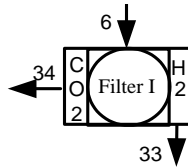
$$C_4 = C_{23} = C_{30}$$

Gas compressor 5-6



$$\dot{C}_5 + \dot{C}_{W5-6} + \dot{Z}_{C5-6} = \dot{C}_6$$

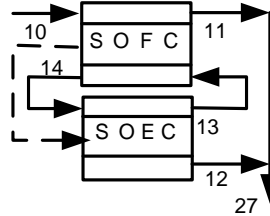
Filter



$$\dot{C}_6 + \dot{Z}_F = \dot{C}_{33} + \dot{C}_{34}$$

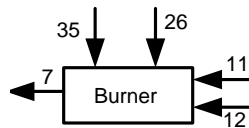
$$\frac{\dot{C}_6}{\dot{E}x_6} = \frac{\dot{C}_{33}}{\dot{E}x_{33}} + \frac{\dot{C}_{34}}{\dot{E}x_{34}}$$

Lumped SOFC-SOEC



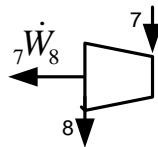
$$\dot{C}_{10} + \dot{Z}_{SOFC_SOEC} = \dot{C}_{27}$$

Burner



$$\dot{C}_{27} + \dot{C}_{35} + \dot{C}_{26} + \dot{Z}_{Burner} = \dot{C}_7$$

Gas turbine



$$\dot{C}_7 + \dot{Z}_{7-8} = \dot{C}_8 + \dot{C}_{t7-8}$$

$$\dot{C}_8 = 0$$

APPENDIX B

EES to simulate the systems

B1. System I

```
{Program System I performs calculations for energetic and Exergoeconomic of system I}
{This code finds mass, temperature and pressure at different states of the system I}
{The system includes gasifier, water gas shift, heat exchanger and steam reforming}
P_0=101.325[kPa];T_0=298[k]
R_bar=8.314[kJ/kg-K]
{Data from biomass gasification}
M_dot_3=0.27/1000*MW_H2O";Cp_H2O=4.18[kJ/kg-K]"
M_dot_1=0.32/1000*99.48
"Total hydrogen and products from gasification"
{N_H2=1.114/1000[kmol/s];N_CH4=0.0003469/1000[kmol/s];N_CO=0.7662/1000[kg/s];N_CO2
=0.2062/1000[kmol/s]; N_tar=0.04058/1000[kmol/s];N_char=0.06401/1000[kmol/s]}
MW_CH4=16.043;MW_CO=28.011;MW_CO2=44.01;MW_H2=2.016[kg/kmol];MW_H2O=18.
015;MW_air=28.97[kJ/kg-K]
MW_O2=32[kg/kmol];MW_N2=28.013[kg/kmol];MW_tar=78.11[kg/kmol];MW_char=12[kg/k
mol]
Cp_char=0.708[kJ/kg-K];Cp_air=1.004[kJ/kg-K]
"Standard exergies for the compounds"
EPS_ch_H2=236100[kJ/kmol];EPS_ch_CO=275100;EPS_ch_CO2=19870;EPS_ch_CH4=83165
0;EPS_ch_H2O=9500[kJ/kmol];EPS_ch_O2=3971[kJ/kmol];EPS_ch_N2=720[kJ/kmol]
EPS_ch_air=0.21*EPS_ch_O2+0.79*EPS_ch_N2

{Calculations for the adiabatic burner with 100%efficiency}
tar_26=N_tar;char_26=N_char;N_26=tar_26+char_26
P_26=120[kPa];DELTAHF_char=0
DELTAH_char_26=4.18*(4.03*(T_26-T_0)+0.00114*(T_26^2/2-T_0^2/2))+2.04*10^5*(1/T_26-
1/T_0)
S_char_26=4.18*(4.03*(LN(T_26)-LN(T_0))+0.00114*(T_26-T_0)+1.02*10^5*(1/T_26^2-
1/T_0^2))-R_bar*LN(P_26/P_0*char_26/N_26)
EX_ph_char_26=DELTAH_char_26-T_0*S_char_26
EPS_ch_char=410260[kJ/kmol]
EX_ch_char_26=char_26/N_26*(EPS_ch_char+R_bar*T_0*LN(char_26/N_26))
EX_char_26=char_26*(EX_ch_char_26+EX_ph_char_26)

{Calculation of enthalpy &exergy of tar}
N_C=48.01/12;N_H=6.04;A1_tar=37.1635;A2_tar=-
31.4767;A3_tar=0.564682;A4_tar=20.1145;A5_tar=54.3111;A6_tar=44.6712;C_f=48.0;H_f=6.0
4;O_f=45.43;N_f=0.15;S_f=0.05
DELTAH_tar_26=N_C*DELTAHF_CO2+N_H/2*DELTAHF_H2O+(0.00422*MW_tar*(T_26^
2-T_0^2)/2-30.980)
{S_star in kJ/kmol carbon K}
S_star_26=A1_tar+A2_tar*EXP(-
A3_tar*(H_f/C_f+N_f))+A4_tar*(O_f/(C_f+N_f))+A5_tar*(N_f/(C_f+N_f))+A6_tar*(S_f/(C_f+
N_f))
```

$S_{tar_26} = S_{star_26} + 0.00422 * MW_{tar} * (T_{26} - T_0) - R_{bar} * LN(P_{26}/P_0 * tar_{26}/N_{26})$
 $EX_{ph_tar_26} = DELTAH_{tar_26} * tar_{26} - T_0 * S_{tar_26} * tar_{26}$
 $EPS_{ch_tar} = 3303600 \text{ [kJ/kmol]}$
 $X_{tar_26} = tar_{26}/N_{26}$
 $EX_{ch_tar_26} = X_{tar_26} * (EPS_{ch_tar} + R_{bar} * T_0 * LN(X_{tar_26}))$
 $EX_{tar_26} = EX_{ph_tar_26} + tar_{26} * EX_{ch_tar_26}$
 $EX_{26} = EX_{char_26} + EX_{tar_26}$
 {Chemical exergy of tar is disregarded}
 $EX_2 = EX_{26} + EX_{36}$

{State 36}

$P_{36} = 120 \text{ [kPa]}$; $T_{36} = T_{26}$
 $H2_{36} = N_{H2}$; $CH4_{36} = N_{CH4}$; $CO_{36} = N_{CO}$; $CO2_{36} = N_{CO2}$
 $N_{36} = N_{H2} + N_{CH4} + N_{CO} + N_{CO2}$
 $MW_{36} = H2_{36}/N_{36} * MW_{H2} + CH4_{36}/N_{36} * MW_{CH4} + CO_{36}/N_{36} * MW_{CO} + CO2_{36}/N_{36} * MW_{CO2}$
 $M_{dot_36} = N_{36} * MW_{36}$

{Calculations of delta enthalpy for hydrogen in kJ/kmol at heat exchanger 36-5 inlet}

$A_{H2} = 29.11$; $B_{H2} = -0.1916 * 10^{(-2)}$; $C_{H2} = 0.4003 * 10^{(-5)}$; $D_{H2} = -0.8704 * 10^{(-9)}$; $DELTAHF_{H2} = 0.0$; $DELTA_{S_{H2}} = 130.68 \text{ [kJ/kmol-K]}$
 $DELTAH_{H2_36} = A_{H2} * (T_{36} - T_0) + B_{H2} * (T_{36}^2 - T_0^2)/2 + C_{H2} * (T_{36}^3 - T_0^3)/3 + D_{H2} * (T_{36}^4 - T_0^4)/4$
 $S_{H2_36} = A_{H2} * (LN(T_{36}) - LN(T_0)) + B_{H2} * (T_{36} - T_0) + C_{H2} * (T_{36}^2 - T_0^2)/2 + D_{H2} * (T_{36}^3 - T_0^3)/3 - R_{bar} * LN(P_{36}/P_0 * H2_{36}/N_{36})$
 $EX_{ph_H2_36} = DELTAH_{H2_36} - T_0 * S_{H2_36}$
 $EX_{ch_H2_36} = H2_{36}/N_{36} * (EPS_{ch_H2} + R_{bar} * T_0 * LN(H2_{36}/N_{36}))$

{Calculations of delta enthalpy for carbon monoxide in kJ/kmol at heat exchanger 36-5 inlet}

$A_{CO} = 28.16$; $B_{CO} = 0.1675 * 10^{(-2)}$; $C_{CO} = 0.5372 * 10^{(-5)}$; $D_{CO} = -2.222 * 10^{(-9)}$; $DELTAHF_{CO} = -110.53 \text{ [kJ/mol]}$; $DELTA_{S_{CO}} = 197.65 \text{ [kJ/kmol-K]}$
 $DELTAH_{CO_36} = A_{CO} * (T_{36} - T_0) + B_{CO} * (T_{36}^2 - T_0^2)/2 + C_{CO} * (T_{36}^3 - T_0^3)/3 + D_{CO} * (T_{36}^4 - T_0^4)/4$
 $S_{CO_36} = A_{CO} * (LN(T_{36}) - LN(T_0)) + B_{CO} * (T_{36} - T_0) + C_{CO} * (T_{36}^2 - T_0^2)/2 + D_{CO} * (T_{36}^3 - T_0^3)/3 - R_{bar} * LN(P_{36}/P_0 * CO_{36}/N_{36})$
 $EX_{ph_CO_36} = DELTAH_{CO_36} - T_0 * S_{CO_36}$
 $EX_{ch_CO_36} = CO_{36}/N_{36} * (EPS_{ch_CO} + R_{bar} * T_0 * LN(CO_{36}/N_{36}))$

{Calculations of delta enthalpy for carbon dioxide in kJ/kmol at heat exchanger 36-5 inlet}

$A_{CO2} = 22.26$; $B_{CO2} = 5.981 * 10^{(-2)}$; $C_{CO2} = -3.501 * 10^{(-5)}$; $D_{CO2} = 7.469 * 10^{(-9)}$; $DELTAHF_{CO2} = -393.52 \text{ [kJ/mol]}$; $DELTA_{S_{CO2}} = 213.8 \text{ [kJ/kmol-K]}$
 $DELTAH_{CO2_36} = A_{CO2} * (T_{36} - T_0) + B_{CO2} * (T_{36}^2 - T_0^2)/2 + C_{CO2} * (T_{36}^3 - T_0^3)/3 + D_{CO2} * (T_{36}^4 - T_0^4)/4$
 $S_{CO2_36} = A_{CO2} * (LN(T_{36}) - LN(T_0)) + B_{CO2} * (T_{36} - T_0) + C_{CO2} * (T_{36}^2 - T_0^2)/2 + D_{CO2} * (T_{36}^3 - T_0^3)/3 - R_{bar} * LN(P_{36}/P_0 * CO2_{36}/N_{36})$
 $EX_{ph_CO2_36} = DELTAH_{CO2_36} - T_0 * S_{CO2_36}$
 $EX_{ch_CO2_36} = CO2_{36}/N_{36} * (EPS_{ch_CO2} + R_{bar} * T_0 * LN(CO2_{36}/N_{36}))$

{Calculations of delta enthalpy for methane in kJ/kmol at heat exchanger 36-5 inlet}

$A_{CH4}=19.89; B_{CH4}=5.204 \cdot 10^{-2}; C_{CH4}=1.269 \cdot 10^{-5}; D_{CH4}=-11.01 \cdot 10^{-9};$
 $\Delta H_{f,CH4}=-74.8[\text{kJ/mol}]; \Delta S_{CH4}=186.16[\text{kJ/kmol-K}]$
 $\Delta H_{CH4,36}=A_{CH4} \cdot (T_{36}-T_0)+B_{CH4} \cdot (T_{36}^2-T_0^2)/2+C_{CH4} \cdot (T_{36}^3-T_0^3)/3+D_{CH4} \cdot (T_{36}^4-T_0^4)/4$
 $S_{CH4,36}=A_{CH4} \cdot (\ln(T_{36})-\ln(T_0))+B_{CH4} \cdot (T_{36}-T_0)+C_{CH4} \cdot (T_{36}^2-T_0^2)/2+D_{CH4} \cdot (T_{36}^3-T_0^3)/3-R_{bar} \cdot \ln(P_{36}/P_0 \cdot CH4_{36}/N_{36})$
 $EX_{ph,CH4,36}=\Delta H_{CH4,36}-T_0 \cdot S_{CH4,36}$
 $EX_{ch,CH4,36}=CH4_{36}/N_{36} \cdot (EPS_{ch,CH4}+R_{bar} \cdot T_0 \cdot \ln(CH4_{36}/N_{36}))$

"Enthalpy at heat exchanger 36-5 inlet"

$\Delta H_{36}=H2_{36} \cdot \Delta H_{H2,36}+CO_{36} \cdot (\Delta H_{f,CO} \cdot 1000+\Delta H_{CO,36})+CO2_{36} \cdot (\Delta H_{f,CO2} \cdot 1000+\Delta H_{CO2,36})+CH4_{36} \cdot (\Delta H_{f,CH4} \cdot 1000+\Delta H_{CH4,36})$

"Total number of moles at steam reforming inlet"

$N_{SRi}=N_{36}+H2O_{15}$

"State 15"

$T_{15}=T_{20}$

$P_{15}=P_{36}$

$H2O_{15}=N_{CH4}; N_{15}=H2O_{15}; M_{dot,15}=H2O_{15} \cdot MW_{H2O}$ "Steam consumed by steam reforming reaction"

{Calculations of delta enthalpy for water in kJ/ kmol at steam reforming inlet}

$A_{H2O}=32.24; B_{H2O}=0.1923 \cdot 10^{-2}; C_{H2O}=1.055 \cdot 10^{-5}; D_{H2O}=-3.595 \cdot 10^{-9};$
 $\Delta H_{f,H2O}=-241.83[\text{kJ/mol}]; \Delta S_{H2O}=188.83[\text{kJ/kmol-K}]$

$\Delta H_{H2O,15}=A_{H2O} \cdot (T_{15}-T_0)+B_{H2O} \cdot (T_{15}^2-T_0^2)/2+C_{H2O} \cdot (T_{15}^3-T_0^3)/3+D_{H2O} \cdot (T_{15}^4-T_0^4)/4$

$S_{H2O,15}=A_{H2O} \cdot (\ln(T_{15})-\ln(T_0))+B_{H2O} \cdot (T_{15}-T_0)+C_{H2O} \cdot (T_{15}^2-T_0^2)/2+D_{H2O} \cdot (T_{15}^3-T_0^3)/3$

$EX_{ph,H2O,15}=\Delta H_{H2O,15}-T_0 \cdot S_{H2O,15}$

$EX_{ch,H2O,15}=H2O_{15}/N_{SRi} \cdot (EPS_{ch,H2O}+R_{bar} \cdot T_0 \cdot \ln(H2O_{15}/N_{SRi}))$

"Physical and chemical exergy with flow at SRi"

$EX_{ph,SRi}=CO_{36} \cdot EX_{ph,CO,36}+CO2_{36} \cdot EX_{ph,CO2,36}+CH4_{36} \cdot EX_{ph,CH4,36}+H2_{36} \cdot EX_{ph,H2,36}+H2O_{15} \cdot EX_{ph,H2O,15}$

$EX_{ch,SRi}=CO_{36} \cdot EX_{ch,CO,36}+CO2_{36} \cdot EX_{ch,CO2,36}+CH4_{36} \cdot EX_{ch,CH4,36}+H2_{36} \cdot EX_{ch,H2,36}+H2O_{15} \cdot EX_{ch,H2O,15}$

$EX_{SRi}=EX_{ph,SRi}+EX_{ch,SRi}$

$EX_{36}=CO_{36} \cdot (EX_{ph,CO,36}+EX_{ch,CO,36})+CO2_{36} \cdot (EX_{ph,CO2,36}+EX_{ch,CO2,36})+CH4_{36} \cdot (EX_{ph,CH4,36}+EX_{ch,CH4,36})+H2_{36} \cdot (EX_{ph,H2,36}+EX_{ch,H2,36})$

$EX_{15}=H2O_{15} \cdot (EX_{ph,H2O,15}+EX_{ch,H2O,15})$

"State 17"

$P_{17}=P_{36}-0.05 \cdot P_{36}$

$CO_{17}=CH4_{36}+N_{CO}; CO2_{17}=CO2_{36}; H2_{17}=3 \cdot CH4_{36}+H2_{36}$

$N_{17}=H2_{17}+CO_{17}+CO2_{17}$

$MW_{17}=H2_{17}/N_{17} \cdot MW_{H2}+CO_{17}/N_{17} \cdot MW_{CO}+CO2_{17}/N_{17} \cdot MW_{CO2}$

$M_{dot,17}=N_{17} \cdot MW_{17}$

$N_{SRe}=N_{17}$

{ Calculations of delta enthalpy for hydrogen in kJ/kmol at steam reforming exit}
 $DELTAH_H2_17 = A_H2*(T_17-T_0) + B_H2*(T_17^2-T_0^2)/2 + C_H2*(T_17^3-T_0^3)/3 + D_H2*(T_17^4-T_0^4)/4$
 $S_H2_17 = A_H2*(LN(T_17)-LN(T_0)) + B_H2*(T_17-T_0) + C_H2*(T_17^2-T_0^2)/2 + D_H2*(T_17^3-T_0^3)/3 - R_bar*LN(P_17/P_0*(H2_17/N_SRe))$
 $EX_ph_H2_17 = DELTAH_H2_17 - T_0*S_H2_17$
 $EX_ch_H2_17 = H2_17/N_17*(EPS_ch_H2 + R_bar*T_0*LN(H2_17/N_SRe))$

{ Calculations of delta enthalpy for carbon monoxide in kJ/kmol at steam reforming exit}
 $DELTAH_CO_17 = A_CO*(T_17-T_0) + B_CO*(T_17^2-T_0^2)/2 + C_CO*(T_17^3-T_0^3)/3 + D_CO*(T_17^4-T_0^4)/4$
 $S_CO_17 = A_CO*(LN(T_17)-LN(T_0)) + B_CO*(T_17-T_0) + C_CO*(T_17^2-T_0^2)/2 + D_CO*(T_17^3-T_0^3)/3 - R_bar*LN(P_17/P_0*(CO_17/N_SRe))$
 $EX_ph_CO_17 = DELTAH_CO_17 - T_0*S_CO_17$
 $EX_ch_CO_17 = CO_17/N_17*(EPS_ch_CO + R_bar*T_0*LN(CO_17/N_SRe))$

{ Calculations of delta enthalpy for carbon dioxide in kJ/kmol at steam reforming exit}
 $DELTAH_CO2_17 = A_CO2*(T_17-T_0) + B_CO2*(T_17^2-T_0^2)/2 + C_CO2*(T_17^3-T_0^3)/3 + D_CO2*(T_17^4-T_0^4)/4$
 $S_CO2_17 = A_CO2*(LN(T_17)-LN(T_0)) + B_CO2*(T_17-T_0) + C_CO2*(T_17^2-T_0^2)/2 + D_CO2*(T_17^3-T_0^3)/3 - R_bar*LN(P_17/P_0*(CO2_17/N_SRe))$
 $EX_ph_CO2_17 = DELTAH_CO2_17 - T_0*S_CO2_17$
 $EX_ch_CO2_17 = CO2_17/N_17*(EPS_ch_CO2 + R_bar*T_0*LN(CO2_17/N_SRe))$

$DELTAH_17 = CO_17*(DELTAH_CO_17 + DELTAHF_CO*1000) + CO2_17*(DELTAHF_CO2*1000 + DELTAH_CO2_17) + H2_17*DELTAH_H2_17$

"Physical and chemical exergies with flow at SRe"

$EX_ph_SRe = CO_17*EX_ph_CO_17 + CO2_17*EX_ph_CO2_17 + H2_17*EX_ph_H2_17$
 $EX_ch_SRe = CO_17*EX_ch_CO_17 + CO2_17*EX_ch_CO2_17 + H2_17*EX_ch_H2_17$
 $EX_SRe = EX_ph_SRe + EX_ch_SRe$
 $EX_17 = EX_SRe$

"Exergy destroyed in SR"

$EX_Ir_SR2 = T_0*(H2_17*(S_H2_17 + DELTA_S_H2) + CO2_17*(S_CO2_17 + DELTA_S_CO2) + CO_17*(S_CO_17 + DELTA_S_CO))$
 $EX_Ir_SR1 = T_0*(CH4_36*(S_CH4_36 + DELTA_S_CH4) + CO2_36*(S_CO2_36 + DELTA_S_CO2) + CO_36*(S_CO_36 + DELTA_S_CO) + H2O_15*(S_H2O_15 + DELTA_S_H2O))$
 $EX_Ir_SR = EX_Ir_SR2 - EX_Ir_SR1$

{ Energy balance of the steam reforming reactor to find T_17 }

$SR_A = H2_36*DELTAH_H2_36 + CH4_36*(DELTAHF_CH4*1000 + DELTAH_CH4_36) + CO2_36*(DELTAHF_CO2*1000 + DELTAH_CO2_36)$
 $SR_B = CO_36*(DELTAHF_CO*1000 + DELTAH_CO_36) + H2O_15*(DELTAHF_H2O*1000 + DELTAH_H2O_15)$
 $SR_1 = SR_A + SR_B$
 $SR_2 = H2_17*DELTAH_H2_17 + CO_17*(DELTAHF_CO*1000 + DELTAH_CO_17) + CO2_17*(DELTAHF_CO2*1000 + DELTAH_CO2_17)$
 $SR_2 = SR_1$ "From which will find exit temperature from steam reformer, T_17"

"State 18"

$$P_{18}=P_{17}-0.05*P_{17}$$

$$CO_{18}=CO_{17}; CO2_{18}=CO2_{17}; H2_{18}=H2_{17}$$

$$N_{18}=H2_{18}+CO_{18}+CO2_{18}$$

$$MW_{18}=H2_{18}/N_{18}*MW_{H2}+CO_{18}/N_{18}*MW_{CO}+CO2_{18}/N_{18}*MW_{CO2}$$

$$M_{dot_{18}}=N_{18}*MW_{18}$$

{Calculations of delta enthalpy for hydrogen in kJ/kmol at steam reforming exit}

$$DELTAH_{H2_{18}}=A_{H2}*(T_{18}-T_0)+B_{H2}*(T_{18}^2-T_0^2)/2+C_{H2}*(T_{18}^3-T_0^3)/3+D_{H2}*(T_{18}^4-T_0^4)/4$$

$$S_{H2_{18}}=A_{H2}*(LN(T_{18})-LN(T_0))+B_{H2}*(T_{18}-T_0)+C_{H2}*(T_{18}^2-T_0^2)/2+D_{H2}*(T_{18}^3-T_0^3)/3-R_{bar}*LN(P_{18}/P_0*H2_{18}/N_{18})$$

$$EX_{ph_{H2_{18}}}=DELTAH_{H2_{18}}-T_0*S_{H2_{18}}$$

$$EX_{ch_{H2_{18}}}=H2_{18}/N_{18}*(EPS_{ch_{H2}}+R_{bar}*T_0*LN(H2_{18}/N_{18}))$$

{Calculations of delta enthalpy for carbon monoxide in kJ/kmol at steam reforming exit}

$$DELTAH_{CO_{18}}=A_{CO}*(T_{18}-T_0)+B_{CO}*(T_{18}^2-T_0^2)/2+C_{CO}*(T_{18}^3-T_0^3)/3+D_{CO}*(T_{18}^4-T_0^4)/4$$

$$S_{CO_{18}}=A_{CO}*(LN(T_{18})-LN(T_0))+B_{CO}*(T_{18}-T_0)+C_{CO}*(T_{18}^2-T_0^2)/2+D_{CO}*(T_{18}^3-T_0^3)/3-R_{bar}*LN(P_{18}/P_0*CO_{18}/N_{18})$$

$$EX_{ph_{CO_{18}}}=DELTAH_{CO_{18}}-T_0*S_{CO_{18}}$$

$$EX_{ch_{CO_{18}}}=CO_{18}/N_{18}*(EPS_{ch_{CO}}+R_{bar}*T_0*LN(CO_{18}/N_{18}))$$

{Calculations of delta enthalpy for carbon dioxide in kJ/kmol at steam reforming exit}

$$DELTAH_{CO2_{18}}=A_{CO2}*(T_{18}-T_0)+B_{CO2}*(T_{18}^2-T_0^2)/2+C_{CO2}*(T_{18}^3-T_0^3)/3+D_{CO2}*(T_{18}^4-T_0^4)/4$$

$$S_{CO2_{18}}=A_{CO2}*(LN(T_{18})-LN(T_0))+B_{CO2}*(T_{18}-T_0)+C_{CO2}*(T_{18}^2-T_0^2)/2+D_{CO2}*(T_{18}^3-T_0^3)/3-R_{bar}*LN(P_{18}/P_0*CO2_{18}/N_{18})$$

$$EX_{ph_{CO2_{18}}}=DELTAH_{CO2_{18}}-T_0*S_{CO2_{18}}$$

$$EX_{ch_{CO2_{18}}}=CO2_{18}/N_{18}*(EPS_{ch_{CO2}}+R_{bar}*T_0*LN(CO2_{18}/N_{18}))$$

"Physical and chemical exergies with flow at state 18"

$$EX_{ph_{18}}=CO_{18}*EX_{ph_{CO_{18}}}+CO2_{18}*EX_{ph_{CO2_{18}}}+H2_{18}*EX_{ph_{H2_{18}}}$$

$$EX_{ch_{18}}=CO_{18}*EX_{ch_{CO_{18}}}+CO2_{18}*EX_{ch_{CO2_{18}}}+H2_{18}*EX_{ch_{H2_{18}}}$$

$$EX_{18}=EX_{ph_{18}}+EX_{ch_{18}}$$

$$DELTAH_{18}=CO_{18}*(DELTAH_{CO_{18}}+DELTAHF_{CO}*1000)+CO2_{18}*(DELTAHF_{CO2}*1000+DELTAH_{CO2_{18}})+H2_{18}*DELTAH_{H2_{18}}$$

$$Q_{dot_{17_{18}}}=DELTAH_{17}-DELTAH_{18}$$

{Assume no pressure drop in the heat recovery steam generation 7-8}

$$H2O_7=M_{dot_7}/MW_{H2O}; M_{dot_7}=M_{dot_3}; N_7=H2O_7$$

$$T_7=T_0$$

$$P_7=120[\text{kPa}] \text{ "From main supply"}$$

$$h_7=\text{Enthalpy (Steam, } T=T_7, P=P_7)$$

$$S_7=\text{Entropy (Steam, } T=T_7, P=P_7)$$

$$EX_{ph_{H2O_7}}=h_7-T_0*S_7$$

$$EX_{ch_{H2O_7}}=H2O_7/N_7*(EPS_{ch_{H2O}}+R_{bar}*T_0*LN(H2O_7/N_7))$$

"Exergy at heat exchanger 7-8 inlet"

$$EX_{ph_7} = M_{dot_7} * EX_{ph_H2O_7}$$

$$EX_{ch_7} = H2O_7 * EX_{ch_H2O_7}$$

$$EX_7 = EX_{ph_7} + EX_{ch_7}$$

"State 8"

$$M_{dot_8} = M_{dot_7}; H2O_8 = H2O_7; N_8 = N_7$$

$$T_8 = T_{17-7} [K]; P_8 = P_7$$

$$h_8 = \text{Enthalpy (Steam, } T=T_8, P=P_8)$$

$$S_8 = \text{Entropy (Steam, } T=T_8, P=P_8)$$

$$EX_{ph_H2O_8} = h_8 - T_0 * S_8$$

$$EX_{ch_H2O_8} = H2O_8 / N_8 * (EPS_{ch_H2O} + R_{bar} * T_0 * \ln(H2O_8 / N_8))$$

"Exergy at heat exchanger 7-8 exit"

$$EX_{ph_8} = M_{dot_8} * EX_{ph_H2O_8}$$

$$EX_{ch_8} = H2O_8 * EX_{ch_H2O_8}$$

$$EX_8 = EX_{ph_8} + EX_{ch_8}$$

$$Q_{dot_7_8} = M_{dot_7} * (h_8 - h_7)$$

$$Q_{dot_17_18} = Q_{dot_7_8} \text{ "To find } T_{18}$$

"Exergy destroyed in heat exchanger 17_18&7_8"

$$EX_{Ir_17} = T_0 * (H2_{17} * (S_{H2_17} + \Delta S_{H2}) + CO2_{17} * (S_{CO2_17} + \Delta S_{CO2}) + CO_{17} * (S_{CO_17} + \Delta S_{CO}))$$

$$EX_{Ir_18} = T_0 * (H2_{18} * (S_{H2_18} + \Delta S_{H2}) + CO2_{18} * (S_{CO2_18} + \Delta S_{CO2}) + CO_{18} * (S_{CO_18} + \Delta S_{CO}))$$

$$EX_{Ir_HE_17_18} = EX_{Ir_17} - EX_{Ir_18}$$

$$EX_{Ir_7} = T_0 * (H2O_7 * (S_7 + \Delta S_{H2O}))$$

$$EX_{Ir_8} = T_0 * (H2O_8 * (S_8 + \Delta S_{H2O}))$$

$$EX_{Ir_HE_7_8} = EX_{Ir_8} - EX_{Ir_7}$$

$$EX_{Ir_17_18_7_8} = EX_{Ir_HE_17_18} + EX_{Ir_HE_7_8}$$

{ Calculations for steam shift reaction }

{ Calculations of delta enthalpy for steam in kJ/kmol at steam shift inlet }

$$H2O_{21} = CO_{18}; P_{21} = P_{18}; T_{21} = 500$$

$$M_{dot_21} = H2O_{21} * MW_{H2O}; N_{21} = H2O_{21}$$

$$\Delta H_{H2O_21} = A_{H2O} * (T_{21} - T_0) + B_{H2O} * (T_{21}^2 - T_0^2) / 2 + C_{H2O} * (T_{21}^3 - T_0^3) / 3 + D_{H2O} * (T_{21}^4 - T_0^4) / 4$$

$$S_{H2O_21} = A_{H2O} * (\ln(T_{21}) - \ln(T_0)) + B_{H2O} * (T_{21} - T_0) + C_{H2O} * (T_{21}^2 - T_0^2) / 2 + D_{H2O} * (T_{21}^3 - T_0^3) / 3 - R_{bar} * \ln(P_{21} / P_0 * H2O_{21} / N_{SSi})$$

$$EX_{ph_H2O_21} = \Delta H_{H2O_21} - T_0 * S_{H2O_21}$$

$$EX_{ch_H2O_21} = H2O_{21} / N_{SSi} * (EPS_{ch_H2O} + R_{bar} * T_0 * \ln(H2O_{21} / N_{SSi}))$$

$$EX_{21} = H2O_{21} * (EX_{ph_H2O_21} + EX_{ch_H2O_21})$$

"Physical exergy and chemical exergy at SSi"

$$EX_{ph_SSi} = CO_{18} * EX_{ph_CO_18} + CO2_{18} * EX_{ph_CO2_18} + H2_{18} * EX_{ph_H2_18} + H2O_{21} * EX_{ph_H2O_21}$$

$$EX_{ch_SSi} = CO_{18} * EX_{ch_CO_18} + CO2_{18} * EX_{ch_CO2_18} + H2_{18} * EX_{ch_H2_18} + H2O_{21} * EX_{ch_H2O_21}$$

$$EX_{SSi} = EX_{ph_SSi} + EX_{ch_SSi}$$

{ calculate delta enthalpy for carbon dioxide in kJ/kmol at steam shift exit}
 $CO2_{19}=CO2_{18}+CO_{36}$; $H2_{19}=H2_{18}+CO_{18}$; $P_{19}=P_{18}-0.05*P_{18}$
 $N_{19}=CO2_{19}+H2_{19}$
 $MW_{19}=H2_{19}/N_{19}*MW_{H2}+CO2_{19}/N_{19}*MW_{CO2}$
 $M_{dot_{19}}=N_{19}*MW_{19}$
 $N_{SSi}=N_{18}+H2O_{21}$
 $N_{SSe}=N_{19}$

$DELTAH_{CO2_{19}}= A_{CO2}*(T_{19}-T_0)+B_{CO2}*(T_{19}^2-T_0^2)/2+C_{CO2}*(T_{19}^3-T_0^3)/3+D_{CO2}*(T_{19}^4-T_0^4)/4$
 $S_{CO2_{19}}= A_{CO2}*(LN(T_{19})-LN(T_0))+B_{CO2}*(T_{19}-T_0)+C_{CO2}*(T_{19}^2-T_0^2)/2+D_{CO2}*(T_{19}^3-T_0^3)/3-R_{bar}*LN(P_{19}/P_0*CO2_{19}/N_{SSe})$
 $EX_{ph_{CO2_{19}}}=DELTAH_{CO2_{19}}-T_0*S_{CO2_{19}}$
 $EX_{ch_{CO2_{19}}}=CO2_{19}/N_{SSe}*(EPS_{ch_{CO2}}+R_{bar}*T_0*LN(CO2_{19}/N_{SSe}))$

{ Calculations of delta enthalpy for hydrogen in kJ/kmol at steam shift exit}
 $DELTAH_{H2_{19}}= A_{H2}*(T_{19}-T_0)+B_{H2}*(T_{19}^2-T_0^2)/2+C_{H2}*(T_{19}^3-T_0^3)/3+D_{H2}*(T_{19}^4-T_0^4)/4$
 $S_{H2_{19}}= A_{H2}*(LN(T_{19})-LN(T_0))+B_{H2}*(T_{19}-T_0)+C_{H2}*(T_{19}^2-T_0^2)/2+D_{H2}*(T_{19}^3-T_0^3)/3-R_{bar}*LN(P_{19}/P_0*H2_{19}/N_{SSe})$
 $EX_{ph_{H2_{19}}}=DELTAH_{H2_{19}}-T_0*S_{H2_{19}}$
 $EX_{ch_{H2_{19}}}=H2_{19}/N_{SSe}*(EPS_{ch_{H2}}+R_{bar}*T_0*LN(H2_{19}/N_{SSe}))$

"Physical exergy and chemical exergy at SSe"

$EX_{ph_{SSe}}=H2_{19}*EX_{ph_{H2_{19}}}+CO2_{19}*EX_{ph_{CO2_{19}}}$
 $EX_{ch_{SSe}}=H2_{19}*EX_{ch_{H2_{19}}}+CO2_{19}*EX_{ch_{CO2_{19}}}$
 $EX_{SSe}=EX_{ph_{SSe}}+EX_{ch_{SSe}}$
 $EX_{19}=EX_{SSe}$
 $DELTAH_{19}=H2_{19}*DELTAH_{H2_{19}}+CO2_{19}*(DELTAH_{CO2_{19}}+DELTAHF_{CO2}*1000)$

"Exergy destroyed in steam shift reactor"

$EX_{Ir_{SS}}=T_0*(H2_{19}*(S_{H2_{19}}+DELTA_{S_{H2}})+CO2_{19}*(S_{CO2_{19}}+DELTA_{S_{CO2}})-H2O_{21}*(S_{H2O_{21}}+DELTA_{S_{H2O}})-H2_{18}*(S_{H2_{18}}+DELTA_{S_{H2}})-CO2_{18}*(S_{CO2_{18}}+DELTA_{S_{CO2}})-CO_{18}*(S_{CO_{18}}+DELTA_{S_{CO}}))$
 { Calculations for temperature at steam shift reactor exit, T₁₉}
 $SS_A=CO_{18}*(DELTAH_{CO_{18}}+DELTAHF_{CO}*1000)+CO2_{18}*(DELTAHF_{CO}*1000+DELTAH_{CO2_{18}})$
 $SS_B=H2_{18}*DELTAH_{H2_{18}}+H2O_{21}*(DELTAHF_{H2O}*1000+DELTAH_{H2O_{21}})$
 $SS_1=SS_A+SS_B$
 $SS_2=H2_{19}*DELTAH_{H2_{19}}+CO2_{19}*(DELTAHF_{CO2}*1000+DELTAH_{CO2_{19}})$
 $SS_1-SS_2=0$ "To calculate T₁₉"
 $Q_{dot_{19_5}}=DELTAH_{19}-DELTAH_5$

{ Calculations for heat exchanger 19_5 & 28_20 }

$H2O_{20}=4*(H2O_{21}+H2O_{15})$
 $M_{dot_{20}}=H2O_{20}*MW_{H2O}$; $N_{20}=H2O_{20}$
 $P_{20}=P_{21}$
 $DELTAH_{H2O_{20}}= A_{H2O}*(T_{20}-T_0)+B_{H2O}*(T_{20}^2-T_0^2)/2+C_{H2O}*(T_{20}^3-T_0^3)/3+D_{H2O}*(T_{20}^4-T_0^4)/4$

$S_{H2O_20} = A_{H2O}*(LN(T_{20})-LN(T_0))+B_{H2O}*(T_{20}-T_0)+C_{H2O}*(T_{20}^2-T_0^2)/2$
 $+ D_{H2O}*(T_{20}^3-T_0^3)/3-R_{bar}*LN(P_{20}/P_0*H2O_{20}/N_{20})$
 $EX_{ph_H2O_20}=DELTAH_{H2O_20}-T_0*S_{H2O_20}$
 $EX_{ch_H2O_20}=H2O_{20}/N_{20}*(EPS_{ch_H2O}+R_{bar}*T_0*LN(H2O_{20}/N_{20}))$

"Physical and chemical exergies with flow at heat exchanger 28_20"

$EX_{20}=H2O_{20}*EX_{ph_H2O_20}+H2O_{20}*EX_{ch_H2O_20}$

"State 28"

$T_{28}=T_0;P_{28}=P_{20};H2O_{28}=H2O_{20};N_{28}=H2O_{28};M_{dot_28}=M_{dot_20}$
 $DELTAH_{H2O_28} = A_{H2O}*(T_{28}-T_0)+B_{H2O}*(T_{28}^2-T_0^2)/2 + C_{H2O}*(T_{28}^3-$
 $T_0^3)/3 + D_{H2O}*(T_{28}^4-T_0^4)/4$
 $S_{H2O_28} = A_{H2O}*(LN(T_{28})-LN(T_0))+B_{H2O}*(T_{28}-T_0)+C_{H2O}*(T_{28}^2-T_0^2)/2 +$
 $D_{H2O}*(T_{28}^3-T_0^3)/3-R_{bar}*LN(P_{28}/P_0*H2O_{28}/N_{28})$
 $EX_{ph_H2O_28}=DELTAH_{H2O_28}-T_0*S_{H2O_28}$
 $EX_{ch_H2O_28}=H2O_{28}/N_{28}*(EPS_{ch_H2O}+R_{bar}*T_0*LN(H2O_{28}/N_{28}))$
 $EX_{28}=H2O_{28}*EX_{ph_H2O_28}+H2O_{28}*EX_{ch_H2O_28}$
 $Q_{dot_28_20}=H2O_{20}*(DELTAH_{H2O_20}+DELTAHF_{H2O}*1000-DELTAH_{H2O_28}-$
 $DELTAHF_{H2O}*1000)$
 $Q_{dot_28_20}=Q_{dot_19_5}$ "To find T_20"

"Exergy destroyed in heat exchanger 19_22&28_20"

$EX_{Ir_19}=T_0*(H2_{19}*(S_{H2_19}+DELTA_{S_H2})+CO2_{19}*(S_{CO2_19}+DELTA_{S_CO2}))$
 $EX_{Ir_5}=T_0*(H2_{5}*(S_{H2_5}+DELTA_{S_H2})+CO2_{5}*(S_{CO2_5}+DELTA_{S_CO2}))$
 $EX_{Ir_HE_19_5}=EX_{Ir_19}-EX_{Ir_5}$
 $EX_{Ir_20}=T_0*(H2O_{20}*(S_{H2O_20}+DELTA_{S_H2O}))$
 $EX_{Ir_28}=T_0*(H2O_{28}*(S_{H2O_28}+DELTA_{S_H2O}))$
 $EX_{Ir_HE_28_20}=EX_{Ir_20}-EX_{Ir_28}$
 $EX_{Ir_19_5_28_20}=EX_{Ir_HE_19_5}+EX_{Ir_HE_28_20}$

"State 4"

$M_{dot_4}=M_{dot_3};H2O_4=M_{dot_4}/MW_{H2O};N_4=H2O_4$
 $T_4=500[K];P_4=120[kPa]$
 $h_4=Enthalpy(Steam,T=T_4,P=P_4)$
 $S_4=Entropy(Steam,T=T_4,P=P_4)$
 $EX_{ph_H2O_4}=h_4-T_0*S_4$
 $EX_{ch_H2O_4}=H2O_4/N_4*(EPS_{ch_H2O}+R_{bar}*T_0*LN(H2O_4/N_4))$

"Exergy at heat exchanger 4 exit"

$EX_{ph_4}=M_{dot_4}*EX_{ph_H2O_4}$
 $EX_{ch_4}=H2O_4*EX_{ch_H2O_4}$
 $EX_4=EX_{ph_4}+EX_{ch_4}$

"Compression 5-6"

"State 5"

$T_5=T_0$
 $CO2_5=CO2_{19};H2_5=H2_{19};N_5=CO2_5+H2_5;M_{dot_5}=N_5*MW_5$
 $P_5=P_{19}-0.05*P_{19}$
 $MW_5=H2_5/N_5*MW_{H2}+CO2_5/N_5*MW_{CO2}$

$$Cp_CO2_5=A_CO2+B_CO2*T_5+C_CO2*T_5^2+D_CO2*T_5^3$$

$$Cp_H2_5=A_H2+B_H2*T_5+C_H2*T_5^2+D_H2*T_5^3$$

$$Cv_CO2_5=Cp_CO2_5-R_bar$$

$$Cv_H2_5=Cp_H2_5-R_bar$$

$$Cp_5=CO2_5/N_5*Cp_CO2_5+H2_5/N_5*Cp_H2_5$$

$$Cv_5=CO2_5/N_5*Cv_CO2_5+H2_5/N_5*Cv_H2_5$$

$$Gama_gas=Cp_5/Cv_5$$

{ Calculations of delta enthalpy for carbon dioxide in kJ/kmol at steam shift exit }

$$DELTAH_CO2_5= A_CO2*(T_5-T_0)+B_CO2*(T_5^2-T_0^2)/2+C_CO2*(T_5^3-T_0^3)/3+D_CO2*(T_5^4-T_0^4)/4$$

$$S_CO2_5= A_CO2*(LN(T_5)-LN(T_0))+B_CO2*(T_5-T_0)+C_CO2*(T_5^2-T_0^2)/2 + D_CO2*(T_5^3-T_0^3)/3-R_bar*LN(P_5/P_0*CO2_5/N_5)$$

$$EX_ph_CO2_5=DELTAH_CO2_5-T_0*S_CO2_5$$

$$EX_ch_CO2_5=CO2_5/N_5*(EPS_ch_CO2+R_bar*T_0*LN(CO2_5/N_5))$$

{ Calculations of delta enthalpy for hydrogen in kJ/kmol at steam shift exit }

$$DELTAH_H2_5= A_H2*(T_5-T_0)+B_H2*(T_5^2-T_0^2)/2 + C_H2*(T_5^3-T_0^3)/3 + D_H2*(T_5^4-T_0^4)/4$$

$$S_H2_5= A_H2*(LN(T_5)-LN(T_0))+B_H2*(T_5-T_0)+C_H2*(T_5^2-T_0^2)/2 + D_H2*(T_5^3-T_0^3)/3-R_bar*LN(P_5/P_0*H2_5/N_5)$$

$$EX_ph_H2_5=DELTAH_H2_5-T_0*S_H2_5$$

$$EX_ch_H2_5=H2_5/N_5*(EPS_ch_H2+R_bar*T_0*LN(H2_5/N_5))$$

"Physical exergy and chemical exergy at 5"

$$EX_ph_5=H2_5*EX_ph_H2_5+CO2_5*EX_ph_CO2_5$$

$$EX_ch_5=H2_5*EX_ch_H2_5+CO2_5*EX_ch_CO2_5$$

$$EX_5=EX_ph_5+EX_ch_5$$

$$DELTAH_5=H2_5*DELTAH_H2_5+CO2_5*(DELTAH_CO2_5+DELTAHF_CO2*1000)$$

"State 6" Eta_c=0.8

$$CO2_6=CO2_5;H2_6=H2_5;N_6=CO2_6+H2_6;M_dot_6=M_dot_5$$

$$P_6=1.9*P_5$$

$$P_6=P_5*(1+Eta_c*(T_6/T_5-1))^(Gama_gas/(Gama_gas-1))"$$

To find T_6"

{ Calculations of delta enthalpy for carbon dioxide in kJ/kmol at steam shift exit }

$$DELTAH_CO2_6= A_CO2*(T_6-T_0)+B_CO2*(T_6^2-T_0^2)/2+C_CO2*(T_6^3-T_0^3)/3+D_CO2*(T_6^4-T_0^4)/4$$

$$S_CO2_6= A_CO2*(LN(T_6)-LN(T_0))+B_CO2*(T_6-T_0)+C_CO2*(T_6^2-T_0^2)/2 + D_CO2*(T_6^3-T_0^3)/3-R_bar*LN(P_6/P_0*CO2_6/N_6)$$

$$EX_ph_CO2_6=DELTAH_CO2_6-T_0*S_CO2_6$$

$$EX_ch_CO2_6=CO2_6/N_6*(EPS_ch_CO2+R_bar*T_0*LN(CO2_6/N_6))$$

{ Calculations of delta enthalpy for hydrogen in kJ/kmol at steam shift exit }

$$DELTAH_H2_6= A_H2*(T_6-T_0) +B_H2*(T_6^2-T_0^2)/2 + C_H2*(T_6^3-T_0^3)/3 + D_H2*(T_6^4-T_0^4)/4$$

$$S_H2_6= A_H2*(LN(T_6)-LN(T_0))+B_H2*(T_6-T_0)+C_H2*(T_6^2-T_0^2)/2 + D_H2*(T_6^3-T_0^3)/3-R_bar*LN(P_6/P_0*H2_6/N_6)$$

EX_ph_H2_6=DELTAH_H2_6-T_0*S_H2_6
EX_ch_H2_6=H2_6/N_6*(EPS_ch_H2+R_bar*T_0*LN(H2_6/N_6))

"Physical exergy and chemical exergy at compressor 5-6 exit, state 6 "

EX_ph_6=H2_6*EX_ph_H2_6+CO2_6*EX_ph_CO2_6
EX_ch_6=H2_6*EX_ch_H2_6+CO2_6*EX_ch_CO2_6
EX_6=EX_ph_6+EX_ch_6

"Enthalpy at compressor inlet"

DELTAH_6=H2_6*DELTAH_H2_6+CO2_6*(DELTAH_CO2_6+DELTAHF_CO2*1000)

"Exergy destroyed in compressor 5_6"

EX_Ir_Comp5_6_e=T_0*(H2_6*(S_H2_6+DELTA_S_H2)+CO2_6*(S_CO2_6+DELTA_S_CO2))
EX_Ir_Comp5_6_i=T_0*(H2_5*(S_H2_5+DELTA_S_H2)+CO2_5*(S_CO2_5+DELTA_S_CO2))
EX_Ir_Comp5_6=EX_Ir_Comp5_6_e-EX_Ir_Comp5_6_i+W_dot_5_6

"Work done on compressor 5-6"

W_dot_5_6=DELTAH_6-DELTAH_5

"Calculations for hydrogen line "

P_33=(P_6-0.05*P_6)*H2_6/N_6
T_33=T_6
H2_33=H2_6; M_dot_33=H2_33*MW_H2; N_33=H2_33
DELTAH_H2_33=DELTAH_H2_6
S_H2_33= A_H2*(LN(T_33)-LN(T_0))+B_H2*(T_33-T_0)+C_H2*(T_33^2-T_0^2)/2 +
D_H2*(T_33^3-T_0^3)/3-R_bar*LN(P_33/P_0*H2_33/N_33)
EX_ph_H2_33=DELTAH_H2_33-T_0*S_H2_33
EX_ch_H2_33=H2_33/N_33*(EPS_ch_H2+R_bar*T_0*LN(H2_33/N_33))
EX_33=H2_33*(EX_ph_H2_33+EX_ch_H2_33)
H2_Yield=H2_33

"Calculations for carbon dioxide line "

P_34=(P_6-0.05*P_6)*CO2_6/N_6
T_34=T_6
CO2_34=CO2_6; M_dot_34=CO2_34*MW_CO2; N_34=CO2_34
DELTAH_CO2_34=DELTAH_CO2_6
S_CO2_34= A_CO2*(LN(T_34)-LN(T_0))+B_H2*(T_34-T_0)+C_H2*(T_34^2-T_0^2)/2 +
D_H2*(T_34^3-T_0^3)/3-R_bar*LN(P_34/P_0*CO2_34/N_34)
EX_ph_CO2_34=DELTAH_CO2_34-T_0*S_CO2_34
EX_ch_CO2_34=CO2_34/N_34*(EPS_ch_CO2+R_bar*T_0*LN(CO2_34/N_34))
EX_34=CO2_34*(EX_ph_CO2_34+EX_ch_CO2_34)
CO2_Emission=CO2_34

"Efficiency calculations"

LHV_biomass=19005[kJ/kg]
LHV_H2=120000[kJ/kg]
M_dot_H2=H2_33*MW_H2
Eta_H2=LHV_H2*M_dot_H2/(LHV_biomass*M_dot_1)*100"Efficiency considers H2 only"
Eta_EX_H2=EX_33/(BETA*M_dot_1*LHV_biomass)*100"Efficiency considers H2 only"
EX_Gasifier=EX_biomass+EX_4-EX_2

BETA=1.173

$$EX_1 = M_{dot_1} * BETA * LHV_{biomass}$$

"Economic"

$$TAO = 8000 [\text{hr/yr}]; ER = 1 \{ \text{Exchange rate is one} \}$$

$$Pr = 2 * 3600 * 10^{(-6)} \text{ "Biomass price \$/kWh"}$$

$$FC_{dot_f} = Pr * LHV_{biomass} * TAO / ER \text{ "Energetic cost"}$$

$$C_{dot_1} = FC_{dot_f} / TAO * (1/BETA) \text{ "Exergetic cost"}$$

"Cost balance and auxiliary equations"

$$C_{dot_4} + C_{dot_1} + Z_{dot_Gasifier} = C_{dot_2} \text{ "Gasifier"}$$

$$Z_{dot_Gasifier} = 1.047; C_{dot_1} = c_1 * EX_{Biomass}; C_{dot_2} = c_2 * EX_2; C_{dot_4} = c_4 * EX_4$$

$$c_4 = 0.1046$$

$$Z_{OBJ_Gasifier} = Z_{dot_Gasifier} + EX_{d_gasifier} * C_2$$

$$C_{dot_2} + Z_{dot_Seperator} = C_{dot_{26}} + C_{dot_{36}} \text{ "Seperator to find } c_{26} \text{"}$$

$$Z_{dot_Seperator} = 0.083; C_{dot_{26}} = c_{26} * EX_{26}; C_{dot_{36}} = c_{36} * EX_{36}$$

$$C_{dot_2} / Ex_2 = C_{dot_{36}} / Ex_{36}$$

$$C_{dot_{36}} + C_{dot_{15}} + Z_{dot_SR} = C_{dot_{17}} \text{ "Steam reforming to find } c_{17} \text{"}$$

$$Z_{dot_SR} = 1.339; C_{dot_{15}} = c_{15} * EX_{15}; C_{dot_{17}} = c_{17} * EX_{17}$$

$$c_{15} = c_4$$

$$Z_{OBJ_SR} = Z_{dot_SR} + EX_{Ir_SR} * C_{17}$$

$$C_{dot_{17}} + C_{dot_7} + Z_{dot_HE1} = C_{dot_{18}} + C_{dot_8} \text{ "Heat exchanger I to find } c_{10}, c_{18} \text{"}$$

$$Z_{dot_HE1} = 0.748 [\$/\text{hr}]; C_{dot_{18}} = c_{18} * EX_{18}; C_{dot_7} = c_7 * EX_7; C_{dot_8} = c_8 * EX_8$$

$$C_{dot_{17}} / Ex_{17} = C_{dot_{18}} / Ex_{18}$$

$$c_7 = 0$$

$$Z_{OBJ_HE1} = Z_{dot_HE1} + EX_{Ir_{17_18_7_8}} * C_{18}$$

$$C_{dot_{18}} + C_{dot_{21}} + Z_{dot_SS} = C_{dot_{19}} \text{ "Steam shift, to find } c_{19} \text{"}$$

$$Z_{dot_SS} = 1.339 [\$/\text{s}]; C_{dot_{19}} = c_{19} * EX_{19}; C_{dot_{21}} = c_{21} * EX_{21}$$

$$c_{21} = c_4$$

$$Z_{OBJ_SS} = Z_{dot_SS} + EX_{Ir_{SS}} * C_{19}$$

$$C_{dot_{28}} + C_{dot_{19}} + Z_{dot_HE2} = C_{dot_5} + C_{dot_{20}} \text{ "Heat exchanger II"}$$

$$Z_{dot_HE2} = 0.748; C_{dot_{28}} = c_{28} * EX_{28}; C_{dot_{20}} = c_{20} * EX_{20}$$

$$C_{28} = 0; C_{20} = C_4$$

$$C_{dot_5} = c_5 * EX_5$$

$$Z_{OBJ_HE2} = Z_{dot_HE2} + EX_{Ir_{19_5_28_20}} * C_5$$

$$C_{dot_5} + C_{dot_{w_5_6}} + Z_{dot_{5_6}} = C_{dot_6} \text{ "Gas compressor 5-6 to find } c_5 \text{"}$$

$$Z_{dot_{5_6}} = 1.591 [\$/\text{s}]; C_{dot_{w_5_6}} = c_{5_6} * W_{dot_{5_6}}; C_{dot_6} = c_6 * EX_6$$

$$c_{5_6} = 0.1046$$

$$Z_{OBJ_{5_6}} = Z_{dot_{5_6}} + EX_{Ir_{COmp5_6}} * C_6$$

$$C_{dot_6} + Z_{dot_Filter1} = C_{dot_{33}} + C_{dot_{34}} \text{ "Filter 1 to find } c_{33}, c_{34} \text{"}$$

$$Z_{dot_Filter1} = 0.256; C_{dot_{33}} = c_{33} * EX_{33}; C_{dot_{34}} = c_{34} * EX_{34}$$

$$C_{dot_6} / Ex_6 = C_{dot_{33}} / Ex_{33} + C_{dot_{34}} / Ex_{34}$$

$$Z_{OBJ_Filter1} = Z_{dot_Filter1}$$

Z_OBJ=Z_OBJ_SS+Z_OBJ_HE1+Z_OBJ_HE2+Z_OBJ_SR+Z_OBJ_Filter1+Z_OBJ_5_6+Z_OBJ_
Gasifier

B2. System II

{The hybrid system includes gasifier, SOFC, steam turbine and gas turbine}

"The code performs the optimization of system II"

{The code finds mass, temperature and pressure at different states of the system II which utilises hydrogen from biomass gasification in hybrid system}

$P_0=101.325[\text{kPa}]; T_0=298[\text{k}]$

$R_{\text{bar}}=8.314[\text{kJ/kg-K}]$

{Data from biomass gasification}

$M_{\text{dot}_3}=0.27/1000*MW_{\text{H}_2\text{O}}; C_{p_{\text{H}_2\text{O}}}=4.18[\text{kJ/kg-K}]$

$M_{\text{dot}_1}=0.32/1000*99.48$

"Total hydrogen and products from gasification"

$\{N_{\text{H}_2}=1.114/1000[\text{kmol/s}]; N_{\text{CH}_4}=0.0003469/1000[\text{kmol/s}]; N_{\text{CO}}=0.7662/1000[\text{kg/s}]; N_{\text{CO}_2}=0.2062/1000[\text{kmol/s}]; N_{\text{tar}}=0.04058/1000[\text{kmol/s}]; N_{\text{char}}=0.06401/1000[\text{kmol/s}]\}$

$MW_{\text{CH}_4}=16.043; MW_{\text{CO}}=28.011; MW_{\text{CO}_2}=44.01; MW_{\text{H}_2}=2.016[\text{kg/kmol}]; MW_{\text{H}_2\text{O}}=18.015; MW_{\text{air}}=28.97[\text{kJ/kg-K}]$

$MW_{\text{O}_2}=32[\text{kg/kmol}]; MW_{\text{N}_2}=28.013[\text{kg/kmol}]; MW_{\text{tar}}=78.11[\text{kg/kmol}]; MW_{\text{char}}=12[\text{kg/kmol}]$

$C_{p_{\text{char}}}=0.708[\text{kJ/kg-K}]; C_{p_{\text{air}}}=1.004[\text{kJ/kg-K}]$

"Standard exergies for the compounds"

$EPS_{\text{ch}_{\text{H}_2}}=236100[\text{kJ/kmol}]; EPS_{\text{ch}_{\text{CO}}}=275100; EPS_{\text{ch}_{\text{CO}_2}}=19870; EPS_{\text{ch}_{\text{CH}_4}}=831650; EPS_{\text{ch}_{\text{H}_2\text{O}}}=9500[\text{kJ/kmol}]; EPS_{\text{ch}_{\text{O}_2}}=3971[\text{kJ/kmol}]; EPS_{\text{ch}_{\text{N}_2}}=720[\text{kJ/kmol}]$

$EPS_{\text{ch}_{\text{air}}}=0.21*EPS_{\text{ch}_{\text{O}_2}}+0.79*EPS_{\text{ch}_{\text{N}_2}}$

$N_{\text{H}_2\text{SOFC}}=0.0004091[\text{kmol/s}]$ "Hydrogen fed for one cell"

$N_{\text{H}_2\text{R}}=N_{\text{H}_2}*U_{\text{f}}$

$N_{\text{O}_2}=1/2*N_{\text{H}_2}$

$N_{\text{tot}}=N_{\text{H}_2}+N_{\text{CO}}+N_{\text{CO}_2}+N_{\text{CH}_4}+N_{\text{tar}}+N_{\text{char}}$

$X_{\text{H}_2}=N_{\text{H}_2}/N_{\text{tot}}*100; X_{\text{CO}}=N_{\text{CO}}/N_{\text{tot}}*100; X_{\text{CH}_4}=N_{\text{CH}_4}/N_{\text{tot}}*100; X_{\text{CO}_2}=N_{\text{CO}_2}/N_{\text{tot}}*100$

{fuel and air utilization factor}

$U_{\text{f}}=0.95; U_{\text{air}}=0.20$

{calaculate supplied air where air contains 21% O2}

$N_{\text{air}}=N_{\text{O}_2}/0.21$

{Calculations for the adiabatic burner with 100% efficiency}

{Calculations of number of moles at the burner inlet}

$T_{11}=T_{14}; T_{13}=T_{6}$ "They are given"

$\text{tar}_{26}=N_{\text{tar}}; \text{char}_{26}=N_{\text{char}}$

$\text{H}_2_{11}=(1-U_{\text{f}})*N_{\text{H}_2}; \text{O}_2_{11}=(1-$

$U_{\text{f}})*2*N_{\text{O}_2}; \text{N}_2_{11}=79/21*N_{\text{O}_2}; N_{11}=\text{H}_2_{11}+\text{O}_2_{11}+\text{N}_2_{11}$

$\text{H}_2_{13}=N_{\text{H}_2}$

$M_{\text{dot}_{13}}=\text{H}_2_{13}*MW_{\text{H}_2}$

$\text{air}_{35}=M_{\text{dot}_{35}}/MW_{\text{air}}$

$N_{\text{bi}}=\text{tar}_{26}+\text{char}_{26}+\text{H}_2_{11}+\text{O}_2_{11}+\text{N}_2_{11}+\text{air}_{35}$ "Number of moles at the burner inlet"

$P_{11}=P_{\text{SOFC}}$

{Calculations of flue gas at the burner exit}

{Calculations of enthalpy of hydrogen at the burner inlet}

$A_{\text{H}_2}=29.11; B_{\text{H}_2}=-0.1916*10^{(-2)}; C_{\text{H}_2}=0.4003*10^{(-5)}; D_{\text{H}_2}=-0.8704*10^{(-9)}; \text{DELTA}_{\text{HF}_{\text{H}_2}}=0.0; \text{DELTA}_{\text{S}_{\text{H}_2}}=130.68[\text{kJ/kmol-K}]$

$\Delta H_{H2_11} = A_{H2}*(T_{11}-T_0) + B_{H2}*(T_{11}^2-T_0^2)/2 + C_{H2}*(T_{11}^3-T_0^3)/3 + D_{H2}*(T_{11}^4-T_0^4)/4$
 $S_{H2_11} = A_{H2}*(\ln(T_{11})-\ln(T_0)) + B_{H2}*(T_{11}-T_0) + C_{H2}*(T_{11}^2-T_0^2)/2 + D_{H2}*(T_{11}^3-T_0^3)/3 - R_{bar}*\ln(P_{11}/P_0*H2_11/N_{bi})$
 $EX_{ph_H2_11} = \Delta H_{H2_11} - T_0*(S_{H2_11})$
 $EX_{ch_H2_11} = H2_11/N_{bi}*(EPS_{ch_H2} + R_{bar}*T_0*\ln(H2_11/N_{bi}))$

{ Calculations of enthalpy of oxygen at the burner inlet }

$\Delta H_{F_air} = 0$
 $A_{O2} = 25.48; B_{O2} = 1.520*10^{-2}; C_{O2} = -0.7155*10^{-5}; D_{O2} = 1.312*10^{-9}; \Delta H_{F_O2} = 0.0; \Delta S_{O2} = 205.04 [kJ/kmol-K]$
 $\Delta H_{O2_11} = A_{O2}*(T_{11}-T_0) + B_{O2}*(T_{11}^2-T_0^2)/2 + C_{O2}*(T_{11}^3-T_0^3)/3 + D_{O2}*(T_{11}^4-T_0^4)/4$
 $S_{O2_11} = A_{O2}*(\ln(T_{11})-\ln(T_0)) + B_{O2}*(T_{11}-T_0) + C_{O2}*(T_{11}^2-T_0^2)/2 + D_{O2}*(T_{11}^3-T_0^3)/3 - R_{bar}*\ln(P_{11}/P_0*O2_11/N_{bi})$
 $EX_{ph_O2_11} = \Delta H_{O2_11} - T_0*(S_{O2_11})$
 $EX_{ch_O2_11} = O2_11/N_{bi}*(EPS_{ch_O2} + R_{bar}*T_0*\ln(O2_11/N_{bi}))$

{ Calculations of enthalpy of nitrogen at the burner inlet }

$A_{N2} = 28.90; B_{N2} = -0.1571*10^{-2}; C_{N2} = 0.8081*10^{-5}; D_{N2} = -2.873*10^{-9}; \Delta H_{F_N2} = 0.0; \Delta S_{N2} = 191.61 [kJ/kmol-K]$
 $\Delta H_{N2_11} = A_{N2}*(T_{11}-T_0) + B_{N2}*(T_{11}^2-T_0^2)/2 + C_{N2}*(T_{11}^3-T_0^3)/3 + D_{N2}*(T_{11}^4-T_0^4)/4$
 $S_{N2_11} = A_{N2}*(\ln(T_{11})-\ln(T_0)) + B_{N2}*(T_{11}-T_0) + C_{N2}*(T_{11}^2-T_0^2)/2 + D_{N2}*(T_{11}^3-T_0^3)/3 - R_{bar}*\ln(P_{11}/P_0*N2_11/N_{bi})$
 $EX_{ph_N2_11} = \Delta H_{N2_11} - T_0*(S_{N2_11})$
 $EX_{ch_N2_11} = N2_11/N_{bi}*(EPS_{ch_N2} + R_{bar}*T_0*\ln(N2_11/N_{bi}))$
 $EX_{11} = H2_11*(EX_{ph_H2_11} + EX_{ch_H2_11}) + N2_11*(EX_{ph_N2_11} + EX_{ch_N2_11}) + O2_11*(EX_{ph_O2_11} + EX_{ch_O2_11})$
 $M_{dot_11} = H2_11*MW_{H2} + N2_11*MW_{N2} + O2_11*MW_{O2}$

{ Calculation of enthalpy & exergy of air at the burner inlet }

$A_{air} = 28.11; B_{air} = 0.1967*10^{-2}; C_{air} = 0.4802*10^{-5}; D_{air} = 1.966*10^{-9}; \Delta S_{air} = 1.69528/28.97 [kJ/kmol-K]$
 $\Delta H_{air_35} = A_{air}*(T_{35}-T_0) + B_{air}*(T_{35}^2-T_0^2)/2 + C_{air}*(T_{35}^3-T_0^3)/3 + D_{air}*(T_{35}^4-T_0^4)/4$
 $S_{air_35} = A_{air}*(\ln(T_{35})-\ln(T_0)) + B_{air}*(T_{35}-T_0) + C_{air}*(T_{35}^2-T_0^2)/2 + D_{air}*(T_{35}^3-T_0^3)/3 - R_{bar}*\ln(P_{35}/P_0*air_35/N_{bi})$
 $EX_{ph_air_35} = \Delta H_{air_35} - T_0*(S_{air_35})$
 $EX_{ch_air_35} = air_35/N_{bi}*(EPS_{ch_air} + R_{bar}*T_0*\ln(air_35/N_{bi}))$
 $EX_{35} = EX_{ph_air_35} + EX_{ch_air_35}$

{ Calculations of enthalpy & exergy of char at the burner inlet }

$\Delta H_{F_char} = 0$
 $P_{26} = P_{10}$
 $\Delta H_{char_26} = 4.18*(4.03*(T_{26}-T_0) + 0.00114*(T_{26}^2/2 - T_0^2/2) + 2.04*10^5*(1/T_{26} - 1/T_0))$
 $S_{char_26} = 4.18*(4.03*(\ln(T_{26})-\ln(T_0)) + 0.00114*(T_{26}-T_0) + 1.02*10^5*(1/T_{26} - 1/T_0^2)) - R_{bar}*\ln(P_{26}/P_0*char_26/N_{bi})$

$EX_{ph_char_26} = \Delta H_{char_26} - T_0 \cdot S_{char_26}$
 $EPS_{ch_char} = 410260 \text{ [kJ/kmol]}$
 $EX_{ch_char_26} = char_26 / N_{bi} \cdot (EPS_{ch_char} + R_{bar} \cdot T_0 \cdot \ln(char_26 / N_{bi}))$
 $EX_{char_26} = char_26 \cdot (EX_{ch_char_26} + EX_{ph_char_26})$

{Calculations of enthalpy & exergy of tar at the burner inlet}

$N_C = 48.01/12; N_H = 6.04; A1_{tar} = 37.1635; A2_{tar} = 31.4767; A3_{tar} = 0.564682; A4_{tar} = 20.1145; A5_{tar} = 54.3111; A6_{tar} = 44.6712; C_f = 48.0; H_f = 6.04; O_f = 45.43; N_f = 0.15; S_f = 0.05$
 $\Delta H_{tar_26} = N_C \cdot \Delta H_{f_CO2} + N_H / 2 \cdot \Delta H_{f_H2O} + (0.00422 \cdot MW_{tar} \cdot (T_{26}^2 - T_0^2) / 2 - 30.980)$
 $S_{star_26} = A1_{tar} + A2_{tar} \cdot \exp(-A3_{tar} \cdot (H_f / C_f + N_f)) + A4_{tar} \cdot (O_f / (C_f + N_f)) + A5_{tar} \cdot (N_f / (C_f + N_f)) + A6_{tar} \cdot (S_f / (C_f + N_f))$
 $S_{tar_26} = S_{star_26} + 0.00422 \cdot MW_{tar} \cdot (T_{26} - T_0) - R_{bar} \cdot \ln(P_{26} / P_0 \cdot tar_26 / N_{bi})$
 $EX_{ph_tar_26} = \Delta H_{tar_26} \cdot tar_26 - T_0 \cdot S_{tar_26} \cdot tar_26$
 $EPS_{ch_tar} = 3303600 \text{ [kJ/kmol]}$
 $X_{tar_26} = tar_26 / N_{bi}$
 $EX_{ch_tar_26} = X_{tar_26} \cdot (EPS_{ch_tar} + R_{bar} \cdot T_0 \cdot \ln(X_{tar_26}))$
 $EX_{tar_26} = EX_{ph_tar_26} + tar_26 \cdot EX_{ch_tar_26}$
 $EX_{26} = EX_{char_26} + EX_{tar_26}$
 {Chemical exergy of tar is disregarded}
 $EX_2 = EX_{26} + EX_{36}$

"Physical and chemical exergies with flow at burner inlet, states 26,11,35 "

$EX_{ph_bi} = EX_{ph_tar_26} + char_26 \cdot EX_{ph_char_26} + air_{35} \cdot EX_{ph_air_35} + N2_{11} \cdot EX_{ph_N2_11} + H2_{11} \cdot EX_{ph_H2_11} + O2_{11} \cdot EX_{ph_O2_11}$
 $EX_{ch_bi} = tar_26 \cdot EX_{ch_tar_26} + char_26 \cdot EX_{ch_char_26} + air_{35} \cdot EX_{ch_air_35} + N2_{11} \cdot EX_{ch_N2_11} + H2_{11} \cdot EX_{ch_H2_11} + O2_{11} \cdot EX_{ch_O2_11}$
 $EX_{bi} = EX_{ph_bi} + EX_{ch_bi}$

"Destruction exergy in the burner"

$EX_{Ir_burner_e} = T_0 \cdot (H2O_7 \cdot (S_{H2O_7} + \Delta S_{H2O}) + CO2_7 \cdot (S_{CO2_7} + \Delta S_{CO2}) + N2_7 \cdot (S_{N2_7} + \Delta S_{N2}) + air_7 \cdot (S_{air_7} + \Delta S_{air}))$
 $EX_{Ir_burner_i} = T_0 \cdot (H2_{11} \cdot (S_{H2_11} + \Delta S_{H2}) + O2_{11} \cdot (S_{O2_11} + \Delta S_{O2}) + N2_{11} \cdot (S_{N2_11} + \Delta S_{N2}) + air_{35} \cdot (S_{air_35} + \Delta S_{air}))$
 $EX_{Ir_burner} = EX_{Ir_burner_e} - EX_{Ir_burner_i}$

{Gas turbine calculations 7-8: exit temperature, exit pressure, gas mass flow rate}

$\eta_t = 0.80$

$A_{tar} = -36.22; B_{tar} = 48.475 \cdot 10^{(-2)}; C_{tar} = -31.57 \cdot 10^{(-5)}; D_{tar} = 77.62 \cdot 10^{(-9)}$

{Calculation of temperature of flue gas at the burner exit or at the turbine inlet}

$B_1 = tar_26 \cdot \Delta H_{tar_26} + char_26 \cdot \Delta H_{char_26} + H2_{11} \cdot \Delta H_{H2_11} + O2_{11} \cdot \Delta H_{O2_11} + N2_{11} \cdot \Delta H_{N2_11} + air_{35} \cdot \Delta H_{air_35}$

"State 7"

$H2O_7 = H2_{11} + 3 \cdot tar_26$

$CO2_7 = Char_26 + 6 \cdot tar_26$

$O2_{consumed} = Char_26 + 7.5 \cdot tar_26 + H2_{11} / 2$ "O2 consumed"

$O2_{consumed} = O2_{11} + O2_{35}$ "O2₁₁ < O2_{consumed} take more from 35"

$N2_35=O2_35*79/21$
 $air_7=air_35-N2_35-O2_35$ " Air exits turbine 7-8"
 $N2_7=N2_11$ "inert"
 $N_7=H2O_7+CO2_7+N2_7+air_7$
 $MW_7=H2O_7/N_7*MW_H2O+CO2_7/N_7*MW_CO2+N2_7/N_7*MW_N2+air_7/N_7*MW_air$
 $M_dot_7=N_7*MW_7$
 $Cp_N2_7=A_N2+B_N2*T_7+C_N2*T_7^2+D_N2*T_7^3$
 $Cp_CO2_7=A_CO2+B_CO2*T_7+C_CO2*T_7^2+D_CO2*T_7^3$
 $Cp_H2O_7=A_H2O+B_H2O*T_7+C_H2O*T_7^2+D_H2O*T_7^3$
 $Cp_air_7=A_air+B_air*T_7+C_air*T_7^2+D_air*T_7^3$
 $Cp_7=H2O_7/N_7*Cp_H2O_7+CO2_7/N_7*Cp_CO2_7+N2_7/N_7*Cp_N2_7+air_7/N_7*Cp_air_7$
 $Cv_7=Cp_7-R_bar$
 $Gama_7=Cp_7/Cv_7$

$DELTAH_CO2_7= A_CO2*(T_7-T_0)+B_CO2*(T_7^2-T_0^2)/2+C_CO2*(T_7^3-T_0^3)/3+D_CO2*(T_7^4-T_0^4)/4$
 $S_CO2_7= A_CO2*(LN(T_7)-LN(T_0))+B_CO2*(T_7-T_0)+C_CO2*(T_7^2-T_0^2)/2 + D_CO2*(T_7^3-T_0^3)/3-R_bar*LN(P_7/P_0*CO2_7/N_7)$
 $EX_ph_CO2_7=DELTAH_CO2_7-T_0*(S_CO2_7)$
 $EX_ch_CO2_7=CO2_7/N_7*(EPS_ch_CO2+R_bar*T_0*LN(CO2_7/N_7))$

$DELTAH_air_7= A_air*(T_7-T_0)+B_air*(T_7^2-T_0^2)/2+C_air*(T_7^3-T_0^3)/3+D_air*(T_7^4-T_0^4)/4$
 $S_air_7= A_air*(LN(T_7)-LN(T_0))+B_air*(T_7-T_0)+C_air*(T_7^2-T_0^2)/2 + D_air*(T_7^3-T_0^3)/3-R_bar*LN(P_7/P_0*air_7/N_7)$
 $EX_ph_air_7=DELTAH_air_7-T_0*(S_air_7)$
 $EX_ch_air_7=air_7/N_7*(EPS_ch_air+R_bar*T_0*LN(air_7/N_7))$

$DELTAH_N2_7= A_N2*(T_7-T_0)+B_N2*(T_7^2-T_0^2)/2+C_N2*(T_7^3-T_0^3)/3+D_N2*(T_7^4-T_0^4)/4$
 $S_N2_7= A_N2*(LN(T_7)-LN(T_0))+B_N2*(T_7-T_0)+C_N2*(T_7^2-T_0^2)/2 + D_N2*(T_7^3-T_0^3)/3-R_bar*LN(P_7/P_0*N2_7/N_7)$
 $EX_ph_N2_7=DELTAH_N2_7-T_0*(S_N2_7)$
 $EX_ch_N2_7=N2_7/N_7*(EPS_ch_N2+R_bar*T_0*LN(N2_7/N_7))$

$DELTAH_H2O_7= A_H2O*(T_7-T_0)+B_H2O*(T_7^2-T_0^2)/2+C_H2O*(T_7^3-T_0^3)/3+D_H2O*(T_7^4-T_0^4)/4$
 $S_H2O_7= A_H2O*(LN(T_7)-LN(T_0))+B_H2O*(T_7-T_0)+C_H2O*(T_7^2-T_0^2)/2 + D_H2O*(T_7^3-T_0^3)/3-R_bar*LN(P_7/P_0*H2O_7/N_7)$
 $EX_ph_H2O_7=DELTAH_H2O_7-T_0*(S_H2O_7)$
 $EX_ch_H2O_7=H2O_7/N_7*(EPS_ch_H2O+R_bar*T_0*LN(H2O_7/N_7))$

"Physical and chemical exergies with flow at turbine 7_8 inlet, state 7"
 $EX_ph_7=CO2_7*EX_ph_CO2_7+air_7*EX_ph_air_7+N2_7*EX_ph_N2_7+H2O_7*EX_ph_H2O_7$
 $EX_ch_7=CO2_7*EX_ch_CO2_7+air_7*EX_ch_air_7+N2_7*EX_ch_N2_7+H2O_7*EX_ch_H2O_7$
 $EX_7=EX_ph_7+EX_ch_7$

"State 8"

$T_{fg}=363[K]$; $P_{fg}=P_0+0.1$ " Assumed flue gas temperature and flue gas pressure at which will leave the system"

$T_8=T_{fg}$

$P_8=P_{fg}$ " Pressure of the flue gas at exit "

$CO2_8=CO2_7$; $air_8=air_7$; $N2_8=N2_7$; $H2O_8=H2O_7$

$N_8=N_7$; $M_{dot_8}=M_{dot_7}$

$DELTAH_{CO2_8}=A_{CO2}*(T_8-T_0)+B_{CO2}*(T_8^2-T_0^2)/2+C_{CO2}*(T_8^3-T_0^3)/3+D_{CO2}*(T_8^4-T_0^4)/4$

$S_{CO2_8}=A_{CO2}*(LN(T_8)-LN(T_0))+B_{CO2}*(T_8-T_0)+C_{CO2}*(T_8^2-T_0^2)/2+D_{CO2}*(T_8^3-T_0^3)/3-R_{bar}*LN(P_8/P_0*CO2_8/N_8)$

$EX_{ph_{CO2_8}}=DELTAH_{CO2_8}-T_0*(S_{CO2_8})$

$EX_{ch_{CO2_8}}=CO2_8/N_8*(EPS_{ch_{CO2}}+R_{bar}*T_0*LN(CO2_8/N_8))$

$DELTAH_{air_8}=A_{air}*(T_8-T_0)+B_{air}*(T_8^2-T_0^2)/2+C_{air}*(T_8^3-T_0^3)/3+D_{air}*(T_8^4-T_0^4)/4$

$S_{air_8}=A_{air}*(LN(T_8)-LN(T_0))+B_{air}*(T_8-T_0)+C_{air}*(T_8^2-T_0^2)/2+D_{air}*(T_8^3-T_0^3)/3-R_{bar}*LN(P_8/P_0*air_8/N_8)$

$EX_{ph_{air_8}}=DELTAH_{air_8}-T_0*(S_{air_8})$

$EX_{ch_{air_8}}=air_8/N_8*(EPS_{ch_{air}}+R_{bar}*T_0*LN(air_8/N_8))$

$DELTAH_{N2_8}=A_{N2}*(T_8-T_0)+B_{N2}*(T_8^2-T_0^2)/2+C_{N2}*(T_8^3-T_0^3)/3+D_{N2}*(T_8^4-T_0^4)/4$

$S_{N2_8}=A_{N2}*(LN(T_8)-LN(T_0))+B_{N2}*(T_8-T_0)+C_{N2}*(T_8^2-T_0^2)/2+D_{N2}*(T_8^3-T_0^3)/3-R_{bar}*LN(P_8/P_0*N2_8/N_8)$

$EX_{ph_{N2_8}}=DELTAH_{N2_8}-T_0*(S_{N2_8})$

$EX_{ch_{N2_8}}=N2_8/N_8*(EPS_{ch_{N2}}+R_{bar}*T_0*LN(N2_8/N_8))$

$DELTAH_{H2O_8}=A_{H2O}*(T_8-T_0)+B_{H2O}*(T_8^2-T_0^2)/2+C_{H2O}*(T_8^3-T_0^3)/3+D_{H2O}*(T_8^4-T_0^4)/4$

$S_{H2O_8}=A_{H2O}*(LN(T_8)-LN(T_0))+B_{H2O}*(T_8-T_0)+C_{H2O}*(T_8^2-T_0^2)/2+D_{H2O}*(T_8^3-T_0^3)/3-R_{bar}*LN(P_8/P_0*H2O_8/N_8)$

$EX_{ph_{H2O_8}}=DELTAH_{H2O_8}-T_0*(S_{H2O_8})$

$EX_{ch_{H2O_8}}=H2O_8/N_8*(EPS_{ch_{H2O}}+R_{bar}*T_0*LN(H2O_8/N_8))$

"Physical and chemical exergies with flow at turbine 7_8 exit"

$EX_{ph_8}=CO2_8*EX_{ph_{CO2_8}}+air_8*EX_{ph_{air_8}}+N2_8*EX_{ph_{N2_8}}+H2O_8*EX_{ph_{H2O_8}}$

$EX_{ch_8}=CO2_8*EX_{ch_{CO2_8}}+air_8*EX_{ch_{air_8}}+N2_8*EX_{ch_{N2_8}}+H2O_8*EX_{ch_{H2O_8}}$

$EX_8=0$

"Exergy destruction in turbine 7_8"

$EX_{Ir_{Tur_{7_8_e}}}=T_0*(H2O_8*(S_{H2O_8}+DELTA_{S_{H2O}})+CO2_8*(S_{CO2_8}+DELTA_{S_{CO2}})+N2_8*(S_{N2_8}+DELTA_{S_{N2}})+air_8*(S_{air_8}+DELTA_{S_{air}}))$

$EX_{Ir_{Tur_{7_8_i}}}=T_0*(H2O_7*(S_{H2O_7}+DELTA_{S_{H2O}})+CO2_7*(S_{CO2_7}+DELTA_{S_{CO2}})+N2_7*(S_{N2_7}+DELTA_{S_{N2}})+air_7*(S_{air_7}+DELTA_{S_{air}}))$

$EX_{Ir_{Tur_{7_8}}}=EX_{Ir_{Tur_{7_8_i}}}-EX_{Ir_{Tur_{7_8_e}}}$

"Enthalpy at the burner exit and turbine inlet is the same"

$$B_1 = CO2_7 * (\Delta H_{CO2_7} + \Delta H_{f,CO2} * 1000) + H2O_7 * (\Delta H_{H2O_7} + \Delta H_{f,H2O} * 1000) + air_7 * \Delta H_{air_7} + N2_7 * \Delta H_{N2_7}$$

{Calculation of temperature at gas turbine 7-8 exit}

$$B_4 = CO2_7 * (\Delta H_{CO2_8} + \Delta H_{f,CO2} * 1000) + H2O_7 * (\Delta H_{H2O_8} + \Delta H_{f,H2O} * 1000) + air_7 * \Delta H_{air_8} + N2_7 * \Delta H_{N2_8}$$

$$W_{dot_7_8} = B_1 - B_4$$

{compressor 24-25 which compresses air from ambient temperature, T₂₄ to a temperature of T₂₅ need by SOFC}

$$T_{24} = T_0; P_{24} = P_0$$

$$P_{35} = P_{10}$$

$$P_{25} = P_{35} + 0.05 * P_{35}$$

$$M_{dot_25} = M_{dot_24}; M_{dot_35} = M_{dot_25}$$

$$air_{24} = M_{dot_24} / MW_{air}; N_{24} = air_{24}$$

$$air_{25} = M_{dot_25} / MW_{air}; N_{25} = air_{25}$$

{Compressor inlet temperature, inlet pressure and exit pressure are known}

$P_{25} = P_{24} * (1 + \eta_c * (T_{25}/T_{24} - 1))^{(\gamma_{air}/(\gamma_{air} - 1))}$ to find exit compressor temperature, T₂₅"

$$\Delta H_{air_24} = A_{air} * (T_{24} - T_0) + B_{air} * (T_{24}^2 - T_0^2) / 2 + C_{air} * (T_{24}^3 - T_0^3) / 3 + D_{air} * (T_{24}^4 - T_0^4) / 4$$

$$S_{air_24} = A_{air} * (\ln(T_{24}) - \ln(T_0)) + B_{air} * (T_{24} - T_0) + C_{air} * (T_{24}^2 - T_0^2) / 2 + D_{air} * (T_{24}^3 - T_0^3) / 3 - R_{bar} * \ln(P_{24}/P_0 * air_{24}/N_{24})$$

$$EX_{ph_air_24} = \Delta H_{air_24} - T_0 * (S_{air_24})$$

$$EX_{ch_air_24} = air_{35} / N_{bi} * (\epsilon_{PS_ch_air} + R_{bar} * T_0 * \ln(air_{24}/N_{24}))$$

"physical and chemical exergies at compressor 24_25 inlet, state 24"

$$EX_{ph_24} = air_{24} * EX_{ph_air_24}$$

$$EX_{ch_24} = air_{24} * EX_{ch_air_24}$$

$$EX_{24} = EX_{ph_24} + EX_{ch_24}$$

$$\Delta H_{air_25} = A_{air} * (T_{25} - T_0) + B_{air} * (T_{25}^2 - T_0^2) / 2 + C_{air} * (T_{25}^3 - T_0^3) / 3 + D_{air} * (T_{25}^4 - T_0^4) / 4$$

$$S_{air_25} = A_{air} * (\ln(T_{25}) - \ln(T_0)) + B_{air} * (T_{25} - T_0) + C_{air} * (T_{25}^2 - T_0^2) / 2 + D_{air} * (T_{25}^3 - T_0^3) / 3 - R_{bar} * \ln(P_{25}/P_0 * air_{25}/N_{25})$$

$$EX_{ph_air_25} = \Delta H_{air_25} - T_0 * (S_{air_25})$$

$$EX_{ch_air_25} = air_{25} / N_{25} * (\epsilon_{PS_ch_air} + R_{bar} * T_0 * \ln(air_{25}/N_{25}))$$

"physical and chemical exergies at compressor 24_25 inlet, state 25"

$$EX_{ph_25} = air_{25} * EX_{ph_air_25}$$

$$EX_{ch_25} = air_{25} * EX_{ch_air_25}$$

$$EX_{25} = EX_{ph_25} + EX_{ch_25}$$

"Exergy destruction in compressor 24_25"

$$EX_{Ir_Comp24_25} = T_0 * (air_{25} * (S_{air_25} + \Delta S_{air}) - air_{24} * (S_{air_24} + \Delta S_{air}))$$

"Exergy destroyed in heat exchanger 25_35"

$$EX_{Ir_HE_25_35} = T_0 * (air_{35} * (S_{air_35} + \Delta S_{air}) - air_{25} * (S_{air_25} + \Delta S_{air}))$$

"Work of compressor 24-25"

$$W_{dot_24_25} = air_{24} * (\Delta H_{air_25} - \Delta H_{air_24})$$

$$P_{r_24_25} = P_{25} / P_{24}$$

T_35=430" Assumed"

{Heat exchanger line 25-35}

$Q_{dot_25_35} = air_{35} * (DELTAH_{air_35} - DELTAH_{air_25})$

{Heat exchanger line 36-5}

$Q_{dot_36_5} = Q_{dot_25_35}$ "To find M_dot_24"

$P_{36} = P_3; T_{36} = T_{26}$

$H2_{36} = N_{H2}; CH4_{36} = N_{CH4}; CO_{36} = N_{CO}; CO2_{36} = N_{CO2}$

$N_{36} = N_{H2} + N_{CH4} + N_{CO} + N_{CO2}$

$MW_{36} = H2_{36}/N_{36} * MW_{H2} + CH4_{36}/N_{36} * MW_{CH4} + CO_{36}/N_{36} * MW_{CO} + CO2_{36}/N_{36} * MW_{CO2}$

$M_{dot_36} = N_{36} * MW_{36}$

"Heat exchange in heat exchanger 36-5"

$Q_{dot_36_5} = DELTAH_{36} - DELTAH_5$

{Calculations for compressor 5-6 which compresses CH4, H2, CO, CO2 from gasifier temperature to steam reforming reactor temperature}

{T_5 is the temperature at which gasification takes place; T_6 is the temperature preferred to take reforming reaction place}

$T_5 = T_0 + 200$

$P_5 = P_3$ "Atmospheric gasification"

$P_6 = 1.9 * P_5$

$P_6 = P_5 * (1 + Eta_c * (T_6/T_5 - 1))^{(Gama_{gas}/(Gama_{gas} - 1))}$ "To find T_5"

$H2_5 = H2_{36}; CH4_5 = CH4_{36}; CO_5 = CO_{36}; CO2_5 = CO2_{36}$

$N_5 = N_{36}; MW_5 = MW_{36}; M_{dot_5} = M_{dot_36}$

$Cp_{CH4_5} = A_{CH4} + B_{CH4} * T_5 + C_{CH4} * T_5^2 + D_{CH4} * T_5^3$

$Cp_{CO_5} = A_{CO} + B_{CO} * T_5 + C_{CO} * T_5^2 + D_{CO} * T_5^3$

$Cp_{CO2_5} = A_{CO2} + B_{CO2} * T_5 + C_{CO2} * T_5^2 + D_{CO2} * T_5^3$

$Cp_{H2_5} = A_{H2} + B_{H2} * T_5 + C_{H2} * T_5^2 + D_{H2} * T_5^3$

$Cv_{CH4_5} = Cp_{CH4_5} - R_{bar}$

$Cv_{CO_5} = Cp_{CO_5} - R_{bar}$

$Cv_{CO2_5} = Cp_{CO2_5} - R_{bar}$

$Cv_{H2_5} = Cp_{H2_5} - R_{bar}$

$Cp_5 = CO2_5/N_5 * Cp_{CO2_5} + CO_5/N_5 * Cp_{CO_5} + CH4_5/N_5 * Cp_{CH4_5} + H2_5/N_5 * Cp_{H2_5}$

$Cv_5 = CO2_5/N_5 * Cv_{CO2_5} + CO_5/N_5 * Cv_{CO_5} + CH4_5/N_5 * Cv_{CH4_5} + H2_5/N_5 * Cv_{H2_5}$

$Gama_{gas} = Cp_5 / Cv_5$

{calculate delta enthalpy for hydrogen in kJ/kmol at heat exchanger 36-5 inlet}

$DELTAH_{H2_36} = A_{H2} * (T_{36} - T_0) + B_{H2} * (T_{36}^2 - T_0^2) / 2 + C_{H2} * (T_{36}^3 - T_0^3) / 3 + D_{H2} * (T_{36}^4 - T_0^4) / 4$

$S_{H2_36} = A_{H2} * (LN(T_{36}) - LN(T_0)) + B_{H2} * (T_{36} - T_0) + C_{H2} * (T_{36}^2 - T_0^2) / 2 + D_{H2} * (T_{36}^3 - T_0^3) / 3 - R_{bar} * LN(P_{36}/P_0 * H2_{36}/N_{36})$

$EX_{ph_H2_36} = DELTAH_{H2_36} - T_0 * (S_{H2_36})$

$$EX_ch_H2_36=H2_36/N_36*(EPS_ch_H2+R_bar*T_0*LN(H2_36/N_36))$$

{ calculate delta enthalpy for carbon monoxide in kJ/kmol at heat exchanger 36-5 inlet }

$$\begin{aligned} DELTAH_CO_36 &= A_CO*(T_36-T_0)+B_CO*(T_36^2-T_0^2)/2+C_CO*(T_36^3- \\ &T_0^3)/3+D_CO*(T_36^4-T_0^4)/4 \\ S_CO_36 &= A_CO*(LN(T_36)-LN(T_0))+B_CO*(T_36-T_0)+C_CO*(T_36^2-T_0^2)/2 + \\ &D_CO*(T_36^3-T_0^3)/3-R_bar*LN(P_36/P_0*CO_36/N_36) \\ EX_ph_CO_36 &= DELTAH_CO_36-T_0*(S_CO_36) \\ EX_ch_CO_36 &= CO_36/N_36*(EPS_ch_CO+R_bar*T_0*LN(CO_36/N_36)) \end{aligned}$$

{ Calculation of delta enthalpy for carbon dioxide in kJ/kmol at heat exchanger 36-5 inlet }

$$\begin{aligned} DELTAH_CO2_36 &= A_CO2*(T_36-T_0)+B_CO2*(T_36^2-T_0^2)/2+C_CO2*(T_36^3- \\ &T_0^3)/3+D_CO2*(T_36^4-T_0^4)/4 \\ S_CO2_36 &= A_CO2*(LN(T_36)-LN(T_0))+B_CO2*(T_36-T_0)+C_CO2*(T_36^2-T_0^2)/2 + \\ &D_CO2*(T_36^3-T_0^3)/3-R_bar*LN(P_36/P_0*CO2_36/N_36) \\ EX_ph_CO2_36 &= DELTAH_CO2_36-T_0*(S_CO2_36) \\ EX_ch_CO2_36 &= CO2_36/N_36*(EPS_ch_CO2+R_bar*T_0*LN(CO2_36/N_36)) \end{aligned}$$

{ calculate delta enthalpy for methane in kJ/kmol at heat exchanger 36-5 inlet }

$$\begin{aligned} DELTAH_CH4_36 &= A_CH4*(T_36-T_0)+B_CH4*(T_36^2-T_0^2)/2+C_CH4*(T_36^3- \\ &T_0^3)/3+D_CH4*(T_36^4-T_0^4)/4 \\ S_CH4_36 &= A_CH4*(LN(T_36)-LN(T_0))+B_CH4*(T_36-T_0)+C_CH4*(T_36^2-T_0^2)/2 + \\ &D_CH4*(T_36^3-T_0^3)/3-R_bar*LN(P_36/P_0*CH4_36/N_36) \\ EX_ph_CH4_36 &= DELTAH_CH4_36-T_0*(S_CH4_36) \\ EX_ch_CH4_36 &= CH4_36/N_36*(EPS_ch_CH4+R_bar*T_0*LN(CH4_36/N_36)) \end{aligned}$$

"Physical and chemical exergy with flow at heat exchanger 36_5 inlet"

$$\begin{aligned} EX_ph_36 &= CO_36*EX_ph_CO_36+CO2_36*EX_ph_CO2_36+H2_36*EX_ph_H2_36+CH4_36 \\ &*EX_ph_CH4_36 \\ EX_ch_36 &= CO_36*EX_ch_CO_36+CO2_36*EX_ch_CO2_36+H2_36*EX_ch_H2_36+CH4_36 \\ &*EX_ch_CH4_36 \\ EX_36 &= EX_ph_36+EX_ch_36 \end{aligned}$$

"Exergy destruction in heat exchanger 36_5"

$$\begin{aligned} EX_Ir_HE_36_5_i &= T_0*(H2_36*(S_H2_36+DELTA_S_H2)+CO_36*(S_CO_36+DELTA_S_C \\ &O)+CO2_36*(S_CO2_36+DELTA_S_CO2)+CH4_36*(S_CH4_36+DELTA_S_CH4)) \\ EX_Ir_HE_36_5_e &= T_0*(H2_5*(S_H2_5+DELTA_S_H2)+CO_5*(S_CO_5+DELTA_S_CO)+ \\ &CO2_5*(S_CO2_5+DELTA_S_CO2)+CH4_5*(S_CH4_5+DELTA_S_CH4)) \\ EX_Ir_HE_36_5 &= EX_Ir_HE_36_5_e-EX_Ir_HE_36_5_i \end{aligned}$$

"Enthalpy at heat exchanger 36-5 inlet"

$$\begin{aligned} DELTAH_36 &= H2_36*DELTAH_H2_36+CO_36*(DELTAHF_CO*1000+DELTAH_CO_36)+C \\ &O2_36*(DELTAHF_CO2*1000+DELTAH_CO2_36)+CH4_36*(DELTAHF_CH4*1000+DELTA \\ &H_CH4_36) \end{aligned}$$

{ Calculate delta enthalpy for hydrogen in kJ/kmol at heat exchanger 36-5 exit }

$$\begin{aligned} DELTAH_H2_5 &= A_H2*(T_5-T_0)+B_H2*(T_5^2-T_0^2)/2 + C_H2*(T_5^3-T_0^3)/3 + \\ &D_H2*(T_5^4-T_0^4)/4 \\ S_H2_5 &= A_H2*(LN(T_5)-LN(T_0))+B_H2*(T_5-T_0)+C_H2*(T_5^2-T_0^2)/2 + \\ &D_H2*(T_5^3-T_0^3)/3-R_bar*LN(P_5/P_0*H2_5/N_5) \end{aligned}$$

$$\begin{aligned} EX_{ph_H2_5} &= DELTAH_{H2_5} - T_0 * (S_{H2_5}) \\ EX_{ch_H2_5} &= H2_5 / N_5 * (EPS_{ch_H2} + R_{bar} * T_0 * LN(H2_5 / N_5)) \end{aligned}$$

{ Calculations of delta enthalpy for carbon monoxide in kJ/kmol at heat exchanger 36-5 exit }

$$\begin{aligned} DELTAH_{CO_5} &= A_{CO} * (T_5 - T_0) + B_{CO} * (T_5^2 - T_0^2) / 2 + C_{CO} * (T_5^3 - T_0^3) / 3 + D_{CO} * (T_5^4 - T_0^4) / 4 \\ S_{CO_5} &= A_{CO} * (LN(T_5) - LN(T_0)) + B_{CO} * (T_5 - T_0) + C_{CO} * (T_5^2 - T_0^2) / 2 + D_{CO} * (T_5^3 - T_0^3) / 3 - R_{bar} * LN(P_5 / P_0 * CO_5 / N_5) \\ EX_{ph_CO_5} &= DELTAH_{CO_5} - T_0 * (S_{CO_5}) \\ EX_{ch_CO_5} &= CO_5 / N_5 * (EPS_{ch_CO} + R_{bar} * T_0 * LN(CO_5 / N_5)) \end{aligned}$$

{ Calculations of delta enthalpy for carbon dioxide in kJ/kmol at heat exchanger 36-5 exit }

$$\begin{aligned} DELTAH_{CO2_5} &= A_{CO2} * (T_5 - T_0) + B_{CO2} * (T_5^2 - T_0^2) / 2 + C_{CO2} * (T_5^3 - T_0^3) / 3 + D_{CO2} * (T_5^4 - T_0^4) / 4 \\ S_{CO2_5} &= A_{CO2} * (LN(T_5) - LN(T_0)) + B_{CO2} * (T_5 - T_0) + C_{CO2} * (T_5^2 - T_0^2) / 2 + D_{CO2} * (T_5^3 - T_0^3) / 3 - R_{bar} * LN(P_5 / P_0 * CO2_5 / N_5) \\ EX_{ph_CO2_5} &= DELTAH_{CO2_5} - T_0 * (S_{CO2_5}) \\ EX_{ch_CO2_5} &= CO2_5 / N_5 * (EPS_{ch_CO2} + R_{bar} * T_0 * LN(CO2_5 / N_5)) \end{aligned}$$

{ Calculations delta enthalpy for methane in kJ/kmol at heat exchanger 36-5 exit }

$$\begin{aligned} DELTAH_{CH4_5} &= A_{CH4} * (T_5 - T_0) + B_{CH4} * (T_5^2 - T_0^2) / 2 + C_{CH4} * (T_5^3 - T_0^3) / 3 + D_{CH4} * (T_5^4 - T_0^4) / 4 \\ S_{CH4_5} &= A_{CH4} * (LN(T_5) - LN(T_0)) + B_{CH4} * (T_5 - T_0) + C_{CH4} * (T_5^2 - T_0^2) / 2 + D_{CH4} * (T_5^3 - T_0^3) / 3 - R_{bar} * LN(P_5 / P_0 * CH4_5 / N_5) \\ EX_{ph_CH4_5} &= DELTAH_{CH4_5} - T_0 * (S_{CH4_5}) \\ EX_{ch_CH4_5} &= CH4_5 / N_5 * (EPS_{ch_CH4} + R_{bar} * T_0 * LN(CH4_5 / N_5)) \end{aligned}$$

"Physical and chemical exergy at compressor 5-6 inlet, state 5"

$$\begin{aligned} EX_{ph_5} &= CO_5 * EX_{ph_CO_5} + CO2_5 * EX_{ph_CO2_5} + H2_5 * EX_{ph_H2_5} + CH4_5 * EX_{ph_CH4_5} \\ EX_{ch_5} &= CO_5 * EX_{ch_CO_5} + CO2_5 * EX_{ch_CO2_5} + H2_5 * EX_{ch_H2_5} + CH4_5 * EX_{ch_CH4_5} \\ EX_5 &= EX_{ph_5} + EX_{ch_5} \end{aligned}$$

"Enthalpy at heat exchanger 36-5 exit or compressor inlet"

$$\begin{aligned} DELTAH_5 &= H2_5 * DELTAH_{H2_5} + CO_5 * (DELTAHF_{CO} * 1000 + DELTAH_{CO_5}) + CO2_5 * (DELTAHF_{CO2} * 1000 + DELTAH_{CO2_5}) + CH4_5 * (DELTAHF_{CH4} * 1000 + DELTAH_{CH4_5}) \end{aligned}$$

"State 6"

$$\begin{aligned} H2_6 &= H2_5; CO_6 = CO_5; CO2_6 = CO2_5; CH4_6 = CH4_5 \\ N_6 &= H2_6 + CO_6 + CO2_6 + CH4_6 \\ M_{dot_6} &= H2_6 * MW_{H2} + CO_6 * MW_{CO} + CO2_6 * MW_{CO2} + CH4_6 * MW_{CH4} \end{aligned}$$

{ Calculations of delta enthalpy for hydrogen in kJ/kmol at compressor 5-6 exit }

$$\begin{aligned} DELTAH_{H2_6} &= A_{H2} * (T_6 - T_0) + B_{H2} * (T_6^2 - T_0^2) / 2 + C_{H2} * (T_6^3 - T_0^3) / 3 + D_{H2} * (T_6^4 - T_0^4) / 4 \\ S_{H2_6} &= A_{H2} * (LN(T_6) - LN(T_0)) + B_{H2} * (T_6 - T_0) + C_{H2} * (T_6^2 - T_0^2) / 2 + D_{H2} * (T_6^3 - T_0^3) / 3 - R_{bar} * LN(P_6 / P_0 * H2_6 / N_6) \\ EX_{ph_H2_6} &= DELTAH_{H2_6} - T_0 * (S_{H2_6}) \\ EX_{ch_H2_6} &= H2_6 / N_6 * (EPS_{ch_H2} + R_{bar} * T_0 * LN(H2_6 / N_6)) \end{aligned}$$

{ Calculations of delta enthalpy for carbon monoxide in kJ/kmol at compressor 5-6 exit }

$$\text{DELTAH_CO_6} = A_CO*(T_6-T_0)+B_CO*(T_6^2-T_0^2)/2+C_CO*(T_6^3-T_0^3)/3+D_CO*(T_6^4-T_0^4)/4$$

$$S_CO_6 = A_CO*(\text{LN}(T_6)-\text{LN}(T_0))+B_CO*(T_6-T_0)+C_CO*(T_6^2-T_0^2)/2 + D_CO*(T_6^3-T_0^3)/3-R_bar*\text{LN}(P_6/P_0*CO_6/N_6)$$

$$\text{EX_ph_CO_6} = \text{DELTAH_CO_6}-T_0*(S_CO_6)$$

$$\text{EX_ch_CO_6} = CO_6/N_6*(\text{EPS_ch_CO}+R_bar*T_0*\text{LN}(CO_6/N_6))$$

{ Calculations of delta enthalpy for carbon dioxide in kJ/kmol at compressor 5-6 exit }

$$\text{DELTAH_CO2_6} = A_CO2*(T_6-T_0)+B_CO2*(T_6^2-T_0^2)/2+C_CO2*(T_6^3-T_0^3)/3+D_CO2*(T_6^4-T_0^4)/4$$

$$S_CO2_6 = A_CO2*(\text{LN}(T_6)-\text{LN}(T_0))+B_CO2*(T_6-T_0)+C_CO2*(T_6^2-T_0^2)/2 + D_CO2*(T_6^3-T_0^3)/3-R_bar*\text{LN}(P_6/P_0*CO2_6/N_6)$$

$$\text{EX_ph_CO2_6} = \text{DELTAH_CO2_6}-T_0*(S_CO2_6)$$

$$\text{EX_ch_CO2_6} = CO2_6/N_6*(\text{EPS_ch_CO2}+R_bar*T_0*\text{LN}(CO2_6/N_6))$$

{ Calculations of delta enthalpy for methane in kJ/kmol at compressor 5-6 exit }

$$\text{DELTAH_CH4_6} = A_CH4*(T_6-T_0)+B_CH4*(T_6^2-T_0^2)/2+C_CH4*(T_6^3-T_0^3)/3+D_CH4*(T_6^4-T_0^4)/4$$

$$S_CH4_6 = A_CH4*(\text{LN}(T_6)-\text{LN}(T_0))+B_CH4*(T_6-T_0)+C_CH4*(T_6^2-T_0^2)/2 + D_CH4*(T_6^3-T_0^3)/3-R_bar*\text{LN}(P_6/P_0*CH4_6/N_6)$$

$$\text{EX_ph_CH4_6} = \text{DELTAH_CH4_6}-T_0*(S_CH4_6)$$

$$\text{EX_ch_CH4_6} = CH4_6/N_6*(\text{EPS_ch_CH4}+R_bar*T_0*\text{LN}(CH4_6/N_6))$$

"Physical and chemical exergy at compressor 5-6 exit, state 6"

$$\text{EX_ph_6} = CO_6*\text{EX_ph_CO_6}+CO2_6*\text{EX_ph_CO2_6}+H2_6*\text{EX_ph_H2_6}+CH4_6*\text{EX_ph_CH4_6}$$

$$\text{EX_ch_6} = CO_6*\text{EX_ch_CO_6}+CO2_6*\text{EX_ch_CO2_6}+H2_6*\text{EX_ch_H2_6}+CH4_6*\text{EX_ch_CH4_6}$$

$$\text{EX_6} = \text{EX_ph_6}+\text{EX_ch_6}$$

"Exergy destruction in compressor 5_6"

$$\text{EX_Ir_Comp5_6_e} = T_0*(H2_6*(S_H2_6+\text{DELTA_S_H2})+CO_6*(S_CO_6+\text{DELTA_S_CO})+CO2_6*(S_CO2_6+\text{DELTA_S_CO2})+CH4_6*(S_CH4_6+\text{DELTA_S_CH4}))$$

$$\text{EX_Ir_Comp5_6_i} = T_0*(H2_5*(S_H2_5+\text{DELTA_S_H2})+CO_5*(S_CO_5+\text{DELTA_S_CO})+CO2_5*(S_CO2_5+\text{DELTA_S_CO2})+CH4_5*(S_CH4_5+\text{DELTA_S_CH4}))$$

$$\text{EX_Ir_Comp5_6} = \text{EX_Ir_Comp5_6_e}-\text{EX_Ir_Comp5_6_i}$$

"Enthalpy at heat exchanger 36-5 exit or compressor inlet"

$$\text{DELTAH_6} = H2_6*\text{DELTAH_H2_6}+CO_6*(\text{DELTAHF_CO}*1000+\text{DELTAH_CO_6})+CO2_6*(\text{DELTAHF_CO2}*1000+\text{DELTAH_CO2_6})+CH4_6*(\text{DELTAHF_CH4}*1000+\text{DELTAH_CH4_6})$$

"Work done on compressor 5-6"

$$W_dot_5_6 = (\text{DELTAH_6}-\text{DELTAH_5})$$

"Total number of moles at steam reforming inlet"

$$N_SRi = CH4_16+CO_16+CO2_16+H2O_15$$

"State 16"

CH4_16=N_CH4; CO_16=N_CO; CO2_16=N_CO2; H2O_15=N_CH4" Molar flow from gasification process"

$T_{16}=T_6$
 $P_{16}=P_{13}$
 $N_{16}=\text{CH}_4_{16}+\text{CO}_{16}+\text{CO}_2_{16}$ "All primary hydrogen is sent to SOFC"
 $M_{\text{dot}}_{16}=\text{CH}_4_{16}*\text{MW}_{\text{CH}_4}+\text{CO}_{16}*\text{MW}_{\text{CO}}+\text{CO}_2_{16}*\text{MW}_{\text{CO}_2}$

{Calculations of delta enthalpy for carbon monoxide at steam reformer inlet}
 $A_{\text{CO}}=28.16$; $B_{\text{CO}}=0.1675*10^{(-2)}$; $C_{\text{CO}}=0.5372*10^{(-5)}$; $D_{\text{CO}}=-2.222*10^{(-9)}$; $\text{DELTAHF}_{\text{CO}}=-110.53[\text{kJ/mol}]$; $\text{DELTA}_{\text{S}_{\text{CO}}}=197.65[\text{kJ/kmol-K}]$
 $\text{DELTAH}_{\text{CO}}_{16}=A_{\text{CO}}*(T_{16}-T_0)+B_{\text{CO}}*(T_{16}^2-T_0^2)/2+C_{\text{CO}}*(T_{16}^3-T_0^3)/3+D_{\text{CO}}*(T_{16}^4-T_0^4)/4$
 $S_{\text{CO}}_{16}=A_{\text{CO}}*(\text{LN}(T_{16})-\text{LN}(T_0))+B_{\text{CO}}*(T_{16}-T_0)+C_{\text{CO}}*(T_{16}^2-T_0^2)/2+D_{\text{CO}}*(T_{16}^3-T_0^3)/3-R_{\text{bar}}*\text{LN}(P_{16}/P_0*\text{CO}_{16}/N_{\text{SRi}})$
 $\text{EX}_{\text{ph}_{\text{CO}}}_{16}=\text{DELTAH}_{\text{CO}}_{16}-T_0*(S_{\text{CO}}_{16})$
 $\text{EX}_{\text{ch}_{\text{CO}}}_{16}=\text{CO}_{16}/N_{\text{SRi}}*(\text{EPS}_{\text{ch}_{\text{CO}}}+R_{\text{bar}}*T_0*\text{LN}(\text{CO}_{16}/N_{\text{SRi}}))$

{Calculations of delta enthalpy for carbon dioxide at steam reformer inlet}
 $A_{\text{CO}_2}=22.26$; $B_{\text{CO}_2}=5.981*10^{(-2)}$; $C_{\text{CO}_2}=-3.501*10^{(-5)}$; $D_{\text{CO}_2}=-7.469*10^{(-9)}$; $\text{DELTAHF}_{\text{CO}_2}=-393.52[\text{kJ/mol}]$; $\text{DELTA}_{\text{S}_{\text{CO}_2}}=213.8[\text{kJ/kmol-K}]$
 $\text{DELTAH}_{\text{CO}_2}_{16}=A_{\text{CO}_2}*(T_{16}-T_0)+B_{\text{CO}_2}*(T_{16}^2-T_0^2)/2+C_{\text{CO}_2}*(T_{16}^3-T_0^3)/3+D_{\text{CO}_2}*(T_{16}^4-T_0^4)/4$
 $S_{\text{CO}_2}_{16}=A_{\text{CO}_2}*(\text{LN}(T_{16})-\text{LN}(T_0))+B_{\text{CO}_2}*(T_{16}-T_0)+C_{\text{CO}_2}*(T_{16}^2-T_0^2)/2+D_{\text{CO}_2}*(T_{16}^3-T_0^3)/3-R_{\text{bar}}*\text{LN}(P_{16}/P_0*\text{CO}_2_{16}/N_{\text{SRi}})$
 $\text{EX}_{\text{ph}_{\text{CO}_2}_{16}}=\text{DELTAH}_{\text{CO}_2}_{16}-T_0*(S_{\text{CO}_2}_{16})$
 $\text{EX}_{\text{ch}_{\text{CO}_2}_{16}}=\text{CO}_2_{16}/N_{\text{SRi}}*(\text{EPS}_{\text{ch}_{\text{CO}_2}}+R_{\text{bar}}*T_0*\text{LN}(\text{CO}_2_{16}/N_{\text{SRi}}))$

{Calculations of delta enthalpy for methane in kJ/kmol at steam reforming inlet}
 $A_{\text{CH}_4}=19.89$; $B_{\text{CH}_4}=5.204*10^{(-2)}$; $C_{\text{CH}_4}=1.269*10^{(-5)}$; $D_{\text{CH}_4}=-11.01*10^{(-9)}$; $\text{DELTAHF}_{\text{CH}_4}=-74.8[\text{kJ/mol}]$; $\text{DELTA}_{\text{S}_{\text{CH}_4}}=186.16[\text{kJ/kmol-K}]$
 $\text{DELTAH}_{\text{CH}_4}_{16}=A_{\text{CH}_4}*(T_{16}-T_0)+B_{\text{CH}_4}*(T_{16}^2-T_0^2)/2+C_{\text{CH}_4}*(T_{16}^3-T_0^3)/3+D_{\text{CH}_4}*(T_{16}^4-T_0^4)/4$
 $S_{\text{CH}_4}_{16}=A_{\text{CH}_4}*(\text{LN}(T_{16})-\text{LN}(T_0))+B_{\text{CH}_4}*(T_{16}-T_0)+C_{\text{CH}_4}*(T_{16}^2-T_0^2)/2+D_{\text{CH}_4}*(T_{16}^3-T_0^3)/3-R_{\text{bar}}*\text{LN}(P_{16}/P_0*\text{CH}_4_{16}/N_{\text{SRi}})$
 $\text{EX}_{\text{ph}_{\text{CH}_4}_{16}}=\text{DELTAH}_{\text{CH}_4}_{16}-T_0*(S_{\text{CH}_4}_{16})$
 $\text{EX}_{\text{ch}_{\text{CH}_4}_{16}}=\text{CH}_4_{16}/N_{\text{SRi}}*(\text{EPS}_{\text{ch}_{\text{CH}_4}}+R_{\text{bar}}*T_0*\text{LN}(\text{CH}_4_{16}/N_{\text{SRi}}))$

"State 15"

$T_{15}=T_{14}$ "Temperature of by product water same as SOFC temperature"
 $P_{15}=P_{14}$ "pressure of by product water same as SOFC pressure"
 $N_{15}=\text{H}_2\text{O}_{15}$ "Steam consumed by steam reforming reaction"
 $M_{\text{dot}}_{15}=\text{H}_2\text{O}_{15}*\text{MW}_{\text{H}_2\text{O}}$

{Calculations of delta enthalpy for water in kJ/ kmol at steam reforming inlet}
 $A_{\text{H}_2\text{O}}=32.24$; $B_{\text{H}_2\text{O}}=0.1923*10^{(-2)}$; $C_{\text{H}_2\text{O}}=1.055*10^{(-5)}$; $D_{\text{H}_2\text{O}}=-3.595*10^{(-9)}$; $\text{DELTAHF}_{\text{H}_2\text{O}}=-241.83[\text{kJ/mol}]$; $\text{DELTA}_{\text{S}_{\text{H}_2\text{O}}}=188.83[\text{kJ/kmol-K}]$
 $\text{DELTAH}_{\text{H}_2\text{O}}_{15}=A_{\text{H}_2\text{O}}*(T_{15}-T_0)+B_{\text{H}_2\text{O}}*(T_{15}^2-T_0^2)/2+C_{\text{H}_2\text{O}}*(T_{15}^3-T_0^3)/3+D_{\text{H}_2\text{O}}*(T_{15}^4-T_0^4)/4$
 $S_{\text{H}_2\text{O}}_{15}=A_{\text{H}_2\text{O}}*(\text{LN}(T_{15})-\text{LN}(T_0))+B_{\text{H}_2\text{O}}*(T_{15}-T_0)+C_{\text{H}_2\text{O}}*(T_{15}^2-T_0^2)/2+D_{\text{H}_2\text{O}}*(T_{15}^3-T_0^3)/3$
 $\text{EX}_{\text{ph}_{\text{H}_2\text{O}}}_{15}=\text{DELTAH}_{\text{H}_2\text{O}}_{15}-T_0*(S_{\text{H}_2\text{O}}_{15})$
 $\text{EX}_{\text{ch}_{\text{H}_2\text{O}}}_{15}=\text{H}_2\text{O}_{15}/N_{\text{SRi}}*(\text{EPS}_{\text{ch}_{\text{H}_2\text{O}}}+R_{\text{bar}}*T_0*\text{LN}(\text{H}_2\text{O}_{15}/N_{\text{SRi}}))$

"Physical and chemical exergy with flow at SRi"

$$EX_ph_SRi=CO_16*EX_ph_CO_16+CO2_16*EX_ph_CO2_16+CH4_16*EX_ph_CH4_16+H2O_15*EX_ph_H2O_15$$

$$EX_ch_SRi=CO_16*EX_ch_CO_16+CO2_16*EX_ch_CO2_16+CH4_16*EX_ch_CH4_16+H2O_15*EX_ch_H2O_15$$

$$EX_SRi=EX_ph_SRi+EX_ch_SRi$$

$$EX_16=CO_16*(EX_ph_CO_16+EX_ch_CO_16)+CO2_16*(EX_ph_CO2_16+EX_ch_CO2_16)+CH4_16*(EX_ph_CH4_16+EX_ch_CH4_16)$$

$$EX_15=H2O_15*(EX_ph_H2O_15+EX_ch_H2O_15)$$

"State 17"

$$P_17=P_16-0.05*P_16$$

$$CO_17=CH4_16+N_CO; CO2_17=CO2_16; H2_17=3*CH4_16$$

$$N_17=H2_17+CO_17+CO2_17$$

$$MW_17=H2_17/N_17*MW_H2+CO_17/N_17*MW_CO+CO2_17/N_17*MW_CO2$$

$$M_dot_17=N_17*MW_17$$

$$N_SRe=N_17$$

{Calculations of delta enthalpy for hydrogen in kJ/kmol at steam reforming exit}

$$DELTAH_H2_17= A_H2*(T_17-T_0)+B_H2*(T_17^2-T_0^2)/2 + C_H2*(T_17^3-T_0^3)/3 + D_H2*(T_17^4-T_0^4)/4$$

$$S_H2_17= A_H2*(LN(T_17)-LN(T_0))+B_H2*(T_17-T_0)+C_H2*(T_17^2-T_0^2)/2 + D_H2*(T_17^3-T_0^3)/3-R_bar*LN(P_17/P_0*H2_17/N_SRe)$$

$$EX_ph_H2_17=DELTAH_H2_17-T_0*(S_H2_17)$$

$$EX_ch_H2_17=H2_17/N_17*(EPS_ch_H2+R_bar*T_0*LN(H2_17/N_SRe))$$

{Calculations of delta enthalpy for carbon monoxide in kJ/kmol at steam reforming exit}

$$DELTAH_CO_17= A_CO*(T_17-T_0)+B_CO*(T_17^2-T_0^2)/2+C_CO*(T_17^3-T_0^3)/3+D_CO*(T_17^4-T_0^4)/4$$

$$S_CO_17= A_CO*(LN(T_17)-LN(T_0))+B_CO*(T_17-T_0)+C_CO*(T_17^2-T_0^2)/2 + D_CO*(T_17^3-T_0^3)/3-R_bar*LN(P_17/P_0*CO_17/N_SRe)$$

$$EX_ph_CO_17=DELTAH_CO_17-T_0*(S_CO_17)$$

$$EX_ch_CO_17=CO_17/N_17*(EPS_ch_CO+R_bar*T_0*LN(CO_17/N_SRe))$$

{Calculations of delta enthalpy for carbon dioxide in kJ/kmol at steam reforming exit}

$$DELTAH_CO2_17= A_CO2*(T_17-T_0)+B_CO2*(T_17^2-T_0^2)/2+C_CO2*(T_17^3-T_0^3)/3+D_CO2*(T_17^4-T_0^4)/4$$

$$S_CO2_17= A_CO2*(LN(T_17)-LN(T_0))+B_CO2*(T_17-T_0)+C_CO2*(T_17^2-T_0^2)/2 + D_CO2*(T_17^3-T_0^3)/3-R_bar*LN(P_17/P_0*CO2_17/N_SRe)$$

$$EX_ph_CO2_17=DELTAH_CO2_17-T_0*(S_CO2_17)$$

$$EX_ch_CO2_17=CO2_17/N_17*(EPS_ch_CO2+R_bar*T_0*LN(CO2_17/N_SRe))$$

"Physical and chemical exergies with flow at SRe"

$$EX_ph_SRe=CO_17*EX_ph_CO_17+CO2_17*EX_ph_CO2_17+H2_17*EX_ph_H2_17$$

$$EX_ch_SRe=CO_17*EX_ch_CO_17+CO2_17*EX_ch_CO2_17+H2_17*EX_ch_H2_17$$

$$EX_SRe=EX_ph_SRe+EX_ch_SRe$$

"Exergy destruction in SR"

$EX_{Ir_SR2}=T_0*(H2_{17}*(S_{H2_17}+DELTA_S_{H2})+CO2_{17}*(S_{CO2_17}+DELTA_S_{CO2})+CO_{17}*(S_{CO_17}+DELTA_S_{CO}))$
 $EX_{Ir_SR1}=T_0*(CH4_{16}*(S_{CH4_16}+DELTA_S_{CH4})+CO2_{16}*(S_{CO2_16}+DELTA_S_{CO2})+CO_{16}*(S_{CO_16}+DELTA_S_{CO})+H2O_{15}*(S_{H2O_15}+DELTA_S_{H2O}))$
 $EX_{Ir_SR}=EX_{Ir_SR2}-EX_{Ir_SR1}$

{Energy balance to find T₁₇}
 $SR_A=CH4_{16}*(DELTAHF_{CH4}*1000+DELTAH_{CH4_16})+CO2_{16}*(DELTAHF_{CO2}*1000+DELTAH_{CO2_16})$
 $SR_B=CO_{16}*(DELTAHF_{CO}*1000+DELTAH_{CO_16})+H2O_{15}*(DELTAHF_{H2O}*1000+DELTAH_{H2O_15})$
 $SR_1=SR_A+SR_B$
 $SR_2=H2_{17}*DELTAH_{H2_17}+CO_{17}*(DELTAHF_{CO}*1000+DELTAH_{CO_17})+CO2_{17}*(DELTAHF_{CO2}*1000+DELTAH_{CO2_17})$
 $SR_2=SR_1$ "From which will find exit temperature from steam reformer, T₁₇"

{Calculations for heat exchanger 17-18}
 "State 18"
 $P_{18}=P_{17}-P_{17}*0.05$ "Pressure of flow gas is given in terms of mole fraction"
 $T_{18}=T_0$ "Assumed exit temperature preferred to met gas shift reaction in the next step"
 $N_{18}=N_{17}$
 $M_{dot_18}=M_{dot_17}$
 $DELTAH_{18}=H2_{18}*DELTAH_{H2_18}+CO_{18}*(DELTAHF_{CO}*1000+DELTAH_{CO_18})+CO2_{18}*(DELTAHF_{CO2}*1000+DELTAH_{CO2_18})$
 $DELTAH_{17}=H2_{17}*DELTAH_{H2_17}+CO_{17}*(DELTAHF_{CO}*1000+DELTAH_{CO_17})+CO2_{17}*(DELTAHF_{CO2}*1000+DELTAH_{CO2_17})$

"Heat need to be extracted before gas shift reaction"
 $Q_{dot_17_18}=(DELTAH_{17}-DELTAH_{18})$

{Calculations for air preheating}
 $Gama_air=1.4$; $Eta_c=0.80$
 $T_{SOFC}=1000$ [K]"SOFC temperature"
 $P_{SOFC}=120$ [kPa]"SOFC pressure"
 $P_{10}=P_{SOFC}$
 $M_{dot_10}=N_{air}*MW_{air}$

"Compressor 0-9"
 $P_9=P_{10}$
 $P_9=P_0*(1+Eta_c*(T_9/T_0-1))^{(Gama_air/(Gama_air-1))}$
 $air_9=N_{air}$; $N_9=air_9$
 $DELTAH_{air_9}=A_{air}*(T_9-T_0)+B_{air}*(T_9^2-T_0^2)/2+C_{air}*(T_9^3-T_0^3)/3+D_{air}*(T_9^4-T_0^4)/4$
 $S_{air_9}=A_{air}*(LN(T_9)-LN(T_0))+B_{air}*(T_9-T_0)+C_{air}*(T_9^2-T_0^2)/2+D_{air}*(T_9^3-T_0^3)/3-R_{bar}*LN(P_9/P_0*air_9/N_9)$
 $EX_{ph_air_9}=DELTAH_{air_9}-T_0*(S_{air_9})$
 $EX_{ch_air_9}=air_9/N_9*(EPS_{ch_air}+R_{bar}*T_0*LN(air_9/N_9))$
 $h_{air_9}=A_{air}*T_9+B_{air}*T_9^2/2+C_{air}*T_9^3/3+D_{air}*T_9^4/4$
 "Physical and chemical exergy at compressor 0-9 exit"

$EX_{ph_9} = air_9 * EX_{ph_air_9}$
 $EX_{ch_9} = air_9 * EX_{ch_air_9}$
 $EX_9 = EX_{ph_9} + EX_{ch_9}$
 $air_0 = N_{air}; N_0 = air_0$
 $DELTAH_{air_0} = A_{air} * (T_0 - T_0) + B_{air} * (T_0^2 - T_0^2) / 2 + C_{air} * (T_0^3 - T_0^3) / 3 + D_{air} * (T_0^4 - T_0^4) / 4$
 $S_{air_0} = A_{air} * (LN(T_0) - LN(T_0)) + B_{air} * (T_0 - T_0) + C_{air} * (T_0^2 - T_0^2) / 2 + D_{air} * (T_0^3 - T_0^3) / 3 - R_{bar} * LN(P_0 / P_0 * air_0 / N_0)$
 $EX_{ph_air_0} = DELTAH_{air_0} - T_0 * (S_{air_0})$
 $EX_{ch_air_0} = air_0 / N_0 * (EPS_{ch_air} + R_{bar} * T_0 * LN(air_0 / N_0))$
 "Physical and chemical exergy at compressor 0-9 inlet"
 $EX_{ph_0} = air_0 * EX_{ph_air_0}$
 $EX_{ch_0} = air_0 * EX_{ch_air_0}$
 $EX_0 = EX_{ph_0} + EX_{ch_0}$
 "Exergy destruction in compressor 0-9"
 $EX_{Ir_COmp_0_9} = T_0 * (air_9 * (S_{air_9} + DELTA_{S_air}) - air_0 * (S_{air_0} + DELTA_{S_air}))$
 $W_{dot_0_9} = M_{dot_9} * Cp_{air} * (T_9 - T_0)$ "Work rate done on compressor 0-9"
 $M_{dot_9} = M_{dot_10}$
 $air_{10} = N_{air}; N_{10} = air_{10}$ "Air is that need for electrochemical reaction"
 $Q_{dot_9_10} = M_{dot_10} * Cp_{air} * (T_{10} - T_9)$
 $Q_{dot_17_18} = Q_{dot_9_10}$ "To find T_{10} , Temperature of the preheating air"

"Calculations for SOFC"

$N_{SOFCi} = air_{10} + H2_{13}$
 $N_{SOFCe} = H2O_{14} + H2_{11} + O2_{11} + N2_{11}$

"State 10"

$DELTAH_{air_10} = A_{air} * (T_{10} - T_0) + B_{air} * (T_{10}^2 - T_0^2) / 2 + C_{air} * (T_{10}^3 - T_0^3) / 3 + D_{air} * (T_{10}^4 - T_0^4) / 4$
 $S_{air_10} = A_{air} * (LN(T_{10}) - LN(T_0)) + B_{air} * (T_{10} - T_0) + C_{air} * (T_{10}^2 - T_0^2) / 2 + D_{air} * (T_{10}^3 - T_0^3) / 3 - R_{bar} * LN(P_{10} / P_0 * air_{10} / N_{SOFCi})$
 $EX_{ph_air_10} = DELTAH_{air_10} - T_0 * (S_{air_10})$
 $EX_{ch_air_10} = air_{10} / N_{SOFCi} * (EPS_{ch_air} + R_{bar} * T_0 * LN(air_{10} / N_{SOFCi}))$
 $EX_{10} = air_{10} * (EX_{ph_air_10} + EX_{ch_air_10})$
 $h_{air_10} = A_{air} * T_{10} + B_{air} * T_{10}^2 / 2 + C_{air} * T_{10}^3 / 3 + D_{air} * T_{10}^4 / 4$

"State 13"

$P_{13} = P_{10} + 0.05 * P_{10}$
 $DELTAH_{H2_13} = A_{H2} * (T_{13} - T_0) + B_{H2} * (T_{13}^2 - T_0^2) / 2 + C_{H2} * (T_{13}^3 - T_0^3) / 3 + D_{H2} * (T_{13}^4 - T_0^4) / 4$
 $S_{H2_13} = A_{H2} * (LN(T_{13}) - LN(T_0)) + B_{H2} * (T_{13} - T_0) + C_{H2} * (T_{13}^2 - T_0^2) / 2 + D_{H2} * (T_{13}^3 - T_0^3) / 3 - R_{bar} * LN(P_{13} / P_0 * H2_{13} / N_{SOFCi})$
 $EX_{ph_H2_13} = DELTAH_{H2_13} - T_0 * (S_{H2_13})$
 $EX_{ch_H2_13} = H2_{13} / N_{SOFCi} * (EPS_{ch_H2} + R_{bar} * T_0 * LN(H2_{13} / N_{SOFCi}))$
 $EX_{13} = H2_{13} * (EX_{ph_H2_13} + EX_{ch_H2_13})$

"Physical and chemical exergy with flow in to SOFC"

$EX_{ph_SOFCi} = air_{10} * EX_{ph_air_10} + H2_{13} * EX_{ph_H2_13}$
 $EX_{ch_SOFCi} = air_{10} * EX_{ch_air_10} + H2_{13} * EX_{ch_H2_13}$
 $EX_{SOFCi} = EX_{ph_SOFCi} + EX_{ch_SOFCi}$

"State 14"

$H_2O_{14}=N_{H2}; M_{dot_{14}}=H_2O_{14}*MW_{H2O}$ "Producer steam in SOFC"

$T_{14}=T_{SOFC}; P_{14}=P_{10}$

$DELTAH_{H2O_{14}}=A_{H2O}*(T_{14}-T_0)+B_{H2O}*(T_{14}^2-T_0^2)/2+C_{H2O}*(T_{14}^3-T_0^3)/3+D_{H2O}*(T_{14}^4-T_0^4)/4$

$S_{H2O_{14}}=A_{H2O}*(LN(T_{14})-LN(T_0))+B_{H2O}*(T_{14}-T_0)+C_{H2O}*(T_{14}^2-T_0^2)/2+D_{H2O}*(T_{14}^3-T_0^3)/3-R_{bar}*LN(P_{14}/P_0*H_2O_{14}/N_{SOFCe})$

$EX_{ph_{H2O_{14}}}=DELTAH_{H2O_{14}}-T_0*(S_{H2O_{14}})$

$EX_{ch_{H2O_{14}}}=H_2O_{14}/N_{SOFCe}*(EPS_{ch_{H2O}}+R_{bar}*T_0*LN(H_2O_{14}/N_{SOFCe}))$

$EX_{14}=H_2O_{14}*(EX_{ph_{H2O_{14}}}+EX_{ch_{H2O_{14}}})$

$EX_{ch_{H2_{11}SOFCe}}=H_2_{11}/N_{SOFCe}*(EPS_{ch_{H2}}+R_{bar}*T_0*LN(H_2_{11}/N_{SOFCe}))$

$EX_{ch_{O2_{11}SOFCe}}=O_2_{11}/N_{SOFCe}*(EPS_{ch_{O2}}+R_{bar}*T_0*LN(O_2_{11}/N_{SOFCe}))$

$EX_{ch_{N2_{11}SOFCe}}=N_2_{11}/N_{SOFCe}*(EPS_{ch_{N2}}+R_{bar}*T_0*LN(N_2_{11}/N_{SOFCe}))$

"Physical and chemical exergy with flow out SOFC"

$EX_{ph_{SOFCe}}=N_2_{11}*EX_{ph_{N2_{11}}}+O_2_{11}*EX_{ph_{O2_{11}}}+H_2_{11}*EX_{ph_{H2_{11}}}+H_2O_{14}*EX_{ph_{H2O_{14}}}$

$EX_{ch_{SOFCe}}=N_2_{11}*EX_{ch_{N2_{11}SOFCe}}+O_2_{11}*EX_{ch_{O2_{11}SOFCe}}+H_2_{11}*EX_{ch_{H2_{11}SOFCe}}+H_2O_{14}*EX_{ch_{H2O_{14}}}$

$EX_{SOFCe}=EX_{ph_{SOFCe}}+EX_{ch_{SOFCe}}$

"Destruction exergy in SOFC"

$EX_{Ir_{SOFC2}}=T_0*(H_2_{11}*(S_{H2_{11}}+DELTA_{S_{H2}})+O_2_{11}*(S_{O2_{11}}+DELTA_{S_{O2}})+H_2O_{14}*(S_{H2O_{14}}+DELTA_{S_{H2O}})+N_2_{11}*(S_{N2_{11}}+DELTA_{S_{N2}}))$

$EX_{Ir_{SOFC1}}=T_0*(air_{10}*(S_{air_{10}}+DELTA_{S_{air}})+H_2_{13}*(S_{H2_{13}}+DELTA_{S_{H2}}))$

$EX_{Ir_{SOFC}}=EX_{Ir_{SOFC2}}-EX_{Ir_{SOFC1}}$

$SOFC_e=W_{dot_{SOFC}}*N_{1SOFC}/1000+H_2_{11}*DELTAH_{H2_{11}}+O_2_{11}*DELTAH_{O2_{11}}+N_2_{11}*DELTAH_{N2_{11}}+H_2O_{14}*(DELTAHF_{H2O}*1000+DELTAH_{H2O_{14}})$

$SOFC_i=H_2_{13}*DELTAH_{H2_{13}}+air_{10}*DELTAH_{air_{10}}$

$SOFC_e=SOFC_i$ "Energy balance for SOFC"

{ Calculations for the heat recovery steam generation 3-4 to meet T_4 required for gasification process }

{ Assume no pressure drop in the heat recovery steam generation 3-4 }

$H_2O_3=M_{dot_3}/MW_{H2O}; N_3=H_2O_3$

$T_3=T_0$

$T_4=500[K]$ "The temperature of the injected steam, M_{dot_4} is the amount of injected steam"

$P_3=120[kPa]; P_4=P_3$ "From main supply"

$h_3=$ Enthalpy (Steam, $T=T_3, P=P_3$)

$S_3=$ Entropy (Steam, $T=T_3, P=P_3$)

$EX_{ph_{H2O_3}}=h_3-T_0*S_3$

$EX_{ch_{H2O_3}}=H_2O_3/N_3*(EPS_{ch_{H2O}}+R_{bar}*T_0*LN(H_2O_3/N_3))$

"Exergy at heat exchanger 3-4 inlet"

$EX_{ph_3}=M_{dot_3}*EX_{ph_{H2O_3}}$

$EX_{ch_3}=H_2O_3*EX_{ch_{H2O_3}}$

$EX_3=EX_{ph_3}+EX_{ch_3}$

"State 4"

$M_{dot_4}=M_{dot_3}; H_2O_4=H_2O_3; N_4=N_3$

$h_4 = \text{Enthalpy (Steam, } T=T_4, P=P_4)$
 $S_4 = \text{Entropy (Steam, } T=T_4, P=P_4)$
 $EX_{ph_H2O_4} = h_4 - T_0 * S_4$
 $EX_{ch_H2O_4} = H2O_4 / N_4 * (EPS_{ch_H2O} + R_{bar} * T_0 * \ln(H2O_4 / N_4))$
 "Exergy at heat exchanger 3-4 exit"
 $EX_{ph_4} = M_{dot_3} * EX_{ph_H2O_4}$
 $EX_{ch_4} = H2O_4 * EX_{ch_H2O_4}$
 $EX_4 = EX_{ph_4} + EX_{ch_4}$
 $EX_{Ir_3_4} = T_0 * M_{dot_3} * (S_4 - S_3)$
 $Q_{dot_3_4} = M_{dot_3} * (h_4 - h_3)$ "Heat need to generate steam required for gasification"

{Calculations for heat exchanger 3_4 & 20_21}
 "Enthalpies from steam tables"
 $H2O_{20} = H2O_{21}$
 $M_{dot_20} = H2O_{20} * MW_{H2O}; N_{20} = H2O_{20}$
 $M_{dot_21} = M_{dot_20}$
 $T_{20} = T_{14}; P_{20} = P_{10}$
 $h_{20} = \text{Enthalpy (Steam, } T=T_{20}, P=P_{20})$
 $S_{20} = \text{Entropy (Steam, } T=T_{20}, P=P_{20})$
 $EX_{ph_H2O_20} = h_{20} - T_0 * S_{20}$
 $EX_{ch_H2O_20} = H2O_{20} / N_{20} * (EPS_{ch_H2O} + R_{bar} * T_0 * \ln(H2O_{20} / N_{20}))$
 "Physical and chemical exergies with flow at heat exchanger inlet"
 $EX_{20} = M_{dot_20} * EX_{ph_H2O_20} + H2O_{20} * EX_{ch_H2O_20}$
 $EX_{21} = H2O_{21} * EX_{ph_H2O_21} + H2O_{21} * EX_{ch_H2O_21}$

"Exergy destruction in heat exchanger 20_21"
 $EX_{Ir_20_21} = T_0 * (H2O_{21} * (S_{H2O_21} + \Delta S_{H2O}) - M_{dot_20} * S_{20})$
 $Q_{dot_20_21} = Q_{dot_3_4}$ "Heat transferred from line 20-21"
 $Q_{dot_20_21} = M_{dot_20} * (h_{20} - h_{21})$
 $P_{21} = P_{18}$
 $T_{21} = \text{Temperature (Steam, } h=h_{21}, P=P_{21})$
 $H2O_{21} = CO_{18}$

{Extra steam after steam reforming}
 "State 27"
 $H2O_{19} = H2O_{14} - H2O_{15}$
 $M_{dot_19} = H2O_{19} * MW_{H2O}; M_{dot_27} = H2O_{27} * MW_{H2O}; N_{27} = H2O_{27}$
 $M_{dot_27} = M_{dot_19} - M_{dot_20}$
 $T_{27} = T_{14}; P_{27} = P_{10}$
 $h_{27} = \text{Enthalpy (Steam, } T=T_{27}, P=P_{27})$
 $S_{27} = \text{Entropy (Steam, } T=T_{27}, P=P_{27})$
 $EX_{ph_H2O_27} = h_{27} - T_0 * S_{27}$
 $EX_{ch_H2O_27} = H2O_{27} / N_{27} * (EPS_{ch_H2O} + R_{bar} * T_0 * \ln(H2O_{27} / N_{27}))$
 "Physical and chemical exergies with steam at point 27"
 $EX_{ph_27} = M_{dot_27} * EX_{ph_H2O_27}$
 $EX_{ch_27} = H2O_{27} * EX_{ch_H2O_27}$
 $EX_{27} = EX_{ph_27} + EX_{ch_27}$

{Calculations for steam shift reaction}
 {H2O_21 should be at T_21 & with molar flow rate required for the shift reaction}

$CO_{18}=CO_{17}; CO_{2,18}=CO_{2,17}; H_{2,18}=H_{2,17}$
 $CO_{2,22}=CO_{2,17}+CO_{16}; H_{2,22}=H_{2,18}+CO_{18}$
 $N_{22}=CO_{2,22}+H_{2,22}+H_2O_{21}$
 $MW_{22}=H_{2,22}/N_{22}*MW_{H_2}+CO_{2,22}/N_{22}*MW_{CO_2}$
 $M_{dot_{22}}=N_{22}*MW_{22}$
 $P_{22}=P_{18}-0.05*P_{18}$
 $N_{SSi}=CO_{18}+CO_{2,18}+H_{2,18}+H_2O_{21}$
 {Calculate delta enthalpy for carbon monoxide in kJ/kmol at steam shift inlet}
 $DELTAH_{CO_{18}}= A_{CO}*(T_{18}-T_0)+B_{CO}*(T_{18}^2-T_0^2)/2+C_{CO}*(T_{18}^3-T_0^3)/3+D_{CO}*(T_{18}^4-T_0^4)/4$
 $S_{CO_{18}}= A_{CO}*(LN(T_{18})-LN(T_0))+B_{CO}*(T_{18}-T_0)+C_{CO}*(T_{18}^2-T_0^2)/2 + D_{CO}*(T_{18}^3-T_0^3)/3-R_{bar}*LN(P_{18}/P_0*CO_{18}/N_{SSi})$
 $EX_{ph_{CO_{18}}}=DELTAH_{CO_{18}}-T_0*(S_{CO_{18}})$
 $EX_{ch_{CO_{18}}}=CO_{18}/N_{SSi}*(EPS_{ch_{CO}}+R_{bar}*T_0*LN(CO_{18}/N_{SSi}))$
 {Calculation of delta enthalpy for carbon dioxide in kJ/kmol at steam shift inlet}
 $DELTAH_{CO_{2,18}}= A_{CO_2}*(T_{18}-T_0)+B_{CO_2}*(T_{18}^2-T_0^2)/2+C_{CO_2}*(T_{18}^3-T_0^3)/3+D_{CO_2}*(T_{18}^4-T_0^4)/4$
 $S_{CO_{2,18}}= A_{CO_2}*(LN(T_{18})-LN(T_0))+B_{CO_2}*(T_{18}-T_0)+C_{CO_2}*(T_{18}^2-T_0^2)/2 + D_{CO_2}*(T_{18}^3-T_0^3)/3-R_{bar}*LN(P_{18}/P_0*CO_{2,18}/N_{SSi})$
 $EX_{ph_{CO_{2,18}}}=DELTAH_{CO_{2,18}}-T_0*(S_{CO_{2,18}})$
 $EX_{ch_{CO_{2,18}}}=CO_{2,18}/N_{SSi}*(EPS_{ch_{CO_2}}+R_{bar}*T_0*LN(CO_{2,18}/N_{SSi}))$

 {Calculation of delta enthalpy for hydrogen in kJ/kmol at steam shift inlet}
 $DELTAH_{H_{2,18}}= A_{H_2}*(T_{18}-T_0)+B_{H_2}*(T_{18}^2-T_0^2)/2 + C_{H_2}*(T_{18}^3-T_0^3)/3 + D_{H_2}*(T_{18}^4-T_0^4)/4$
 $S_{H_{2,18}}= A_{H_2}*(LN(T_{18})-LN(T_0))+B_{H_2}*(T_{18}-T_0)+C_{H_2}*(T_{18}^2-T_0^2)/2 + D_{H_2}*(T_{18}^3-T_0^3)/3-R_{bar}*LN(P_{18}/P_0*H_{2,18}/N_{SSi})$
 $EX_{ph_{H_{2,18}}}=DELTAH_{H_{2,18}}-T_0*(S_{H_{2,18}})$
 $EX_{ch_{H_{2,18}}}=H_{2,18}/N_{SSi}*(EPS_{ch_{H_2}}+R_{bar}*T_0*LN(H_{2,18}/N_{SSi}))$

 {Calculation of delta enthalpy for steam in kJ/kmol at steam shift inlet}
 $DELTAH_{H_2O_{21}}= A_{H_2O}*(T_{21}-T_0)+B_{H_2O}*(T_{21}^2-T_0^2)/2 + C_{H_2O}*(T_{21}^3-T_0^3)/3 + D_{H_2O}*(T_{21}^4-T_0^4)/4$
 $S_{H_2O_{21}}= A_{H_2O}*(LN(T_{21})-LN(T_0))+B_{H_2O}*(T_{21}-T_0)+C_{H_2O}*(T_{21}^2-T_0^2)/2 + D_{H_2O}*(T_{21}^3-T_0^3)/3-R_{bar}*LN(P_{21}/P_0*H_2O_{21}/N_{SSi})$
 $EX_{ph_{H_2O_{21}}}=DELTAH_{H_2O_{21}}-T_0*(S_{H_2O_{21}})$
 $EX_{ch_{H_2O_{21}}}=H_2O_{21}/N_{SSi}*(EPS_{ch_{H_2O}}+R_{bar}*T_0*LN(H_2O_{21}/N_{SSi}))$
 "Physical exergy and chemical exergy at SSi"
 $EX_{ph_{SSi}}=CO_{18}*EX_{ph_{CO_{18}}}+CO_{2,18}*EX_{ph_{CO_{2,18}}}+H_{2,18}*EX_{ph_{H_{2,18}}}+H_2O_{21}*EX_{ph_{H_2O_{21}}}$
 $EX_{ch_{SSi}}=CO_{18}*EX_{ch_{CO_{18}}}+CO_{2,18}*EX_{ch_{CO_{2,18}}}+H_{2,18}*EX_{ch_{H_{2,18}}}+H_2O_{21}*EX_{ch_{H_2O_{21}}}$
 $EX_{SSi}=EX_{ph_{SSi}}+EX_{ch_{SSi}}$
 $N_{SSe}=CO_{2,22}+H_{2,22}$
 {Calculation of delta enthalpy for carbon dioxide in kJ/kmol at steam shift exit}
 $DELTAH_{CO_{2,22}}= A_{CO_2}*(T_{22}-T_0)+B_{CO_2}*(T_{22}^2-T_0^2)/2+C_{CO_2}*(T_{22}^3-T_0^3)/3+D_{CO_2}*(T_{22}^4-T_0^4)/4$
 $S_{CO_{2,22}}= A_{CO_2}*(LN(T_{22})-LN(T_0))+B_{CO_2}*(T_{22}-T_0)+C_{CO_2}*(T_{22}^2-T_0^2)/2 + D_{CO_2}*(T_{22}^3-T_0^3)/3-R_{bar}*LN(P_{22}/P_0*CO_{2,22}/N_{SSe})$
 $EX_{ph_{CO_{2,22}}}=DELTAH_{CO_{2,22}}-T_0*(S_{CO_{2,22}})$

$$EX_ch_CO2_22=CO2_22/N_SSe*(EPS_ch_CO2+R_bar*T_0*LN(CO2_22/N_SSe))$$

{Calculation of delta enthalpy for hydrogen in kJ/kmol at steam shift exit}

$$DELTAH_H2_22= A_H2*(T_22-T_0)+B_H2*(T_22^2-T_0^2)/2 + C_H2*(T_22^3-T_0^3)/3 + D_H2*(T_22^4-T_0^4)/4$$

$$S_H2_22 = A_H2*(LN(T_22)-LN(T_0))+B_H2*(T_22-T_0)+C_H2*(T_22^2-T_0^2)/2 + D_H2*(T_22^3-T_0^3)/3-R_bar*LN(P_22/P_0*H2_22/N_SSe)$$

$$EX_ph_H2_22=DELTAH_H2_22-T_0*(S_H2_22)$$

$$EX_ch_H2_22=H2_22/N_SSe*(EPS_ch_H2+R_bar*T_0*LN(H2_22/N_SSe))$$

$$EX_H2_22=H2_22*EX_ph_H2_22+H2_22*EX_ch_H2_22$$

$$EX_CO2_22=CO2_22*EX_ph_CO2_22+CO2_22*EX_ch_CO2_22$$

"Physical exergy and chemical exergy at SSe"

$$EX_ph_SSe=H2_22*EX_ph_H2_22+CO2_22*EX_ph_CO2_22$$

$$EX_ch_SSe=H2_22*EX_ch_H2_22+CO2_22*EX_ch_CO2_22$$

$$EX_SSe=EX_ph_SSe+EX_ch_SSe$$

$$EX_22=EX_SSe$$

"Exergy destruction in steam shift reactor"

$$EX_Ir_SS=T_0*(H2_22*(S_H2_22+DELTA_S_H2)+CO2_22*(S_CO2_22+DELTA_S_CO2)-H2O_21*(S_H2O_21+DELTA_S_H2O)-H2_18*(S_H2_18+DELTA_S_H2)-CO2_18*(S_CO2_18+DELTA_S_CO2)-CO_18*(S_CO_18+DELTA_S_CO))$$

"Exergy destruction in heat exchanger 17_18&9_10"

$$EX_ph_18=CO_18*EX_ph_CO_18+CO2_18*EX_ph_CO2_18+H2_18*EX_ph_H2_18$$

$$EX_ch_18=CO_18*EX_ch_CO_18+CO2_18*EX_ch_CO2_18+H2_18*EX_ch_H2_18$$

$$EX_18=EX_ph_18+EX_ch_18$$

$$EX_17=EX_SRe$$

$$EX_Ir_17=T_0*(H2_17*(S_H2_17+DELTA_S_H2)+CO2_17*(S_CO2_17+DELTA_S_CO2)+CO_17*(S_CO_17+DELTA_S_CO))$$

$$EX_Ir_18=T_0*(H2_18*(S_H2_18+DELTA_S_H2)+CO2_18*(S_CO2_18+DELTA_S_CO2)+CO_18*(S_CO_18+DELTA_S_CO))$$

$$EX_Ir_HE_17_18=EX_Ir_17-EX_Ir_18$$

$$EX_Ir_HE_9_10=T_0*(air_10*(S_air_10+DELTA_S_air)-air_9*(S_air_9+DELTA_S_air))$$

{Calculation for temperature at steam shift reactor exit, T_22}

$$SS_A=CO_18*(DELTAH_CO_18+DELTAHF_CO*1000)+CO2_18*(DELTAHF_CO2*1000+DELTAH_CO2_18)$$

$$SS_B=H2_18*DELTAH_H2_18+H2O_21*(DELTAHF_H2O*1000+DELTAH_H2O_21)$$

$$SS_1=SS_A+SS_B$$

$$SS_2=H2_22*DELTAH_H2_22+CO2_22*(DELTAHF_CO2*1000+DELTAH_CO2_22)$$

$$SS_1-SS_2=0 \text{ "To calculate } T_22 \text{ "}$$

"Calculations for hydrogen line"

$$P_33=(P_22-0.05*P_22)*H2_22/N_22$$

$$T_33=T_22$$

$$H2_33=H2_22;M_dot_33=H2_33*MW_H2;N_33=H2_33$$

$$DELTAH_H2_33=DELTAH_H2_22$$

$$S_H2_33= A_H2*(LN(T_22)-LN(T_0))+B_H2*(T_22-T_0)+C_H2*(T_22^2-T_0^2)/2 + D_H2*(T_22^3-T_0^3)/3-R_bar*LN(P_33/P_0*H2_33/N_33)$$

$$EX_ph_H2_33=DELTAH_H2_33-T_0*(S_H2_33)$$

$$EX_ch_H2_33=H2_33/N_33*(EPS_ch_H2+R_bar*T_0*LN(H2_33/N_33))$$

$$EX_33=H2_33*(EX_ph_H2_33+EX_ch_H2_33)$$

H2_Yield=H2_22

"Calculations for carbon dioxide line"

$P_{34}=(P_{22}-0.05*P_{22})*CO2_{22}/N_{22}$

$T_{34}=T_{22}$

$CO2_{34}=CO2_{22}; M_{dot_{34}}=CO2_{34}*MW_{CO2}; N_{34}=CO2_{34}$

$DELTAH_{CO2_{34}}=DELTAH_{CO2_{22}}$

$S_{CO2_{34}}=A_{CO2}*(LN(T_{22})-LN(T_0))+B_{H2}*(T_{22}-T_0)+C_{H2}*(T_{22}^2-T_0^2)/2 + D_{H2}*(T_{22}^3-T_0^3)/3-R_{bar}*LN(P_{34}/P_0*CO2_{34}/N_{34})$

$EX_{ph_{CO2_{34}}}=DELTAH_{CO2_{34}}-T_0*S_{CO2_{34}}$

$EX_{ch_{CO2_{34}}}=CO2_{34}/N_{34}*(EPS_{ch_{CO2}}+R_{bar}*T_0*LN(CO2_{34}/N_{34}))$

$EX_{34}=CO2_{34}*(EX_{ph_{CO2_{34}}}+EX_{ch_{CO2_{34}}})$

$CO2_{Emission}=CO2_{22}$

"Efficiency calculations"

$LHV_{biomass}=19005[kJ/kg]$

$W_{dot_{SOFC}}=52.37[W]$ "From SOFC calculations"

$W_{dot_{SOFC_AC}}=W_{dot_{SOFC}}*0.95$

$N_{SOFC}=N_{H2}*1000/N_{H2_SOFC}$

$W_{dot_{STACK}}=W_{dot_{SOFC}}*N1_{SOFC}$

$LHV_{H2}=120000[kJ/kg]$

$Eta_{el_tur}=(W_{dot_{7_8}}-W_{dot_{5_6}}-W_{dot_{24_25}}-W_{dot_{0_9}})*0.90/(M_{dot_1}*19005)*100$

"SOFC efficiency"

$Eta_{el_SOFC}=W_{dot_{SOFC_AC}}/(N_{H2_SOFC}*LHV_{H2}*2.016)*100$ "Efficiency of SOFC"

$Eta_{el_Overall}=Eta_{el_SOFC}+Eta_{el_tur}$

$Eta_{EX_el_Overall}=Eta_{EX_el_SOFC}+Eta_{EX_el_tur}$

$Eta_{H2}=(DELTAH_{H2_33}/MW_{H2})/LHV_{biomass}*100$ "Efficiency when take H2 only in consideration"

$EX_{H2_13}=H2_{13}*EX_{ph_{H2_13}}+H2_{13}*EX_{ch_{H2_13}}$

$Eta_{EX_el_tur}=(W_{dot_{7_8}}-W_{dot_{5_6}}-W_{dot_{24_25}}-W_{dot_{0_9}})*0.90/(BETA*M_{dot_1}*LHV_{biomass})*100$

$Eta_{EX_Steam}=EX_{27}/(BETA*M_{dot_1}*LHV_{biomass})*100$

$Eta_{EX_H2}=EX_{33}/(BETA*M_{dot_1}*LHV_{biomass})*100$ "Efficiency when take H2 only in consideration"

$Eta_{EX_el_SOFC}=W_{dot_{STACK}}/1000/(1.173*M_{dot_1}*LHV_{biomass})*100$

$EX_{Ir_{3_4_20_21}}=EX_{Ir_{3_4}}+EX_{Ir_{20_21}}$ "Heat exchanger 3_4&20_21"

$EX_{Ir_{36_5_25_35}}=EX_{Ir_{HE_{36_5}}}+EX_{Ir_{HE_{25_35}}}$ "Heat exchanger 36_5&25_35"

$EX_{Ir_{17_18_9_10}}=EX_{Ir_{HE_{17_18}}}+EX_{Ir_{HE_{9_10}}}$ "Heat exchanger 17_18&9_10"

$EX_1=M_{dot_1}*BETA*LHV_{biomass}$

$EX_{d_gasifier}=EX_1+EX_4-EX_2$

"Economic"

$TAO=8000[hr/yr]; BETA=1.173; ER=1$ {exchange rate is one}

$Pr=2*3600*10^{(-6)}$ "Biomass price \$/kWh"

$FC_{dot_f}=Pr*LHV_{biomass}*M_{dot_1}*TAO/ER$ "Energetic cost"

$C_{dot_1}=FC_{dot_f}/TAO*(1/BETA)$ "Exergetic cost"

"Cost balance and auxiliary equations"

$C_{dot_4}+C_{dot_1}+Z_{dot_Gasifier}=C_{dot_2}$ "Gasifier"

$Z_{dot_Gasifier}=1.047; C_{dot_1}=c_1*EX_{Biomass}; C_{dot_2}=c_2*EX_2; C_{dot_4}=c_4*EX_4$

$Z_{OBJ_Gasifier}=Z_{dot_Gasifier}+EX_{d_gasifier}*C_2$

$C_{\dot{2}}+Z_{\dot{\text{Seperator}}}=C_{\dot{26}}+C_{\dot{36}}$ "Seperator to find c_{26} "
 $Z_{\dot{\text{Seperator}}}=0.083$; $C_{\dot{26}}=c_{26} \cdot EX_{26}$; $C_{\dot{36}}=c_{36} \cdot EX_{36}$
 $C_{\dot{2}}/Ex_2=C_{\dot{36}}/Ex_{36}$

$C_{\dot{24}}+C_{\dot{w}_{24,25}}+Z_{\dot{24,25}}=C_{\dot{25}}$ "Air compressor 24-25 to find c_{25} "
 $Z_{\dot{24,25}}=2.511$; $C_{\dot{w}_{24,25}}=c_{24,25} \cdot W_{\dot{24,25}}$
 $c_{24,25}=0.1046$
 $C_{24}=0$; $C_{\dot{24}}=c_{24} \cdot Ex_{24}$; $C_{\dot{25}}=c_{25} \cdot Ex_{25}$
 $Z_{\text{OBJ}_{24,25}}=Z_{\dot{24,25}}+EX_{\text{Ir_Comp}_{24,25}} \cdot C_{25}$

$C_{\dot{36}}+C_{\dot{25}}+Z_{\dot{\text{HE1}}}=C_{\dot{5}}+C_{\dot{35}}$ "Heat exchanger 1 to find c_{35}, c_{36} "
 $Z_{\dot{\text{HE1}}}=0.748$; $C_{\dot{5}}=c_5 \cdot EX_5$; $C_{\dot{35}}=c_{35} \cdot EX_{35}$
 $C_5=C_{36}$
 $Z_{\text{OBJ}_{\text{HE1}}}=Z_{\dot{\text{HE1}}}+EX_{\text{Ir}_{36,5,25,35}} \cdot C_{36}$

$C_{\dot{5}}+C_{\dot{w}_{5,6}}+Z_{\dot{5,6}}=C_{\dot{6}}$ "Gas compressor 5-6 to find c_5 "
 $Z_{\dot{5,6}}=1.591$ [\$/s]; $C_{\dot{w}_{5,6}}=c_{5,6} \cdot W_{\dot{5,6}}$; $C_{\dot{6}}=c_6 \cdot EX_6$
 $c_{5,6}=0.1046$
 $Z_{\text{OBJ}_{5,6}}=Z_{\dot{5,6}}+EX_{\text{Ir_Comp}_{5,6}} \cdot C_6$

$C_{\dot{6}}+Z_{\dot{\text{Filter1}}}=C_{\dot{16}}+C_{\dot{13}}$ "Filter 1 to find c_6, c_{13} "
 $Z_{\dot{\text{Filter1}}}=0.256$; $C_{\dot{16}}=c_{16} \cdot EX_{16}$; $C_{\dot{13}}=c_{13} \cdot EX_{13}$
 $C_{\dot{13}}/Ex_{13}=C_{\dot{16}}/Ex_{16}$
 $Z_{\text{OBJ}_{\text{Filter1}}}=Z_{\dot{\text{Filter1}}}$

$C_{\dot{16}}+C_{\dot{15}}+Z_{\dot{\text{SR}}}=C_{\dot{17}}$ "Steam reforming to find c_{16} "
 $Z_{\dot{\text{SR}}}=1.339$; $C_{\dot{15}}=c_{15} \cdot EX_{15}$; $C_{\dot{17}}=c_{17} \cdot EX_{17}$
 $C_{15}=c_{14}$
 $Z_{\text{OBJ}_{\text{SR}}}=Z_{\dot{\text{SR}}}+EX_{\text{Ir}_{\text{SR}}} \cdot C_{17}$

$C_{\dot{0}}+C_{\dot{w}_{0,9}}+Z_{\dot{0,9}}=C_{\dot{9}}$ "Air compressor 0-9 to find c_9 "
 $Z_{\dot{0,9}}=2.511$; $C_{\dot{w}_{0,9}}=c_{0,9} \cdot W_{\dot{0,9}}$; $C_{\dot{0}}=c_0 \cdot EX_0$
 $c_{0,9}=0.1046$
 $c_0=0$
 $Z_{\text{OBJ}_{0,9}}=Z_{\dot{0,9}}+EX_{\text{Ir_Comp}_{0,9}} \cdot C_9$

$C_{\dot{17}}+C_{\dot{9}}+Z_{\dot{\text{HE2}}}=C_{\dot{18}}+C_{\dot{10}}$ "Heat exchanger 2 to find c_{10}, c_{17} "
 $Z_{\dot{\text{HE2}}}=0.748$ [\$/hr]; $C_{\dot{18}}=c_{18} \cdot EX_{18}$; $C_{\dot{9}}=c_9 \cdot EX_9$; $C_{\dot{10}}=c_{10} \cdot EX_{10}$
 $C_{\dot{17}}/Ex_{17}=C_{\dot{18}}/Ex_{18}$
 $Z_{\text{OBJ}_{\text{HE2}}}=Z_{\dot{\text{HE2}}}+EX_{\text{Ir}_{17,18,9,10}} \cdot C_{18}$

$C_{\dot{3}}+C_{\dot{20}}+Z_{\dot{\text{HE3}}}=C_{\dot{21}}+C_{\dot{4}}$ "Heat exchanger 3"
 $Z_{\dot{\text{HE3}}}=0.748$; $C_{\dot{3}}=c_3 \cdot EX_3$; $C_{\dot{20}}=c_{20} \cdot EX_{20}$; $C_{\dot{21}}=c_{21} \cdot EX_{21}$
 $C_{\dot{20}}/Ex_{20}=C_{\dot{21}}/Ex_{21}$
 $C_3=0$; $C_{20}=c_{14}$
 $Z_{\text{OBJ}_{\text{HE3}}}=Z_{\dot{\text{HE3}}}+EX_{\text{Ir}_{3,4,20,21}} \cdot C_{21}$

$C_{\dot{18}}+C_{\dot{21}}+Z_{\dot{\text{SS}}}=C_{\dot{22}}$ "Steam shift, to find c_{18} "
 $Z_{\dot{\text{SS}}}=1.339$ [\$/s]; $C_{\dot{22}}=c_{22} \cdot EX_{22}$

$$Z_OBJ_SS=Z_dot_SS+EX_Ir_SS*C_22$$

$$\begin{aligned}C_dot_22+Z_dot_Filter2&=C_dot_33+C_dot_34\text{"Filter 2"} \\Z_dot_Filter2&=0.256;C_dot_33=c_33*EX_33;C_dot_34=c_34*EX_34 \\C_dot_22/EX_22&=C_dot_33/EX_33+C_dot_34/EX_34 \\Z_OBJ_Filter2&=Z_dot_Filter2\end{aligned}$$

"This is done only for SOFC because its number changes with gasification temperature and therefore its cost"

$$\begin{aligned}A_SOFC&=100[\text{cm}^2] \\A_STACK&=100*A_SOFC;N_STACK=N1_SOFC*A_SOFC/A_STACK \\Cost_SOFC&=0.1442*A_SOFC \\C_STACK&=(2.7*Cost_SOFC*N1_SOFC+2.50695*N_STACK*A_SOFC) \\S_STACK&=0.10*C_STACK \\PWF&=1/(1+0.10)^{25};PW=C_STACK-S_STACK*PWF \\CRF&=0.10*(0.10+1)^{25}/((0.10+1)^{25}-1) \\Z_dot_SOFC&=CRF*PW*1.06/8000 \\C_dot_13+C_dot_10+Z_dot_SOFC&=C_dot_14+C_dot_11+C_dot_W_SOFC\text{"SOFC to find }c_11\text{"} \\C_dot_W_SOFC&=c_SOFC*N1_SOFC*W_dot_SOFC_AC/1000;C_dot_11=c_11*EX_11;C_dot_14=c_14*EX_14 \\C_14&=c_11 \\Z_OBJ_SOFC&=Z_dot_SOFC+EX_Ir_SOFC*C_11\end{aligned}$$

"State 27"

$$\begin{aligned}C_dot_14/EX_14&=C_dot_27/EX_27 \\C_dot_27&=c_27*EX_27\end{aligned}$$

$$\begin{aligned}C_dot_11+C_dot_26+C_dot_35+Z_dot_burner&=C_dot_7\text{"Burner to find }c_7\text{"} \\Z_dot_burner&=1.339;C_dot_7=c_7*EX_7 \\Z_OBJ_burner&=Z_dot_burner+EX_Ir_burner*C_7\end{aligned}$$

$$\begin{aligned}C_dot_7+Z_dot_7_8&=C_dot_8+C_dot_w_7_8\text{"Turbine 7-8 to find }c_8\text{"} \\Z_dot_7_8&=5.859;C_dot_w_7_8=C_7_8*W_dot_7_8;C_dot_8=c_8*EX_8 \\C_7_8&=0.1046 \\C_8&=0 \\Z_OBJ_Tur_7_8&=Z_dot_7_8+EX_Ir_Tur_7_8*C_7\end{aligned}$$

"Total objective function"

$$\begin{aligned}Z_OBJ&=Z_OBJ_Tur_7_8+Z_OBJ_burner+Z_OBJ_SOFC+Z_OBJ_Filter2+Z_OBJ_SS+Z_OBJ_HE3+Z_OBJ_HE2+Z_OBJ_0_9+Z_OBJ_SR+Z_OBJ_Filter1+Z_OBJ_5_6+Z_OBJ_HE1+Z_OBJ_J_24_25+Z_OBJ_Gasifier\end{aligned}$$

B3. System III

{Program EEs to perform calculations for Exergoeconomic of system III, Z_dot as system ii.
Z_dot for the coupled SOEC_SOFC is assumed 2*Z_dot for SOFC
{This code finds mass, temperature and pressure at different states of the system III}
{The hybrid system includes gasifier, SOFC, SOEC and gas turbine}

P_0=101.325[kPa];T_0=298[k]
R_bar=8.314[kJ/kg-K]
{Data from biomass gasification}
M_dot_3=0.27/1000*MW_H2O;Cp_H2O=4.18[kJ/kg-K]
M_dot_1=0.32/1000*99.48
"Total hydrogen and products from gasification"
{N_H2=1.114/1000[kmol/s];N_CH4=0.0003469/1000[kmol/s];N_CO=0.7662/1000[kg/s];N_CO2
=0.2062/1000[kmol/s]; N_tar=0.04058/1000[kmol/s];N_char=0.06401/1000[kmol/s]}
MW_CH4=16.043;MW_CO=28.011;MW_CO2=44.01;MW_H2=2.016[kg/kmol];MW_H2O=18.
015;MW_air=28.97[kJ/kg-K]
MW_O2=32[kg/kmol];MW_N2=28.013[kg/kmol];MW_tar=78.11[kg/kmol];MW_char=12[kg/k
mol]
Cp_char=0.708[kJ/kg-K];Cp_air=1.004[kJ/kg-K]
"Standard exergies for the compounds"
EPS_ch_H2=236100[kJ/kmol];EPS_ch_CO=275100;EPS_ch_CO2=19870;EPS_ch_CH4=83165
0;EPS_ch_H2O=9500[kJ/kmol];EPS_ch_O2=3971[kJ/kmol];EPS_ch_N2=720[kJ/kmol]
EPS_ch_air=0.21*EPS_ch_O2+0.79*EPS_ch_N2
N_H2_SOFC=0.0004091[kmol/s]"Hydrogen fed for one cell"
{N_SOFC=2723[cells]"Total number of cells"}
N_H2R=N_H2*U_f
N_O2=1/2*N_H2
A_SOFC=100
{fuel and air utilization factor}
U_f=0.95;U_air=0.20

{calaculate supplied air where air contains 21% O2}
N_air=N_O2/0.21

{Calculations for the adiabatic burner with 100% efficiency}
{calculation of number of moles at the burner inlet}
{T_26=1023[K]}; T_11=T_14;T_13=T_12"They are given"
tar_26=N_tar; char_26=N_char
H2_11=0; O2_11=(1-U_f)*N_O2;N2_11=79/21*N_O2;N_11=O2_11+N2_11
H2_13=N_H2
air_35=M_dot_35/MW_air
N_bi=tar_26+char_26+O2_11+N2_11+air_35+O2_12"Number of moles at the burner inlet"
P_11=P_SOFC
{Calculation of flue gas at the burner exit}
{Calculation of enthalpy of hydrogen at the burner inlet}
A_H2=29.11;B_H2=-0.1916*10⁽⁻²⁾;C_H2=0.4003*10⁽⁻⁵⁾;D_H2=-0.8704*10⁽⁻⁹⁾;
DELTAHF_H2=0.0;DELTA_S_H2=130.68[kJ/kmol-K]

DELTAH_H2_11=0
S_H2_11=0

EX_ph_H2_11=0
EX_ch_H2_11=0

{Calculation of enthalpy of oxygen at the burner inlet} DELTAHF_air=0
A_O2=25.48;B_O2=1.520*10⁽⁻²⁾;C_O2=-0.7155*10⁽⁻⁵⁾;D_O2=1.312*10⁽⁻⁹⁾;DELTAHF_O2=0.0;DELTA_S_O2=205.04[kJ/kmol-K]
DELTAH_O2_11= A_O2*(T_11-T_0)+B_O2*(T_11²-T_0²)/2+C_O2*(T_11³-T_0³)/3+D_O2*(T_11⁴-T_0⁴)/4
S_O2_11= A_O2*(LN(T_11)-LN(T_0))+B_O2*(T_11-T_0)+C_O2*(T_11²-T_0²)/2 + D_O2*(T_11³-T_0³)/3-R_bar*LN(P_11/P_0*O2_11/N_SOFCe)
EX_ph_O2_11=DELTAH_O2_11-T_0*S_O2_11
EX_ch_O2_11=O2_11/N_SOFCe*(EPS_ch_O2+R_bar*T_0*LN(O2_11/N_SOFCe))

{Calculation of enthalpy of nitrogen at the burner inlet}
A_N2=28.90;B_N2=-0.1571*10⁽⁻²⁾;C_N2=0.8081*10⁽⁻⁵⁾;D_N2=-2.873*10⁽⁻⁹⁾;DELTAHF_N2=0.0;DELTA_S_N2=191.61[kJ/kmol-K]
DELTAH_N2_11= A_N2*(T_11-T_0)+B_N2*(T_11²-T_0²)/2+C_N2*(T_11³-T_0³)/3+D_N2*(T_11⁴-T_0⁴)/4
S_N2_11= A_N2*(LN(T_11)-LN(T_0))+B_N2*(T_11-T_0)+C_N2*(T_11²-T_0²)/2 + D_N2*(T_11³-T_0³)/3-R_bar*LN(P_11/P_0*N2_11/N_SOFCe)
EX_ph_N2_11=DELTAH_N2_11-T_0*S_N2_11
EX_ch_N2_11=N2_11/N_SOFCe*(EPS_ch_N2+R_bar*T_0*LN(N2_11/N_SOFCe))
EX_11=H2_11*(EX_ph_H2_11+EX_ch_H2_11)+N2_11*(EX_ph_N2_11+EX_ch_N2_11)+O2_11*(EX_ph_O2_11+EX_ch_O2_11)
M_dot_11=N2_11*MW_N2+O2_11*MW_O2

{Calculation of enthalpy & exergy of air at the burner inlet}
A_air=28.11;B_air=0.1967*10⁽⁻²⁾;C_air=0.4802*10⁽⁻⁵⁾;D_air=1.966*10⁽⁻⁹⁾;DELTA_S_air=1.69528/28.97 [kJ/kmol-K]
DELTAH_air_35= A_air*(T_35-T_0)+B_air*(T_35²-T_0²)/2+C_air*(T_35³-T_0³)/3+D_air*(T_35⁴-T_0⁴)/4
S_air_35= A_air*(LN(T_35)-LN(T_0))+B_air*(T_35-T_0)+C_air*(T_35²-T_0²)/2 + D_air*(T_35³-T_0³)/3-R_bar*LN(P_35/P_0*air_35/N_bi)
EX_ph_air_35=DELTAH_air_35-T_0*S_air_35
EX_ch_air_35=air_35/N_bi*(EPS_ch_air+R_bar*T_0*LN(air_35/N_bi))
EX_35=EX_ph_air_35+EX_ch_air_35

{Calculation of enthalpy & exergy of char at the burner inlet}
P_26=P_3; DELTAHF_char=0
DELTAH_char_26=4.18*(4.03*(T_26-T_0)+0.00114*(T_26²/2-T_0²/2)+2.04*10⁵*(1/T_26-1/T_0))
S_char_26=4.18*(4.03*(LN(T_26)-LN(T_0))+0.00114*(T_26-T_0)+1.02*10⁵*(1/T_26²-1/T_0²))-R_bar*LN(P_26/P_0*char_26/N_bi)
EX_ph_char_26=DELTAH_char_26-T_0*S_char_26
EPS_ch_char=410260[kJ/kmol]
EX_ch_char_26=char_26/N_bi*(EPS_ch_char+R_bar*T_0*LN(char_26/N_bi))
EX_char_26=char_26*(EX_ch_char_26+EX_ph_char_26)

{Calculation of enthalpy & exergy of tar at the burner inlet}

$N_C=48.01/12; N_H=6.04; A1_tar=37.1635; A2_tar=-$
 $31.4767; A3_tar=0.564682; A4_tar=20.1145; A5_tar=54.3111; A6_tar=44.6712; C_f=48.0; H_f=6.0$
 $4; O_f=45.43; N_f=0.15; S_f=0.05$
 $DELTAH_tar_26=N_C*DELTAHF_CO2+N_H/2*DELTAHF_H2O+(0.00422*MW_tar*(T_26^$
 $2-T_0^2)/2-30.980)$
 {S_star in kJ/kmol carbon K}
 $S_star_26=A1_tar+A2_tar*EXP(-$
 $A3_tar*(H_f/C_f+N_f))+A4_tar*(O_f/(C_f+N_f))+A5_tar*(N_f/(C_f+N_f))+A6_tar*(S_f/(C_f+$
 $N_f))$
 $S_tar_26=S_star_26+0.00422*MW_tar*(T_26-T_0)-R_bar*LN(P_26/P_0*tar_26/N_bi)$
 $EX_ph_tar_26=DELTAH_tar_26*tar_26-T_0*S_tar_26*tar_26$
 $EPS_ch_tar=3303600$ [kJ/kmol]
 $X_tar_26=tar_26/N_bi$
 $EX_ch_tar_26=X_tar_26*(EPS_ch_tar+R_bar*T_0*LN(X_tar_26))$
 $EX_tar_26=EX_ph_tar_26+tar_26*EX_ch_tar_26$
 $EX_26=EX_char_26+EX_tar_26$
 {Chemical exergy of tar is disregarded}
 $EX_2=EX_26+EX_36$
 "Physical and chemical exergies with flow at burner inlet, states 26,11,12,35 "
 $EX_ph_bi=EX_ph_tar_26+char_26*EX_ph_char_26+air_35*EX_ph_air_35+N2_11*EX_ph_N2$
 $_11+H2_11*EX_ph_H2_11+O2_11*EX_ph_O2_11+O2_12*EX_ph_O2_12$
 $EX_ch_bi=tar_26*EX_ch_tar_26+char_26*EX_ch_char_26+air_35*EX_ch_air_35+N2_11*EX$
 $_ch_N2_11+H2_11*EX_ch_H2_11+O2_11*EX_ch_O2_11+O2_12*EX_ch_O2_12$
 $EX_bi=EX_ph_bi+EX_ch_bi$

 "Destroyed exergy in the burner"
 $EX_Ir_burner_e=T_0*(H2O_7*(S_H2O_7+DELTA_S_H2O)+CO2_7*(S_CO2_7+DELTA_S_$
 $CO2)+N2_7*(S_N2_7+DELTA_S_N2)+air_7*(S_air_7+DELTA_S_air))$
 $EX_Ir_burner_i=T_0*(S_tar_26*tar_26+char_26*S_char_26+O2_11*(S_O2_11+DELTA_S_O2$
 $) +O2_12*(S_O2_12+DELTA_S_O2)+N2_11*(S_N2_11+DELTA_S_N2)+air_35*(S_air_35+D$
 $ELTA_S_air))$
 $EX_Ir_burner=EX_Ir_burner_e-EX_Ir_burner_i$

 {Gas turbine calculations 7-8: exit temperature, exit pressure, gas mass flow rate}
 $Eta_t=0.80$
 $M_dot_8=M_dot_7$

 {Calculation of temperature of flue gas at the burner exit or at the turbine inlet}
 $B_1=tar_26*DELTAH_tar_26+char_26*DELTAH_char_26+H2_11*DELTAH_H2_11+O2_11*$
 $DELTAH_O2_11+N2_11*DELTAH_N2_11+air_35*DELTAH_air_35$

 "State 7"
 $H2O_7=3*tar_26$
 $CO2_7=Char_26+6*tar_26$
 "O2 only change"
 $O2_consumed=Char_26+7.5*tar_26$ "O2 consumed"
 $O2_consumed=O2_11+O2_35+O2_12$ "O2_11+O2_12<O2_consumed take more from 35"
 "From the above two equations we can find how much more oxygen is needed"
 $N2_35=O2_35*79/21$
 "Excess air that used to control burner temperature and left the burner"

$air_7=air_{35-N2_{35}-O2_{35}}$ "Air exits turbine 7-8"
 $N2_7=N2_{11}$ "inert"
 $N_7=H2O_7+CO2_7+N2_7+air_7$
 $MW_7=H2O_7/N_7*MW_{H2O}+CO2_7/N_7*MW_{CO2}+N2_7/N_7*MW_{N2}+air_7/N_7*MW_{air}$
 $M_{dot_7}=N_7*MW_7$
 $P_7=P_3$
 $Cp_{N2_7}=A_{N2}+B_{N2}*T_7+C_{N2}*T_7^2+D_{N2}*T_7^3$
 $Cp_{CO2_7}=A_{CO2}+B_{CO2}*T_7+C_{CO2}*T_7^2+D_{CO2}*T_7^3$
 $Cp_{H2O_7}=A_{H2O}+B_{H2O}*T_7+C_{H2O}*T_7^2+D_{H2O}*T_7^3$
 $Cp_{air_7}=A_{air}+B_{air}*T_7+C_{air}*T_7^2+D_{air}*T_7^3$
 $Cp_7=H2O_7/N_7*Cp_{H2O_7}+CO2_7/N_7*Cp_{CO2_7}+N2_7/N_7*Cp_{N2_7}+air_7/N_7*Cp_{air_7}$
 $Cv_7=Cp_7-R_{bar}$
 $Gama_7=Cp_7/Cv_7$

$DELTAH_{CO2_7}=A_{CO2}*(T_7-T_0)+B_{CO2}*(T_7^2-T_0^2)/2+C_{CO2}*(T_7^3-T_0^3)/3+D_{CO2}*(T_7^4-T_0^4)/4$
 $S_{CO2_7}=A_{CO2}*(LN(T_7)-LN(T_0))+B_{CO2}*(T_7-T_0)+C_{CO2}*(T_7^2-T_0^2)/2+D_{CO2}*(T_7^3-T_0^3)/3-R_{bar}*LN(P_7/P_0*CO2_7/N_7)$
 $EX_{ph_{CO2_7}}=DELTAH_{CO2_7}-T_0*S_{CO2_7}$
 $EX_{ch_{CO2_7}}=CO2_7/N_7*(EPS_{ch_{CO2}}+R_{bar}*T_0*LN(CO2_7/N_7))$

$DELTAH_{air_7}=A_{air}*(T_7-T_0)+B_{air}*(T_7^2-T_0^2)/2+C_{air}*(T_7^3-T_0^3)/3+D_{air}*(T_7^4-T_0^4)/4$
 $S_{air_7}=A_{air}*(LN(T_7)-LN(T_0))+B_{air}*(T_7-T_0)+C_{air}*(T_7^2-T_0^2)/2+D_{air}*(T_7^3-T_0^3)/3-R_{bar}*LN(P_7/P_0*air_7/N_7)$
 $EX_{ph_{air_7}}=DELTAH_{air_7}-T_0*S_{air_7}$
 $EX_{ch_{air_7}}=air_7/N_7*(EPS_{ch_{air}}+R_{bar}*T_0*LN(air_7/N_7))$

$DELTAH_{N2_7}=A_{N2}*(T_7-T_0)+B_{N2}*(T_7^2-T_0^2)/2+C_{N2}*(T_7^3-T_0^3)/3+D_{N2}*(T_7^4-T_0^4)/4$
 $S_{N2_7}=A_{N2}*(LN(T_7)-LN(T_0))+B_{N2}*(T_7-T_0)+C_{N2}*(T_7^2-T_0^2)/2+D_{N2}*(T_7^3-T_0^3)/3-R_{bar}*LN(P_7/P_0*N2_7/N_7)$
 $EX_{ph_{N2_7}}=DELTAH_{N2_7}-T_0*S_{N2_7}$
 $EX_{ch_{N2_7}}=N2_7/N_7*(EPS_{ch_{N2}}+R_{bar}*T_0*LN(N2_7/N_7))$

$DELTAH_{H2O_7}=A_{H2O}*(T_7-T_0)+B_{H2O}*(T_7^2-T_0^2)/2+C_{H2O}*(T_7^3-T_0^3)/3+D_{H2O}*(T_7^4-T_0^4)/4$
 $S_{H2O_7}=A_{H2O}*(LN(T_7)-LN(T_0))+B_{H2O}*(T_7-T_0)+C_{H2O}*(T_7^2-T_0^2)/2+D_{H2O}*(T_7^3-T_0^3)/3-R_{bar}*LN(P_7/P_0*H2O_7/N_7)$
 $EX_{ph_{H2O_7}}=DELTAH_{H2O_7}-T_0*S_{H2O_7}$
 $EX_{ch_{H2O_7}}=H2O_7/N_7*(EPS_{ch_{H2O}}+R_{bar}*T_0*LN(H2O_7/N_7))$

"Physical and chemical exergies with flow at turbine 7_8 inlet, state 7"
 $EX_{ph_7}=CO2_7*EX_{ph_{CO2_7}}+air_7*EX_{ph_{air_7}}+N2_7*EX_{ph_{N2_7}}+H2O_7*EX_{ph_{H2O_7}}$
 $EX_{ch_7}=CO2_7*EX_{ch_{CO2_7}}+air_7*EX_{ch_{air_7}}+N2_7*EX_{ch_{N2_7}}+H2O_7*EX_{ch_{H2O_7}}$
 $EX_7=EX_{ph_7}+EX_{ch_7}$

"Enthalpy at the burner exit or turbine inlet are the same"

$$B_1=CO2_7*(DELTAH_{CO2_7}+DELTAHF_{CO2}*1000)+H2O_7*(DELTAH_{H2O_7}+DELTAHF_{H2O}*1000)+air_7*DELTAH_{air_7}+N2_7*DELTAH_{N2_7}$$

"State 8"

$T_{fg}=363[K]$; $P_{fg}=P_0+0.1$ "The assumed flue gas temperature and flue gas pressure at which will leave the system"

$$T_8=T_{fg}$$

$P_8=P_{fg}$ "Pressure of the flue gas at exit"

$$CO2_8=CO2_7; air_8=air_7; N2_8=N2_7; H2O_8=H2O_7$$

$$N_8=N_7$$

$$DELTAH_{CO2_8}=A_{CO2}*(T_8-T_0)+B_{CO2}*(T_8^2-T_0^2)/2+C_{CO2}*(T_8^3-T_0^3)/3+D_{CO2}*(T_8^4-T_0^4)/4$$

$$S_{CO2_8}=A_{CO2}*(LN(T_8)-LN(T_0))+B_{CO2}*(T_8-T_0)+C_{CO2}*(T_8^2-T_0^2)/2+D_{CO2}*(T_8^3-T_0^3)/3-R_{bar}*LN(P_8/P_0*CO2_8/N_8)$$

$$EX_{ph_{CO2_8}}=DELTAH_{CO2_8}-T_0*S_{CO2_8}$$

$$EX_{ch_{CO2_8}}=CO2_8/N_8*(EPS_{ch_{CO2}}+R_{bar}*T_0*LN(CO2_8/N_8))$$

$$DELTAH_{air_8}=A_{air}*(T_8-T_0)+B_{air}*(T_8^2-T_0^2)/2+C_{air}*(T_8^3-T_0^3)/3+D_{air}*(T_8^4-T_0^4)/4$$

$$S_{air_8}=A_{air}*(LN(T_8)-LN(T_0))+B_{air}*(T_8-T_0)+C_{air}*(T_8^2-T_0^2)/2+D_{air}*(T_8^3-T_0^3)/3-R_{bar}*LN(P_8/P_0*air_8/N_8)$$

$$EX_{ph_{air_8}}=DELTAH_{air_8}-T_0*S_{air_8}$$

$$EX_{ch_{air_8}}=air_8/N_8*(EPS_{ch_{air}}+R_{bar}*T_0*LN(air_8/N_8))$$

$$DELTAH_{N2_8}=A_{N2}*(T_8-T_0)+B_{N2}*(T_8^2-T_0^2)/2+C_{N2}*(T_8^3-T_0^3)/3+D_{N2}*(T_8^4-T_0^4)/4$$

$$S_{N2_8}=A_{N2}*(LN(T_8)-LN(T_0))+B_{N2}*(T_8-T_0)+C_{N2}*(T_8^2-T_0^2)/2+D_{N2}*(T_8^3-T_0^3)/3-R_{bar}*LN(P_8/P_0*N2_8/N_8)$$

$$EX_{ph_{N2_8}}=DELTAH_{N2_8}-T_0*S_{N2_8}$$

$$EX_{ch_{N2_8}}=N2_8/N_8*(EPS_{ch_{N2}}+R_{bar}*T_0*LN(N2_8/N_8))$$

$$DELTAH_{H2O_8}=A_{H2O}*(T_8-T_0)+B_{H2O}*(T_8^2-T_0^2)/2+C_{H2O}*(T_8^3-T_0^3)/3+D_{H2O}*(T_8^4-T_0^4)/4$$

$$S_{H2O_8}=A_{H2O}*(LN(T_8)-LN(T_0))+B_{H2O}*(T_8-T_0)+C_{H2O}*(T_8^2-T_0^2)/2+D_{H2O}*(T_8^3-T_0^3)/3-R_{bar}*LN(P_8/P_0*H2O_8/N_8)$$

$$EX_{ph_{H2O_8}}=DELTAH_{H2O_8}-T_0*S_{H2O_8}$$

$$EX_{ch_{H2O_8}}=H2O_8/N_8*(EPS_{ch_{H2O}}+R_{bar}*T_0*LN(H2O_8/N_8))$$

"Physical and chemical exergies with flow at turbine 7_8 exit"

$$EX_{ph_8}=CO2_8*EX_{ph_{CO2_8}}+air_8*EX_{ph_{air_8}}+N2_8*EX_{ph_{N2_8}}+H2O_8*EX_{ph_{H2O_8}}$$

$$EX_{ch_8}=CO2_8*EX_{ch_{CO2_8}}+air_8*EX_{ch_{air_8}}+N2_8*EX_{ch_{N2_8}}+H2O_8*EX_{ch_{H2O_8}}$$

$$EX_8=EX_{ph_8}+EX_{ch_8}$$

"Exergy destroyed in turbine 7_8"

$$EX_{Ir_{Tur_{7_8}}}=T_0*(H2O_8*(S_{H2O_8}+DELTA_{S_{H2O}})+CO2_8*(S_{CO2_8}+DELTA_{S_{CO2}})+N2_8*(S_{N2_8}+DELTA_{S_{N2}})+air_8*(S_{air_8}+DELTA_{S_{air}}))$$

$$EX_{Ir_Tur_7_8_i} = T_0 * (H_2O_7 * (S_{H_2O_7} + \Delta S_{H_2O}) + CO_2_7 * (S_{CO_2_7} + \Delta S_{CO_2}) + N_2_7 * (S_{N_2_7} + \Delta S_{N_2}) + air_7 * (S_{air_7} + \Delta S_{air}))$$

$$EX_{Ir_Tur_7_8} = EX_{Ir_Tur_7_8_i} - EX_{Ir_Tur_7_8_e}$$

"Enthalpy at turbine inlet"

$$B_4 = CO_2_8 * (\Delta H_{CO_2_8} + \Delta H_{F_{CO_2}} * 1000) + H_2O_8 * (\Delta H_{H_2O_8} + \Delta H_{F_{H_2O}} * 1000) + air_8 * \Delta H_{air_8} + N_2_8 * \Delta H_{N_2_8}$$

"Work of Turbine 7_8"

$$W_{dot_7_8} = B_1 - B_4$$

{Compressor 24-25 which compresses air from ambient temperature, T₂₄ to a temperature of T₂₅ need by SOFC}

$$T_{24} = T_0; P_{24} = P_0$$

$$P_{35} = P_{10}$$

$$P_{25} = P_{35} + 0.05 * P_{35}$$

$$M_{dot_25} = M_{dot_24}; M_{dot_35} = M_{dot_25}$$

$$air_{24} = M_{dot_24} / MW_{air}; N_{24} = air_{24}$$

$$air_{25} = M_{dot_25} / MW_{air}; N_{25} = air_{25}$$

{Compressor inlet temperature, inlet pressure and exit pressure are known}

$P_{25} = P_{24} * (1 + \eta_c * (T_{25}/T_{24} - 1))^{(\gamma_{air}/(\gamma_{air} - 1))}$ to find exit compressor temperature, T₂₅"

$$\Delta H_{air_24} = A_{air} * (T_{24} - T_0) + B_{air} * (T_{24}^2 - T_0^2) / 2 + C_{air} * (T_{24}^3 - T_0^3) / 3 + D_{air} * (T_{24}^4 - T_0^4) / 4$$

$$S_{air_24} = A_{air} * (\ln(T_{24}) - \ln(T_0)) + B_{air} * (T_{24} - T_0) + C_{air} * (T_{24}^2 - T_0^2) / 2 + D_{air} * (T_{24}^3 - T_0^3) / 3 - R_{bar} * \ln(P_{24}/P_0 * air_{24}/N_{24})$$

$$EX_{ph_air_24} = \Delta H_{air_24} - T_0 * S_{air_24}$$

$$EX_{ch_air_24} = air_{35} / N_{bi} * (EPS_{ch_air} + R_{bar} * T_0 * \ln(air_{24}/N_{24}))$$

"physical and chemical exergies at compressor 24_25 inlet, state 24"

$$EX_{ph_24} = air_{24} * EX_{ph_air_24}$$

$$EX_{ch_24} = air_{24} * EX_{ch_air_24}$$

$$EX_{24} = EX_{ph_24} + EX_{ch_24}$$

$$\Delta H_{air_25} = A_{air} * (T_{25} - T_0) + B_{air} * (T_{25}^2 - T_0^2) / 2 + C_{air} * (T_{25}^3 - T_0^3) / 3 + D_{air} * (T_{25}^4 - T_0^4) / 4$$

$$S_{air_25} = A_{air} * (\ln(T_{25}) - \ln(T_0)) + B_{air} * (T_{25} - T_0) + C_{air} * (T_{25}^2 - T_0^2) / 2 + D_{air} * (T_{25}^3 - T_0^3) / 3 - R_{bar} * \ln(P_{25}/P_0 * air_{25}/N_{25})$$

$$EX_{ph_air_25} = \Delta H_{air_25} - T_0 * S_{air_25}$$

$$EX_{ch_air_25} = air_{25} / N_{25} * (EPS_{ch_air} + R_{bar} * T_0 * \ln(air_{25}/N_{25}))$$

"physical and chemical exergies at compressor 24_25 inlet, state 25"

$$EX_{ph_25} = air_{25} * EX_{ph_air_25}$$

$$EX_{ch_25} = air_{25} * EX_{ch_air_25}$$

$$EX_{25} = EX_{ph_25} + EX_{ch_25}$$

"Exergy destroyed in compressor 24_25"

$$EX_{Ir_Comp24_25} = T_0 * (air_{25} * (S_{air_25} + \Delta S_{air}) - air_{24} * (S_{air_24} + \Delta S_{air}))$$

"Exergy destroyed in heat exchanger 25_35"

$$EX_{Ir_HE_25_35} = T_0 * (air_{35} * (S_{air_35} + \Delta S_{air}) - air_{25} * (S_{air_25} + \Delta S_{air}))$$

"Work of compressor 24-25"

$W_{dot_{24,25}} = air_{24} * (DELTAH_{air_{25}} - DELTAH_{air_{24}})$
 $P_{r_{24,25}} = P_{25} / P_{24}$ {pressure ratio; one of parameters need to study}
 $T_{35} = 430$ "Assumed"

{Heat exchanger line 25-35}
 $Q_{dot_{25,35}} = air_{35} * (DELTAH_{air_{35}} - DELTAH_{air_{25}})$

{Heat exchanger line 36-5}
 $P_{36} = P_3; T_{36} = T_{26}$
 $H2_{36} = N_{H2}; CH4_{36} = N_{CH4}; CO_{36} = N_{CO}; CO2_{36} = N_{CO2}$
 $N_{36} = N_{H2} + N_{CH4} + N_{CO} + N_{CO2}$
 $MW_{36} = H2_{36} / N_{36} * MW_{H2} + CH4_{36} / N_{36} * MW_{CH4} + CO_{36} / N_{36} * MW_{CO} + CO2_{36} / N_{36} * MW_{CO2}$
 $M_{dot_{36}} = N_{36} * MW_{36}$
 $Q_{dot_{36,16}} = Q_{dot_{25,35}}$ "To find $M_{dot_{24}}$ "

"Heat exchange in heat exchanger 36-5"
 $Q_{dot_{36,16}} = DELTAH_{36} - DELTAH_{16}$

{calculate delta enthalpy for hydrogen in kJ/kmol at heat exchanger 36-5 inlet}
 $DELTAH_{H2_{36}} = A_{H2} * (T_{36} - T_0) + B_{H2} * (T_{36}^2 - T_0^2) / 2 + C_{H2} * (T_{36}^3 - T_0^3) / 3 + D_{H2} * (T_{36}^4 - T_0^4) / 4$
 $S_{H2_{36}} = A_{H2} * (LN(T_{36}) - LN(T_0)) + B_{H2} * (T_{36} - T_0) + C_{H2} * (T_{36}^2 - T_0^2) / 2 + D_{H2} * (T_{36}^3 - T_0^3) / 3 - R_{bar} * LN(P_{36} / P_0 * H2_{36} / N_{36})$
 $EX_{ph_{H2_{36}}} = DELTAH_{H2_{36}} - T_0 * S_{H2_{36}}$
 $EX_{ch_{H2_{36}}} = H2_{36} / N_{36} * (EPS_{ch_{H2}} + R_{bar} * T_0 * LN(H2_{36} / N_{36}))$

{calculate delta enthalpy for carbon monoxide in kJ/kmol at heat exchanger 36-5 inlet}
 $DELTAH_{CO_{36}} = A_{CO} * (T_{36} - T_0) + B_{CO} * (T_{36}^2 - T_0^2) / 2 + C_{CO} * (T_{36}^3 - T_0^3) / 3 + D_{CO} * (T_{36}^4 - T_0^4) / 4$
 $S_{CO_{36}} = A_{CO} * (LN(T_{36}) - LN(T_0)) + B_{CO} * (T_{36} - T_0) + C_{CO} * (T_{36}^2 - T_0^2) / 2 + D_{CO} * (T_{36}^3 - T_0^3) / 3 - R_{bar} * LN(P_{36} / P_0 * CO_{36} / N_{36})$
 $EX_{ph_{CO_{36}}} = DELTAH_{CO_{36}} - T_0 * S_{CO_{36}}$
 $EX_{ch_{CO_{36}}} = CO_{36} / N_{36} * (EPS_{ch_{CO}} + R_{bar} * T_0 * LN(CO_{36} / N_{36}))$

{calculate delta enthalpy for carbon dioxide in kJ/kmol at heat exchanger 36-5 inlet}
 $DELTAH_{CO2_{36}} = A_{CO2} * (T_{36} - T_0) + B_{CO2} * (T_{36}^2 - T_0^2) / 2 + C_{CO2} * (T_{36}^3 - T_0^3) / 3 + D_{CO2} * (T_{36}^4 - T_0^4) / 4$
 $S_{CO2_{36}} = A_{CO2} * (LN(T_{36}) - LN(T_0)) + B_{CO2} * (T_{36} - T_0) + C_{CO2} * (T_{36}^2 - T_0^2) / 2 + D_{CO2} * (T_{36}^3 - T_0^3) / 3 - R_{bar} * LN(P_{36} / P_0 * CO2_{36} / N_{36})$
 $EX_{ph_{CO2_{36}}} = DELTAH_{CO2_{36}} - T_0 * S_{CO2_{36}}$
 $EX_{ch_{CO2_{36}}} = CO2_{36} / N_{36} * (EPS_{ch_{CO2}} + R_{bar} * T_0 * LN(CO2_{36} / N_{36}))$

{calculate delta enthalpy for methane in kJ/kmol at heat exchanger 36-5 inlet}
 $DELTAH_{CH4_{36}} = A_{CH4} * (T_{36} - T_0) + B_{CH4} * (T_{36}^2 - T_0^2) / 2 + C_{CH4} * (T_{36}^3 - T_0^3) / 3 + D_{CH4} * (T_{36}^4 - T_0^4) / 4$
 $S_{CH4_{36}} = A_{CH4} * (LN(T_{36}) - LN(T_0)) + B_{CH4} * (T_{36} - T_0) + C_{CH4} * (T_{36}^2 - T_0^2) / 2 + D_{CH4} * (T_{36}^3 - T_0^3) / 3 - R_{bar} * LN(P_{36} / P_0 * CH4_{36} / N_{36})$
 $EX_{ph_{CH4_{36}}} = DELTAH_{CH4_{36}} - T_0 * S_{CH4_{36}}$
 $EX_{ch_{CH4_{36}}} = CH4_{36} / N_{36} * (EPS_{ch_{CH4}} + R_{bar} * T_0 * LN(CH4_{36} / N_{36}))$

"Physical and chemical exergy with flow at heat exchanger 36_5 inlet"

EX_ph_36=CO_36*EX_ph_CO_36+CO2_36*EX_ph_CO2_36+H2_36*EX_ph_H2_36+CH4_36*EX_ph_CH4_36

EX_ch_36=CO_36*EX_ch_CO_36+CO2_36*EX_ch_CO2_36+H2_36*EX_ch_H2_36+CH4_36*EX_ch_CH4_36

EX_36=EX_ph_36+EX_ch_36

"Exergy destroyed in heat exchanger 36_5"

EX_Ir_HE_36_16_i=T_0*(H2_36*(S_H2_36+DELTA_S_H2)+CO_36*(S_CO_36+DELTA_S_CO)+CO2_36*(S_CO2_36+DELTA_S_CO2)+CH4_36*(S_CH4_36+DELTA_S_CH4))

EX_Ir_HE_36_16_e=T_0*(H2_16*(S_H2_16+DELTA_S_H2)+CO_16*(S_CO_16+DELTA_S_CO)+CO2_16*(S_CO2_16+DELTA_S_CO2)+CH4_16*(S_CH4_16+DELTA_S_CH4))

EX_Ir_HE_36_16=EX_Ir_HE_36_16_i-EX_Ir_HE_36_16_e

"Enthalpy at heat exchanger 36-5 inlet"

DELTAH_36=H2_36*DELTAH_H2_36+CO_36*(DELTAHF_CO*1000+DELTAH_CO_36)+CO2_36*(DELTAHF_CO2*1000+DELTAH_CO2_36)+CH4_36*(DELTAHF_CH4*1000+DELTAH_CH4_36)

DELTAH_16=H2_16*DELTAH_H2_16+CO_16*(DELTAHF_CO*1000+DELTAH_CO_16)+CO2_16*(DELTAHF_CO2*1000+DELTAH_CO2_16)+CH4_16*(DELTAHF_CH4*1000+DELTAH_CH4_16)

"Total number of moles at steam reforming inlet"

N_SRi=CH4_16+CO_16+CO2_16+H2_16+H2O_15

"State 16"

CH4_16=N_CH4;CO_16=N_CO;CO2_16=N_CO2;H2_16=N_H2"Molar flow from gasification process"

T_16=T_0+100

P_16=P_36

N_16=CH4_16+CO_16+CO2_16+H2_16"No hydrogen sent to SOFC from gasification"

M_dot_16=M_dot_36

{Calculation of delta enthalpy for carbon monoxide at steam reformer inlet}

A_CO=28.16;B_CO=0.1675*10⁽⁻²⁾;C_CO=0.5372*10⁽⁻⁵⁾;D_CO=-2.222*10⁽⁻⁹⁾;DELTAHF_CO=-110.53[kJ/mol];DELTA_S_CO=197.65[kJ/kmol-K]

DELTAH_CO_16= A_CO*(T_16-T_0) +B_CO*(T_16²-T_0²)/2+C_CO*(T_16³-T_0³)/3+D_CO*(T_16⁴-T_0⁴)/4

S_CO_16= A_CO*(LN (T_16)-LN (T_0)) +B_CO*(T_16-T_0)+C_CO*(T_16²-T_0²)/2 + D_CO*(T_16³-T_0³)/3-R_bar*LN(P_16/P_0*CO_16/N_SRi)

EX_ph_CO_16=DELTAH_CO_16-T_0*S_CO_16

EX_ch_CO_16=CO_16/N_SRi*(EPS_ch_CO+R_bar*T_0*LN (CO_16/N_SRi))

{calculate delta enthalpy for carbon dioxide at steam reformer inlet}

A_CO2=22.26;B_CO2=5.981*10⁽⁻²⁾;C_CO2=-3.501*10⁽⁻⁵⁾;D_CO2=-7.469*10⁽⁻⁹⁾;DELTAHF_CO2=-393.52[kJ/mol];DELTA_S_CO2=213.8[kJ/kmol-K]

DELTAH_CO2_16= A_CO2*(T_16-T_0)+B_CO2*(T_16²-T_0²)/2+C_CO2*(T_16³-T_0³)/3+D_CO2*(T_16⁴-T_0⁴)/4

$$S_{CO2_16} = A_{CO2} * (\ln(T_{16}) - \ln(T_0)) + B_{CO2} * (T_{16} - T_0) + C_{CO2} * (T_{16}^2 - T_0^2) / 2 + D_{CO2} * (T_{16}^3 - T_0^3) / 3 - R_{bar} * \ln(P_{16} / P_0 * CO2_16 / N_{SRi})$$

$$EX_{ph_CO2_16} = \Delta H_{CO2_16} - T_0 * S_{CO2_16}$$

$$EX_{ch_CO2_16} = CO2_16 / N_{SRi} * (\epsilon_{ch_CO2} + R_{bar} * T_0 * \ln(CO2_16 / N_{SRi}))$$

{ calculate delta enthalpy for methane in kJ/kmol at steam reforming inlet }

$$A_{CH4} = 19.89; B_{CH4} = 5.204 * 10^{-2}; C_{CH4} = 1.269 * 10^{-5}; D_{CH4} = -11.01 * 10^{-9}; \Delta H_{f,CH4} = -74.8 \text{ [kJ/mol]}; \Delta S_{CH4} = 186.16 \text{ [kJ/kmol-K]}$$

$$\Delta H_{CH4_16} = A_{CH4} * (T_{16} - T_0) + B_{CH4} * (T_{16}^2 - T_0^2) / 2 + C_{CH4} * (T_{16}^3 - T_0^3) / 3 + D_{CH4} * (T_{16}^4 - T_0^4) / 4$$

$$S_{CH4_16} = A_{CH4} * (\ln(T_{16}) - \ln(T_0)) + B_{CH4} * (T_{16} - T_0) + C_{CH4} * (T_{16}^2 - T_0^2) / 2 + D_{CH4} * (T_{16}^3 - T_0^3) / 3 - R_{bar} * \ln(P_{16} / P_0 * CH4_16 / N_{SRi})$$

$$EX_{ph_CH4_16} = \Delta H_{CH4_16} - T_0 * S_{CH4_16}$$

$$EX_{ch_CH4_16} = CH4_16 / N_{SRi} * (\epsilon_{ch_CH4} + R_{bar} * T_0 * \ln(CH4_16 / N_{SRi}))$$

{ Calculations of delta enthalpy for H2 in kJ/kmol at steam reforming inlet }

$$\Delta H_{H2_16} = A_{H2} * (T_{16} - T_0) + B_{H2} * (T_{16}^2 - T_0^2) / 2 + C_{H2} * (T_{16}^3 - T_0^3) / 3 + D_{H2} * (T_{16}^4 - T_0^4) / 4$$

$$S_{H2_16} = A_{H2} * (\ln(T_{16}) - \ln(T_0)) + B_{H2} * (T_{16} - T_0) + C_{H2} * (T_{16}^2 - T_0^2) / 2 + D_{H2} * (T_{16}^3 - T_0^3) / 3 - R_{bar} * \ln(P_{16} / P_0 * H2_16 / N_{16})$$

$$EX_{ph_H2_16} = \Delta H_{H2_16} - T_0 * S_{H2_16}$$

$$EX_{ch_H2_16} = H2_16 / N_{16} * (\epsilon_{ch_H2} + R_{bar} * T_0 * \ln(H2_16 / N_{16}))$$

"State 15"

$T_{15} = T_{20}$ "Temperature of by product water same as SOFC temperature"

$P_{15} = P_{20}$ "pressure of by product water same as SOFC pressure"

$H2O_{15} = N_{CH4}; N_{15} = H2O_{15}; M_{dot_{15}} = H2O_{15} * MW_{H2O}$ "Steam consumed by steam reforming reaction"

{ Calculations of delta enthalpy for water in kJ/ kmol at steam reforming inlet }

$$A_{H2O} = 32.24; B_{H2O} = 0.1923 * 10^{-2}; C_{H2O} = 1.055 * 10^{-5}; D_{H2O} = -3.595 * 10^{-9}; \Delta H_{f,H2O} = -241.83 \text{ [kJ/mol]}; \Delta S_{H2O} = 188.83 \text{ [kJ/kmol-K]}$$

$$\Delta H_{H2O_15} = A_{H2O} * (T_{15} - T_0) + B_{H2O} * (T_{15}^2 - T_0^2) / 2 + C_{H2O} * (T_{15}^3 - T_0^3) / 3 + D_{H2O} * (T_{15}^4 - T_0^4) / 4$$

$$S_{H2O_15} = A_{H2O} * (\ln(T_{15}) - \ln(T_0)) + B_{H2O} * (T_{15} - T_0) + C_{H2O} * (T_{15}^2 - T_0^2) / 2 + D_{H2O} * (T_{15}^3 - T_0^3) / 3$$

$$EX_{ph_H2O_15} = \Delta H_{H2O_15} - T_0 * S_{H2O_15}$$

$$EX_{ch_H2O_15} = H2O_{15} / N_{SRi} * (\epsilon_{ch_H2O} + R_{bar} * T_0 * \ln(H2O_{15} / N_{SRi}))$$

"Physical and chemical exergy with flow at SRi"

$$EX_{ph_SRi} = CO_{16} * EX_{ph_CO_{16}} + CO2_{16} * EX_{ph_CO2_{16}} + CH4_{16} * EX_{ph_CH4_{16}} + H2_{16} * EX_{ph_H2_{16}} + H2O_{15} * EX_{ph_H2O_{15}}$$

$$EX_{ch_SRi} = CO_{16} * EX_{ch_CO_{16}} + CO2_{16} * EX_{ch_CO2_{16}} + CH4_{16} * EX_{ch_CH4_{16}} + H2_{16} * EX_{ch_H2_{16}} + H2O_{15} * EX_{ch_H2O_{15}}$$

$$EX_{SRi} = EX_{ph_SRi} + EX_{ch_SRi}$$

$$EX_{16} = CO_{16} * (EX_{ph_CO_{16}} + EX_{ch_CO_{16}}) + CO2_{16} * (EX_{ph_CO2_{16}} + EX_{ch_CO2_{16}}) + CH4_{16} * (EX_{ph_CH4_{16}} + EX_{ch_CH4_{16}}) + H2_{16} * (EX_{ph_H2_{16}} + EX_{ch_H2_{16}})$$

$$EX_{15} = H2O_{15} * (EX_{ph_H2O_{15}} + EX_{ch_H2O_{15}})$$

"State 17"

$P_{17}=P_{16}-0.05*P_{16}$
 $CO_{17}=CH4_{16}+N_{CO};CO2_{17}=CO2_{16};H2_{17}=3*CH4_{16}+H2_{16}$
 $N_{17}=H2_{17}+CO_{17}+CO2_{17}$
 $MW_{17}=H2_{17}/N_{17}*MW_{H2}+CO_{17}/N_{17}*MW_{CO}+CO2_{17}/N_{17}*MW_{CO2}$
 $M_{dot_{17}}=N_{17}*MW_{17}$
 $N_{SRe}=N_{17}$

{calculate delta enthalpy for hydrogen in kJ/kmol at steam reforming exit}
 $DELTAH_{H2_{17}}=A_{H2}*(T_{17}-T_0)+B_{H2}*(T_{17}^2-T_0^2)/2+C_{H2}*(T_{17}^3-T_0^3)/3+D_{H2}*(T_{17}^4-T_0^4)/4$
 $S_{H2_{17}}=A_{H2}*(LN(T_{17})-LN(T_0))+B_{H2}*(T_{17}-T_0)+C_{H2}*(T_{17}^2-T_0^2)/2+D_{H2}*(T_{17}^3-T_0^3)/3-R_{bar}*LN(P_{17}/P_0*H2_{17}/N_{SRe})$
 $EX_{ph_{H2_{17}}}=DELTAH_{H2_{17}}-T_0*S_{H2_{17}}$
 $EX_{ch_{H2_{17}}}=H2_{17}/N_{17}*(EPS_{ch_{H2}}+R_{bar}*T_0*LN(H2_{17}/N_{SRe}))$

{Calculation of delta enthalpy for carbon monoxide in kJ/kmol at steam reforming exit}
 $DELTAH_{CO_{17}}=A_{CO}*(T_{17}-T_0)+B_{CO}*(T_{17}^2-T_0^2)/2+C_{CO}*(T_{17}^3-T_0^3)/3+D_{CO}*(T_{17}^4-T_0^4)/4$
 $S_{CO_{17}}=A_{CO}*(LN(T_{17})-LN(T_0))+B_{CO}*(T_{17}-T_0)+C_{CO}*(T_{17}^2-T_0^2)/2+D_{CO}*(T_{17}^3-T_0^3)/3-R_{bar}*LN(P_{17}/P_0*CO_{17}/N_{SRe})$
 $EX_{ph_{CO_{17}}}=DELTAH_{CO_{17}}-T_0*S_{CO_{17}}$
 $EX_{ch_{CO_{17}}}=CO_{17}/N_{17}*(EPS_{ch_{CO}}+R_{bar}*T_0*LN(CO_{17}/N_{SRe}))$

{Calculations of delta enthalpy for carbon dioxide in kJ/kmol at steam reforming exit}
 $DELTAH_{CO2_{17}}=A_{CO2}*(T_{17}-T_0)+B_{CO2}*(T_{17}^2-T_0^2)/2+C_{CO2}*(T_{17}^3-T_0^3)/3+D_{CO2}*(T_{17}^4-T_0^4)/4$
 $S_{CO2_{17}}=A_{CO2}*(LN(T_{17})-LN(T_0))+B_{CO2}*(T_{17}-T_0)+C_{CO2}*(T_{17}^2-T_0^2)/2+D_{CO2}*(T_{17}^3-T_0^3)/3-R_{bar}*LN(P_{17}/P_0*CO2_{17}/N_{SRe})$
 $EX_{ph_{CO2_{17}}}=DELTAH_{CO2_{17}}-T_0*S_{CO2_{17}}$
 $EX_{ch_{CO2_{17}}}=CO2_{17}/N_{17}*(EPS_{ch_{CO2}}+R_{bar}*T_0*LN(CO2_{17}/N_{SRe}))$

"Physical and chemical exergies with flow at SRe"
 $EX_{ph_{SRe}}=CO_{17}*EX_{ph_{CO_{17}}}+CO2_{17}*EX_{ph_{CO2_{17}}}+H2_{17}*EX_{ph_{H2_{17}}}$
 $EX_{ch_{SRe}}=CO_{17}*EX_{ch_{CO_{17}}}+CO2_{17}*EX_{ch_{CO2_{17}}}+H2_{17}*EX_{ch_{H2_{17}}}$
 $EX_{SRe}=EX_{ph_{SRe}}+EX_{ch_{SRe}}$

"Exergy destruction in SR"
 $EX_{Ir_{SR2}}=T_0*(H2_{17}*(S_{H2_{17}}+DELTA_{S_{H2}})+CO2_{17}*(S_{CO2_{17}}+DELTA_{S_{CO2}})+CO_{17}*(S_{CO_{17}}+DELTA_{S_{CO}}))$
 $EX_{Ir_{SR1}}=T_0*(CH4_{16}*(S_{CH4_{16}}+DELTA_{S_{CH4}})+CO2_{16}*(S_{CO2_{16}}+DELTA_{S_{CO2}})+CO_{16}*(S_{CO_{16}}+DELTA_{S_{CO}})+H2O_{15}*(S_{H2O_{15}}+DELTA_{S_{H2O}}))$
 $EX_{Ir_{SR}}=EX_{Ir_{SR2}}-EX_{Ir_{SR1}}$

{Energy balance of the steam reforming reactor to find T₁₇}
 $SR_A=H2_{16}*DELTAH_{H2_{16}}+CH4_{16}*(DELTAHF_{CH4}*1000+DELTAH_{CH4_{16}})+CO2_{16}*(DELTAHF_{CO2}*1000+DELTAH_{CO2_{16}})$
 $SR_B=CO_{16}*(DELTAHF_{CO}*1000+DELTAH_{CO_{16}})+H2O_{15}*(DELTAHF_{H2O}*1000+DELTAH_{H2O_{15}})$
 $SR_1=SR_A+SR_B$

$$SR_2 = H2_{17} * DELTAH_{H2_{17}} + CO_{17} * (DELTAHF_{CO} * 1000 + DELTAH_{CO_{17}}) + CO2_{17} * (DELTAHF_{CO2} * 1000 + DELTAH_{CO2_{17}})$$

SR_2=SR_1"From which will find exit temperature from steam reformer, T_17"

{Calculations for heat exchanger 17-18}

"State 18"

P_18=P_17-P_17*0.05"Pressure of flow gas is given in terms of mole fraction"

T_18=T_0+13"Assumed exit temperature preferred to met gas shift reaction in the next step"

N_18=N_17

M_dot_18=M_dot_17

$$DELTAH_{18} = H2_{18} * DELTAH_{H2_{18}} + CO_{18} * (DELTAHF_{CO} * 1000 + DELTAH_{CO_{18}}) + CO2_{18} * (DELTAHF_{CO2} * 1000 + DELTAH_{CO2_{18}})$$

$$DELTAH_{17} = H2_{17} * DELTAH_{H2_{17}} + CO_{17} * (DELTAHF_{CO} * 1000 + DELTAH_{CO_{17}}) + CO2_{17} * (DELTAHF_{CO2} * 1000 + DELTAH_{CO2_{17}})$$

"Heat need to be extracted before gas shift reaction"

$$Q_{dot_{17_{18}}} = (DELTAH_{17} - DELTAH_{18})$$

{Calculations for air preheating}

Gama_air=1.4; Eta_c=0.80

T_SOFC=1000[K]"SOFC temperature"

P_SOFC=120[kPa]"SOFC pressure"

P_10=P_SOFC

M_dot_10=N_air*MW_air

"Compressor 0-9"

P_9=P_10

$$P_9 = P_0 * (1 + Eta_c * (T_9/T_0 - 1))^{Gama_air / (Gama_air - 1)}$$

air_9=N_air; N_9=air_9

$$DELTAH_{air_9} = A_{air} * (T_9 - T_0) + B_{air} * (T_9^2 - T_0^2) / 2 + C_{air} * (T_9^3 - T_0^3) / 3 + D_{air} * (T_9^4 - T_0^4) / 4$$

$$S_{air_9} = A_{air} * (\ln(T_9) - \ln(T_0)) + B_{air} * (T_9 - T_0) + C_{air} * (T_9^2 - T_0^2) / 2 + D_{air} * (T_9^3 - T_0^3) / 3 - R_{bar} * \ln(P_9/P_0 * air_9/N_9)$$

$$EX_{ph_air_9} = DELTAH_{air_9} - T_0 * S_{air_9}$$

$$EX_{ch_air_9} = air_9/N_9 * (EPS_{ch_air} + R_{bar} * T_0 * \ln(air_9/N_9))$$

$$h_{air_9} = A_{air} * T_9 + B_{air} * T_9^2 / 2 + C_{air} * T_9^3 / 3 + D_{air} * T_9^4 / 4$$

"Physical and chemical exergy at compressor 0-9 exit"

$$EX_{ph_9} = air_9 * EX_{ph_air_9}$$

$$EX_{ch_9} = air_9 * EX_{ch_air_9}$$

$$EX_9 = EX_{ph_9} + EX_{ch_9}$$

air_0=N_air; N_0=air_0

$$DELTAH_{air_0} = A_{air} * (T_0 - T_0) + B_{air} * (T_0^2 - T_0^2) / 2 + C_{air} * (T_0^3 - T_0^3) / 3 + D_{air} * (T_0^4 - T_0^4) / 4$$

$$S_{air_0} = A_{air} * (\ln(T_0) - \ln(T_0)) + B_{air} * (T_0 - T_0) + C_{air} * (T_0^2 - T_0^2) / 2 + D_{air} * (T_0^3 - T_0^3) / 3 - R_{bar} * \ln(P_0/P_0 * air_0/N_0)$$

$$EX_{ph_air_0} = DELTAH_{air_0} - T_0 * S_{air_0}$$

$$EX_{ch_air_0} = air_0/N_0 * (EPS_{ch_air} + R_{bar} * T_0 * \ln(air_0/N_0))$$

"Physical and chemical exergy at compressor 0-9 inlet"

$$EX_{ph_0} = air_0 * EX_{ph_air_0}$$

$$EX_{ch_0} = air_0 * EX_{ch_air_0}$$

$$EX_0 = EX_{ph_0} + EX_{ch_0}$$

"Exergy destruction in compressor 0-9"

$$EX_{Ir_Comp_0_9} = T_0 * (air_9 * (S_{air_9} + DELTA_{S_air}) - air_0 * (S_{air_0} + DELTA_{S_air}))$$

$$W_{dot_0_9} = M_{dot_9} * Cp_{air} * (T_9 - T_0) \text{ "Work rate done on compressor 0-9"}$$

$$M_{dot_9} = M_{dot_10}$$

air_10=N_air" Air that needs for electrochemical reaction"

$$Q_{dot_9_10} = air_9 * (h_{air_10} - h_{air_9})$$

$$Q_{dot_17_18} = Q_{dot_9_10} \text{ "To find } T_{10}, \text{ Temperature of the preheating air"}$$

"Calculations for SOFC-SOEC"

$$N_{SOFCi} = air_{10}$$

$$N_{SOFCe} = O2_{11} + N2_{11} + O2_{12}$$

"State 10"

$$DELTAH_{air_10} = A_{air} * (T_{10} - T_0) + B_{air} * (T_{10}^2 - T_0^2) / 2 + C_{air} * (T_{10}^3 - T_0^3) / 3 + D_{air} * (T_{10}^4 - T_0^4) / 4$$

$$S_{air_10} = A_{air} * (\ln(T_{10}) - \ln(T_0)) + B_{air} * (T_{10} - T_0) + C_{air} * (T_{10}^2 - T_0^2) / 2 + D_{air} * (T_{10}^3 - T_0^3) / 3 - R_{bar} * \ln(P_{10} / P_0 * air_{10} / N_{SOFCi})$$

$$EX_{ph_air_10} = DELTAH_{air_10} - T_0 * S_{air_10}$$

$$EX_{ch_air_10} = air_{10} / N_{SOFCi} * (EPS_{ch_air} + R_{bar} * T_0 * \ln(air_{10} / N_{SOFCi}))$$

$$EX_{10} = air_{10} * (EX_{ph_air_10} + EX_{ch_air_10})$$

$$h_{air_10} = A_{air} * T_{10} + B_{air} * T_{10}^2 / 2 + C_{air} * T_{10}^3 / 3 + D_{air} * T_{10}^4 / 4$$

"Physical and chemical exergy with flow in to SOFC"

$$EX_{ph_SOFCi} = air_{10} * EX_{ph_air_10}$$

$$EX_{ch_SOFCi} = air_{10} * EX_{ch_air_10}$$

$$EX_{SOFCi} = EX_{ph_SOFCi} + EX_{ch_SOFCi}$$

"State 12 is added after adding SOEC"

$$U_{F_SOEC} = U_f; P_{12} = P_{14}; T_{12} = T_{14}$$

$$O2_{12} = U_{F_SOEC} * N_{O2}$$

$$DELTAH_{O2_12} = A_{O2} * (T_{12} - T_0) + B_{O2} * (T_{12}^2 - T_0^2) / 2 + C_{O2} * (T_{12}^3 - T_0^3) / 3 + D_{O2} * (T_{12}^4 - T_0^4) / 4$$

$$S_{O2_12} = A_{O2} * (\ln(T_{12}) - \ln(T_0)) + B_{O2} * (T_{12} - T_0) + C_{O2} * (T_{12}^2 - T_0^2) / 2 + D_{O2} * (T_{12}^3 - T_0^3) / 3 - R_{bar} * \ln(P_{12} / P_0 * O2_{12} / N_{SOFCe})$$

$$EX_{ph_O2_12} = DELTAH_{O2_12} - T_0 * S_{O2_12}$$

$$EX_{ch_O2_12} = O2_{12} / N_{SOFCe} * (EPS_{ch_H2O} + R_{bar} * T_0 * \ln(O2_{12} / N_{SOFCe}))$$

$$EX_{12} = O2_{12} * (EX_{ph_O2_12} + EX_{ch_O2_12})$$

"State 14"

$$O2_{10} = 21 / 100 * air_{10}; H2O_{14} = 0.5 * O2_{10}; M_{dot_14} = H2O_{14} * MW_{H2O} \text{ "Producer steam in SOFC"}$$

$$T_{14} = T_{SOFC}; P_{14} = P_{10}$$

$\Delta H_{H_2O,14} = A_{H_2O} \cdot (T_{14} - T_0) + B_{H_2O} \cdot (T_{14}^2 - T_0^2) / 2 + C_{H_2O} \cdot (T_{14}^3 - T_0^3) / 3 + D_{H_2O} \cdot (T_{14}^4 - T_0^4) / 4$
 $S_{H_2O,14} = A_{H_2O} \cdot (\ln(T_{14}) - \ln(T_0)) + B_{H_2O} \cdot (T_{14} - T_0) + C_{H_2O} \cdot (T_{14}^2 - T_0^2) / 2 + D_{H_2O} \cdot (T_{14}^3 - T_0^3) / 3 - R_{bar} \cdot \ln(P_{14} / P_0 \cdot H_{2O,14} / N_{SOFCe})$
 $EX_{ph,H_2O,14} = \Delta H_{H_2O,14} - T_0 \cdot S_{H_2O,14}$
 $EX_{ch,H_2O,14} = H_{2O,14} / N_{SOFCe} \cdot (EPS_{ch,H_2O} + R_{bar} \cdot T_0 \cdot \ln(H_{2O,14} / N_{SOFCe}))$
 $EX_{14} = H_{2O,14} \cdot (EX_{ph,H_2O,14} + EX_{ch,H_2O,14})$
 $EX_{ch,H_2,11,SOFCe} = 0$
 $EX_{ch,O_2,11,SOFCe} = O_{2,11} / N_{SOFCe} \cdot (EPS_{ch,O_2} + R_{bar} \cdot T_0 \cdot \ln(O_{2,11} / N_{SOFCe}))$
 $EX_{ch,N_2,11,SOFCe} = N_{2,11} / N_{SOFCe} \cdot (EPS_{ch,N_2} + R_{bar} \cdot T_0 \cdot \ln(N_{2,11} / N_{SOFCe}))$

"Physical and chemical exergy with flow out SOFC-SOEC"

$EX_{ph,SOFCe} = N_{2,11} \cdot EX_{ph,N_2,11} + O_{2,11} \cdot EX_{ph,O_2,11} + O_{2,12} \cdot EX_{ph,O_2,12}$
 $EX_{ch,SOFCe} = N_{2,11} \cdot EX_{ch,N_2,11,SOFCe} + O_{2,11} \cdot EX_{ch,O_2,11,SOFCe} + O_{2,12} \cdot EX_{ch,O_2,12}$
 $EX_{SOFCe} = EX_{ph,SOFCe} + EX_{ch,SOFCe}$

"Destruction exergy in SOFC-SOEC"

$EX_{Ir,SOFC2} = T_0 \cdot (O_{2,11} \cdot (S_{O_2,11} + \Delta S_{O_2}) + O_{2,12} \cdot (S_{O_2,12} + \Delta S_{O_2}) + N_{2,11} \cdot (S_{N_2,11} + \Delta S_{N_2}))$
 $EX_{Ir,SOFC1} = T_0 \cdot air_{10} \cdot (S_{air,10} + \Delta S_{air})$
 $EX_{Ir,SOFC} = EX_{Ir,SOFC2} - EX_{Ir,SOFC1}$

$SOFC_e = W_{dot,SOFC} \cdot N_{1,SOFC} / 1000 + O_{2,11} \cdot \Delta H_{O_2,11} + N_{2,11} \cdot \Delta H_{N_2,11} + O_{2,12} \cdot (\Delta H_{O_2,12} \cdot 1000 + \Delta H_{O_2,12})$
 $SOFC_i = air_{10} \cdot \Delta H_{air,10}$
 $SOFC_e = SOFC_i$

{ Calculations for the heat recovery steam generation 3-4 to meet T_4 required for gasification process }

{ Assume no pressure drop in the heat recovery steam generation 3-4 }

$H_{2O,3} = M_{dot,3} / MW_{H_2O}$; $N_3 = H_{2O,3}$

$T_3 = T_0$

"The temperature of the injected steam, $M_{dot,4}$ is the amount of injected steam"

$P_3 = 120$ [kPa] "From main supply"

$h_3 =$ Enthalpy (Steam, $T = T_3, P = P_3$)

$S_3 =$ Entropy (Steam, $T = T_3, P = P_3$)

$EX_{ph,H_2O,3} = h_3 - T_0 \cdot S_3$

$EX_{ch,H_2O,3} = H_{2O,3} / N_3 \cdot (EPS_{ch,H_2O} + R_{bar} \cdot T_0 \cdot \ln(H_{2O,3} / N_3))$

"Exergy at heat exchanger 3-4 inlet"

$EX_{ph,3} = M_{dot,3} \cdot EX_{ph,H_2O,3}$

$EX_{ch,3} = M_{dot,3} / MW_{H_2O} \cdot EX_{ch,H_2O,3}$

$EX_3 = EX_{ph,3} + EX_{ch,3}$

"State 4"

$M_{dot,4} = M_{dot,3}$; $H_{2O,4} = H_{2O,3}$; $N_4 = N_3$

$T_4 = 500$ [K]; $P_4 = P_3$

$h_4 =$ Enthalpy (Steam, $T = T_4, P = P_4$)

$S_4 =$ Entropy (Steam, $T = T_4, P = P_4$)

$$EX_{ph_H2O_4} = h_4 - T_0 * S_4$$

$$EX_{ch_H2O_4} = H2O_4 / N_4 * (EPS_{ch_H2O} + R_{bar} * T_0 * LN(H2O_4 / N_4))$$

"Exergy at heat exchanger 3-4 exit"

$$EX_{ph_4} = M_{dot_3} * EX_{ph_H2O_4}$$

$$EX_{ch_4} = H2O_4 * EX_{ch_H2O_4}$$

$$EX_4 = EX_{ph_4} + EX_{ch_4}$$

"State 23"

$$M_{dot_23} = M_{dot_30}$$

$$M_{dot_4}; T_{23} = T_{30}; P_{23} = P_{30}; H2O_{23} = M_{dot_23} / MW_{H2O}; N_{23} = H2O_{23}$$

$$DELTAH_{H2O_23} = A_{H2O} * (T_{23} - T_0) + B_{H2O} * (T_{23}^2 - T_0^2) / 2 + C_{H2O} * (T_{23}^3 - T_0^3) / 3 + D_{H2O} * (T_{23}^4 - T_0^4) / 4$$

$$S_{H2O_23} = A_{H2O} * (LN(T_{23}) - LN(T_0)) + B_{H2O} * (T_{23} - T_0) + C_{H2O} * (T_{23}^2 - T_0^2) / 2 + D_{H2O} * (T_{23}^3 - T_0^3) / 3 - R_{bar} * LN(P_{23} / P_0 * H2O_{23} / N_{23})$$

$$EX_{ph_H2O_23} = DELTAH_{H2O_23} - T_0 * S_{H2O_23}$$

$$EX_{ch_H2O_23} = H2O_{23} / N_{23} * (EPS_{ch_H2O} + R_{bar} * T_0 * LN(H2O_{23} / N_{23}))$$

$$EX_{23} = H2O_{23} * (EX_{ph_H2O_23} + EX_{ch_H2O_23})$$

{ Calculations for steam shift reaction }

{ H2O_21 should be at T_21 & with molar flow rate required for the shift reaction }

$$CO_{18} = CO_{17}; CO2_{18} = CO2_{17}; H2_{18} = H2_{17}$$

$$CO2_{22} = CO2_{17} + CO_{16}; H2_{22} = H2_{18} + CO_{18}$$

$$N_{22} = CO2_{22} + H2_{22} + H2O_{21}$$

$$MW_{22} = H2_{22} / N_{22} * MW_{H2} + CO2_{22} / N_{22} * MW_{CO2}$$

$$M_{dot_22} = N_{22} * MW_{22}$$

$$CO2_{19} = CO2_{22}; H2_{19} = H2_{22}; N_{19} = CO2_{19} + H2_{19}; P_{19} = P_{22}; M_{dot_19} = M_{dot_22}$$

$$P_{22} = P_{18} - 0.05 * P_{18}$$

$$N_{SSi} = CO_{18} + CO2_{18} + H2_{18} + H2O_{21}$$

{ Calculations of delta enthalpy for carbon monoxide in kJ/kmol at steam shift inlet }

$$DELTAH_{CO_18} = A_{CO} * (T_{18} - T_0) + B_{CO} * (T_{18}^2 - T_0^2) / 2 + C_{CO} * (T_{18}^3 - T_0^3) / 3 + D_{CO} * (T_{18}^4 - T_0^4) / 4$$

$$S_{CO_18} = A_{CO} * (LN(T_{18}) - LN(T_0)) + B_{CO} * (T_{18} - T_0) + C_{CO} * (T_{18}^2 - T_0^2) / 2 + D_{CO} * (T_{18}^3 - T_0^3) / 3 - R_{bar} * LN(P_{18} / P_0 * CO_{18} / N_{SSi})$$

$$EX_{ph_CO_18} = DELTAH_{CO_18} - T_0 * S_{CO_18}$$

$$EX_{ch_CO_18} = CO_{18} / N_{SSi} * (EPS_{ch_CO} + R_{bar} * T_0 * LN(CO_{18} / N_{SSi}))$$

{ Calculations of delta enthalpy for carbon dioxide in kJ/kmol at steam shift inlet }

$$DELTAH_{CO2_18} = A_{CO2} * (T_{18} - T_0) + B_{CO2} * (T_{18}^2 - T_0^2) / 2 + C_{CO2} * (T_{18}^3 - T_0^3) / 3 + D_{CO2} * (T_{18}^4 - T_0^4) / 4$$

$$S_{CO2_18} = A_{CO2} * (LN(T_{18}) - LN(T_0)) + B_{CO2} * (T_{18} - T_0) + C_{CO2} * (T_{18}^2 - T_0^2) / 2 + D_{CO2} * (T_{18}^3 - T_0^3) / 3 - R_{bar} * LN(P_{18} / P_0 * CO2_{18} / N_{SSi})$$

$$EX_{ph_CO2_18} = DELTAH_{CO2_18} - T_0 * S_{CO2_18}$$

$$EX_{ch_CO2_18} = CO2_{18} / N_{SSi} * (EPS_{ch_CO2} + R_{bar} * T_0 * LN(CO2_{18} / N_{SSi}))$$

{ Calculations of delta enthalpy for hydrogen in kJ/kmol at steam shift inlet }

$$DELTAH_{H2_18} = A_{H2} * (T_{18} - T_0) + B_{H2} * (T_{18}^2 - T_0^2) / 2 + C_{H2} * (T_{18}^3 - T_0^3) / 3 + D_{H2} * (T_{18}^4 - T_0^4) / 4$$

$$S_{H2_18} = A_{H2} * (LN(T_{18}) - LN(T_0)) + B_{H2} * (T_{18} - T_0) + C_{H2} * (T_{18}^2 - T_0^2) / 2 + D_{H2} * (T_{18}^3 - T_0^3) / 3 - R_{bar} * LN(P_{18} / P_0 * H2_{18} / N_{SSi})$$

$$EX_{ph_H2_18} = \Delta H_{H2_18} - T_0 * S_{H2_18}$$

$$EX_{ch_H2_18} = H2_{18} / N_{SSi} * (\epsilon_{ch_H2} + R_{bar} * T_0 * \ln(H2_{18} / N_{SSi}))$$

{ calculate delta enthalpy for steam in kJ/kmol at steam shift inlet }

$$H2O_{21} = CO_{18}; P_{21} = P_{18}; T_{21} = T_{20}$$

$$\Delta H_{H2O_21} = A_{H2O} * (T_{21} - T_0) + B_{H2O} * (T_{21}^2 - T_0^2) / 2 + C_{H2O} * (T_{21}^3 - T_0^3) / 3 + D_{H2O} * (T_{21}^4 - T_0^4) / 4$$

$$S_{H2O_21} = A_{H2O} * (\ln(T_{21}) - \ln(T_0)) + B_{H2O} * (T_{21} - T_0) + C_{H2O} * (T_{21}^2 - T_0^2) / 2 + D_{H2O} * (T_{21}^3 - T_0^3) / 3 - R_{bar} * \ln(P_{21} / P_0 * H2O_{21} / N_{SSi})$$

$$EX_{ph_H2O_21} = \Delta H_{H2O_21} - T_0 * S_{H2O_21}$$

$$EX_{ch_H2O_21} = H2O_{21} / N_{SSi} * (\epsilon_{ch_H2O} + R_{bar} * T_0 * \ln(H2O_{21} / N_{SSi}))$$

$$EX_{21} = H2O_{21} * (EX_{ph_H2O_21} + EX_{ch_H2O_21})$$

"Physical exergy and chemical exergy at SSi"

$$EX_{ph_SSi} = CO_{18} * EX_{ph_CO_18} + CO2_{18} * EX_{ph_CO2_18} + H2_{18} * EX_{ph_H2_18} + H2O_{21} * EX_{ph_H2O_21}$$

$$EX_{ch_SSi} = CO_{18} * EX_{ch_CO_18} + CO2_{18} * EX_{ch_CO2_18} + H2_{18} * EX_{ch_H2_18} + H2O_{21} * EX_{ch_H2O_21}$$

$$EX_{SSi} = EX_{ph_SSi} + EX_{ch_SSi}$$

$$N_{SSe} = N_{19}$$

{ Calculations of delta enthalpy for carbon dioxide in kJ/kmol at steam shift exit }

$$\Delta H_{CO2_19} = A_{CO2} * (T_{19} - T_0) + B_{CO2} * (T_{19}^2 - T_0^2) / 2 + C_{CO2} * (T_{19}^3 - T_0^3) / 3 + D_{CO2} * (T_{19}^4 - T_0^4) / 4$$

$$S_{CO2_19} = A_{CO2} * (\ln(T_{19}) - \ln(T_0)) + B_{CO2} * (T_{19} - T_0) + C_{CO2} * (T_{19}^2 - T_0^2) / 2 + D_{CO2} * (T_{19}^3 - T_0^3) / 3 - R_{bar} * \ln(P_{19} / P_0 * CO2_{19} / N_{SSe})$$

$$EX_{ph_CO2_19} = \Delta H_{CO2_19} - T_0 * S_{CO2_19}$$

$$EX_{ch_CO2_19} = CO2_{19} / N_{SSe} * (\epsilon_{ch_CO2} + R_{bar} * T_0 * \ln(CO2_{19} / N_{SSe}))$$

{ Calculations of delta enthalpy for hydrogen in kJ/kmol at steam shift exit }

$$\Delta H_{H2_19} = A_{H2} * (T_{19} - T_0) + B_{H2} * (T_{19}^2 - T_0^2) / 2 + C_{H2} * (T_{19}^3 - T_0^3) / 3 + D_{H2} * (T_{19}^4 - T_0^4) / 4$$

$$S_{H2_19} = A_{H2} * (\ln(T_{19}) - \ln(T_0)) + B_{H2} * (T_{19} - T_0) + C_{H2} * (T_{19}^2 - T_0^2) / 2 + D_{H2} * (T_{19}^3 - T_0^3) / 3 - R_{bar} * \ln(P_{19} / P_0 * H2_{19} / N_{SSe})$$

$$EX_{ph_H2_19} = \Delta H_{H2_19} - T_0 * S_{H2_19}$$

$$EX_{ch_H2_19} = H2_{19} / N_{SSe} * (\epsilon_{ch_H2} + R_{bar} * T_0 * \ln(H2_{19} / N_{SSe}))$$

"Physical exergy and chemical exergy at SSe"

$$EX_{ph_SSe} = H2_{19} * EX_{ph_H2_19} + CO2_{19} * EX_{ph_CO2_19}$$

$$EX_{ch_SSe} = H2_{19} * EX_{ch_H2_19} + CO2_{19} * EX_{ch_CO2_19}$$

$$EX_{SSe} = EX_{ph_SSe} + EX_{ch_SSe}$$

$$EX_{19} = EX_{SSe}$$

"Exergy destruction in steam shift reactor"

$$EX_{Ir_SS} = T_0 * (H2_{19} * (S_{H2_19} + \Delta S_{H2}) + CO2_{19} * (S_{CO2_19} + \Delta S_{CO2}) - H2O_{21} * (S_{H2O_21} + \Delta S_{H2O}) - H2_{18} * (S_{H2_18} + \Delta S_{H2}) - CO2_{18} * (S_{CO2_18} + \Delta S_{CO2}) - CO_{18} * (S_{CO_18} + \Delta S_{CO}))$$

"Exergy destruction in heat exchanger 17_18&9_10"

$$EX_{ph_18} = CO_{18} * EX_{ph_CO_18} + CO2_{18} * EX_{ph_CO2_18} + H2_{18} * EX_{ph_H2_18}$$

$EX_{ch_18} = CO_{18} * EX_{ch_CO_18} + CO_{2_18} * EX_{ch_CO2_18} + H_{2_18} * EX_{ch_H2_18}$
 $EX_{18} = EX_{ph_18} + EX_{ch_18}$
 $EX_{17} = EX_{SRe}$
 $EX_{Ir_17} = T_{0} * (H_{2_17} * (S_{H2_17} + DELTA_{S_H2}) + CO_{2_17} * (S_{CO2_17} + DELTA_{S_CO2}) + CO_{17} * (S_{CO_17} + DELTA_{S_CO}))$
 $EX_{Ir_18} = T_{0} * (H_{2_18} * (S_{H2_18} + DELTA_{S_H2}) + CO_{2_18} * (S_{CO2_18} + DELTA_{S_CO2}) + CO_{18} * (S_{CO_18} + DELTA_{S_CO}))$
 $EX_{Ir_HE_17_18} = EX_{Ir_17} - EX_{Ir_18}$
 $EX_{Ir_HE_9_10} = T_{0} * (air_{10} * (S_{air_10} + DELTA_{S_air}) - air_{9} * (S_{air_9} + DELTA_{S_air}))$
 $EX_{Ir_17_18_9_10} = EX_{Ir_HE_17_18} + EX_{Ir_HE_9_10}$ Heat exchanger 17_18&9_10"

{Calculations for temperature at steam shift reactor exit, T_19}
 $SS_A = CO_{18} * (DELTA_{H_CO_18} + DELTA_{HF_CO} * 1000) + CO_{2_18} * (DELTA_{HF_CO2} * 1000 + DELTA_{H_CO2_18})$
 $SS_B = H_{2_18} * DELTA_{H_H2_18} + H_{2O_21} * (DELTA_{HF_H2O} * 1000 + DELTA_{H_H2O_21})$
 $SS_1 = SS_A + SS_B$
 $SS_2 = H_{2_19} * DELTA_{H_H2_19} + CO_{2_19} * (DELTA_{HF_CO2} * 1000 + DELTA_{H_CO2_19})$
 $SS_1 - SS_2 = 0$ "To calculate T_19"

"State 22"

$DELTA_{H_19} = H_{2_19} * DELTA_{H_H2_19} + CO_{2_19} * (DELTA_{H_CO2_19} + DELTA_{HF_CO2} * 1000)$
 $DELTA_{H_22} = H_{2_22} * DELTA_{H_H2_22} + CO_{2_22} * (DELTA_{H_CO2_22} + DELTA_{HF_CO2} * 1000)$
 $Q_{dot_19_22} = DELTA_{H_19} - DELTA_{H_22}$
 {Calculations of delta enthalpy for carbon dioxide in kJ/kmol at steam shift exit}
 $DELTA_{H_CO2_22} = A_{CO2} * (T_{22} - T_0) + B_{CO2} * (T_{22}^2 - T_0^2) / 2 + C_{CO2} * (T_{22}^3 - T_0^3) / 3 + D_{CO2} * (T_{22}^4 - T_0^4) / 4$
 $S_{CO2_22} = A_{CO2} * (LN(T_{22}) - LN(T_0)) + B_{CO2} * (T_{22} - T_0) + C_{CO2} * (T_{22}^2 - T_0^2) / 2 + D_{CO2} * (T_{22}^3 - T_0^3) / 3 - R_{bar} * LN(P_{22} / P_0 * CO_{2_22} / N_{22})$
 $EX_{ph_CO2_22} = DELTA_{H_CO2_22} - T_0 * S_{CO2_22}$
 $EX_{ch_CO2_22} = CO_{2_22} / N_{22} * (EPS_{ch_CO2} + R_{bar} * T_0 * LN(CO_{2_19} / N_{SSe}))$

{Calculations for heat exchanger 19_22& 28_20}

$H_{2O_20} = H_{2O_21} + H_{2O_15}$
 $M_{dot_20} = H_{2O_20} * MW_{H2O}; N_{20} = H_{2O_20}$
 $M_{dot_21} = H_{2O_21} * MW_{H2O}; N_{21} = H_{2O_21}$
 $T_{20} = T_{19} - 7; P_{20} = P_{18}$
 $DELTA_{H_H2O_20} = A_{H2O} * (T_{20} - T_0) + B_{H2O} * (T_{20}^2 - T_0^2) / 2 + C_{H2O} * (T_{20}^3 - T_0^3) / 3 + D_{H2O} * (T_{20}^4 - T_0^4) / 4$
 $S_{H2O_20} = A_{H2O} * (LN(T_{20}) - LN(T_0)) + B_{H2O} * (T_{20} - T_0) + C_{H2O} * (T_{20}^2 - T_0^2) / 2 + D_{H2O} * (T_{20}^3 - T_0^3) / 3 - R_{bar} * LN(P_{20} / P_0 * H_{2O_20} / N_{20})$
 $EX_{ph_H2O_20} = DELTA_{H_H2O_20} - T_0 * S_{H2O_20}$
 $EX_{ch_H2O_20} = H_{2O_20} / N_{20} * (EPS_{ch_H2O} + R_{bar} * T_0 * LN(H_{2O_20} / N_{20}))$

"Physical and chemical exergies with flow at heat exchanger 28_20"

$EX_{20} = H_{2O_20} * EX_{ph_H2O_20} + H_{2O_20} * EX_{ch_H2O_20}$

"State 28"

$T_{28} = T_0; P_{28} = P_{20}; H_{2O_28} = H_{2O_20}; N_{28} = H_{2O_20}$
 $DELTA_{H_H2O_28} = A_{H2O} * (T_{28} - T_0) + B_{H2O} * (T_{28}^2 - T_0^2) / 2 + C_{H2O} * (T_{28}^3 - T_0^3) / 3 + D_{H2O} * (T_{28}^4 - T_0^4) / 4$

$S_{H2O_28} = A_{H2O}*(LN(T_{28})-LN(T_0))+B_{H2O}*(T_{28}-T_0)+C_{H2O}*(T_{28}^2-T_0^2)/2 +$
 $D_{H2O}*(T_{28}^3-T_0^3)/3-R_{bar}*LN(P_{28}/P_0*H2O_{28}/N_{28})$
 $EX_{ph_H2O_28}=DELTAH_{H2O_28}-T_0*S_{H2O_28}$
 $EX_{ch_H2O_28}=H2O_{28}/N_{28}*(EPS_{ch_H2O}+R_{bar}*T_0*LN(H2O_{28}/N_{28}))$
 $EX_{28}=H2O_{28}*EX_{ph_H2O_28}+H2O_{28}*EX_{ch_H2O_28}$
 $Q_{dot_28_20}=H2O_{20}*(DELTAH_{H2O_20}+DELTAHF_{H2O}*1000-DELTAH_{H2O_28}-$
 $DELTAHF_{H2O}*1000)$
 $Q_{dot_28_20}=Q_{dot_19_22}$ "To find T_22"

{calculate delta enthalpy for hydrogen in kJ/kmol at steam shift exit}
 $DELTAH_{H2_22} = A_{H2}*(T_{22}-T_0)+B_{H2}*(T_{22}^2-T_0^2)/2 + C_{H2}*(T_{22}^3-T_0^3)/3 +$
 $D_{H2}*(T_{22}^4-T_0^4)/4$
 $S_{H2_22} = A_{H2}*(LN(T_{22})-LN(T_0))+B_{H2}*(T_{22}-T_0)+C_{H2}*(T_{22}^2-T_0^2)/2 +$
 $D_{H2}*(T_{22}^3-T_0^3)/3-R_{bar}*LN(P_{22}/P_0*H2_{22}/N_{22})$
 $EX_{ph_H2_22}=DELTAH_{H2_22}-T_0*S_{H2_22}$
 $EX_{ch_H2_22}=H2_{22}/N_{22}*(EPS_{ch_H2}+R_{bar}*T_0*LN(H2_{22}/N_{22}))$

"Physical exergy and chemical exergy at 22"
 $EX_{ph_22}=H2_{22}*EX_{ph_H2_22}+CO2_{22}*EX_{ph_CO2_22}$
 $EX_{ch_22}=H2_{22}*EX_{ch_H2_22}+CO2_{22}*EX_{ch_CO2_22}$
 $EX_{22}=EX_{ph_22}+EX_{ch_22}$

"Exergy destruction in heat exchanger 19_22&28_20;22_5&29_30"
 $EX_{Ir_19}=T_0*(H2_{19}*(S_{H2_19}+DELTA_{S_H2})+CO2_{19}*(S_{CO2_19}+DELTA_{S_CO2}))$
 $EX_{Ir_22}=T_0*(H2_{22}*(S_{H2_22}+DELTA_{S_H2})+CO2_{22}*(S_{CO2_22}+DELTA_{S_CO2}))$
 $EX_{Ir_20}=T_0*(H2O_{20}*(S_{H2O_20}+DELTA_{S_H2O}))$
 $EX_{Ir_30}=T_0*(H2O_{30}*(S_{H2O_30}+DELTA_{S_H2O}))$
 $EX_{Ir_28}=T_0*(H2O_{28}*(S_{H2O_28}+DELTA_{S_H2O}))$
 $EX_{Ir_29}=T_0*(H2O_{29}*(S_{H2O_29}+DELTA_{S_H2O}))$
 $EX_{Ir_HE_28_20}=EX_{Ir_20}-EX_{Ir_28}$
 $EX_{Ir_HE_19_22}=EX_{Ir_19}-EX_{Ir_22}$
 $EX_{Ir_HE_29_30}=EX_{Ir_30}-EX_{Ir_29}$
 $EX_{Ir_19_22_28_20}=EX_{Ir_HE_19_22}+EX_{Ir_HE_28_20}$
 $EX_{Ir_HE_22_5}=EX_{Ir_22}-EX_{Ir_Comp5_6_i}$
 $EX_{Ir_22_5_29_30}=EX_{Ir_HE_22_5}+EX_{Ir_HE_29_30}$

"Heat exchanger 22-5"
 $Q_{dot_22_5}=DELTAH_{22}-DELTAH_5$
 $Q_{dot_29_30}=DELTAH_{30}-DELTAH_{29}$
 $Q_{dot_22_5}=Q_{dot_29_30}$ "To find water exit temperature T_29"

$P_{30}=P_{29}; T_{30}=500; H2O_{30}=H2O_{29}; N_{30}=H2O_{30}; M_{dot_30}=H2O_{30}*MW_{H2O}$
 $DELTAH_{H2O_30} = A_{H2O}*(T_{30}-T_0)+B_{H2O}*(T_{30}^2-T_0^2)/2 + C_{H2O}*(T_{30}^3-$
 $T_0^3)/3 + D_{H2O}*(T_{30}^4-T_0^4)/4$
 $S_{H2O_30} = A_{H2O}*(LN(T_{30})-LN(T_0))+B_{H2O}*(T_{30}-T_0)+C_{H2O}*(T_{30}^2-T_0^2)/2 +$
 $D_{H2O}*(T_{30}^3-T_0^3)/3-R_{bar}*LN(P_{30}/P_0*H2O_{30}/N_{30})$
 $DELTAH_{30}=H2O_{30}*DELTAH_{H2O_30}$
 $EX_{ph_H2O_30}=DELTAH_{H2O_30}-T_0*S_{H2O_30}$
 $EX_{ch_H2O_30}=H2O_{30}/N_{30}*(EPS_{ch_H2O}+R_{bar}*T_0*LN(H2O_{30}/N_{30}))$
 $EX_{30}=H2O_{30}*EX_{ph_H2O_30}+H2O_{30}*EX_{ch_H2O_30}$

"State 29"

$T_{29}=T_0; P_{29}=P_0; N_{29}=H_2O_{29}; M_{dot_{29}}=M_{dot_{30}}$
 $DELTAH_{H_2O_{29}}= A_{H_2O}*(T_{29}-T_0)+B_{H_2O}*(T_{29}^2-T_0^2)/2 + C_{H_2O}*(T_{29}^3-T_0^3)/3 + D_{H_2O}*(T_{29}^4-T_0^4)/4$
 $S_{H_2O_{29}}= A_{H_2O}*(LN(T_{29})-LN(T_0))+B_{H_2O}*(T_{29}-T_0)+C_{H_2O}*(T_{29}^2-T_0^2)/2 + D_{H_2O}*(T_{29}^3-T_0^3)/3-R_{bar}*LN(P_{29}/P_0*H_2O_{29}/N_{29})$
 $DELTAH_{29}=H_2O_{29}*DELTAH_{H_2O_{29}}$

$EX_{ph_{H_2O_{29}}}=DELTAH_{H_2O_{29}}-T_0*S_{H_2O_{29}}$
 $EX_{ch_{H_2O_{29}}}=H_2O_{29}/N_{29}*(EPS_{ch_{H_2O}}+R_{bar}*T_0*LN(H_2O_{29}/N_{29}))$
 $EX_{29}=H_2O_{29}*EX_{ph_{H_2O_{29}}}+H_2O_{29}*EX_{ch_{H_2O_{29}}}$

"Compression 5-6"

"State 5"

{ T_6 is the temperature preferred to take reforming reaction pla[ce]

T_5=T_0" Assumed"

P_5=P_22" Known"

H2_5=H2_22; CO2_5=CO2_22

N_5=N_22; M_dot_5=M_dot_22

MW_5=H2_5/N_5*MW_H2+CO2_5/N_5*MW_CO2

Cp_CO2_5=A_CO2+B_CO2*T_5+C_CO2*T_5^2+D_CO2*T_5^3

Cp_H2_5=A_H2+B_H2*T_5+C_H2*T_5^2+D_H2*T_5^3

Cv_CO2_5=Cp_CO2_5-R_bar

Cv_H2_5=Cp_H2_5-R_bar

Cp_5=CO2_5/N_5*Cp_CO2_5+H2_5/N_5*Cp_H2_5

Cv_5=CO2_5/N_5*Cv_CO2_5+H2_5/N_5*Cv_H2_5

Gama_gas=Cp_5/Cv_5

{ Calculate delta enthalpy for hydrogen in kJ/kmol at heat exchanger 36-5 exit }

$DELTAH_{H_2_5}= A_{H_2}*(T_5-T_0)+B_{H_2}*(T_5^2-T_0^2)/2 + C_{H_2}*(T_5^3-T_0^3)/3 + D_{H_2}*(T_5^4-T_0^4)/4$

$S_{H_2_5}= A_{H_2}*(LN(T_5)-LN(T_0))+B_{H_2}*(T_5-T_0)+C_{H_2}*(T_5^2-T_0^2)/2 + D_{H_2}*(T_5^3-T_0^3)/3-R_{bar}*LN(P_5/P_0*H_2_5/N_5)$

$EX_{ph_{H_2_5}}=DELTAH_{H_2_5}-T_0*S_{H_2_5}$

$EX_{ch_{H_2_5}}=H_2_5/N_5*(EPS_{ch_{H_2}}+R_{bar}*T_0*LN(H_2_5/N_5))$

{ calculate delta enthalpy for carbon dioxide in kJ/kmol at heat exchanger 36-5 exit }

$DELTAH_{CO_2_5}= A_{CO_2}*(T_5-T_0)+B_{CO_2}*(T_5^2-T_0^2)/2+C_{CO_2}*(T_5^3-T_0^3)/3+D_{CO_2}*(T_5^4-T_0^4)/4$

$S_{CO_2_5}= A_{CO_2}*(LN(T_5)-LN(T_0))+B_{CO_2}*(T_5-T_0)+C_{CO_2}*(T_5^2-T_0^2)/2 + D_{CO_2}*(T_5^3-T_0^3)/3-R_{bar}*LN(P_5/P_0*CO_2_5/N_5)$

$EX_{ph_{CO_2_5}}=DELTAH_{CO_2_5}-T_0*S_{CO_2_5}$

$EX_{ch_{CO_2_5}}=CO_2_5/N_5*(EPS_{ch_{CO_2}}+R_{bar}*T_0*LN(CO_2_5/N_5))$

"Physical and chemical exergy at compressor 5-6 inlet, state 5"

$EX_{ph_5}=CO_2_5*EX_{ph_{CO_2_5}}+H_2_5*EX_{ph_{H_2_5}}$

$EX_{ch_5}=CO_2_5*EX_{ch_{CO_2_5}}+H_2_5*EX_{ch_{H_2_5}}$

$EX_5=EX_{ph_5}+EX_{ch_5}$

"Enthalpy at heat exchanger 36-5 exit or compressor inlet"

DELTAH_5=H2_5*DELTAH_H2_5+CO2_5*(DELTAHF_CO2*1000+DELTAH_CO2_5)
"State 6"

P_6=1.9*P_5" Assumed"

P_6=P_5*(1+Eta_c*(T_6/T_5-1))^(Gama_gas/(Gama_gas-1))"To find T_6"

H2_6=H2_5;CO2_6=CO2_5

N_6=H2_6+CO2_6

M_dot_6=M_dot_5

{Calculations of delta enthalpy for hydrogen in kJ/kmol at compressor 5-6 exit}

DELTAH_H2_6= A_H2*(T_6-T_0)+B_H2*(T_6^2-T_0^2)/2 + C_H2*(T_6^3-T_0^3)/3 +
D_H2*(T_6^4-T_0^4)/4

S_H2_6= A_H2*(LN(T_6)-LN(T_0))+B_H2*(T_6-T_0)+C_H2*(T_6^2-T_0^2)/2 +

D_H2*(T_6^3-T_0^3)/3-R_bar*LN(P_6/P_0*H2_6/N_6)

EX_ph_H2_6=DELTAH_H2_6-T_0*S_H2_6

EX_ch_H2_6=H2_6/N_6*(EPS_ch_H2+R_bar*T_0*LN(H2_6/N_6))

{calculate delta enthalpy for carbon dioxide in kJ/kmol at compressor 5-6 exit}

DELTAH_CO2_6= A_CO2*(T_6-T_0)+B_CO2*(T_6^2-T_0^2)/2+C_CO2*(T_6^3-
T_0^3)/3+D_CO2*(T_6^4-T_0^4)/4

S_CO2_6= A_CO2*(LN(T_6)-LN(T_0))+B_CO2*(T_6-T_0)+C_CO2*(T_6^2-T_0^2)/2 +

D_CO2*(T_6^3-T_0^3)/3-R_bar*LN(P_6/P_0*CO2_6/N_6)

EX_ph_CO2_6=DELTAH_CO2_6-T_0*S_CO2_6

EX_ch_CO2_6=CO2_6/N_6*(EPS_ch_CO2+R_bar*T_0*LN(CO2_6/N_6))

"Physical and chemical exergy at compressor 5-6 exit, state 6"

EX_ph_6=CO2_6*EX_ph_CO2_6+H2_6*EX_ph_H2_6

EX_ch_6=CO2_6*EX_ch_CO2_6+H2_6*EX_ch_H2_6

EX_6=EX_ph_6+EX_ch_6

"Exergy destruction in compressor 5_6"

EX_Ir_Comp5_6_e=T_0*(H2_6*(S_H2_6+DELTA_S_H2)+CO2_6*(S_CO2_6+DELTA_S_CO2))

EX_Ir_Comp5_6_i=T_0*(H2_5*(S_H2_5+DELTA_S_H2)+CO2_5*(S_CO2_5+DELTA_S_CO2))

EX_Ir_Comp5_6=EX_Ir_Comp5_6_e-EX_Ir_Comp5_6_i+W_dot_5_6

"Enthalpy at heat exchanger 36-5 exit or compressor inlet"

DELTAH_6=H2_6*DELTAH_H2_6+CO2_6*(DELTAHF_CO2*1000+DELTAH_CO2_6)

"Work done on compressor 5-6"

W_dot_5_6=(DELTAH_6-DELTAH_5)

"Calculations for hydrogen line "

P_33=(P_6-0.05*P_6)*H2_5/N_5

T_33=T_6

H2_33=H2_6;M_dot_33=H2_33*MW_H2;N_33=H2_33

DELTAH_H2_33=DELTAH_H2_6

S_H2_33= A_H2*(LN(T_33)-LN(T_0))+B_H2*(T_33-T_0)+C_H2*(T_33^2-T_0^2)/2 +

D_H2*(T_33^3-T_0^3)/3-R_bar*LN(P_33/P_0*H2_33/N_33)

EX_ph_H2_33=DELTAH_H2_33-T_0*S_H2_33

EX_ch_H2_33=H2_33/N_33*(EPS_ch_H2+R_bar*T_0*LN(H2_33/N_33))

EX_33=H2_33*(EX_ph_H2_33+EX_ch_H2_33)

H2_Yield=H2_33

```

"Calculations for carbon dioxide line "
P_34=(P_6-0.05*P_6)*CO2_6/N_6
T_34=T_6
CO2_34=CO2_6;M_dot_34=CO2_34*MW_CO2;N_34=CO2_34
DELTAH_CO2_34=DELTAH_CO2_6
S_CO2_34= A_CO2*(LN(T_34)-LN(T_0))+B_H2*(T_34-T_0)+C_H2*(T_34^2-T_0^2)/2 +
D_H2*(T_34^3-T_0^3)/3-R_bar*LN(P_34/P_0*CO2_34/N_34)
EX_ph_CO2_34=DELTAH_CO2_34-T_0*S_CO2_34
EX_ch_CO2_34=CO2_34/N_34*(EPS_ch_CO2+R_bar*T_0*LN(CO2_34/N_34))
EX_34=CO2_34*(EX_ph_CO2_34+EX_ch_CO2_34)
CO2_Emission=CO2_34
"Efficiency calculations"
LHV_biomass=19005[kJ/kg]
W_dot_SOFC=52.37[W]"From SOFC calculations"
W_dot_SOFC_AC=W_dot_SOFC*0.95
N_SOFC=N_H2*1000/N_H2_SOFC
W_dot_STACK=W_dot_SOFC*N1_SOFC
LHV_H2=120000[kJ/kg]
Eta_el_tur=(W_dot_7_8-W_dot_5_6-W_dot_24_25-W_dot_0_9)*0.90/(M_dot_1*
LHV_biomass)*100
"SOFC efficiency"
Eta_el_SOFC=W_dot_SOFC_AC/(N_H2_SOFC*LHV_H2*2.016)*100"Efficiency of SOFC"
Eta_el_Overall=Eta_el_SOFC+Eta_el_tur
Eta_EX_el_Overall=Eta_EX_el_SOFC+Eta_EX_el_tur
M_dot_H2=H2_33*MW_H2
Eta_H2=LHV_H2*M_dot_H2/(LHV_biomass*M_dot_1)*100"Efficiency when take H2 only in
consideration"
Eta_EX_el_tur=(W_dot_7_8-W_dot_5_6-W_dot_24_25-W_dot_0_9)*0.90/( BETA *M_dot_1*
LHV_biomass)*100
Eta_EX_Steam=(EX_23)/( BETA *M_dot_1* LHV_biomass)*100
Eta_EX_H2=EX_33/( BETA *M_dot_1* LHV_biomass)*100"Efficiency when take H2 only in
consideration"
Eta_EX_el_SOFC=W_dot_STACK/1000/( BETA *M_dot_1* LHV_biomass)*100
EX_Ir_36_16_25_35=EX_Ir_HE_36_16+EX_Ir_HE_25_35"Heat exchanger 36_5&25_35"
EX_Gasifier=EX_biomass+EX_4-EX_2
"Gasifier"
EX_1=M_dot_1*BETA* LHV_biomass
EX_d_gasifier=EX_1+EX_4-EX_2
"Economic"
TAO=8000[hr/yr];BETA=1.173;ER=1 {exchange rate is one}
Pr=2*3600*10^(-6)"Biomass price $/kWh"
FC_dot_f=Pr*LHV_biomass*TAO/ER"Energetic cost"
C_dot_1=FC_dot_f/TAO*(1/BETA)"Exergetic cost"

"Cost balance and auxiliay equations"
C_dot_4+C_dot_1+Z_dot_Gasifier=C_dot_2"Gasifier"
Z_dot_Gasifier=1.047;C_dot_1=c_1*EX_Biomass;C_dot_2=c_2*EX_2;C_dot_4=c_4*EX_4
c_4=c_30
Z_OBJ_Gasifier=Z_dot_Gasifier+EX_d_gasifier*C_2

```

C_dot_2+Z_dot_Separator=C_dot_26+C_dot_36"Seperator to find c_26"
Z_dot_Separator=0.083;C_dot_26=c_26*EX_26;C_dot_36=c_36*EX_36
C_dot_2/Ex_2=C_dot_36/Ex_36

C_dot_24+C_dot_w_24_25+Z_dot_24_25=C_dot_25" Air compressor 24-25 to find c_25"
Z_dot_24_25=2.511;C_dot_w_24_25=c_24_25*W_dot_24_25
c_24_25=0.1046
c_24=0;C_dot_24=c_24*Ex_24;C_dot_25=c_25*Ex_25
Z_OBJ_24_25=Z_dot_24_25+EX_Ir_COmp24_25*C_25

C_dot_36+C_dot_25+Z_dot_HE1=C_dot_16+C_dot_35"Heat exchanger 1 to find c_35, c_16"
Z_dot_HE1= 0.748;C_dot_16=c_16*EX_16;C_dot_35=c_35*EX_35
(C_dot_36-C_dot_16)/(EX_36-EX_16)=(C_dot_35-C_dot_25)/(EX_35-EX_25)
Z_OBJ_HE1=Z_dot_HE1+EX_Ir_36_16_25_35*C_36

C_dot_16+C_dot_15+Z_dot_SR=C_dot_17"Steam reforming to find c_17"
Z_dot_SR=1.339;C_dot_15=c_15*EX_15;C_dot_17=c_17*EX_17
Z_OBJ_SR=Z_dot_SR+EX_Ir_SR*C_17

C_dot_0+C_dot_w_0_9+Z_dot_0_9=C_dot_9" Air compressor 0-9 to find c_9"
Z_dot_0_9=2.511;C_dot_w_0_9=c_0_9*W_dot_0_9;C_dot_0=c_0*EX_0
c_0_9=0.1046
c_0=0
Z_OBJ_0_9=Z_dot_0_9+EX_Ir_COmp_0_9*C_9

C_dot_17+C_dot_9+Z_dot_HE2=C_dot_18+C_dot_10"Heat exchanger 2 to find c_10, c_18"
Z_dot_HE2= 0.748[\$/hr];C_dot_18=c_18*EX_18;C_dot_9=c_9*EX_9;C_dot_10=c_10*EX_10
(C_dot_9-C_dot_10)/(EX_9-EX_10)=(C_dot_17-C_dot_18)/(EX_17-EX_18)"P-rule"
Z_OBJ_HE2=Z_dot_HE2+EX_Ir_17_18_9_10*C_18

C_dot_18+C_dot_21+Z_dot_SS=C_dot_19"Water gas shift, to find c_19"
Z_dot_SS=1.339[\$/s];C_dot_19=c_19*EX_19;C_dot_21=c_21*EX_21
c_21=c_15
Z_OBJ_SS=Z_dot_SS+EX_Ir_SS*C_19

C_dot_28+C_dot_19+Z_dot_HE3=C_dot_22+C_dot_20"Heat exchanger 3"
Z_dot_HE3= 0.748;C_dot_28=c_28*EX_28;C_dot_20=c_20*EX_20;C_dot_22=c_22*EX_22
c_20=c_30
C_28=0;C_20=c_21
Z_OBJ_HE3=Z_dot_HE3+EX_Ir_19_22_28_20*C_20

C_dot_29+C_dot_22+Z_dot_HE4=C_dot_30+C_dot_5"Heat exchanger 4"
Z_dot_HE4= 0.748;C_dot_29=c_29*EX_29;C_dot_30=c_30*EX_30;C_dot_5=c_5*EX_5
C_dot_22/Ex_22=C_dot_5/Ex_5
C_29=0
Z_OBJ_HE4=Z_dot_HE4+EX_Ir_22_5_29_30*C_5

"State 23, excess steam"
c_23=c_30
C_dot_23=c_23*Ex_23

$C_{\dot{5}}+C_{\dot{w}_{5_6}}+Z_{\dot{5}_6}=C_{\dot{6}}$ "Gas compressor 5-6 to find $c_{\dot{5}}$ "
 $Z_{\dot{5}_6}=1.591$ [\$/s]; $C_{\dot{w}_{5_6}}=c_{\dot{5}_6}W_{\dot{5}_6}$; $C_{\dot{6}}=c_{\dot{6}}EX_{\dot{6}}$
 $c_{\dot{5}_6}=0.1046$
 $Z_{OBJ_{5_6}}=Z_{\dot{5}_6}+EX_{Ir_COmp5_6}C_{\dot{6}}$

$C_{\dot{6}}+Z_{\dot{Filter1}}=C_{\dot{33}}+C_{\dot{34}}$ "Filter 1 to find $c_{\dot{33}},c_{\dot{34}}$ "
 $Z_{\dot{Filter1}}=0.256$; $C_{\dot{33}}=c_{\dot{33}}EX_{\dot{33}}$; $C_{\dot{34}}=c_{\dot{34}}EX_{\dot{34}}$
 $C_{\dot{6}}/Ex_{\dot{6}}=C_{\dot{33}}/Ex_{\dot{33}}+C_{\dot{34}}/Ex_{\dot{34}}$
 $Z_{OBJ_Filter1}=Z_{\dot{Filter1}}$

$Z_{\dot{SOFC_SOEC}}=2Z_{\dot{SOFC}}$
 $C_{\dot{27}}=c_{\dot{27}}EX_{\dot{27}}$
 $EX_{\dot{27}}=EX_{\dot{11}}+EX_{\dot{12}}$
 $Z_{OBJ_SOFC}=Z_{\dot{SOFC_SOEC}}+EX_{Ir_SOFC}C_{\dot{27}}$

$C_{\dot{27}}+C_{\dot{26}}+C_{\dot{35}}+Z_{\dot{burner}}=C_{\dot{7}}$ "Burner to find $c_{\dot{27}}$ "
 $Z_{\dot{burner}}=1.339$; $C_{\dot{7}}=c_{\dot{7}}EX_{\dot{7}}$
 $Z_{OBJ_burner}=Z_{\dot{burner}}+EX_{Ir_burner}C_{\dot{7}}$

$C_{\dot{7}}+Z_{\dot{7}_8}=C_{\dot{8}}+C_{\dot{w}_{7_8}}$ "Turbine 7-8 to find $c_{\dot{7}}$ "
 $Z_{\dot{7}_8}=5.859$; $C_{\dot{w}_{7_8}}=C_{\dot{7}_8}W_{\dot{7}_8}$; $C_{\dot{8}}=c_{\dot{8}}EX_{\dot{8}}$
 $C_{\dot{7}_8}=0.1046$
 $C_{\dot{8}}=0$

$Z_{OBJ_Tur_{7_8}}=Z_{\dot{7}_8}+EX_{Ir_Tur_{7_8}}C_{\dot{7}}$
 $Z_{OBJ}=Z_{OBJ_Tur_{7_8}}+Z_{OBJ_burner}+Z_{OBJ_SOFC}+Z_{OBJ_SS}+Z_{OBJ_HE1}+Z_{OBJ_HE2}+Z_{OBJ_HE3}+Z_{OBJ_HE4}+Z_{OBJ_0_9}+Z_{OBJ_SR}+Z_{OBJ_Filter1}+Z_{OBJ_{5_6}}+Z_{OBJ_{24_25}}+Z_{OBJ_Gasifier}$

B4. EES for SOFC and SBG calculations

```
{This code performs SOFC&Biomass gasification calculations}
{Parametric study for hydrogen production from biomass (sawdust wood)-steam gasification}
N_C=48.01/12;N_H=6.04;N_O=45.43/16;N_N=0.15/14
T_0=298[k]; U_0=2[m/s]
T_S=500[k]
R=8.314[kJ/kmol-K]
{Gasifier insulation emissivity, its thermal conductivity and its thickness}
EMISS=0.01;K_ins=0.027[w/mK];X_ins=0.005[m]
{Calculations for delta enthalpy for carbon monoxide}
A_CO=28.16;B_CO=0.1675*10^(-2);C_CO=0.5372*10^(-5);D_CO=-2.222*10^(-9)
DELTA_H_CO= A_CO*(T_1-T_0)+B_CO*(T_1^2-T_0^2)/2+C_CO*(T_1^3-
T_0^3)/3+D_CO*(T_1^4-T_0^4)/4
S_CO= A_CO*(LN(T_1)-LN(T_0))+B_CO*(T_1-T_0)+C_CO*(T_1^2-T_0^2)/2 +
D_CO*(T_1^3-T_0^3)/3
DELTA_HF_CO=-110.53[kJ/mol]
{Calculations for delta enthalpy for carbon dioxide}
A_CO2=22.26;B_CO2=5.981*10^(-2);C_CO2=-3.501*10^(-5);D_CO2=-7.469*10^(-9)
DELTA_H_CO2= A_CO2*(T_1-T_0)+B_CO2*(T_1^2-T_0^2)/2+C_CO2*(T_1^3-
T_0^3)/3+D_CO2*(T_1^4-T_0^4)/4
S_CO2= A_CO2*(LN(T_1)-LN(T_0))+B_CO2*(T_1-T_0)+C_CO2*(T_1^2-T_0^2)/2 +
D_CO2*(T_1^3-T_0^3)/3
DELTA_HF_CO2=-393.52[kJ/mol]
{Calculations for delta enthalpy for water in kJ/ kmol}
A_H2O=32.24;B_H2O=0.1923*10^(-2);C_H2O=1.055*10^(-5);D_H2O=-3.595*10^(-9)
DELTA_H_H2O= A_H2O*(T_S-T_0)+B_H2O*(T_S^2-T_0^2)/2 + C_H2O*(T_S^3-T_0^3)/3
+ D_H2O*(T_S^4-T_0^4)/4
S_H2O = A_H2O*(LN(T_S)-LN(T_0))+B_H2O*(T_S-T_0)+C_H2O*(T_S^2-T_0^2)/2 +
D_H2O*(T_S^3-T_0^3)/3
DELTA_HF_H2O=-241.83[kJ/mol];DELTA_S_H2O=188.83[kJ/kmol-K]
{Calculations for delta enthalpy for hydrogen in kJ/kmol}
A_H2=29.11;B_H2=-0.1916*10^(-2);C_H2=0.4003*10^(-5);D_H2=-0.8704*10^(-9)
DELTA_H_H2= A_H2*(T_1-T_0)+B_H2*(T_1^2-T_0^2)/2 + C_H2*(T_1^3-T_0^3)/3 +
D_H2*(T_1^4-T_0^4)/4
S_H2 = A_H2*(LN(T_1)-LN(T_0))+B_H2*(T_1-T_0)+C_H2*(T_1^2-T_0^2)/2 +
D_H2*(T_1^3-T_0^3)/3
DELTA_HF_H2=0.0;DELTA_S_H2=130.68[kJ/kmol-K]
{Calculations for delta enthalpy for methane in kJ/kmol}
A_CH4=19.89;B_CH4=5.204*10^(-2);C_CH4=1.269*10^(-5);D_CH4=-11.01*10^(-9)
DELTA_H_CH4= A_CH4*(T_1-T_0)+B_CH4*(T_1^2-T_0^2)/2+C_CH4*(T_1^3-
T_0^3)/3+D_CH4*(T_1^4-T_0^4)/4
S_CH4 = A_CH4*(LN(T_1)-LN(T_0))+B_CH4*(T_1-T_0)+C_CH4*(T_1^2-T_0^2)/2 +
D_CH4*(T_1^3-T_0^3)/3
DELTA_HF_CH4=-74.8[kJ/mol]
{Find Gibbs function;multiply by 1000 to homogenise the units}
{Absolute entropy for carbon=5.74 KJ/KmolK}
DELTA_G_1=1000*(2*DELTA_HF_H2-DELTA_HF_CH4)+(2*DELTA_H_H2-
DELTA_H_CH4)
DELTA_G=DELTA_G_1-T_1*(2*S_H2+5.74-S_CH4)
K_1=EXP(-DELTA_G/(R*T_1))
```

$K=1/K_1$
 $TAR=0.01*3598*EXP(-0.0029*T_1)$
 $N_{char}=0.05*ALPHA*N_C$
 "P is the gasification pressure in bars"
 $A=16*(1+0.08*TAR)+8*K*P$
 $B_1=-4*K*P*(0.5*ALPHA*N_H+GAMA+ALPHA*N_C)$
 $B_2=-8*(N_H*ALPHA+2*GAMA-0.06*TAR)*(1+0.08*TAR)$
 $B=B_1+B_2$
 $C=(1+0.08*TAR)*(ALPHA*N_H+2*GAMA-0.06*TAR)^2$
 $X_2=(-B-(B^2-4*A*C)^{0.5})/2/A$
 {N_H2 is a in the global reaction,N_CO2 is c in the global reaction,N_CO is b in the global reaction and X_2 is N_CH4 }
 $N_{CH4}=X_2$
 $N_{tot}=(0.5*N_H*ALPHA+GAMA-2*N_{CH4}+ALPHA*N_C)/(1+0.08*TAR)$
 $N_{H2}=0.5*(N_H*ALPHA-4*N_{CH4}+2*GAMA-0.06*TAR*N_{tot})$
 $N_{CO}=1.90*ALPHA*N_C-N_O*ALPHA-GAMA-2*N_{CH4}-0.12*TAR*N_{tot}$
 $N_{CO2}=N_O*ALPHA+GAMA+N_{CH4}+0.06*TAR*N_{tot}-0.95*ALPHA*N_C$
 $X_{CH4}=N_{CH4}/N_{tot}*100$
 $X_{H2}=N_{H2}/N_{tot}*100$
 $X_{CO}=N_{CO}/N_{tot}*100$
 $X_{CO2}=N_{CO2}/N_{tot}*100$
 $M_{H2}=N_{H2}*2$
 {Physical exergy for CO, CO2, H2 and CH4}
 $EX_{ph_CO}=\Delta H_{CO}-T_0*S_{CO}$
 $EX_{ph_CO2}=\Delta H_{CO2}-T_0*S_{CO2}$
 $EX_{ph_H2}=\Delta H_{H2}-T_0*S_{H2}$
 $EX_{ph_CH4}=\Delta H_{CH4}-T_0*S_{CH4}$
 {Physical exergy in gas product}
 $EX_{ph_gas}=N_{CO}*EX_{ph_CO}+N_{CO2}*EX_{ph_CO2}+N_{H2}*EX_{ph_H2}+N_{CH4}*EX_{ph_CH4}$
 {Chemical exergy for CO, CO2, H2, H2O and CH4}
 {standard chemical exergy for product gas are given in (G72) in kj/kmole}
 $EPS_{ch_H2}=236100;EPS_{ch_CO}=275100;EPS_{ch_CO2}=198700;EPS_{ch_CH4}=831650;EPS_{ch_H2O}=11710$
 {chemical exergy in gas product ref.73}
 $EX_{ch_CO}=X_{CO}/100*EPS_{ch_CO}+R*T_0*X_{CO}/100*LN(X_{CO}/100)$
 $EX_{ch_CO2}=X_{CO2}/100*EPS_{ch_CO2}+R*T_0*X_{CO2}/100*LN(X_{CO2}/100)$
 $EX_{ch_H2}=X_{H2}/100*EPS_{ch_H2}+R*T_0*X_{H2}/100*LN(X_{H2}/100)$
 $EX_{ch_CH4}=X_{CH4}/100*EPS_{ch_CH4}+R*T_0*X_{CH4}/100*LN(X_{CH4}/100)$
 $EX_{ch_gas}=N_{CO}*EX_{ch_CO}+N_{CO2}*EX_{ch_CO2}+N_{H2}*EX_{ch_H2}+N_{CH4}*EX_{ch_CH4}$
 {Total exergy in product gas}
 $EX_{gas}=EX_{ch_gas}+EX_{ph_gas}$
 {Number of moles of biomass and steam inputs}
 $N_{steam}=GAMA$
 $N_{biomass}=ALPHA$
 $M_{steam}=N_{steam}*18$
 $X_{H2O}=N_{steam}/(N_{biomass}+N_{steam})$
 {Total exergy in steam}
 $EX_{ch_H2O}=X_{H2O}*EPS_{ch_H2O}+R*T_0*X_{H2O}*LN(X_{H2O})$

$EX_{ph_H2O} = \Delta H_{H2O} - T_0 \cdot S_{H2O}$
 $EX_{steam} = N_{steam} \cdot (EX_{ch_H2O} + EX_{ph_H2O})$
 {Wood has ultimate
 analysis: $C_f = 48.0; H_f = 6.04; O_f = 45.43; N_f = 0.15; S_f = 0.05; ASH_f = 0.32; HHV = 18.4$
 $C_f = 48.0; H_f = 6.04; O_f = 45.43; N_f = 0.15; S_f = 0.05$
 {The LHV calculated in kJ/kg by using the following relation}
 $LHV_{biomass} = 4.1868/1000 \cdot ((1 + 0.15 \cdot O_f) \cdot (7837.667 \cdot C_f + 33888.889 \cdot H_f - O_f/8))$
 {Use the following relation for beta}
 $BETA = (1.0414 + 0.0177 \cdot (H_f/C_f) - 0.3328 \cdot (O_f/C_f) \cdot (1 + 0.0537 \cdot H_f/C_f)) / (1 - 0.4021 \cdot O_f/C_f)$
 {Fed biomass}
 $MW_{biomass} = 12 \cdot N_C + 1 \cdot N_H + 16 \cdot N_O$
 $M_{biomass} = N_{biomass} \cdot MW_{biomass}$
 $N_{bio_st} = N_{biomass} / N_{steam}$
 $M_{st_bio} = M_{steam} / M_{biomass}$
 $M_{H2_bio} = M_{H2} / M_{biomass}$
 {Energetic efficiency}
 $EN_{biomass} = M_{biomass} \cdot LHV_{biomass}$
 $EN_{H2} = N_{H2} \cdot \Delta H_{H2}$
 $EN_{steam} = N_{steam} \cdot \Delta H_{H2O}$
 $EN_{gas} = N_{H2} \cdot \Delta H_{H2} + N_{CO} \cdot \Delta H_{CO} + N_{CO2} \cdot \Delta H_{CO2} + N_{CH4} \cdot \Delta H_{CH4}$
 {Equations for char}
 $EPS_{ch_char} = 410260$ [kJ/kmol]
 $EX_{ch_char} = EPS_{ch_char}$
 $\Delta H_{char} = 4.18 \cdot (4.03 \cdot (T_1 - T_0) + 0.00114 \cdot (T_1^2/2 - T_0^2/2) + 2.04 \cdot 10^5 \cdot (1/T_1 - 1/T_0))$
 $S_{char} = 4.18 \cdot (4.03 \cdot (\ln(T_1) - \ln(T_0)) + 0.00114 \cdot (T_1 - T_0) + 1.02 \cdot 10^5 \cdot (1/T_1^2 - 1/T_0^2))$
 $EX_{ph_char} = \Delta H_{char} - T_0 \cdot S_{char}$
 $EX_{char} = N_{char} \cdot (EX_{ch_char} + EX_{ph_char})$
 $EN_{char} = N_{char} \cdot \Delta H_{char}$
 {Tar molecular weight as benzen molecular weight C6H6}
 $MW_{tar} = 78.11$
 $N_{tar} = 0.01 \cdot TAR \cdot N_{tot}$
 {Equation for tar}
 $\Delta H_{tar} = N_C \cdot \Delta H_{HF_CO2} + N_H/2 \cdot \Delta H_{HF_H2O} + (0.00422 \cdot (T_1^2 - T_0^2) - 30.980)$
 $EN_{tar} = \Delta H_{tar} \cdot N_{tar} \cdot MW_{tar}$
 $A1_{tar} = 37.1635; A2_{tar} = -$
 $31.4767; A3_{tar} = 0.564682; A4_{tar} = 20.1145; A5_{tar} = 54.3111; A6_{tar} = 44.6712$
 {S_star in kJ/kmol carbon K}
 $S_{star} = A1_{tar} + A2_{tar} \cdot \exp(-$
 $A3_{tar} \cdot (H_f/C_f + N_f)) + A4_{tar} \cdot (O_f/(C_f + N_f)) + A5_{tar} \cdot (N_f/(C_f + N_f)) + A6_{tar} \cdot (S_f/(C_f +$
 $N_f))$
 $S_{tar} = S_{star} + 0.00422 \cdot (T_1 - T_0)$
 $EX_{ph_tar} = \Delta H_{tar} \cdot N_{tar} \cdot MW_{tar} - T_0 \cdot S_{tar} \cdot N_{tar}$
 $EPS_{ch_tar} = 3303600$ [kJ/kmol]
 $X_{tar} = N_{tar} / N_{tot}$
 $EX_{ch_tar} = N_{tar} \cdot (X_{tar} \cdot EPS_{ch_tar} + R \cdot T_0 \cdot X_{tar} \cdot \ln(X_{tar}))$
 {Chemical exergy of tar is disregarded}
 $EX_{tar} = EX_{ph_tar} + EX_{ch_tar}$

{Energy lost from the gasifier wall is calculated by Isachenko, 1977 correlation}

$$(1.9468*(T_w-T_0)^{0.25}*(2.8633*U_0+1)^{0.5}+5.75*10^{-8})*EMISS*(T_w+T_0)*(T_w^2+T_0^2)*(T_w-T_0)-K_{ins}/X_{ins}*(T_1-T_w)=0.0$$

{over all heat transfer coefficient in W/m2/k}

$$H_{overall}=1.9468*(T_w-T_0)^{0.25}*(2.8633*U_0+1)^{0.5}+5.75*10^{-8})*EMISS*(T_w^4-T_0^4)/(T_1-T_0)$$

$$A_{gasifier}=3.14*0.08*0.50$$

{Energy lost from the gasifier}

$$EN_{lost}=A_{gasifier}*H_{overall}*(T_w-T_0)/1000$$

{Energetic efficiencies}

$$ETA_{En1}=EN_{H2}/(EN_{biomass}+EN_{steam})*100$$

$$ETA_{En2}=EN_{gas}/(EN_{biomass}+EN_{steam})*100$$

$$ETA_{En3}=(EN_{gas}+EN_{char}+EN_{tar})/(EN_{biomass}+EN_{steam})*100$$

{Exergy destruction due to energy lost from the gasifier body (thermal exergy)}

$$EX_{destwa}=EN_{lost}*(1-T_0/T_w)$$

{Exergy destructed during the gasification process or internal destroyed}

$$I=EX_{biomass}+EX_{steam}-EX_{gas}-EX_{char}-EX_{tar}-EX_{destwa}$$

$$S_{gen}=I/T_0$$

$$S_{gen_sp}=S_{gen}/M_{biomass}$$

{Exergetic efficiency}

$$EX_{biomass}=BETA*LHV_{biomass}*M_{biomass}$$

$$EX_{H2}=N_{H2}*EX_{ch_H2}+N_{H2}*EX_{ph_H2}$$

$$EX_{gasexH2}=EX_{gas}-EX_{H2}$$

$$ETA_{Ex1}=EX_{H2}/(EX_{biomass}+EX_{steam})*100$$

$$ETA_{Ex2}=EX_{gas}/(EX_{biomass}+EX_{steam})*100$$

$$ETA_{Ex3}=(EX_{gas}+EX_{char}+EX_{tar})/(EX_{biomass}+EX_{steam})*100$$

{Improvement potential}

$$IP=(1-ETA_{Ex1}/100)*I$$

$$EX_{gas_bio}=EX_{gas}/(M_{biomass}*1000)$$

$$EX_{char_bio}=EX_{char}/(M_{biomass}*1000)$$

$$EX_{tar_bio}=EX_{tar}/(M_{biomass}*1000)$$

$$EX_{bio_steam}=(EX_{biomass}+EX_{steam})/(M_{biomass}*1000)$$

$$EX_{phgas_bio}=EX_{ph_gas}/(M_{biomass}*1000)$$

$$EX_{chgas_bio}=EX_{ch_gas}/(M_{biomass}*1000)$$

{Calculations for SOFC}

{DC-AC Inverter efficiency 0.95, Fuel utilization factor 0.95}

$$ETA_{DC_AC}=0.95;U_f=0.95$$

{Reacted H2 moles is U_f*N_{H2} ; F_{FAR} is Faraday constant}

$$F_{FAR}=96485[C/mol]$$

$$N_{H2R}=U_f*N_{H2}$$

$$N_{O2}=2*N_{H2}$$

{Calculate supplied air where air contains 21% O2}

$$N_{air}=N_{O2}/0.21$$

{Current flow in SOFC in A}

$$I_{SOFC}=2*N_{H2_SOFC}*U_f*F_{FAR}$$

$$I_{SOFC}=I_D/1000*A_{SOFC}$$

{Active surface area;Base current density}

$$A_{SOFC}=100 [cm^2]$$

$$I_D=750 [mA/cm^2]$$

$$N_{SOFC}=N_{H2}/N_{H2_SOFC}$$

```

{Exchange current density of anode ;Exchange current density of cathode}
I_DEa=650[ mA/cm2];I_DEc=250[ mA/cm2]
{Effective gaseous diffusivity through the anode ;Effective gaseous diffusivity through the
cathode}
D_effa=0.2[cm2/s];D_effc=0.05[cm2/s]
t_a=0.05[ cm];t_c=0.005 [cm];t_e=0.001[cm];t_cc=0.300[cm]
{Resistivity of air electrode;Resistivity of fuel electrode;Resistivity of electrolyte;Resistivity of
interconnection ohm-cm}
Resist_Air_electrode=0.008114*exp (600/T_SOFC);Resist_Fuel_electrode=0.00298*exp(-
1392/T_SOFC)
Resist_electrolyte=0.00294*exp
(10350/T_SOFC);Resist_interconnection=0.1256*exp(4690/T_SOFC)
{Pressure of the cell; Temperature of the cell}
P_SOFC=120[kPa];T_SOFC=1000[K]
{Calculations of delta enthalpy for water in kJ/ kmol}
DELTAH_H2O= A_H2O*(T_SOFC-T_0)+B_H2O*(T_SOFC^2-T_0^2)/2 +
C_H2O*(T_SOFC^3-T_0^3)/3 + D_H2O*(T_SOFC^4-T_0^4)/4
S_H2O_SOFC = A_H2O*(LN(T_SOFC)-LN(T_0))+B_H2O*(T_SOFC-
T_0)+C_H2O*(T_SOFC^2-T_0^2)/2 + D_H2O*(T_SOFC^3-T_0^3)/3
{Calculations of delta enthalpy for hydrogen in kJ/kmol}
DELTAH_H2= A_H2*(T_SOFC-T_0)+B_H2*(T_SOFC^2-T_0^2)/2 + C_H2*(T_SOFC^3-
T_0^3)/3 + D_H2*(T_SOFC^4-T_0^4)/4
S_H2_SOFC = A_H2*(LN(T_SOFC)-LN(T_0))+B_H2*(T_SOFC-T_0)+C_H2*(T_SOFC^2-
T_0^2)/2 + D_H2*(T_SOFC^3-T_0^3)/3
{Calculations of delta enthalpy for O2 }
A_O2=25.48;B_O2=1.520*10^(-2);C_O2=-0.7155*10^(-5);D_O2=1.312*10^(-9)
DELTAH_O2= A_O2*(T_SOFC-T_0)+B_O2*(T_SOFC^2-T_0^2)/2+C_O2*(T_SOFC^3-
T_0^3)/3+D_O2*(T_SOFC^4-T_0^4)/4
S_O2_SOFC = A_O2*(LN(T_SOFC)-LN(T_0))+B_O2*(T_SOFC-T_0)+C_O2*(T_SOFC^2-
T_0^2)/2 + D_O2*(T_SOFC^3-T_0^3)/3
DELTA_HF_O2=0.0;DELTA_S_O2=205.04[kJ/kmol-K]
{Find Gibbs function, DHF in KJ/mol}
DELTAH_SOFC=((-DELTA_HF_H2-0.5*DELTA_HF_O2+1000*DELTA_HF_H2O)+(-
DELTAH_H2-0.5*DELTAH_O2+DELTAH_H2O))
TDELTA_S_SOFC=T_SOFC*(-S_H2_SOFC-DELTA_S_H2-
0.5*(DELTA_S_O2+S_O2_SOFC)+S_H2O_SOFC+DELTA_S_H2O)
DELTA_G_SOFC=DELTAH_SOFC-TDELTA_S_SOFC
{Open circuit voltage}
V_Oc=-0.5*DELTA_G_SOFC/F_FAR-0.5*R*T_SOFC/F_FAR*LN
((P_H2O/P_SOFC)/(P_H2/P_SOFC*(P_O2/P_SOFC)^0.5))
{The over potentials due to activation}
V_act_a=R*T_SOFC/F_FAR*ARCSINH(I_D/(2*I_DEa ))
V_act_c=R*T_SOFC/F_FAR*ARCSINH(I_D/(2*I_DEc ))
V_Act=V_act_a+V_act_c
{The ohmic over potential, Vohm}
C_SOFC=0.01*(Resist_Air_electrode*t_c+Resist_Fuel_electrode*t_a+Resist_electrolyte*t_e+R
esist_interconnection*t_cc)
{The ohmic symmetry factor, Eosf }
E_osf=(t_c/Resist_Air_electrode+t_cc/Resist_interconnection)/(t_a/Resist_Fuel_electrode+t_cc/
Resist_interconnection)

```

$B_{SOFC} = E_{osf} / (1 + E_{osf})^2$
 {The characteristic length of SOFC, L in t dim}
 $L_{SOFC1} = 1 / (t_a / Resist_{Fuel_electrode} + t_{cc} / Resist_{interconnection})$
 $L_{SOFC2} = 1 / (t_c / Resist_{Air_electrode} + t_{cc} / Resist_{interconnection})$
 $L_{SOFC} = (Resist_{electrolyte} * t_e / (L_{SOFC1} + L_{SOFC2}))^{(0.5)}$
 {Cell pitch length cm}
 $X_{SOFC} = 0.55 [cm]$
 $J = X_{SOFC} / L_{SOFC}$
 {Specific electrical resistance in ohm cm²}
 $R_{Res} = C_{SOFC} * J * (1 / TANH(J) + B_{SOFC} * (J - 2 * TANH(J/2)))$

$V_{Ohm} = R_{Res} * I_D / 1000$
 {Average moles flow of species in fuel and air channels}
 $N_{N2_av} = N_{O2} * (79/21)$
 $N_{O2_av} = (3/2 - U_f) * N_{O2}$
 $N_{H2O_av} = U_f * N_{H2} / 2$
 $N_{H2_av} = (2 * N_{H2} - U_f * N_{H2}) / 2$
 {Concentration of species in fuel and air channels}
 $Y_{O2} = N_{O2_av} / (N_{O2_av} + N_{N2_av})$
 $Y_{N2} = N_{N2_av} / (N_{O2_av} + N_{N2_av})$
 $Y_{H2O} = N_{H2O_av} / (N_{H2_av} + N_{H2O_av})$
 $Y_{H2} = N_{H2_av} / (N_{H2_av} + N_{H2O_av})$
 {Partial pressure of species in fuel and air channels}
 $P_{O2} = P_{SOFC} * Y_{O2}$
 $P_{H2O} = P_{SOFC} * Y_{H2O}$
 $P_{H2} = P_{SOFC} * Y_{H2}$
 $P_{N2} = P_{SOFC} * Y_{N2}$
 {The polarization or concentration over potential, V_{pol}}
 $V_{Pola1} = LN(1 - 0.5 * I_D * R * T_{SOFC} / F_{FAR} * t_a / (D_{effa} * P_{H2}))$
 $V_{Pola2} = LN(1 + 0.5 * I_D * R * T_{SOFC} / F_{FAR} * t_a / (D_{effa} * P_{H2O}))$
 $V_{Pol_a} = -0.5 * R * T_{SOFC} / F_{FAR} * (V_{Pola1} - V_{Pola2})$
 $I_{D1} = 4 * F_{FAR} * P_{O2} * D_{effc} / ((P_{SOFC} - P_{O2}) / P_{SOFC} * R * T_{SOFC} * t_c)$
 $V_{Pol_c} = -0.250 * R * T_{SOFC} / F_{FAR} * LN(1 - I_D / I_{D1})$
 $V_{Pol} = V_{Pol_a} + V_{Pol_c}$
 $V_{Tot} = V_{Act} + V_{Pol} + V_{Ohm}$
 $V_{SOFC} = V_{Oc} - V_{Act} - V_{Ohm} - V_{Pol}$
 $W_{dot_SOFC} = I_{SOFC} * V_{SOFC}$
 $W_{dot_STACK} = N_{SOFC} * W_{dot_SOFC}$
 $LHV_{H2} = 120000 [kJ/kg]$
 $Eta_{SOFC} = W_{dot_SOFC} / (N_{H2_SOFC} * 2.016 * LHV_{H2}) * 100$
 $Eta_{SOFC_El} = W_{dot_SOFC} * Eta_{DC_AC} / (N_{H2_SOFC} * 2.016 * LHV_{H2}) * 100$